

---

**HYDROPHOBINS**  
**FROM *PLEUROTUS OSTREATUS*:**  
**SELF-ASSEMBLING PROTEINS FOR**  
**NANOBIOTECHNOLOGICAL**  
**APPLICATIONS**

---

**Sara Longobardi**

Dottorato in Scienze Biotecnologiche – XXIV ciclo  
Indirizzo Biotecnologie Industriali e Molecolari  
Università di Napoli Federico II







---

**HYDROPHOBINS**  
**FROM *PLEUROTUS OSTREATUS*:**  
**SELF-ASSEMBLING PROTEINS FOR**  
**NANOBIOTECHNOLOGICAL**  
**APPLICATIONS**

---

**Sara Longobardi**

Dottoranda: Sara Longobardi  
Relatore: Prof.ssa Paola Giardina  
Coordinatore: Prof. Giovanni Sannia



*Articolo 9*

*La Repubblica promuove lo sviluppo  
della cultura e la ricerca scientifica e tecnica*

*Articolo 33*

*L'arte e la scienza sono libere e libero ne è l'insegnamento*

*(la Costituzione)*



*A mia madre, per la forza e la  
determinazione che mi ha trasmesso.  
A mio padre, perché tutto quello che  
ho fatto l'ho fatto per amore (philos)  
della conoscenza (sophia).*





<b>Summary</b>	1
<b>Riassunto</b>	2
<b>Abbreviations</b>	7
<b>1 Introduction</b>	9
1.1 The hydrophobins: general features and biological role	10
1.2 Structure of hydrophobins	10
1.3 Hydrophobin self-assembling	12
1.3.1 Self-assembly at interfaces	12
1.3.2 Oligomerization in solution	13
1.3.3 Rodlet formation	14
1.4 Applications	15
1.5 Production of hydrophobins	17
1.6 <i>Pleurotus ostreatus</i> hydrophobins	17
1.7 Outline of the thesis	18
<b>2 Materials and methods</b>	19
2.1 Production of the hydrophobin Vmh2	20
2.2 Characterization of the hydrophobin Vmh2	22
2.3 Characterization of the hydrophobin Vmh2 biofilm	22
<b>3 Results and discussion</b>	25
<b>Section I</b>	26
3.1 Production of the hydrophobin Vmh2	26
3.1.1 Extraction from <i>P. ostreatus</i> cultural medium	26
3.1.2 Extraction from <i>P. ostreatus</i> mycelia	26
3.1.3 Production of the recombinant Vmh2 in <i>E. coli</i>	27
3.1.4 Production of the recombinant Vmh2 in <i>P. pastoris</i>	27
<b>Section II</b>	30
3.2 Characterization of the hydrophobin Vmh2	30
3.2.1 Characterization in solution	30
3.2.2 Biofilm characterization	32
<b>Section III</b>	34
3.3 Applications	34
3.3.1 Immobilization of proteins on Vmh2 biofilm	34
3.3.2 Development of SELDI-TOF-like system	34
3.3.3 Textile material coating	38
3.3.4 Emulsifying properties	39
<b>4 Conclusions</b>	41
<b>5 References</b>	43
<b>Communications, Publications, Courses, Experiences in foreign lab</b>	47
<b>Appendix I</b>	49
Papers	



## Summary

Hydrophobins are a large family of small proteins (about 100 aminoacids), produced by filamentous fungi at different developmental stages, self-assembling at hydrophobic/hydrophilic interfaces into amphipathic biofilm.

A hydrophobin secreted by the basidiomycete fungus *Pleurotus ostreatus*, identified as Vmh2, has been purified both from cultural broth and mycelia. Vmh2 extracted from cultural broth (5-10 mg L<sup>-1</sup>) was found complexed with glucans, identified as cyclodextrins. After separation from glucidic fraction, the protein was not soluble in water but only in less polar solvents. The Vmh2 extraction from *P. ostreatus* mycelia has been optimized, obtaining a higher amount of protein (about 100 mg L<sup>-1</sup>). The recombinant expression of Vmh2 in *Escherichia coli* and *Pichia pastoris* has been also performed, with a yield of about 50 and 30 mg L<sup>-1</sup>, respectively.

The behavior of Vmh2 has been analyzed in different conditions, as solvents, pH, temperature, presence of salts or glucans. When the protein is dissolved in low polar solvents (i.e. 60% ethanol) its structure is characterized by a high content of  $\alpha$ -helix, and it is stable in solution. When the pH increases or in the presence of Ca<sup>2+</sup> ions, a conformational change occurs and a self-assembled  $\beta$ -sheet rich state is formed, rapidly followed by precipitation. When the solvent polarity increases the protein shows an increased tendency to reach hydrophobic/hydrophilic interfaces, with no detectable conformational change. On the other hand a reversible conformational change and reversible aggregation occurs at high temperature. The interaction with glucans (such as glucose) enables the protein to be water soluble. In this condition Vmh2 adopts a  $\beta$ -structure stable in solution, whilst the self-assembled  $\beta$ -sheet rich state occurs after agitation of the solution.

Vmh2 dissolved in ethanol, forms very stable nanometric biofilm by deposition on solid surfaces, such as silicon, changing their wettability (from hydrophobic to hydrophilic). Vmh2 biofilm has been formed also in presence of glucose; in this case the hydrophilicity of the surface increased.

Locally, on the top of Vmh2 biofilm, the presence of some structures rodlet-like has been observed by atomic force microscopy (AFM). The rodlet formation at the water/air interface has been studied in more details preparing Vmh2 biofilm by Langmuir techniques. These rodlets appear to correspond to a hydrophobic bilayer, where conformational changes lead to more rigid structures.

The ability of Vmh2 biofilm to immobilize biological macromolecules has been also verified. Acting as a bioactive substrate to bind other proteins to an inert surface, the biofilm can be used for the fabrication of a new class of hybrid devices, such as biosensors, or for proteomic applications.

Vmh2 biofilm has been also used to modify the wettability of clothing fabrics. In particular, after Vmh2 coating, nylon fabrics became more hydrophobic, hence more waterproof. On the other hand wool (hydrophobic) becomes strongly hydrophilic, improving the wearing comfort and facilitating dyeing process.

Moreover, the emulsification capability of Vmh2 solution has been analysed using three different oils: olive, peanut and almond oil. The stabilization of the emulsion has been evaluated: the emulsions obtained in the presence of Vmh2 are stable at least for two days, and even longer in the cases of the peanut and almond oils.

This work has allowed an improvement of the Vmh2 availability, both as recombinant or extractive protein, to clarify the behaviour of the protein and to verify its applicability in several fields.

## Riassunto

Le idrofobine sono proteine a basso peso molecolare (7-10 KDa) di origine fungina, importanti nella crescita e nello sviluppo dei funghi, in quanto coinvolte nella formazione di strutture aeree, quali ife, spore e corpi fruttiferi e nell'adesione a superfici idrofobiche. Sono caratterizzate dalla presenza di un elevato numero di residui idrofobici e, anche se presentano scarsa identità di sequenza, mostrano un *pattern* caratteristico di otto cisteine formanti quattro ponti disolfurici. Caratteristica peculiare delle idrofobine è quella di auto-assemblare a livello di interfacce idrofiliche-idrofobiche formando biofilm anfipatici, in grado di rendere idrofilica una superficie idrofobica e viceversa. In base alla stabilità del biofilm formato le idrofobine vengono distinte in due classi: le idrofobine di classe I, prodotte sia da Basidiomiceti che da Ascomiceti, formano biofilm molto stabili che possono essere solubilizzati solo con agenti quali acido formico o acido trifluoroacetico (TFA) puro, mentre quelle di classe II, prodotte solo da Ascomiceti, formano biofilm meno stabili, che possono essere solubilizzati anche da soluzioni acquose come il sodio dodecil solfato (SDS) al 2%.

L'idrofobina di classe I più ampiamente caratterizzata è SC3 da *Schizophyllum commune*. E' riportato che SC3 è presente in diversi stati conformazionali: in forma solubile adotta una conformazione con 40% di struttura  $\beta$  e 23% di  $\alpha$ -elica, mentre durante l'auto-assemblamento all'interfaccia aria/acqua passa attraverso uno stato intermedio con incremento del contenuto in  $\alpha$ -elica, che è convertito allo stato finale (stabile) ricco di struttura  $\beta$  (65%). In soluzione il comportamento di SC3 è influenzato da vari parametri: bassa temperatura, pH acidi e basse concentrazioni proteiche tendono a mantenere SC3 in forma monomerica; aumentando la concentrazione si osserva la presenza del dimero in soluzione, mentre elevate temperature e pH alcalini determinano l'associazione della proteina in oligomeri.

Una delle prime osservazioni relative alle idrofobine di classe I riguarda la capacità di formare rodlet, aggregati altamente ordinati simili alle fibrille amiloidi, ossia ricchi di struttura  $\beta$  ed in grado di legare TioflavinaT.

Grazie alle loro caratteristiche peculiari le idrofobine trovano applicazione in svariati campi:

- Nelle biotecnologie alimentari possono essere utilizzate come biotensioattivi o emulsionanti, per migliorare la solubilità di preparati alimentari;
- nell'industria cosmetica per stabilizzare preparati contenenti oli,
- nell'ingegneria biomedica possono essere utilizzate per ricoprire dispositivi medici, come cateteri e vene artificiali, riducendo la possibilità di legame da parte di batteri patogeni a tali superfici.
- Nei sistemi separativi bifasici possono essere sfruttate per purificare proteine di interesse, opportunamente fuse alle idrofobine;
- Nell'immobilizzazione di proteine può essere sfruttata la loro capacità a formare biofilm e ad interagire stabilmente con supporti rigidi, lasciando la proteina libera di ripiegarsi e di svolgere la propria attività;
- Essendo in grado di funzionalizzare superfici, possono essere utilizzate nella creazione di biosensori, come componenti per *lab-on-chip* con applicazioni chimiche e biochimiche e per il *drug delivery*.

Nel gruppo di studio presso cui è stata svolta la presente tesi di dottorato è da tempo oggetto di studio il fungo basidiomicete *Pleurotus ostreatus*, ampiamente

caratterizzato ed utilizzato per la bioconversione di scarti agricoli e di lignocellulosa e per la produzione di enzimi di interesse industriale. In questo fungo sono stati identificati diversi geni codificanti idrofobine, espressi in differenti stadi del ciclo vitale. In particolare è stata purificata dal brodo di coltura del fungo un'idrofobina di classe I identificata come Vmh2, in grado di formare biofilm stabili su superfici solide.

Per poter utilizzare l'idrofobina nei campi di applicazione prima menzionati, risulta necessario raggiungere soddisfacenti livelli di produzione, nonché chiarire il comportamento della proteina in soluzione e le proprietà del biofilm che essa forma. All'interno di questo contesto si inserisce il presente lavoro di ricerca, i cui obiettivi sono stati:

- Estrazione di Vmh2 da *Pleurotus ostreatus*, sia dal terreno di coltura che dal micelio;
- Espressione ricombinante di Vmh2 in *Escherichia coli* e *Pichia pastoris*;
- Caratterizzazione del comportamento di Vmh2 in soluzione;
- Caratterizzazione del biofilm di Vmh2 su superfici solide;
- Valutazione di alcune potenziali applicazioni:
  - Immobilizzazione sul biofilm di Vmh2 di macromolecole biologiche;
  - Analisi della capacità emulsionante di Vmh2;
  - Analisi della capacità di rivestire materiali tessili.

### **Produzione di Vmh2**

Vmh2 è stata purificata dal brodo di coltura di *P. ostreatus* cresciuto in condizioni statiche, con una resa di circa 5-10 mg L<sup>-1</sup>. Analisi dei campioni di proteina solubilizzati in acqua hanno mostrato la presenza di glicani, identificati come ciclo-destrine con un numero di unità di glucosio variabile da 6 a 16, probabilmente prodotte dal fungo a partire dall'amilosio presente nel terreno. Se il campione viene disciolto in etanolo al 60% la frazione glucidica precipita lasciando la proteina libera in soluzione, che però risulta essere non più solubile in acqua. Questo dato suggerisce che l'interazione con i glicani permette la solubilizzazione di Vmh2 in acqua.

Al fine di aumentare i livelli di produzione di Vmh2, è stato messo a punto un sistema di estrazione dal micelio di *P. ostreatus*, seguendo un protocollo che ha permesso di ottenere circa 100 mg L<sup>-1</sup>.

Sono stati inoltre messi a punto sistemi di espressione ricombinante di Vmh2, utilizzando come ospiti il batterio *Escherichia coli* e il lievito *Pichia pastoris*. Nel primo caso Vmh2 è stata espressa come proteina di fusione con la GST (separate da una sequenza riconosciuta dalla proteasi TEV), al fine di aumentarne la solubilità. Tuttavia la proteina è stata ritrovata nei corpi di inclusione. Questi sono stati solubilizzati in un tampone contenente urea, che è stato poi lentamente diluito al fine di permettere l'idrolisi della proteasi. Una volta separata dalla GST, Vmh2 aggrega spontaneamente, permettendo così di ottenere la proteina pura, e correttamente strutturata, con una resa di circa 50 mg L<sup>-1</sup>.

Per quanto riguarda invece l'espressione in *P. pastoris*, sono stati utilizzati due differenti vettori, uno per esprimere la proteina con il peptide segnale omologo (di *P. ostreatus*) e uno per esprimere la proteina con un peptide segnale eterologo (dell' $\alpha$ -factor di *P. pastoris*). Vmh2 è stata recuperata in entrambi i casi dal terreno di coltura, seguendo la stessa procedura ottimizzata per *P. ostreatus*. Risultati ottenuti indicano che l'utilizzo del peptide segnale eterologo permette di ottenere una

maggior quantità di proteina secreta rispetto al peptide segnale omologo, raggiungendo una resa di circa 30 mg L<sup>-1</sup>.

### **Caratterizzazione di Vmh2 in soluzione**

E' stato analizzato il comportamento di Vmh2 in soluzione al variare di alcuni parametri, quali solventi, pH, temperatura, presenza di sali o di glucani.

Vmh2 in etanolo al 60% assume una conformazione con un significativo contributo di  $\alpha$ -elica (30%  $\alpha$ -elica, 20%  $\beta$ -sheet), mostrando inoltre una elevata stabilità in soluzione, anche dopo un mese o dopo induzione dell'aggregazione mediante agitazione meccanica (vortex). Aumentando il pH ( $\geq 6$ ) o in presenza di Ca<sup>2+</sup> si osserva un cambio della struttura secondaria e la rapida aggregazione della proteina in uno stato con maggior contributo di  $\beta$ -sheet, seguita da precipitazione. All'aumentare della temperatura ( $\geq 80^\circ\text{C}$ ) si osserva invece un incremento di conformazione random, cambiamento che risulta reversibile quando la soluzione viene riportata a temperatura ambiente.

Il comportamento di Vmh2 è stato analizzato anche al variare del tipo e della percentuale di solvente. La proteina è stata disciolta in etanolo, isopropanolo, trifluoroetanolo e acetonitrile al 60 ed al 20%, mostrando in tutti i casi una conformazione con maggior contributo di  $\alpha$ -elica, ma una minore solubilità all'aumentare della polarità (20% solvente 80% acqua). Analisi di questi campioni non hanno permesso di rilevare la presenza di aggregati in soluzione, mentre suggeriscono una maggiore tendenza della proteina a raggiungere le interfacce idrofiliche/idrofobiche.

Per chiarire l'interazione proteina/glicani, sono state utilizzate alcune molecole commerciali valutando la loro capacità di solubilizzare Vmh2 di acqua, al pari delle ciclo destrine prodotte dal fungo. Dati ottenuti dimostrano che  $\alpha$ -, $\beta$ - e  $\gamma$ -ciclodestrine, la molecola lineare maltoesoso e anche semplici monomeri di glucosio sono in grado di solubilizzare Vmh2 in acqua. Lo stesso risultato è stato ottenuto utilizzando altri esosi, come mannosio e galattosio, mentre pentosi e polioli sembrano non avere il medesimo effetto. I risultati ottenuti suggeriscono che una molecola di esoso abbia i requisiti strutturali per solubilizzare Vmh2 in acqua.

Vmh2 disciolta in acqua in presenza di glucosio mostra una conformazione stabile con un più elevato contributo di  $\beta$ -sheet (34%  $\beta$ -sheet, 10%  $\alpha$ -elica) e capacità di legare la TioflavinaT (ThT). Dopo induzione dell'aggregazione mediante vortex si osserva un incremento della fluorescenza indotta dal legame con ThT e precipitazione della proteina dopo centrifugazione.

### **Caratterizzazione del biofilm**

Biofilm di Vmh2 disciolta in etanolo al 60% sono stati formati su superfici di silicio cristallino. Mediante analisi ottiche è stato dimostrato che la proteina forma biofilm monostrato (di circa 3 nm) o multistrato, in base alle condizioni di deposizione e di lavaggio. Il biofilm monostrato risulta essere altamente stabile da un punto di vista chimico, essendo resistente a trattamenti basici (in presenza di NaOH) e a detergenti (SDS a 100°C). La proteina anche in presenza di glucosio è in grado di formare biofilm stabili, i quali però presentano uno spessore minore (circa 1.5 nm). Dato che la misura dello spessore del biofilm è determinato dalla media degli spessori in diversi punti è probabile che in questo caso parte della superficie sia ricoperta da Vmh2 e parte dalle più piccole molecole di glucosio.

E' stata anche valutata la capacità del biofilm di Vmh2 di modificare superfici, misurando il valore di angolo di contatto di una goccia d'acqua (WCA) posta sulla

superficie stessa. Il silicio cristallino presenta di norma un WCA di circa 90°, ossia è considerato idrofobico. La presenza del biofilm di Vmh2 in etanolo abbassa il WCA del silicio a circa 44°, rendendo quindi la superficie più idrofilica, mentre il WCA del biofilm di Vmh2 in presenza di glucosio è circa 17°. In quest'ultimo caso probabilmente la presenza di gruppi polari dello zucchero all'interno del biofilm aumenta ulteriormente l'idrofilicità della superficie.

Immagini del biofilm ottenuti mediante microscopia a forza atomica (AFM) hanno mostrato la presenza, in alcune zone, di strutture tipo rodlet. La natura dei rodlet formati all'interfaccia aria/acqua è stata analizzata in più dettaglio, preparando biofilm di Vmh2 mediante tecniche *Langmuir*. I rodlet osservati sembrano corrispondere a *bilayer* idrofobici, la cui formazione è accompagnata da cambi conformazionali che portano ad una più rigida struttura.

## **Applicazioni**

### **- Immobilizzazione di proteine sul biofilm di Vmh2**

E' stata valutata la capacità del biofilm di Vmh2 di immobilizzare proteine, utilizzando l'albumina di siero bovino (BSA) marcata con rodamina e un enzima ossidativo, una laccasi fungina. Nel primo caso la BSA è stata depositata su due chip di silicio, uno ricoperto dal biofilm di Vmh2 e uno no, usato come controllo negativo. Valutando l'emissione di fluorescenza è stato dimostrato che la proteina viene immobilizzata sul silicio solo in presenza del biofilm di Vmh2.

Lo stesso esperimento è stato ripetuto utilizzando la laccasi POXC da *P. ostreatus*, valutando l'effettiva immobilizzazione dell'enzima mediante saggio di attività. Anche in questo caso, i risultati ottenuti dimostrano che solo in presenza del biofilm POXC si immobilizza mantenendo la propria attività catalitica, anche se riutilizzato più volte. Inoltre l'enzima immobilizzato risulta essere significativamente più stabile rispetto a quello in soluzione.

### **Sviluppo di un sistema tipo SELDI-TOF**

Il SELDI-TOF MS (Surface enhanced laser desorption ionization time-of-flight mass spectrometry) è una importante metodologia per effettuare rapide e sensibili analisi di biomolecole, attraverso tecniche di spettrometria di massa di tipo MALDI-TOF, riducendo al minimo le procedure di preparazione del campione, come la purificazione. Questa metodologia si basa sull'utilizzo di piastrine porta-campione opportunamente derivatizzate, in grado di trattenere selettivamente gli analiti di interesse.

In questo contesto è stata verificata la capacità di Vmh2 di formare biofilm su una classica piastrina di acciaio per MALDI-TOF, utilizzando il biofilm per immobilizzare peptidi e anticorpi.

Una miscela di peptidi (derivanti da digestione triptica) è stata depositata sulla piastrina con e senza biofilm di Vmh2, procedendo poi con lavaggi a polarità del solvente decrescente. In assenza del biofilm nessun peptide è stato rilevato già al secondo lavaggio, mentre in presenza del biofilm si osserva la scomparsa dei peptidi più idrofili al diminuire della polarità del solvente, mentre quelli più idrofobici vengono trattenuti, come in una cromatografia a fase inversa.

Sono stati anche immobilizzati anticorpi su una piastrina MALDI, in presenza e in assenza del biofilm. Utilizzando un anticorpo marcato con fluoresceina è stato verificato, osservando l'emissione di fluorescenza, che l'immobilizzazione avviene solo in presenza del biofilm di Vmh2. Al fine di verificare se l'anticorpo immobilizzato mantiene la capacità di legare l'antigene, sono stati usati anticorpi policlonali

specifici. In entrambi i casi lo spettro di massa ha rilevato unicamente la presenza del segnale relativo all'antigene specifico anche partendo da campioni di miscele complesse.

### ***Stabilizzazione di emulsioni***

Dato che le idrofobine sono biosurfattanti, è stata verificata la possibilità di utilizzare Vmh2 nella preparazione e stabilizzazione dei preparati contenente oli, di uso sia in campo cosmetico che alimentare, considerando le caratteristiche delle idrofobine come biosurfattanti. A tale scopo sono stati utilizzati tre differenti oli (oliva, arachidi e mandorle). Vmh2 è stata risospesa in soluzioni al 20% etanolo e miscelata in presenza di ognuno dei tre oli. Le analisi condotte hanno mostrato che, mentre in assenza di Vmh2 si osserva la completa separazione delle fasi, in presenza di Vmh2 l'emulsione in tutti e tre i casi era stabile almeno per 72 ore e oltre una settimana per l'olio di arachidi e mandorla.

### ***Deposizione su materiali tessili***

La capacità di Vmh2 di ricoprire superfici è stata utilizzata anche per rivestire alcuni materiali tessili, come il nylon e la lana, per valutarne l'eventuale cambio di "bagnabilità" andando a osservare l'assorbimento dell'acqua sul tessuto nel tempo. Il nylon (tessuto parzialmente idrofilico) manifestava, dopo trattamento con Vmh2, un forte carattere idrofobico, trattenendo una goccia d'acqua sulla superficie per oltre 2 ore, risultando quindi essere più impermeabile. Invece il campione di lana (tessuto naturalmente idrofobico) diviene altamente idrofilico, risultando essere quindi più facilmente lavabile. In entrambi i casi il biofilm ha mostrato una forte adesione alla superficie e un'elevata stabilità a trattamenti con detergenti anche ad altre temperature.

In conclusione con il presente lavoro di ricerca sono stati conseguiti i seguenti risultati:

- L'ottimizzazione della produzione e dell'estrazione di Vmh2 da *P. ostreatus* ha permesso di ottenere rese soddisfacenti, necessarie per presupporre un potenziale utilizzo della proteina in vari campi di applicazione, tra cui, ad esempio, quello alimentare, dato che viene naturalmente prodotta da un fungo edibile.
- La messa a punto di sistemi di espressione ricombinante di Vmh2, anche in questi casi con buone rese di produzione, pone le basi per la progettazione di idrofobine ingegnerizzate, aventi differenti proprietà a seconda del campo di applicazione.
- I risultati ottenuti dalle analisi di Vmh2 in soluzione contribuiscono a chiarire il comportamento di questa proteina difficile da manipolare a causa della sua tendenza all'aggregazione e ad ottenere le conoscenze necessarie al fine di facilitarne l'utilizzo nei campi di applicazione prima menzionati.
- La caratterizzazione del biofilm di Vmh2 su superfici solide e l'analisi delle sue proprietà hanno permesso di dimostrare che questa proteina può essere utilizzata per funzionalizzare superfici. In particolare, avendo verificato la capacità di immobilizzare macromolecole biologiche, il biofilm di Vmh2 può essere usato come interfaccia biocompatibile per la creazione di dispositivi integrati, quali ad esempio i biosensori, o nello sviluppo di sistemi tipo SELDI-TOF.



## Abbreviations

<b>AFM</b>	Atomic force microscopy
<b>cDNA</b>	Complementary Deoxyribonucleic acid
<b>CD</b>	Circular Dichroism
<b>DTT</b>	Dithiothreitol
<b>GST</b>	Glutathione S-transferase
<b>HPLC</b>	High Performance Liquid Chromatography
<b>LB</b>	Langmuir-Blodgett
<b>LS</b>	Langmuir-Schaefer
<b>MALDI-MS</b>	Matrix assisted laser desorption/ionization-mass spectrometry
<b>NMR Nuclear</b>	Magnetic Resonance
<b>PCR</b>	Polymerase Chain Reaction
<b>PSi</b>	Porous silicon
<b>PDY</b>	Potato Dextrose and Yeast extract
<b>SDS</b>	Sodium Dodecyl Sulfate
<b>SDS-PAGE</b>	SDS Polyacrylamide gel electrophoresis
<b>SELDI-TOF</b>	Surface enhanced laser desorption/ionization-mass spectrometry
<b>Si</b>	Silicon
<b>TEV</b>	Tobacco Etch Virus
<b>TFA</b>	Trifluoroacetic acid
<b>ThT</b>	Thioflavine T (dye)
<b>Vmh2-et</b>	Vmh2 dissolved in 60% ethanol
<b>Vmh2-C</b>	Vmh2 dissolved in water in presence of cyclodextrins
<b>Vmh2-G</b>	Vmh2 dissolved in water in presence of glucose
<b>WCA</b>	Water Contact Angle



## **1. Introduction**

## 1.1 The hydrophobins: general features and biological role

Hydrophobins are a large family of small proteins (about 100 aminoacids), produced by filamentous fungi at different developmental stages, self-assembling at hydrophobic/hydrophilic interfaces into amphipathic biofilm.

Hydrophobins can be secreted out in the surroundings or retained in the fungal structures, such as fruiting bodies or mycelium. Their biological functions seem to be diverse, but always seem to be related to interactions with interfaces or surfaces. Described as the most surface active proteins ever known, hydrophobins play a role as a coating/protective agent, in adhesion, surface modification, or other type of function that require surfactant-like properties [1]. For instance, they allow fungi to escape an aqueous environment, lowering the surface tension (figure 1), and mediate attachment of fungi to hydrophobic surfaces [2]

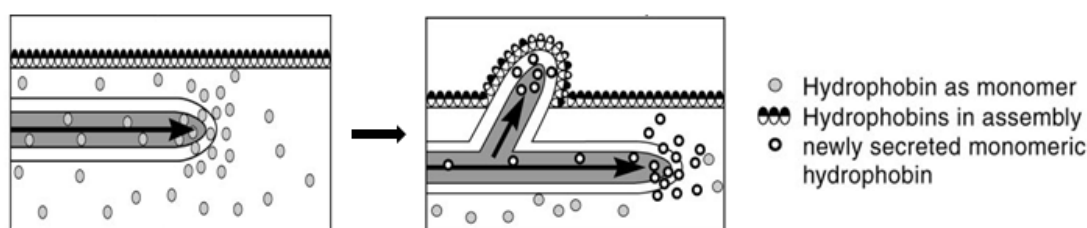
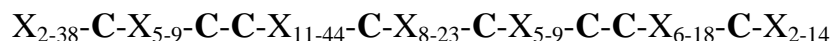


Figure 1: **Schematic model of fungi vegetative mycelia growth.** The hydrophobins secreted into the liquid culture medium form an amphiphilic membrane at water-medium interface, allowing the hyphae to growth into the air.

Despite the low sequence similarity, they have a characteristic pattern of eight cysteine residues forming four nonsequential disulphide bonds that stabilize the structure.



The distribution of the cysteines, the hydrophathy pattern, the morphology and the stability of assembled biofilm allow to divide hydrophobins into two classes: class I and class II. Class I hydrophobin genes have been isolated from ascomycetes and basidiomycetes, while the genes encoding class II hydrophobins have not been identified in basidiomycetes. Class I hydrophobins generate very insoluble assemblies, which can be solubilized only in strong acids such as trifluoroacetic acid or formic acid, whilst assemblies of class II hydrophobins can be solubilized in ethanol or sodium dodecyl sulfate aqueous solutions [3].

## 1.2 Structure of hydrophobins

The structural analysis of proteins and the resulting better comprehension of structure–function relations would allow to understand their biological roles and to choose a suitable one for selected application, or designing new ones with specific desired properties.

The common characteristic of to both class of hydrophobins is a completely conserved pattern of the eight Cys-residues (figure 2), where the second and third, and the sixth and seventh Cys residues are invariably adjacent. The inter-cysteine regions of class II hydrophobins are well conserved. In contrast, in class I

hydrophobins the region between the third and the fourth cystein (loop Cys3-Cys4) varies from 4 to 44 residues, whilst the region between the fourth and the fifth cystein (loop Cys4-Cys5) varies from 8 to 23 residues. [4].

#### Class I hydrophobins

```

SC4  CNSG-PVQ--CCNETTT--VANAQ-KQGLLGG---LLGVVV---GPITGLVGLNCSP---ISVVGV---LFGNSCTA-QTVCCDHVTQNG-----LVN--VGC
PRI2 CNNG-SIQ--CCNSSMTQDRGNLQIAQGVVLGGLLGGLLGLGGLLDLVDLNLALIGVCCSP---ISIVG-----NANTCTQ-QTVCCSNNNFNG-----LIA--LGC
SC3  CTTG-SLS--CCNQVQS---ASSSPVTALLG-----LLGIV-----LDLNVLVGISCSPP---LTVIG-----VGGSGCSA-QTVCCENTQFNG-----LIN--IGC
ABH1 CDVG-EIH--CCDTQQT----PDHTSAAASG---LLGVF-----INLGAFLGFDCTP---ISVLG-----VGGNNCAA-QPVCCGTGNQFTA-----LINA-LDC
EAS  CSID-DYKPYCCQSMMSG-----PAGSPGL-----LNLIP-----VDLSASLG--C-----VVG-----VIGSQCGA-SVKCCDDVTNTGNSFLIINA-ANC
HCF1 CAVGSQIS--CCTTNS--GSD-----ILGNV-----LGGSCLLDN--VSLISSLN-----SNCPAGNTFCPPS-NQDG-----TLNINVSC
MPG1 CGAEKVYS--CCNSKELK--NSKSGAE-----IPIDV-----LSGECKNIPINILTIQLI--PINNFCSD-TVSCCSGEQIG-----LVN--IQC
RODA CGDQAQLS--CCNKATYAG-DVTFDIDEGILAGTLKNLIGGGS---GTEGLGLFNQCSKLDLQIPVIGIPIQALVNQKCKQ-NIACCQNSPSPDASG--SLIGLGLPC

```

#### Class II hydrophobins

```

HFBI  CPPG-LFSNPCCATQVLGLIGLDCCKVPSQNVYDGTDFERNVCAKTGA-QPLCCVAP-VAGQALLC
HFBI  CPTG-LFSNPLCCATNVLDLIGVDCCKTPTIAVDTGAIQAHCAASKGS-KPLCCVAP-VADQALLC
SRH1  CPNG-LYSNPCCGANVLDLVAALDCHTTPRVVLTGPPIQAVCAEAGGKQPLCCVVP-VAGQDILC
CU    CTGL-LQKSPCCNTDILGVANLDCCHGPPSVPTSPSQFQASCVDAGGRSARCCCTLS-LLGLALVC
CRP   CSST-LYSEAQCCATDVLGVADLDCETVPEPTPTASSEFESICATSG-RDAKCCCTIP-LLGQALLC
MGP   CSG--LYGSAQCCATDILGLANLDCGQPSDAPVDADNFSEICAAIG-QRARCCVLP-ILDQGILC
HCF6  CPAN---RVPCQQLSVLGVADVTGASPSGLTSSVSAFEADCAANDG-TTAQCCCLIP-VLGLGLFC
HYD4  CPDGGLLIGTPCCSLDLVGLVLSGECSSPSKTPNSAKEFQETCAASG-QKARCCFLSEVFTLGAFC

```

Figure 2: **Amino acid sequence comparison of class I and II hydrophobins.** (Sunde 2008). The conserved Cys residues are highlighted in yellow with the conserved disulphide bonding pattern indicated with brackets.

In general, class I hydrophobins primary structure comprises 100–125 amino acids and can be glycosylated. The most detailed structural work on a class I hydrophobin has been obtained for the EAS hydrophobin from *Neurospora crassa*, studied by Nuclear Magnetic Resonance [5.]. EAS forms a four stranded  $\beta$ -barrel structure, an additional two stranded  $\beta$ -sheet, interrupted by some disordered regions (Figure 3 A). The structure (about 3 nm of diameter) displays a complete segregation of charged and hydrophobic residues on its surface, forming a hydrophobic patch and making the protein anphipathic.

Class II hydrophobins have shorter sequence comprising 50–100 amino acid residues, and are more easily handled, because of their less tendency to aggregate. The crystal structures of two class II hydrophobins, HFBI and HFBII of *Trichoderma reesei* have been determined, and several other studies on these two proteins have been performed [6]. The class II hydrophobin fold is compact and globular (about 2 nm of diameter) and consists of a small antiparallel  $\beta$ -barrel formed by two hairpins connected by a stretch of a  $\alpha$ -helix, without disordered loop. The helix occupies basically the same region of space as the additional  $\beta$ -sheet in EAS [7]. The overall topology is determined by the cross-linking of the secondary structure via disulphide bonds giving stability thus forming the peculiar amphiphilic structure of the protein (Figure 3 B).

Therefore, by a structural superimposition of EAS and HFBII it is shown that class I and class II hydrophobins share the same fold despite a very low sequence similarity. Large differences are however found in the loops of the  $\beta$ -hairpins of the central  $\beta$ -barrel, indicating a structural reason for different molecular assembling between the two classes.

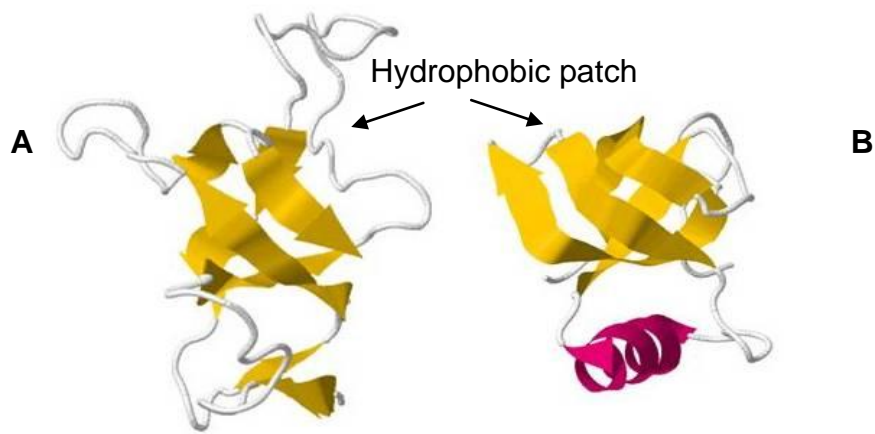


Figure 3: Ribbon diagram of EAS structure (A) and of HFBII structure (B)

Moreover hydrophobins can be post-translationally modified. For instance, SC3 from *Schizophyllum commune* contains 16-22 O-linked mannose units. These sugar molecules influence the properties of the assembled protein [8; 9]

### 1.3 Hydrophobin self-assembly

Hydrophobins can self-assemble in solutions, forming oligomers, or at hydrophobic/hydrophilic interfaces (water/air, water/oil or water/solid surface) into amphiphilic biofilm.

#### 1.3.1 Self-assembly at interfaces

It is demonstrated that class I hydrophobin self-assembling at interfaces is accompanied by change in secondary structure. Water soluble SC3 contains about 23%  $\alpha$ -helix, 40%  $\beta$ -sheet and 16%  $\beta$ -turn [8]. Self-assembly at water-air interface proceed through an intermediate form, with an increase of  $\alpha$ -helical content and a decrease of random coil, which is converted to a stable final state with a higher  $\beta$ -sheet content (65%). The association of SC3 with a hydrophobic surface (Teflon) in water can also induce a  $\alpha$ -helix rich state that is converted to the stable  $\beta$ -sheet upon heating in the presence of detergent. (Figure 3)

In contrast to SC3, self-assembly at water/air interface of class II hydrophobins is not accompanied by change in secondary structure, whilst an increase in helical conformation in the presence of Teflon is observed (Figure 4) [10].

By self-assembly at water/air, hydrophobins decrease the surface tension of the water. This ability has been reported both for class I and class II. Values reported for surface tension of aqueous solutions of hydrophobin range from 45 to 27  $\text{mNm}^{-1}$ , depending on the hydrophobin type and concentration used [10; 11].

By self-assembly on solid surface, hydrophobins can make hydrophilic a hydrophobic material and *vice versa*. The wettability of a solid surface can be estimated measuring the water contact angles (WCA) of a water drop deposited on it. For instance, on hydrophilic surface (WCA < 90 degrees) class I biofilm shows a water contact angle of 120 degrees, whilst class II film seems to be less water repellent (WCA range between 60 and 105 degrees). On the other hand, on hydrophobic surface (WCA > 90 degrees) the wettability of class I biofilm ranges between 36 and 63 degrees, for class II ranges between 22 and 60 degrees [10]. In some cases the wettability could be increased by the presence of sugar molecules. For instance, deglycosylated SC3 biofilm shows a decreased wettability at the hydrophilic side [9]

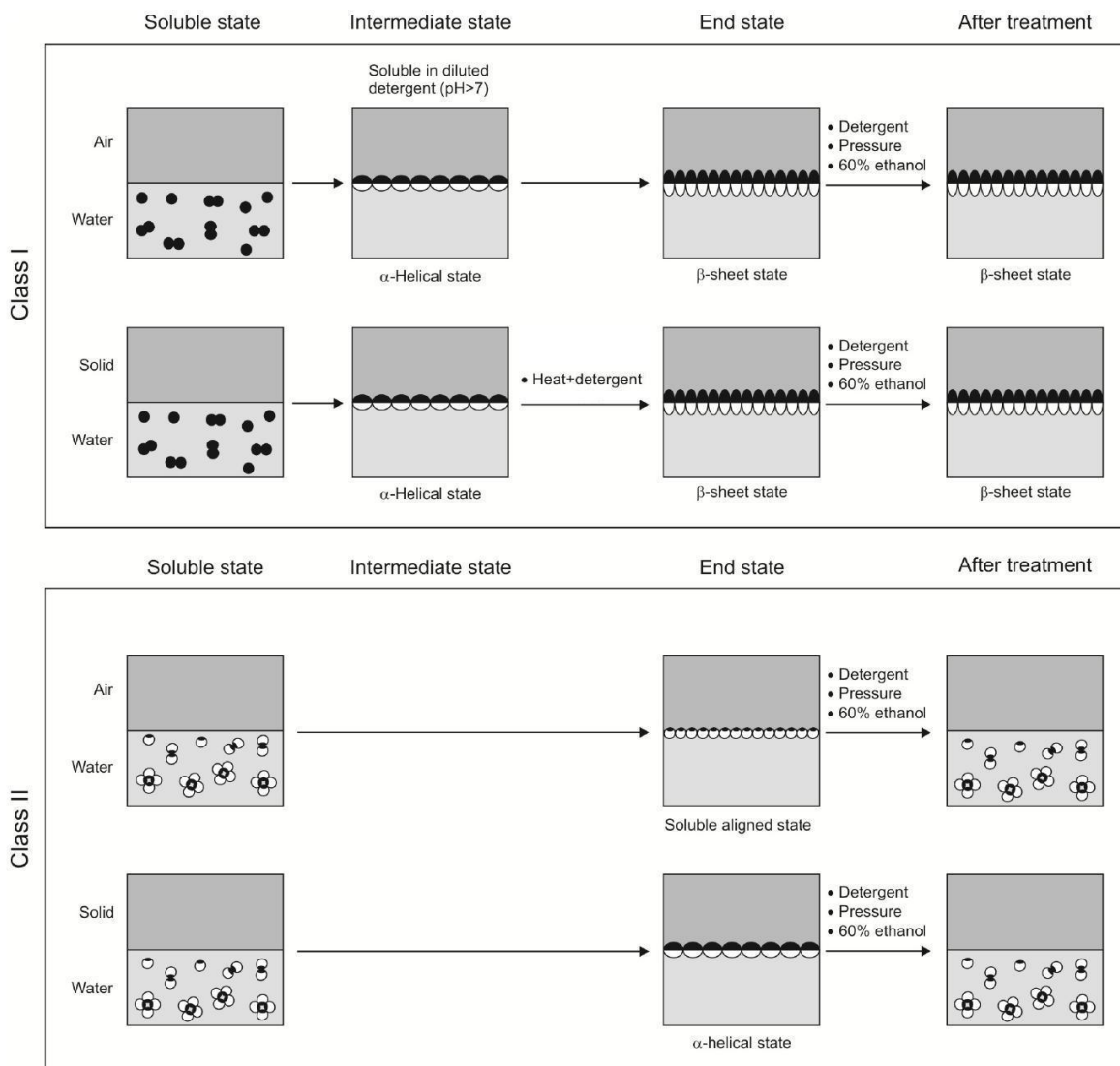


Figure 4: **Model for assembly** of class I (upper panel) and class II (lower panel) hydrophobins at hydrophobic and hydrophilic interfaces (water/air and water/hydrophobic solid)

### 1.3.2 Oligomerization in solution

At a concentration of a few micrograms per millilitre or less SC3 is in its monomeric form. At higher concentration (starting at about  $4 \mu\text{g mL}^{-1}$ ), SC3 is mainly in a dimeric form [12; 13]. The dimeric form is maintained at room temperature and acidic pH, whilst a slow formation of monomer is observed at  $5^\circ\text{C}$ . On the contrary, increasing the temperature or at alkaline pH association of the protein to form oligomers occurs. [14; 15].

A similar behavior has been reported for the recombinant class I hydrophobin H\*protein A [16]. The authors also observed that a strong association occurs in presence of  $\text{Ca}^{2+}$ , whilst this effect did not observed adding  $\text{Na}^+$  to the sample. On the basis of these results, they extended the model of hydrophobins self-assembly in solution previously proposed [14; 15], suggesting that the formation of large agglomerates can be triggered also by bivalent cations bridging and prevented by charge screening with monovalent cations (figure 5).

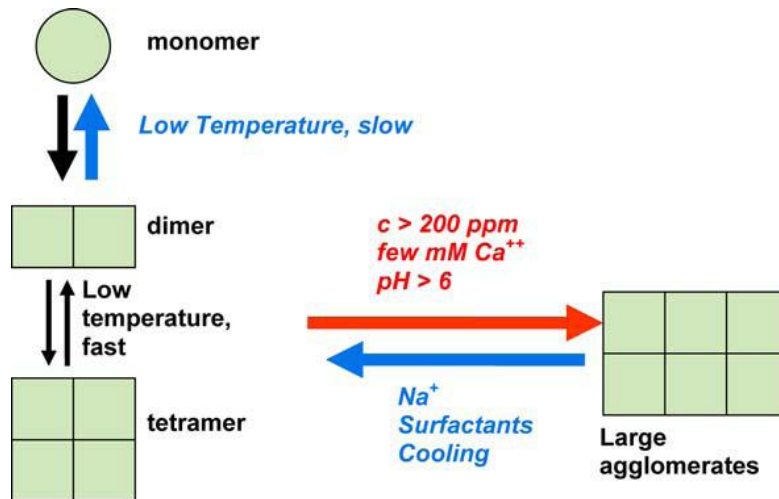


Figure 5: **Scheme of hydrophobin self-association in solution.** [16]

### 1.3.3 Rodlet formation

One of the early observations that were made for class I hydrophobin is the capability to form rodlets [17]. Purified class I hydrophobin have been shown to form rodlets also *in vitro*, drying protein solution on solid surface [8; 18; 19; 20; 21]. The diameter of these rodlets (figure 6) is about 10 nm, whilst the length is typically hundreds of nanometers and depends on the hydrophobin used and its concentration [22, 23].

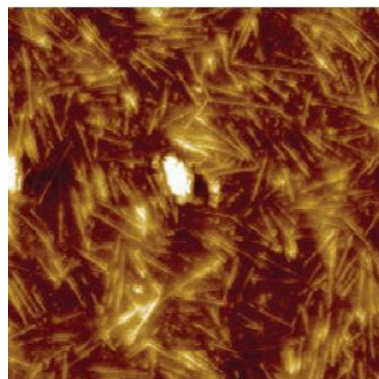


Figure 6: **AFM topography images of rodlets** formed by hydrophobin (HGFI from *Grifola frondosa*) on mica [24].

The rodlets can be formed at the interface air/water too, in a Langmuir trough by multiple compression cycles [24; 25].

Class I hydrophobin rodlets have characteristic similar to amyloid fibrils [26], showing similar spectroscopic changes in the presence of the dyes Thioflavin T (ThT) and Congo Red. The binding of these dyes suggests that the core structure of the rodlets consist of stacked  $\beta$ -sheet (like amyloid fibrils). As a matter of fact the diffraction X-ray pattern of EAS, obtained from unaligned rodlets (produced by vortexing and then harvested by centrifugation) displays reflections, consistent with  $\beta$ -sheet structure [5]. On the other hand, no rodlets have been observed analysing films formed by the purified class II hydrophobins, even if these films have also shown ordered structures [27].



## 1.4 Applications

The intriguing properties of hydrophobins make them of particular interest for numerous potential applications, summarized in table 1.

Application	Example
<b>Industrial applications</b>	
<b>Emulsions</b>	<b>Personal care product, Food industry, Drug delivery</b>
<b>Anti-fouling</b>	<b>Avoidance of binding and growth of undesired microorganisms on surfaces (i.e. ships and panel car)</b>
<b>Gushing factor detection</b>	<b>Identification of hydrophobins responsible for beer over-foaming</b>
<b>High-value applications</b>	
<b>Nanotechnology and diagnostic</b>	<b>Biosensors, Electrodes, DNA/protein Microarrays, Immunological assays</b>
<b>Tissue engineering</b>	<b>Biocompatibility of medical implants and devices</b>
<b>Separation technologies</b>	<b>Co-purification of hybridized protein of interest</b>

Table 1: **Biotechnological applications of hydrophobins.**

The remarkable high surface activity of hydrophobins is similar to that of traditional biosurfactants, such as glycolipids, lipopeptides/lipoproteins, phospholipids, lipopolysaccharides and so on. Hydrophobins can be used as emulsifiers or foaming agents in different branches of industry. In pharmaceutical field they can be used in drug delivery for the formulation of water insoluble drugs [28; 29]. Both personal care and food industries require stable emulsion for some formulation and ingredients. Multinational companies, such as BASF, Unilever or L'Oreal have increased their attention to hydrophobins, due to their properties, as demonstrated by the conspicuous number of patents registered.

The amphiphilic nature of hydrophobins can also be useful in separation technologies by a rapid and efficient detergent-based two phases protein purification system [30]. The first example came from endoglucanase (EGI) of *T. reesei*, whose C-terminus was coupled to hydrophobin HFBI from the same fungus. The purification of this fusion protein using a two-phase system, appeared to be more efficient than that of EGI without the fusion. The total recovery of EGI-HFBI was 90% after such a purification [31].

The ability of hydrophobins to self-assemble on solid supports into amphiphilic coating, can be used to manipulate the binding of various molecules or cells [32]. In view of this hydrophobins could find use in anti-fouling applications, increasing the hydrophobicity of surfaces, or immobilizing growth-inhibiting compound. The antifouling effect can be exploited in the field of biomaterials, where hydrophobin coating can be used to reduce the non-specific binding of proteins (figure 7 a) and bacterial adhesion on surgical instrument and medical implants. On the other hand it could increase the attachment of cells and be useful in tissue engineering. For instance, it has been demonstrated that hydrophobin coating can improve the growth and morphology of fibroblast on Teflon surface (figure 7 b) [33].

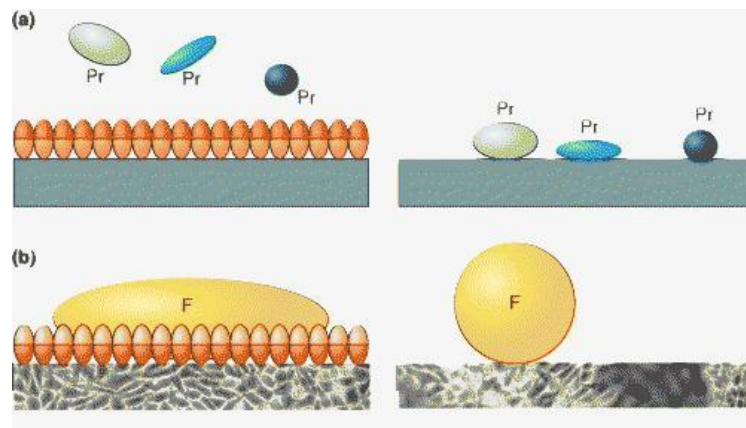


Figure 7: **Schematic representation of some hydrophobin applications.** The figure shows a bare surface on the right, and a surface coated with hydrophobins (orange) on the left. **(a)** Increasing the surface hydrophobicity, aspecific binding of proteins (Pr) is prevented. **(b)** By decreasing the hydrophobicity, growth of human fibroblast (F, in yellow) is promoted.

### Nano-biotechnological applications

Devices such as biosensors or DNA/proteins microarrays are widely used in several fields of research, diagnostic or environmental monitoring. The fabrication of a new generation of hybrid devices, where a biological component is integrated with a micro- or nano-electronic platform, depends on the bio-compatibility of the surfaces and it is necessary in order to immobilize active biological molecules [34]

For this purpose, hydrophobin biofilms can be used to adsorb proteins (i.e. enzymes) on surfaces without losing activity (figure 8).

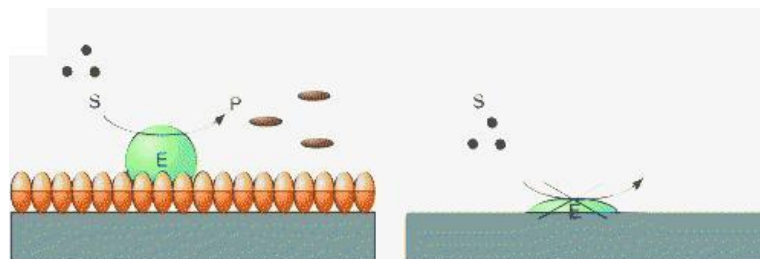


Figure 8. **Schematic immobilization of enzymes on hydrophobins coating.** The presence of hydrophobins (orange) allows immobilization of active enzymes (E, green). S and P are substrates and products, respectively.

It was shown that several types of proteins (glucose oxidase from *A. niger*; bovine serum albumin; chicken egg avidin and monoclonal IgG1) adsorb onto a hydrophobic

solid that was coated with the class I hydrophobin HGFI or the class II hydrophobin HFBI [35; 36]. Thus, hydrophobins can functionalize a solid support, transforming an inert surface into a surface able to retain proteins by charge interactions [36.]. This principle has been used to immobilize enzymes in the development of biosensors [37; 38; 39; 40; 41]. The class I hydrophobin SC3 was used successfully in immobilization of glucose oxidase (GOx) and horseradish peroxidase (HRP) on glassy carbon electrodes. The affinity of these enzymes for their substrate was similar when immobilized and dissolved enzymes were compared. Moreover, GOx was shown to maintain its activity for at least 90 days, even when the biosensor was used repeatedly. Similarly, HRP was still active on the 36th day after immobilization [37]. In principle, both class I and class II hydrophobins can be used to immobilize proteins, acting as biocompatible interface.

## 1.5 Production of hydrophobins

Hydrophobins are available from natural resources (fungi) in milligram amounts [16, 20]. The increasing demand for hydrophobins, in a wide range of applications, leads to a challenge in terms of production and purification of these proteins. The recombinant expression represents a good method for proteins overproduction, besides to be a powerful tool to obtain engineered proteins.

During the last years some examples of recombinant hydrophobins have been described. A production level of 0.6 grams per liter was obtained for a class II hydrophobin from *Trichoderma reesei*, by constructing a *T. reesei* HFBI-overproducing strain containing three copies of the *hfb1* gene [42]. Recently, the class I hydrophobin DewA from *Aspergillus nidulans* was fused to a truncated form of *yaaD* of *Bacillus subtilis* and produced in *Escherichia coli*. Using a pilot plant, this resulted in kilogram scale purified hydrophobin [16].

HGFI from *Grifola frondosa* was expressed in *Pichia pastoris*. The highest secretion level of recombinant protein was approximately 120 mg/L, about 50 times higher than the extractive one [43].

## 1.6 *Pleurotus ostreatus* hydrophobins

The basidiomycetes *Pleurotus ostreatus* is a commercially important edible mushroom, used for the bioconversion of agricultural, industrial, and lignocellulose wastes [44; 45] as a source of enzymes and other chemicals for industrial applications [46; 47], and as an agent for bioremediation [48]. The family of genes coding for *P. ostreatus* hydrophobins is large and complex, and the function of the encoded proteins is regulated by time or developmental stage [49]. Different hydrophobin genes have been isolated from *P. ostreatus*: *vmh1*, *vmh2*, *vmh3*, *Fbh1* [49; 50], *POH2*, *POH3* [51] and *Po.hyd* [52]. The genes coding for vegetative mycelium hydrophobins in *P. ostreatus* are in single copy and encode three different hydrophobins Vmh1, Vmh2 and Vmh3. Vmh1 and Vmh2 are specific of vegetative mycelium, whereas Vmh3 expression also occurs in fruit bodies. The fruit body-specific hydrophobin Fbh1 (or POH1, product of allele of the same gene) and *Po.hyd* [52]. are not expressed during vegetative growth and their expression is spatially regulated in the fruit body. The expression of different hydrophobin genes is under control of different regulatory elements and the proteins have different roles in the fungal development, in order to fulfil its life cycle.

A hydrophobin produced and secreted by *P. ostreatus* mycelia has been identified as Vmh2. The ability of Vmh2 to form stable biofilm on hydrophobic silicon was also verified, suggesting the possibility to use it as mask in micromachining processes for the realization of microsystems [53]. Vmh2 has been also used for the biological passivation of porous silicon, a nanostructured material usable in development of some devices [54].

## 1.7 Outline of the thesis

A deeper knowledge of the properties and behaviours of hydrophobins, both in solution or assembled, is needed to use them for biotechnological applications. For this reason, aims of the present project are:

- Extraction of hydrophobins Vmh2 from *P. ostreatus* cultural broth and mycelia;
- Recombinant production of Vmh2 in *E.coli* and *P. pastoris*;
- Characterization of Vmh2 behaviour in solution;
- Characterization of the Vmh2 biofilm;
- Evaluation of Vmh2 potential applications:
  - Immobilization of biological macromolecules (i.e. proteins, peptides or antibody) on Vmh2 biofilm;
  - Coating of Vmh2 on textile materials,
  - Evaluation of emulsifying capability of Vmh2.

## **2. Materials and Methods**

## 2.1 Production of the hydrophobin Vmh2

The white-rot fungus, *P. ostreatus* (Jacq.:Fr.) Kummer (type: Florida) (ATCC no. MYA-2306) was maintained through periodic transfer at 4°C on potato dextrose agar (Difco) plates in the presence of 0.5% yeast extract. Mycelia were inoculated in 2 l flasks containing 500 ml of potato-dextrose broth (24 g/l) supplemented with 0.5% yeast extract (PDY broth) grown at 28 °C in static or in shaken (150 rpm) mode. After 10 days of fungal growth, mycelia were separated by filtration through gauze.

**Extraction from *P. ostreatus* culture broth-** Hydrophobins were aggregated by air bubbling using a Waring blender. Foam was then collected by centrifugation at 4,000 x g. The precipitate was freeze-dried, treated with 100% trifluoroacetic acid (TFA) for 2hr and sonicated for 30 min. After centrifugation at 3200 x g for 20 min, the supernatant was dried again in a stream of air, and then dissolved in the opportune solvents.

**Extraction from *P. ostreatus* mycelium-** Mycelia were treated twice with 2% SDS in a boiling water bath for 10 min, washed several times with water and once with 60% ethanol to completely remove the detergent. The residue was freeze-dried and treated with TFA in a water bath sonicator (Bandelin Sonorex Digitec) for 10 minutes. The supernatant was dried in a stream of air, dissolved in 60% ethanol and centrifuged (10 min at 3200 x g). The new supernatant was lyophilized and extracted three times with chloroform-methanol 2:1 v/v (10 min in bath sonicator and 10 min incubation at 65°C). The precipitate was again freeze-dried, treated with TFA for 30 min in bath sonicator, dried in a stream of air and dissolved in 60% ethanol. The sample was diluted ten times in water, the pH adjusted at 7 by addition of NH<sub>3</sub>, incubated at 80°C for 10 minutes and vortexed to induce hydrophobin aggregation. The precipitate obtained after centrifugation (10 min at 3200 xg), was treated with TFA as above described and re-dissolved in the appropriate solvents for further analyses.

**Production and purification of the recombinant hydrophobin in *E. coli*-** RNA was extracted from shaken cultures of *P. ostreatus*, using a RNAeasy kit as described by the manufacturer (Qiagen). DNase I treated total RNA was used as a template for RT-PCR using Superscript II (Invitrogen). cDNA was synthesized and amplified with this template using primers corresponding to the N-terminal and C-terminal ends of mature Vmh2 (from D26 to L111 of the sequence whose TrEMBL accession number is Q8WZ12). The vmh2 cDNA was cloned in a pET-derived plasmid vector as a fusion with a 6His-glutathione S-transferase (GST) tag with a TEV (tobacco etch virus) protease cleavage site, thus generating a fusion protein His tag-GST-Vmh2. The resulting vector was transformed into the *E. coli* BL21 DE3 (Novagen). Expression of the fusion protein was induced by adding isopropyl-b-D-thiogalactopyranoside (IPTG, Sigma) at an early exponential-phase culture. After expression induction, the bacteria were harvested by centrifugation, resuspended in a buffer, and disrupted by sonication. The insoluble pellet with the inclusion bodies was dissolved in buffer containing 8 M urea. To reduce urea concentration the sample was slowly diluted drop by drop up to 0.4 M urea. After TEV addition a precipitate was formed. This precipitate was separated by centrifugation, washed several times in water, lyophilized, treated with TFA as above described and dissolved in 60% ethanol. The sample was diluted ten times in water, the pH adjusted at 7 by addition of NH<sub>3</sub>, incubated at 80°C for 10 minutes and vortexed to

induce hydrophobin aggregation. The precipitate obtained after centrifugation was again treated with TFA and re-dissolved in 60% ethanol.

**Production and purification of the recombinant hydrophobin in *Pichia pastoris***- More details are reported on the recombinant expression of Vmh2 in *P. pastoris*, since these data have not been published yet.

The *Pichia pastoris* commercial strain X-33 by Invitrogen was used. This strain was grown in YPDS medium (10 g l<sup>-1</sup> yeast extract; 20 g l<sup>-1</sup> bacto tryptone; 20 g l<sup>-1</sup> glucose; 182.2 g l<sup>-1</sup> sorbitol). Recombinant protein production required the use of BMGY and BMMY mediums (13 g l<sup>-1</sup> yeast nitrogen base with ammonium sulfate without aminoacids; 10 g l<sup>-1</sup> yeast extract; 20 g l<sup>-1</sup> peptone; 100 mM potassium phosphate, pH 6.0; 4x10<sup>-4</sup> g l<sup>-1</sup> biotin; 1% glycerol, for BMGY or 0.5% methanol for BMMY). The commercial plasmids pPICZB and pPICZ $\alpha$ C by Invitrogen, were used for protein expression. Both plasmids contain methanol-inducible AOX1 TT promoter and Zeocin resistance gene. pPICZ $\alpha$ C contains  $\alpha$ -factor gene sequence to address protein secretion in the extracellular medium.

The nucleotide sequence of cDNA encoding for Vmh2 hydrophobin was optimized according to yeast codon usage and a region encoding for the *P. ostreatus* Vmh2 signal peptide was included. In addition, specific restriction sites have been included at both ends of the DNA sequence. The final structure of the insert is: HindIII | EcoRI | N-term – signal peptide | Vmh2 gene – C-term | HindIII | XbaI. Such designed DNA molecule has been obtained as a synthetic gene (MrGene) cloned into a pANY vector.

The vector pPICZB and Vmh2 coding cDNA were subjected to hydrolysis *EcoRI/XbaI*. Then the *EcoRI/XbaI* hydrolyzed Vmh2, including the signal peptide, has been ligated into the *EcoRI/XbaI* digested pPICZB under the control of the AOX1 promoter region.

In order to test a *P. pastoris* signal peptide, pPICZ $\alpha$ C plasmid containing *P. pastoris*  $\alpha$ -factor encoding sequence, was also used.

By PCR experiments sequences corresponding to *XhoI* restriction site and to Kex2 hydrolysis region were added at 5' end of forward primer, whilst *XbaI* restriction site was added to 3' of reverse primer.

(Fw:TTTCTCGAGAAAAGAGACACTCCTTCATGTTCC;

Rev:GATCTAGATTACAAGGAGATGTTGATTGGGGAG).The obtained fragment (*XhoI* | N-term – Vmh2 gene – C-term | *XbaI*) was subjected to a *XhoI/XbaI* digestion and then ligated into the *XhoI/XbaI* digested pPICZ $\alpha$ C plasmid. Vmh2 gene is thus located downstream and in frame to the  $\alpha$ -factor signal peptide encoding sequence.

*P.pastoris* transformation with the linearized DNA fragments (up to 10  $\mu$ g) was performed by electroporation with a Bio-Rad Micro-Pulser apparatus, as specified by the manufacturer. Immediately after, 1 ml of 1M sorbitol was added to the electroporation cuvette and the whole content was transferred to a sterile 15 ml tube. The tube was then incubated at 28°C for 2 hours. 100  $\mu$ l of the cell suspension were spread on YPDS plates containing 100  $\mu$ g ml<sup>-1</sup> of zeocin and incubated from 3-10 days at 28°C until colonies formation. Recombinant cells from solid culture were inoculated in 5 ml BMGY medium in a 50 ml flask. This preculture was grown for one days at 28° C on a rotary shaker (150 rpm), then a volume of suspension sufficient to reach a final OD<sub>600</sub> value of 1.0 was used to inoculate Erlenmeyer baffled flasks containing 1:5 v/v of BMMY medium. Cells were grown on a rotary shaker (150 rpm)

at 28°C and 0.5% of methanol were added to the culture each day of growth to induce protein expression. After 72 hours cultural broth was separated from cells by centrifugation at 3200 xg. Hydrophobin was extracted from broth using the same procedure described for *P. ostreatus*.

## 2.2 Characterization of the hydrophobin Vmh2

**SDS-PAGE-** SDS-polyacrylamide gel electrophoresis (SDS-PAGE) was performed using the Laemmli method (104) with the Bio-Rad Mini Protean III apparatus, using 15% polyacrilamide concentration. The standard used was the Prestained Protein Molecular Weight Marker SM0441 (Fermentas Inc., Glen Burnie, MD, USA). The gels were stained by silver staining.

**Protein concentration determination-** Protein concentrations were evaluated using the PIERCE 660 nm Protein Assay kit. Bovine serum albumin was used as standard.

**Mass spectrometry -** MALDI mass spectra were recorded on a Voyager DE Pro MALDI-TOF mass spectrometer (Applied Biosystems, Foster City, CA). The analyte solutions were mixed with sinapinic acid (20 mg/ml in 70% acetonitrile, TFA 0.1% v/v), or 2,5-Dihydroxybenzoic acid (DHB) (25 mg/ml in 70% acetonitrile) or  $\alpha$ -cyano-4-hydroxycinnamic acid (10 mg/ml in 70% acetonitrile, TFA 0.1% (v/v) as matrixes, applied to the sample plate and air-dried. The spectrometer was used in the linear or reflectron mode. Spectra were calibrated externally.

**Circular dichroism -** Far-UV CD spectra were recorded on a Jasco J715 spectropolarimeter equipped with a Peltier thermostatic cell holder (Jasco model PTC-348), in a quartz cell (0.1-cm light path) from 190 to 250 nm. The temperature was kept at 25° C and the sample compartment was continuously flushed with nitrogen gas. The final spectra were obtained by averaging three scans, using a bandwidth of 1 nm, a step width of 0.5 nm, and a 4 sec averaging per point. The spectra were then corrected for the background signal using a reference solution without the protein. The content of the secondary structure was calculated using the CONTIN method and the reference set 4 [55] available on the Dichroweb server [56].

**Fluorescence analyses-** Fluorescence spectra were recorded at 25°C with a Perkin-Elmer LS50B fluorescence spectrometer. Slit widths were set at 10 nm in both the excitation and emission monochromators. ThT (Sigma- Aldrich, St. Louis, MO, 100 $\mu$ M final concentration) was added to samples. They were excited at 435 nm and emission was monitored from 460 to 600 nm. The spectra were then corrected by subtracting the ThT spectrum.

## 2.3 Characterization of the hydrophobin Vmh2 biofilm

**Immobilization of Vmh2-** Vmh2 solutions at 0.1 mg/ml were spotted on the surfaces. After 1 h, samples were dried for 10 min at 80°C, and then by 2% SDS at 100 °C for 10 minutes. Ellipsometric characterization of the Vmh2 biofilm was performed by a variable-angle spectroscopic ellipsometry model (UVISEL, Horiba-Jobin-Yvon) and by Water Contact Angle (WCA). This procedure was used for the depositions on silicon (single side polished, <100> oriented washed in hydrofluoric acid solution), on MALDI slide and on textile materials.

**Immobilization of laccase-** A drop of the laccase solution has been deposited on Vmh2 modified silicon surface, kept at 4 °C for 1 hour, and then rinsed over night in 50mM phosphate buffer, pH 7. After 16 hours, the silicon biochip has been washed in the same buffer at 25 °C till complete loss of laccase activity in the washing buffer.



Then each chip has been dust-protected and kept at constant humidity conditions when not in use.

**Immobilization of BSA-** Bovine serum albumin (BSA) labelled by rhodamine, was solubilised in water at three different concentration (3, 6, 12  $\mu\text{M}$ ). To assess the protein binding on the chip surface, we have spotted 50  $\mu\text{l}$  of water solution containing the labeled protein on the chips covered by the Vmh2 biofilm. The immobilization has been carried at 4  $^{\circ}\text{C}$  overnight. After incubation, the samples have been rinsed three times in deionized water at room temperature.

**Enzyme assay-**Laccase activity has been assayed at 25 $^{\circ}\text{C}$  using 2,6-dimethoxyphenol (DMP) 10mM in McIlvaine citrate-phosphate buffer, pH 5. Oxidation of DMP has been followed by the absorption increment at 477nm ( $\epsilon_{477} = 14.8 \times 10^3 \text{M}^{-1} \text{cm}^{-1}$ ) using Beckman DU 7500 spectrophotometer (Beckman Instruments). Enzyme activity has been expressed in International Units (IU). Immobilized enzyme has been assayed by silicon dip in 10 ml of McIlvaine citrate-phosphate buffer, pH 5. The absorption increment at 477nm has been followed withdrawing 200  $\mu\text{l}$  of reaction mixture each 30 s for 10 min. The total immobilised activity per unit of silicon (chip) has been calculated as  $\text{U/chip} = \Delta A_{\text{min}}^{-1} / \epsilon \times 10^4$ .

**Immobilization of peptides** - 1  $\mu\text{l}$  of POXC tryptic solution was spotted and dried on MALDI slide wells coated with Vmh2 biofilm. The spots were washed with water, 25% and 50 % acetonitrile (ACN). For the detection of peptides a Voyager DE Pro MALDI-TOF mass spectrometer (Applied Biosystems, Foster City, CA) was used in the reflection mode using  $\alpha$ -cyano-4 hydroxycinnamic acid (10 mg/ml in 70% acetonitrile, TFA 0.1% (v/v) as matrix.

**Immobilization of antibodies** - 1  $\mu\text{l}$  of antibody solutions (fluorescein-anti-rabbit, anti-laccases and anti-GST) was spotted on MALDI slide wells coated with Vmh2 biofilm. After five minutes the drops were removed and the wells were washed three times with water. The protein solutions of laccases and GST-monellin were incubated on antibodies immobilized for five minutes and then all the samples were washed three times with water. For the detection of proteins a Voyager DE Pro MALDI-TOF mass spectrometer (Applied Biosystems, Foster City, CA) was used in the linear mode using sinapinic acid (20 mg/ml in 70% acetonitrile, TFA 0.1% v/v) as matrix.

**Evaluation of emulsifying properties** - Vmh2 was suspended in 20% ethanol at 0,1 mg/ml. The pH of these solutions were adjusted: to pH 2 with addition of TFA 1%, to pH 8 and 10 with addition of  $\text{NH}_3$ . Vmh2 solutions were mixed by vortexing for 20 minutes with three different oils (olive, peanut and almond oil) with a volumetric ratio of 3:1. To evaluate emulsifying capability of Vmh2, several checks were performed at different time points (1h, 2h, 12h, 24h, 48h, 72h) monitoring stability and height of the emulsion phase.



### **3. Results and discussions**

## Section I

### 3.1 Production of the hydrophobin Vmh2

Hydrophobins were purified from *Pleurotus ostreatus* cultural broth and mycelia, using different growth conditions. The recombinant expression of hydrophobin in *Escherichia coli* and *Pichia pastoris* was also performed. Then the protein was characterized.

#### 3.1.1 Extraction from *P. ostreatus* cultural medium

Hydrophobin, identified in a previous study as Vmh2-1, was purified from cultural medium of *P. ostreatus* grown in static cultures. Sequence analysis (hydropathy pattern and spacing between the cysteine residues) and robustness of the aggregates (dissolvable in 100% TFA) demonstrated that it belongs to Class I hydrophobins. The amount of Vmh2 recovered from the cultural broth was between 5 and 10 mg L<sup>-1</sup>. Analyses of protein samples purified from culture medium containing amylose showed the presence of glycans in the hydrophobin aggregates. If the protein was dissolved in 60% ethanol, the glycan fraction precipitated, leaving the protein free in this solution. The free protein was not soluble in water, hence the interaction with glycans enables the protein to be water soluble.

The structure of these glycans matched to  $\alpha$ -(1-4) linked glucose lacking of reducing ends, indicating a cyclic structure (cyclodextrins), and a variable number of monomers, from six to sixteen. The obtained results suggested that the cyclic glucans were produced by the fungus grown in the presence of amylose. In order to analyse hydrophobin/glucans interaction some commercial molecules were tested for their ability of restoring the hydrophobin water solubility. It was demonstrated that pure  $\alpha$ ,  $\beta$  and  $\gamma$  cyclodextrins, the linear molecule maltohexaose and even the simple D-glucose monomer are able to solubilise the hydrophobin Vmh2 in water (see **P3** in Appendix I).

Moreover the ability of other hexoses (i.e. mannose or galactose) to solubilise Vmh2 was also demonstrated, whereas pentoses (i.e. xylose) or polyols (i.e. sorbitol or glycerol) have not the same effect. Therefore, a hexose molecule seems to have the structural requisite to solubilise Vmh2 in water (see **P6** in Appendix I).

#### 3.1.2 Extraction from *P. ostreatus* mycelia

Hydrophobins were also extracted from *P. ostreatus* mycelia, grown in static or shaken cultures. An extraction and purification protocol was set up modifying that one described by Yu *et al* [24], obtaining about 20 milligrams from 1 gr of solid mycelium (corresponding to about 100 mg per litre of culture broth). In the case of shaken cultures, the presence of only one protein was observed and attributed to the same Vmh2 purified from the cultural broth. On the other hand, in static growth conditions another type of hydrophobin, not identified, was also produced. No further investigation has been performed on these samples, whereas Vmh2 extracted from mycelia grown in shaken cultures was characterized. (see **P5** in Appendix I).

### 3.1.3 Production of the recombinant Vmh2 in *E. coli*

Recombinant expression of *vmh2* cDNA was performed in *E. coli* using a construct designed to increase protein solubility. Vmh2 N-terminus was fused to glutathione S-transferase (GST) and to His-6 tag, linked through a sequence coding for a specific protease (TEV protease) site. Despite that, the recombinant protein (rVmh2) was found in inclusion bodies. Hence it was dissolved in urea and then slowly diluted. However, when rVmh2 was freed from the GST tag (after incubation with the TEV protease), spontaneously precipitated in the buffer. The solubilization of these aggregates led to obtain the pure folded protein. The typical yield of rVmh2 was about 50 mg L<sup>-1</sup> of culture. (see **P5** in Appendix I)

### 3.1.4 Production of the recombinant Vmh2 in *P. pastoris*

The recombinant expression of Vmh2 in *P. pastoris* is reported with more details, since these data have not been published yet.

The recombinant expression of Vmh2 in *P. pastoris* was performed using two different vectors: pPICZB in which a fragment containing *P. ostreatus* Vmh2 cDNA and its signal peptide was inserted, and pPICZ $\alpha$ C in which Vmh2 cDNA was located downstream and in frame to the  $\alpha$ -factor signal peptide encoding sequence.

In the first case over 20 recombinant colonies of *P. pastoris* were spread on two solid minimal mediums, in the presence of methanol or dextrose. The colonies growing at the same rate on both medium were selected and spread on solid medium supplemented with *Zeocin* in order to identify colonies containing multiple copies of foreign DNA. Two distinct *P. pastoris* recombinant colonies were selected and grown as described in *Materials and Method* to analyze their protein production. On the third day of growth, the total culture broth (25 ml), was subjected to the standard purification procedure (see *Materials and Method*). The dried supernatant was resuspended in 60% ethanol and analysed by SDS-PAGE. As shown in figure 1 only one of the two colonies (lane 4) produced an amount of protein sufficient to be visualized on SDS-PAGE in these conditions. In any case the protein amount was very low.

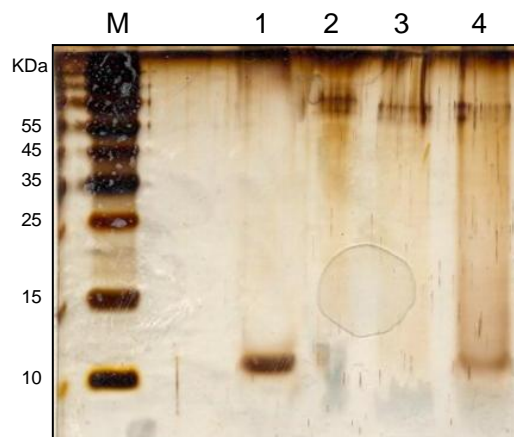


Figure 1: **Silver stained SDS-PAGE.** M: marker; lane 1: Vmh2 from *P. ostreatus*; lane 2: negative control; lane 3: sample extracted from colony 1 of *P.pastoris*; lane 4: sample extracted from colony 2 of *P.pastoris*.

The *P. ostreatus* Vmh2 signal peptide was replaced with the *P. pastoris*  $\alpha$ -factor signal peptide (see *Materials and Method*) to verify if this system led to improve the expression conditions. The same procedure of protein extraction was repeated. The obtained sample was analyzed by SDS-PAGE. As shown in figure 2 a clear and intense band at 10 kDa was detected. It is worth to underline that the protein revealed in this case was extracted from 1 ml of cultural broth.

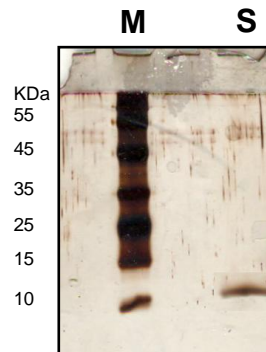


Figure 2. **Silver stained SDS-PAGE.** M: marker; S: Sample extracted from *P.pastoris*.

Results indicated that the use of *P. pastoris*  $\alpha$ -factor signal peptide led to obtain a higher amount of the secreted protein with respect to that of vmh2 native signal peptide. The amount of Vmh2 recovered was evaluated calculating the protein concentrations (see *Materials and method*) of samples derived from three different cultures. The typical yield obtained was about 30 mg L<sup>-1</sup>.

### Evaluation of the production levels

In table 1 the yields obtained from all production systems used are summarized.

	Vmh2 from <i>P.ostreatus</i> broth	Vmh2 from <i>P.ostreatus</i> mycelia	Vmh2 from <i>E.coli</i>	Vmh2 from <i>P. pastoris</i>
Yield (mg L <sup>-1</sup> )	5-10	90-100	40-50	25-30

Table 1: The yields of the four production systems are reported in mg L<sup>-1</sup>

Literature data report that extractive hydrophobins from fungi are available only in milligram amounts. For instance class I hydrophobin ABH3 from *Agaricus bisporus* is extracted from cultural medium with a yield of about 2 mg L<sup>-1</sup>[20], the same order of magnitude obtained for Vmh2 recovered from *P. ostreatus* cultural broth. On the other hand, the extraction from *P. ostreatus* mycelia allowed us to obtain an amount of protein 10 times higher than another cell wall bound class I hydrophobin, HGFI from *G. frondosa* [43].

Moreover the yields of the recombinant Vmh2 from both recombinant expression systems are comparable to those reported in literature for other hydrophobins [57, 43]

A choice between recombinant and extractive proteins could be made, according to specific applications, being both proteins available in adequate amounts. For example, use of extractive protein in the food industry is surely more acceptable with respect to the recombinant one, since it is produced by an edible fungus. On the other hand, the faster production and the possibility to manipulate the protein sequence make the recombinant protein more suitable in other applications (i.e as anti-fouling agent).

## Section II

### 3.2 Characterization of Vmh2

#### 3.2.1 Characterization in solution

The protein behavior in different conditions, as solvents, pH, temperature, presence of salts or glucans was evaluated.

Vmh2 conformation in 60% ethanol showed a significant contribution of  $\alpha$ -helix (figure 3) to the secondary structure (30% of  $\alpha$ -helix respect to 20% of  $\beta$ -sheet). Moreover in this conditions the protein was stable in solution at least for one month, even after vortexing.

Increase of the pH ( $\text{pH} \geq 6$ ) led to a shift towards a Vmh2 structure with a higher  $\beta$  sheet content (figure 3), associated to the formation of an amyloid like,  $\beta$ -sheet rich, assembled state. This state was characterized by ThioflavinT (ThT) fluorescence intensity increase and turbidimetry increase. Analogous behavior was observed in the presence of  $\text{Ca}^{2+}$ , while a monovalent cation, as  $\text{Na}^+$ , had a quite opposite effect, inhibiting the conformational change and self-assembly at pH 6. It has been reported that the recombinant class I hydrophobin H\*protein A, shows propensity to self-assembly in the same conditions [16]. However it is worth noting that Vmh2 self-assembling in these conditions occurs without agitation of the protein solution, differently from other hydrophobins which aggregate after continuous introduction of new hydrophobic:hydrophilic interface.

An increased contribution of random conformation to the Vmh2 structure at high temperature ( $>80^\circ\text{C}$ ) was observed (figure 3). Nevertheless the  $\alpha$ -helix structure can be recovered coming back to room temperature, indicating that this change is reversible.

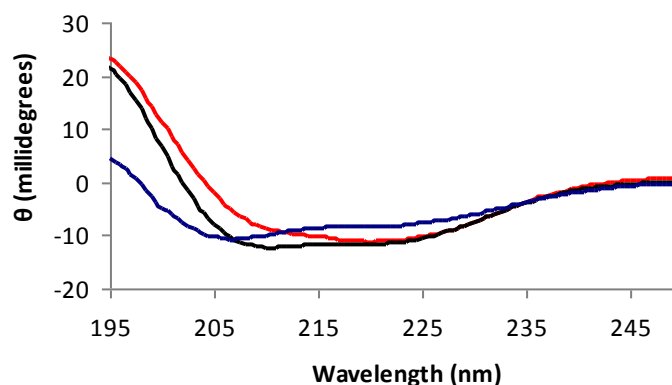


Figure 3: **Typical CD spectra of Vmh2 in 60% ethanol.** The black line represents the protein at  $\text{pH} < 6$ ; the red line represents the protein at  $\text{pH} \geq 6$  or in presence of  $\text{Ca}^{2+}$ ; the blue line represents the protein at  $80^\circ\text{C}$ .

The effect of solvents at different percentage on the Vmh2 behavior was investigated: ethanol, isopropanol, trifluoroethanol (TFE) or acetonitrile (from 60 to 20%) were used. Results showed that the Vmh2 conformation was the same in all cases, but when the solvent percentage decreased the protein amount recovered in solution was reduced.



In order to investigate on the specific parameter affecting the Vmh2 solubility, the surface tension and the dielectric constants (polarity) values of the solvents used were considered. Results showed that the main characteristic affecting Vmh2 behavior is the polarity of the solution rather than its surface tension. Analyses performed in these conditions suggest that in this case loss of soluble protein has to be ascribed to an increase tendency of Vmh2 to reach hydrophilic/hydrophobic interfaces (see **P5** in Appendix I).

Analyses were also performed on the protein dissolved in aqueous solution in the presence of glucose (Vmh2-G). Vmh2-G showed a stable conformation in water with a higher contribution of  $\beta$ -sheet structure (34%) with respect to the  $\alpha$ -helix (10%) even before vortexing (figure 4).

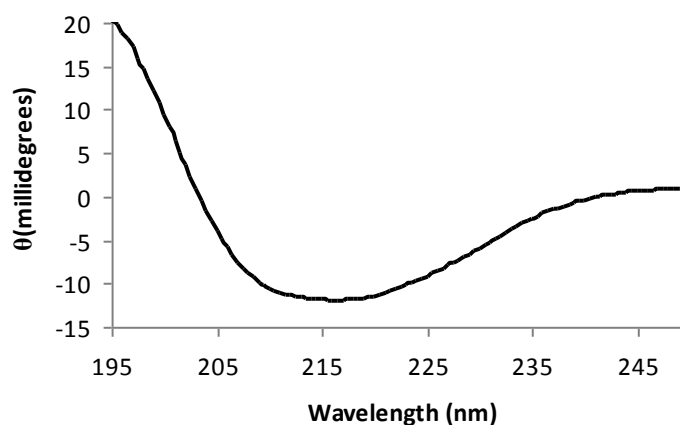


Figure 4: **Typical CD spectra of Vmh2 in water in presence of glucose.**

Moreover Vmh2-G adopted in solution a structure able to bind ThT. This structure could be constituted by small oligomers or even monomers of hydrophobin, because the minimal ThT binding site can be just formed by four consecutive  $\beta$ -strands organized in an aromatic-hydrophobic groove [58] (see **P6** in Appendix I). After vortexing, a slight increase of the fluorescence intensity was observed, and precipitation occurred after centrifugation.

Overall these data suggest that distinct phenomena can occur and are modulated by environmental conditions (figure 5). The protein conformation in 60% ethanol is mainly  $\alpha$ -helix. Starting from the latter condition:

- 1- A conformational change associated with the formation of amyloid like,  $\beta$ -sheet rich, assembled state occurs when the pH increases or in the presence of  $\text{Ca}^{2+}$  ions, without agitation of the protein solution .
- 2- The tendency to reach hydrophobic/hydrophilic interfaces enhances when the solvent polarity increases, with no detectable conformational change.
- 3- A reversible conformational change and reversible aggregation occurs at high temperature.

On the other hand the protein is soluble in water in the presence of glucose, adopting a  $\beta$ -structure. The formation of the self-assembled state occurs after agitation by vortexing.

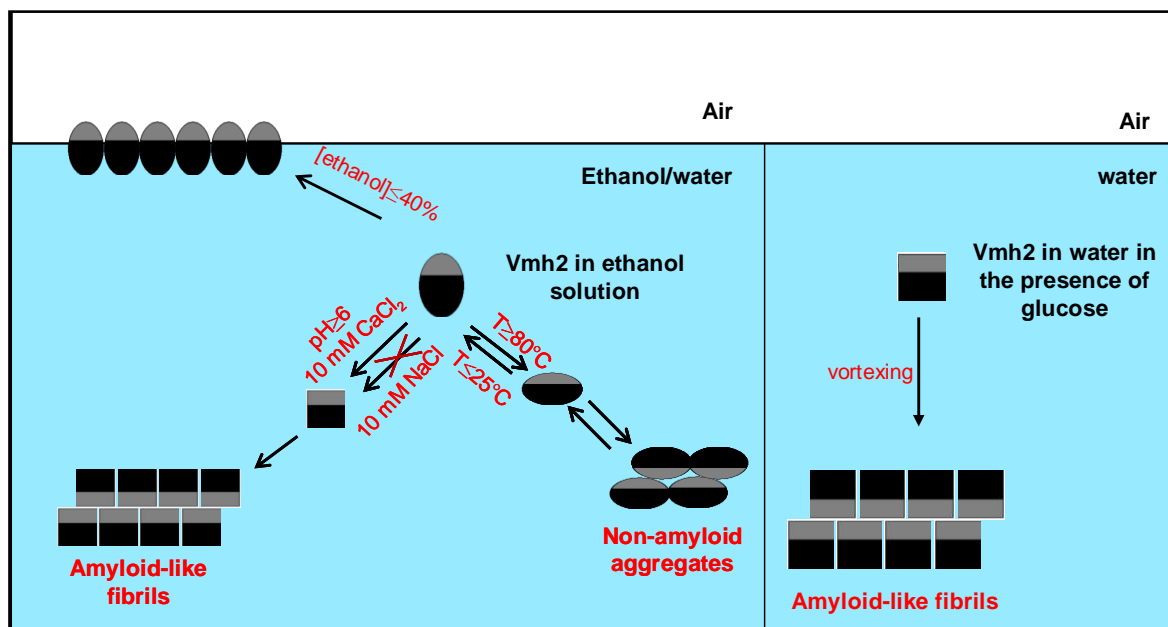


Figure 5: Schematic representation of the Vmh2 self-assembling mechanisms

### 3.2.2 Biofilm characterization

In the previous studies the conditions of Vmh2 deposition on silicon surfaces have been set up as function of, time and temperature of deposition. Silicon is one of the most used materials in the microelectronic industry (i.e. in the integrated circuits in computers or in any electronic instrument) [59]. Nanodevices based on silicon can be used for the development of integrated system as biosensors [60]. The Vmh2 biofilm formed on silicon has been characterized by variable angle spectroscopic ellipsometry (VASE) and an optical model for experimental data fitting has been developed [53,54].

Starting from these preliminary data, Vmh2 dissolved in 60% ethanol (Vmh2-et) was deposited on silicon hydrophobic surfaces and biofilms were formed. Vmh2-et forms monolayer (with a thickness of  $3.1 \pm 0.7$  nm) or multilayer, depending on deposition and washing conditions. The Vmh2-et nanometric monolayer was very stable from the chemical point of view, since it was still present after strong washing in NaOH or SDS at 100°C (see **P1** in Appendix I).

Moreover biofilms of Vmh2 in the presence of glucose (Vmh2-G) were formed, in order to better understand the influence of sugars on the protein self-assembly. A chemically stable, nanometric biofilm was produced by Vmh2-G deposition. The Vmh2-G biofilm can be considered as a mixture of two constituents, glucose and the pure protein. The composite Vmh2-G film self-assembled on silicon was analyzed in comparison to the pure Vmh2-et film.

The optical method used indicated a glucose content of 24% in the composite biofilm, showing a layer thickness of 1.5 nm, smaller than the thickness of the pure hydrophobin self-assembled on silicon (about 3 nm). Then the calculate value of the relative surface concentration of the protein in the Vmh2-et biofilm was about twice than that calculated in the case of Vmh2-G. Even if there is not information on the molecules disposition in the Vmh2-G layer, these results suggest that in this case a large-portion of the surface is covered by the smaller glucose molecules.

Changes in surface wettability due to the presence of the biological films self-assembled on silicon was verified by means of water contact angle (WCA) measurements (Figure 6). The values of the WCA of the bare silicon surface was  $(90.0\pm 0.3)^\circ$ , so it can be defined as hydrophobic. The presence of the Vmh2-et biofilm lowered the WCA value down to  $(44\pm 1)^\circ$ . Therefore this interface is more hydrophilic due to the assembly of the protein into a film with apolar groups disposed towards the hydrophobic silicon and the polar groups on the other side. When the Vmh2-G biofilm was considered, a WCA of  $(17.5\pm 0.5)^\circ$  was measured. Then the presence of polar sugar groups in the structure of the composite biofilm further increases the wettability of the resulting surface. (see **P6** in Appendix I).

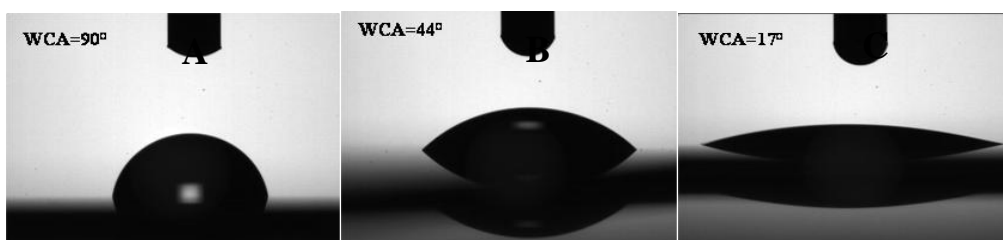


Figure 6: **WCA values.** Panel A: bare silicon; panel B: Vmh2-et biofilm; panel C: Vmh2-G biofilm

By Atomic Force Microscopy (AFM), the presence of rodlets-like structures on top of the Vmh2 biofilm can be randomly observed (figure 7).

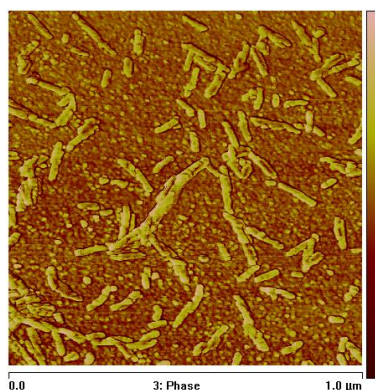


Figure 7: **AFM images of Vmh2 deposited on silicon.**

The rodlet formation at the water/air interface has been studied in more details preparing Vmh2 biofilms by Langmuir techniques. Using Langmuir trough it is possible to obtain protein monolayer both with hydrophobic side exposed to air (Langmuir-Blodgett monolayer or LB) or with hydrophilic side exposed to air (Langmuir-Schaeffer monolayer or LS). LB and LS monolayers, such as bilayer prepared by a combination of LB and LS, were investigated by AFM. Results demonstrated that Vmh2 forms homogenous films in both cases with a similar thickness of about 2.5 nm. When repeated compression-expansion cycles were performed, protein aggregates under forms of rodlets, appeared correspond to a hydrophobic bilayer. Moreover, results indicated that rodlet association proceed via conformational change which led to a more rigid structures. (see **P7** in Appendix I).

## Section III

### 3.3 Applications

#### 3.3.1 Immobilization of proteins on Vmh2 biofilm

The capability of Vmh2-et biofilm to immobilize biological macromolecules was analysed. Fluorescent Bovine Serum Albumin (BSA) and an oxidative enzyme, a fungal laccase, were used.

In the first case, solutions containing a rhodamine labelled BSA were spotted on the Vmh2 biofilm and on bare silicon samples, as a negative control. The fluorescence of silicon-Vmh2-BSA system is brighter than the negative control and is also quite homogeneous on the whole surface. The strength of the interaction between the Vmh2 and the BSA is also verified, since the fluorescent intensities after the overnight washing step do not differ.

In the second case the POXC laccase from *P. ostreatus* was deposited on Vmh2 biofilm. In order to verify the effective immobilization, an enzymatic assay was performed. Results showed that Vmh2 biofilm is able to immobilize the enzyme in the active form and that the immobilized enzyme is significantly more stable than the free form (see **P1** in Appendix I).

Since Vmh2 is able to modify also porous silicon (Psi) structures [53], the possibility to immobilize proteins on this nanostructured material was also verified. Porous silicon is produced from doped crystalline silicon by electrochemical dissolution [61]. Porous silicon can be used as smart transducer material in sensing application, and in particular in the detection of vapors, liquids and biochemical molecules [62].

Solutions containing a rhodamine labelled BSA were spotted on Psi coated with Vmh2. Fluorescence analysis were performed after washing with water showing a homogeneous fluorescence (see **P2** in Appendix I).

All these results suggest that bioactivation of surfaces by Vmh2 biofilm can be a feasible strategy for the fabrication of a new class of hybrid devices.

#### 3.3.2 Development of SELDI-TOF-like system

The development of the SELDI-TOF-like system is reported with more details, since these data have not been published yet.

Surface enhanced laser desorption ionization time-of-flight mass spectrometry (SELDI-TOF MS) is an important tool for the rapid and sensitive analysis of biomolecules. One of the key features of SELDI-TOF-MS is its ability to study complex mixtures from a variety of biological samples with minimal requirements for purification and separation of proteins prior to mass spectrometry [63].

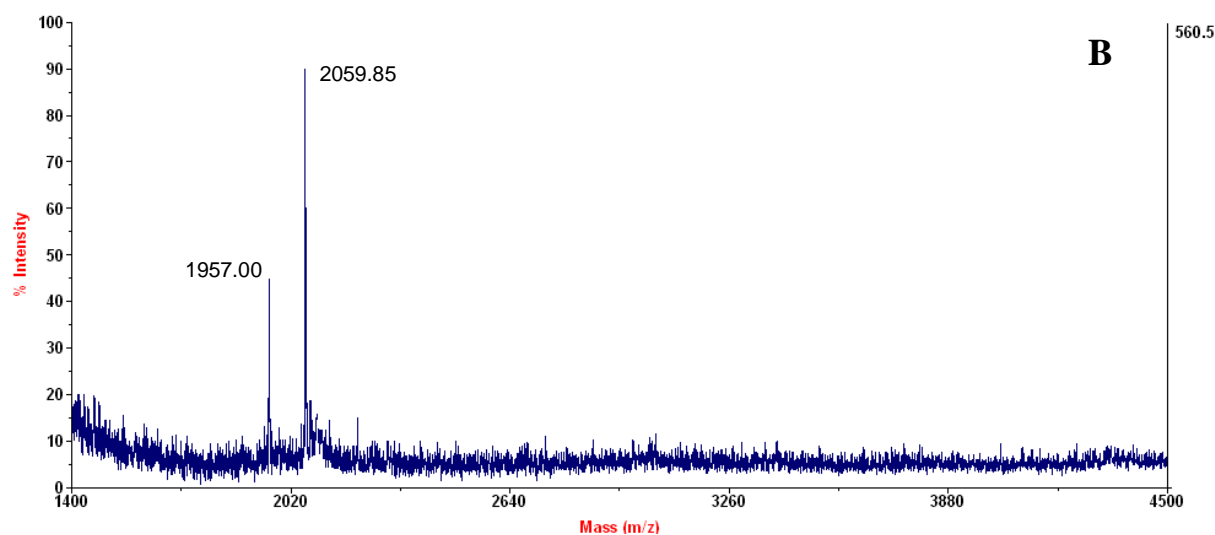
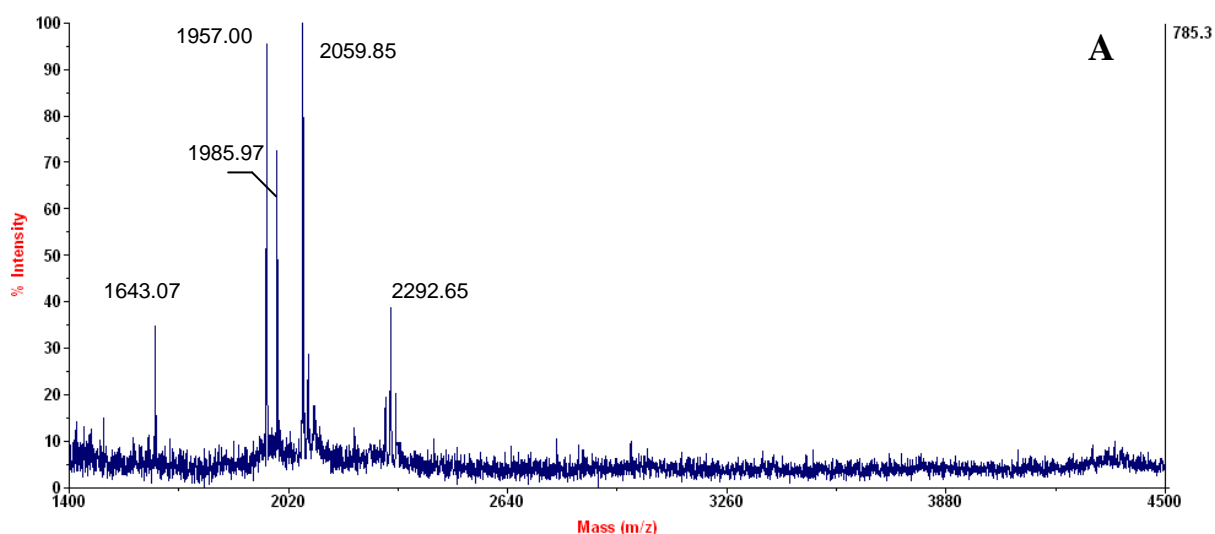
Precoated stainless steel slides are used in SELDI-TOF MS. The coating 'enhances' the surface to bind preferentially a particular class of proteins based on their physiochemical properties. Different coatings give different proteinChip array surfaces, including reverse phase, anionic exchange, cationic exchange and immobilised metal affinity surface [64].

By using different surfaces and different binding/washing conditions a detailed profile of the proteins present in the sample can be obtained. Finally, the detection of proteins is performed using laser for the ionization and a TOF as analyzer [63]. At the

commercial level, SELDI technology was introduced in 1998 by Ciphergen (Ciphergen Biosystems, Palo Alto, CA, USA). Currently, it is provided by Bio-Rad, which have realized more than 600 installations (until to 2008) [65]. This technique has been successfully applied to a number of medical and basic research problems [66; 67]. It is worth to underline that to exploit SELDI-TOF technology it is necessary to have at own disposal a specific mass spectrometry and several proteinChip slides, depending on the specific purpose. The main difficulty is the functionalization of the solid surfaces, a key step for the correct immobilization of biological macromolecules. The ability of Vmh2 biofilm to immobilize proteins was exploited in order to develop a cheap SELDI TOF-like system. A classic MALDI-TOF steel slide was coated with Vmh2 and the biofilm was used as intermediate to immobilize specific peptides and antibodies.

### Immobilization of peptides

Peptides obtained by tryptic hydrolysis of the enzyme POXC (ref) were spotted on the wells in the presence or absence (control) of the Vmh2 biofilm. Each sample was washed three times, decreasing the polarity of the solvent (H<sub>2</sub>O, 25% ACN, 50% ACN) and then the matrix was added. The mass spectra of these samples, obtained using a MALDI-TOF spectrometer, are shown in figure 8.



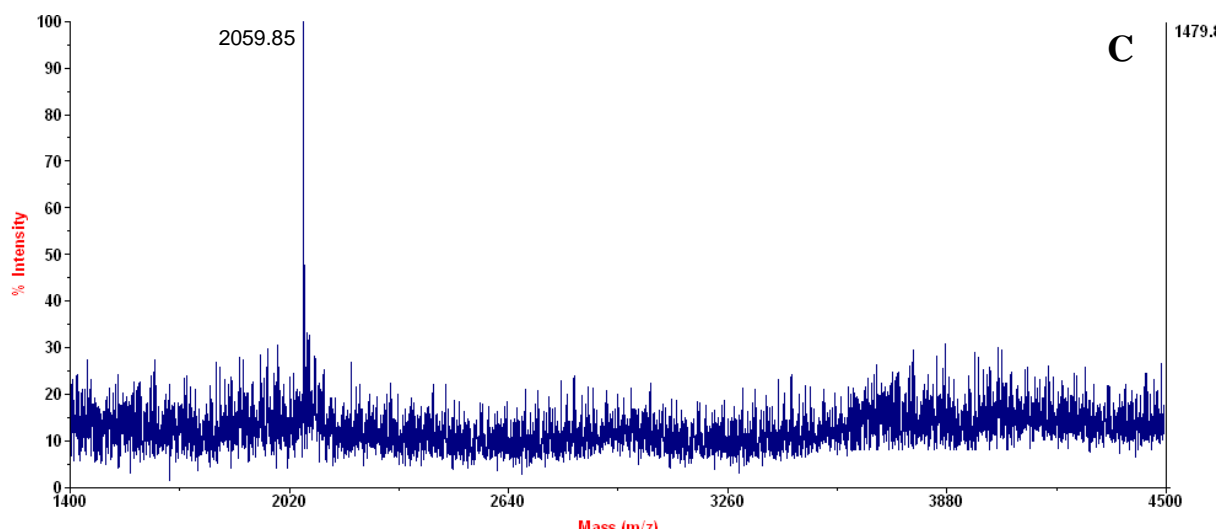


Figure 8: MALDI-MS spectra of peptides immobilized on MALDI slide with Vmh2 biofilm. Panel A: spectrum of the sample after water washing; panel B: spectrum of the sample after washing with 25% ACN; spectrum of the sample after washing with 50% ACN.

After the water washing step (figure 8 A) both samples showed a similar spectrum with five peaks, related to five triptic peptides of POXC. After the washing step with 25% ACN (figure 8 B) two peaks were detectable for the sample spotted in presence of Vmh2 biofilm, whilst no peak was observed for the control, demonstrating that in absence of Vmh2 biofilm no peptide was retained. After the third washing step with 50% ACN (figure 8 C), just one peak was detectable in this sample.

This experiment was repeated several times always obtaining the same result, therefore the method was reproducible.

Analyzing the hydrophathy pattern of the peptides, it is possible to note that the peptides washed out by ACN are the most hydrophilic ones (see table 2). This is probably due to hydrophobic interaction between peptides and Vmh2 biofilm, like in reverse-phase chromatography.

Signals m/z	Corresponding peptides	Hydrophathy pattern	After water washing	After washing in ACN 25%	After washing in ACN 50%
1643	<sup>418</sup> S-R <sup>432</sup>	-			
1957	<sup>271</sup> A-R <sup>290</sup>	++			
1985	<sup>187</sup> Y-R <sup>205</sup>	-			
2059	<sup>254</sup> Y-R <sup>270</sup>	+			
2292	<sup>1</sup> A-R <sup>22</sup>	-			

Table 2: The MALDI signals with the correspondent peptides are reported; the hydrophilic peptides are indicated with -, the hydrophobic ones with +. The blue boxes indicate the presence the peptides after washing.

### Immobilization of antibodies on Vmh2 biofilm and detection of antigens

In order to easily verify the effective immobilization of antibody on the MALDI-TOF steel slide, a fluorescence secondary antibody was used. An antibody conjugated with fluoresceine. was spotted on the wells in the presence or absence of the Vmh2 biofilm. Each sample was washed with water and the fluorescence emission was detected. A fluorescence signal was observed only for the samples spotted in the presence of Vmh2 biofilm. The same procedure was used for further experiments.

Polyclonal antibodies against laccases or BSA were tested to verify if they are able to bind antigens after immobilization. In the first case anti-laccases was immobilized on Vmh2 biofilm (see Materials and method). 1  $\mu\text{l}$  of laccases solution (1 $\mu\text{g}/\mu\text{l}$ ) was deposited on the wells in the presence or absence of the immobilized anti-laccases. A peak of about 66 kDa (figure 9) related to laccase was detected for the sample deposited on the specific antibody immobilized, whilst no signal was observed in absence of it. The same procedure was repeated using ovalbumin as control. When 1  $\mu\text{l}$  of ovalbumin solution (1 $\mu\text{g}/\mu\text{l}$ ) was spotted on immobilized Anti-laccases, no peak was detected. On the other hand, when 1  $\mu\text{l}$  of a mix of laccases and ovalbumin (with a ratio of 1:1) was spotted on immobilized anti-laccases, only the signal related to laccases was detected. These results demonstrate the specificity and the selectivity of the developed system.

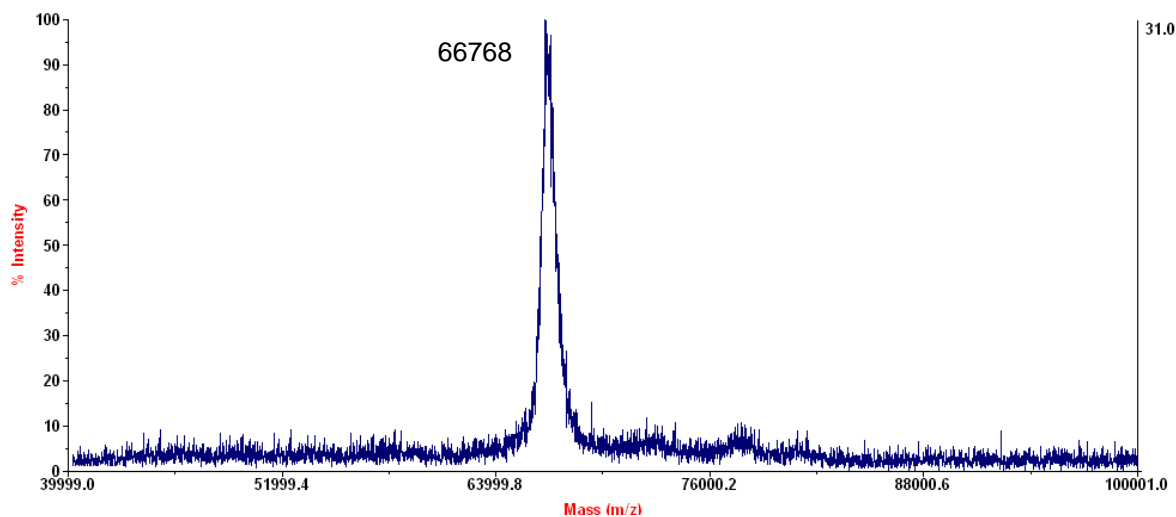


Figure 9: MALDI-MS spectrum of laccase detected by the specific antibody

Further experiments were carried out immobilizing anti-GST antibody on the Vmh2 biofilm. The monellin-GST recombinant fusion protein, kindly provided by research group of prof. Picone, was used for the detection. The sample is an extract of *E. coli* inclusion bodies. When 1  $\mu\text{l}$  of this solution was spotted on immobilized anti-GST, only the signal related to fusion protein (about 40 KDa) was observed, even in presence of ovalbumin 10 mg/ml (figure 10).

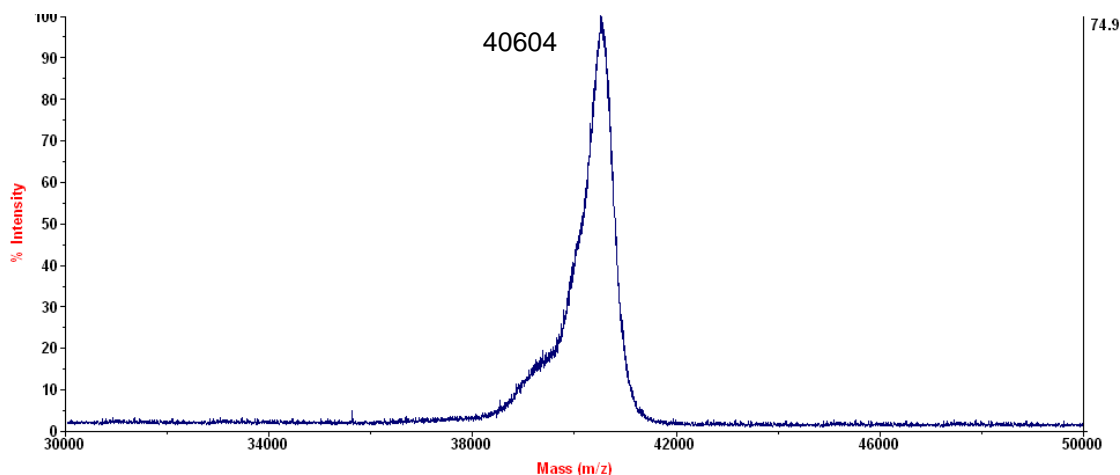


Figure 10 MALDI-MS spectrum of GST-monellin detected by the specific antibody

As a fact, the developed system can be exploited to easily reveal recombinant proteins fused to a tag, such as GST. Moreover complex protein solutions can be analysed by this system without previous treatment (i.e purification).

These results provide the basis for the development of a SELDI TOF-like system, exploiting Vmh2 biofilm and its properties.

### 3.3.3 Textile material coating

The vanguard of the textile industry is looking for new materials and advanced techniques to manufacture improved fabrics and reduce the environment impact caused by chemical processing. As a matter of fact, hydrophobins biofilm can modify the surfaces wettability, making hydrophobic a hydrophilic one, and *viceversa*. For example, it could be interesting to make a cloth waterproof (hydrophobic) to use it in basic rainwear. On the other hand recent research lines are searching for making “superhydrophilic” wool in order to improve the wearing comfort and to facilitate dyeing process. In order to analyze the hydrophobin ability to coat textile material, Vmh2-et solutions were deposited on nylon and wool, using the procedure previously optimized on silicon, and then surfaces wettability was evaluated by measuring water absorption along time. As shown in figure 12, results clearly proved that nylon specimen (hydrophilic) becomes strongly hydrophobic retaining the water drop for over 2 hours. On the other hand wool (hydrophobic) becomes strongly hydrophilic adsorbing quickly the water drop (figure 12).

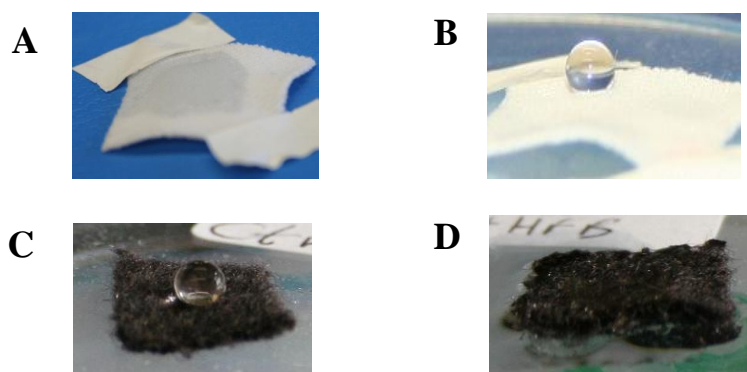


Figure 12. **Qualitative analyses of wettability change of textile material after Vmh2 deposition.** A: nylon (hydrophilic); B: nylon after Vmh2 deposition (hydrophobic); C: wool (hydrophobic); D: wool after Vmh2 deposition (hydrophilic)



No change of the new wettability features were observed after several washing with boiling detergent solution. Therefore, it has been demonstrated that Vmh2 biofilm self-assembled both on nylon and wool fabric cloth samples dramatically change their hydrophilic/hydrophobic nature, exhibiting a strong adhesion to the surface, high resistance to mechanical stress, and great stability to detergent solutions, even at high temperature. Overall results imply the opportunity of industrial usage of Vmh2 hydrophobin to pursue the achievement of new-valuable biomaterial without chemical treatments. This approach could represent a feasible strategy to obtain a new class of bio-material in a sustainable and eco-friendly way.

### 3.3.4 Emulsifying properties

Surface activity of hydrophobins has been accounted for encapsulate and dissolve hydrophobic molecules into aqueous media [68]. Their behavior in solution resembles that of typical surfactants and they self-assemble into amphiphilic membranes. This property might be beneficial for pharmaceutical applications and in the food industry, which both require stable emulsions for certain formulations and ingredients.

The emulsification capacity of Vmh2 solution was analysed using three different oils commonly used in food and healthcare industries: olive, peanut, and almond oil.

A solution of Vmh2 in 20 % ethanol was mixed with each one of the three oils with a volumetric ratio of 3:1. In order to assess emulsifying capability of Vmh2, several checks were performed at different times by monitoring the emulsion stability at different pH values (pH 2, 4, 8, 10). In the experiments performed at acid pH values (between 2-4) the emulsions obtained in the presence of Vmh2 are stable (figure 11) at least for two days, and even longer (up to 7 days) in the cases of the peanut and almond oils. Height of the emulsion phase slightly decrease after 72 hours. On the contrary, tests performed in basic condition (pH>8), showed a quick coalescence of emulsion (within 2-3 hours) until complete separation of phases after 12 hours. This effect can be explained by hydrophobin propensity towards aggregation at basic pH of the solutions (as previously described).

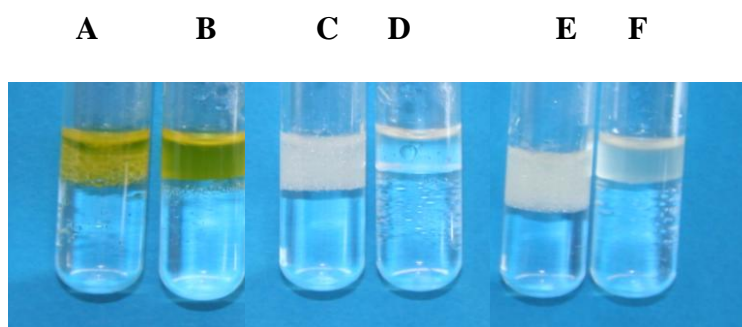


Figure 11: **Emulsions at pH 4 of olive, peanut and almond oil** in the presence (A,C,E) or absence (B,D,F) of Vmh2.

These data indicate the potentiality of the use of the *P. ostreatus* Vmh2 in the stabilization of oil in water emulsions in creams and ointments. Vmh2 acts as a bio-surfactant, self-assembling around oil droplets stabilizing emulsion over time in a pH-dependent manner. Furthermore Vmh2 can be considered a food-grade surfactant, since it has been purified from an edible fungus already consumed in large amounts by people eating this common mushroom (see **P4** in Appendix I).



## 4. Conclusions

Hydrophobins are small proteins (about 100 aminoacids), produced by filamentous fungi at different developmental stages, self-assembling at hydrophobic/hydrophilic interfaces into amphipathic biofilm. The intriguing properties of these proteins make them of great biotechnological interest for numerous applications. They could be used as coatings to increase biocompatibility of medical implants, in cosmetic industry for hair-care products, to immobilize enzymes on surfaces, to create biosensor, or in drug delivery. Hydrophobins have been split in two groups, class I and class II, based on the differences in their hydropathy patterns, spacing of aminoacids between the cysteine residues and properties of the aggregates they form. Class I hydrophobins generate very insoluble assemblies, which can only be dissolved in strong acids (i.e. 100% TFA). Assemblies of Class II can be more easily dissolved in ethanol or sodium dodecyl sulphate.

Adequate production levels and deep knowledge of the properties of hydrophobins, both in solution or assembled, are needed to use them for biotechnological applications. For this reason the present research work has been focused on production and characterization of a class I hydrophobin from *Pleurotus ostreatus*, identified as Vmh2.

Vmh2 has been purified from *Pleurotus ostreatus* mycelia and its recombinant expression in *Escherichia coli* and *Pichia pastoris* has been performed. Being both recombinant and extractive proteins available, a choice between the two proteins according to specific applications can be made.

The characterization of Vmh2 in solution was carried out in different conditions, providing to a deeper knowledge of the protein behavior, necessary to use it for biotechnological applications.

Moreover, the characterization of Vmh2 biofilm and its properties has allowed to verify some of these applications. In particular, the capability of this biofilm to immobilize biological macromolecules suggests that functionalization of surfaces by Vmh2 can be a feasible strategy for the fabrication of a new class of hybrid devices, for biosensing or proteomic research.

Applications of Vmh2 in other industrial fields (such as textile, food and healthcare) has been also verified, demonstrating that Vmh2 is actually a multipurpose protein.

## 5. References

- [1] Linder M. B. *Hydrophobins: Proteins that self-assemble at interfaces*. Current opinion in Colloid & Interface Science (2009); 14: 356-363.
- [2] Wessels J.G.H. *Hydrophobins, proteins that change the nature of the fungal surface*, Adv. Microbial Physiol. (1997); 38: 1-45.
- [3] Wösten H.A.B. and de Vocht M.L. *Hydrophobins, the fungal coat unraveled*. Biochim. Biophys. Acta (2000); 1469: 79-86.
- [4] Sunde M., Kwan A.H., Templeton M.D., Beever R.E., Mackay J.P. *Structural analysis of hydrophobins*. Micron. (2008); 39(7): 773-784.
- [5] Kwan A., Winefield R.D., Sunde M., Matthews J.M., Haverkamp R.G., Templeton M.D., Mackay J.P., Sunde M. *Structural basis for rodlet assembly in fungal hydrophobins*. PNAS (2006); 103:3621-3626.
- [6] Hakanpää J., Linder M., Popov A., Schmidt A., Rouvinen J. *Hydrophobin HFBII in detail: ultrahigh-resolution structure at 0.75 Å*. Biological Crystallography (2006); 62: 356-367.
- [7] Zampieri F., Wosten H.A.B., Scholtmeijer K. *Creating surface Properties Using a Palette of Hydrophobins*. Materials (2010); 3: 4607-4625.
- [8] De Vocht M.L., Scholtmeijer K., van der Vegte E.W., de Vries O.M.H., Sonveaux N., Wosten H.A.B., Ruyschaert J.M., Hadziloannou G., Wessels J.G.H., Robillard G.T. *Structural characterization of the hydrophobin SC3, as monomer and after self-assembly at hydrophobic/hydrophilic interfaces*. Biophys. (1998); 74:2059-2068.
- [9] Scholtmeijer K., Janssen M.I., Gerssen B., De Vocht M.L., van Leeuwen B.M.M., van Kooten T.G., Wosten H.A.B., Wessels J.G.H. *Surface modifications created by using engineered hydrophobins*. Appl. Environ. Microbiol. (2002); 68: 1367-1373.
- [10] Askolin S., Linder M.B., Scholtmeijer K., Tenkanen M., Penttilä M.E., de Vocht M.L., Wosten H.A.B. *Interacion and comparision of a class I hydrophobin from Schizophyllum commune and clas II hydrophobins from Thrichoderma reseei*. Biomacromolecules (2006); 7: 1295-1301.
- [11] Lumsdon S.O., Green J., Stieglitz B. *Adsorption of hydrophobin proteins at hydrophobic and hydrophilic interfaces*. Colloids Surf, B-Biointerfaces (2005); 44: 172-178.
- [12] Wang X., de Vocht M. L., de Jonge J., Poolman B., Robillard G. T. *Structural changes and molecular interactions of hydrophobin SC3 in solution and on a hydrophobic surface*. Protein Sci. (2002); 11: 1172-1181.
- [13] de Vocht M. L., Reviakine I., Ulrich W. P., Bergsma-Schutter W., Wösten H. A., Vogel H., Brisson A., Wessels J. G., Robillard G. T. *Self-assembly of the hydrophobin SC3 proceeds via two structural intermediates*. Protein Sci. (2002); 11: 1199-1205.
- [14] Wang, X., Graveland-Bikker, J. F., De Kruif, C. G., Robillard, G. T. *Oligomerization of hydrophobin SC3 in solution: from soluble state to self-assembly*. Protein Science (2004); 13: 810–821.
- [15] Stroud P..A., Goodwin J.S., Butko P., Cannon G.C., McCormick C.L. *Experimental evidence for multiple assembled states of Sc3 from Schizophyllum commune*. Biomacromolecules (2003); 4:956– 967.
- [16] Wohlleben, W., Subkowski, T., Bollschweiler, C., von Vacano, B., Liu, Y., Schrepp, W., Baus, U. *Recombinantly produced hydrophobins from fungal analogues as highly surface-active performance proteins*. Eur Biophys J. (2010); 39: 457-468.
- [17] Wessels J.G.H. *Developmental regulation of fungal cell-wall formation*. Annu. Rev. Phytopathol. (1994); 32:413-437.
- [18] Wösten H.A.B., Schuren F.H.J. and Wessels J.G.H., *Interfacial self-assembly of a hydrophobin into an amphipathic membrane mediates fungal attachment to hydrophobic surfaces*. EMBO J.(1994); 13: 5848-5854.

- [19] Lugones L.G., Bosscher J.S., Scholtmeyer K., de Vries O.M., Wessels J.G. *An abundant hydrophobin (ABH1) forms hydrophobic rodlet layers in Agaricus bisporus fruiting bodies*. Microbiology. (1996); 142(5): 1321-1329.
- [20] Lugones L.G., Wösten H.A.B. and Wessels J.G.H. *A hydrophobin (ABH3) specifically secreted by vegetatively growing hyphae of Agaricus bisporus (common white button mushroom)*. Microbiology (1998); 144: 2345-2353.
- [21] Mackay J.P., Matthews J.M., Winefield R.D., Mackay L.G., Haverkamp, R.G., Templeton M.D. *The hydrophobin EAS is largely unstructured in solution and functions by forming amyloid-like structures*. Structure (2001); 9: 83-91.
- [22] Linder M.B., Szilvay G.R., Nakari-Setälä T., and Penttilä M.E. *Hydrophobins: the protein amphiphiles of fungi*. FEMS Microbiol. Rev. (2005); 29: 877-896.
- [23] Scherrer S., de Vries O.M.H., Dudler R., Wessels J.G.H. and Honegger R. *Interfacial self-assembly of fungal hydrophobins of the lichen-forming ascomycetes Xanthoria parietina and X. ectaneoides*. Fungal Genet. Biol. (2000); 30: 81-93.
- [24] Yu L., Zhang B., Szilvay G.R., Sun R., Jänis J., Wang Z., Feng S., Xu H., Linder M.B., Qiao M. *Protein HGFI from the edible mushroom Grifola frondosa is a novel 8 kDa class I hydrophobin that forms rodlets in compressed monolayers*. Microbiology (2008); 154: 1677-1685.
- [25] Houmadi S., Ciuchi F., De Santo M.P., De Stefano L., Rea I., Giardina P., Armenante A., Lacaze E., Giocondo M. *Langmuir Blodgett film of hydrophobin protein from Pleurotus ostreatus at air-water interface*. Langmuir (2008); 24(22): 12953-7.
- [26] Butko P., Buford J.P., Goodwin J.S., Stroud P.A., McCormick C.L., Cannon G.C. *Spectroscopic evidence for amyloid-like interfacial self-assembly of hydrophobin SC3*. Biochem. Biophys. Res. Commun. (2001); 280: 212-215.
- [27] Paanen A., Vuorimaa E., Torkkeli M., Penttilä M., Kauranen M., Ikkala O., Lemmetyinen H., Serimaa R., Linder M.B. *Structural hierarchy in molecular films of two class II hydrophobins*. Biochemistry (2003); 42: 5253-5258.
- [28] Akanbi M.H.J., Post E., Meter-Arkema A., Rink R., Robillard G.T, Wang X., Wosten H.A.B., Scholtmeijer K. *Use of hydrophobins in formulation of water insoluble drugs*. Coll and Surfaces B: Biointerfaces (2010); 75(2):526-531.
- [29] Schulz A., Liebeck B.M., John D., Heiss A., Subkowski T., Boker A. *Protein-mineral hybrid capsules from emulsions stabilized with an amphiphilic protein*. J. of Materials Chemistry 2011; 21: 9731-9736.
- [30] Linder M.B., Selber K., Nakari-Setälä T., Qiao M., Kula M.R., Penttilä M. *The hydrophobins HFBI and HFBI from Trichoderma reesei show efficient interactions with non-ionic surfactants in aqueous two-phases systems*. Biomacromolecules (2001). 2: 511-517.
- [31] Collen A., Persson J., Linder M., Nakari-Setälä T., Penttilä M., Tjerneld F., Sivars U., *A novel two-step extraction method with detergent/polymer systems for primary recovery of the fusion protein endoglucanase I -hydrophobin I*. Biochim. Biophys. Acta. (2002); 1569: 139-150.
- [32] Hektor H.J. and Scholtmeijer K. *Hydrophobins: protein with potential*. Curr. Opinion in Biotech (2005); 16: 434-439.
- [33] Janssen M.I., van Leeuwen M.B.M., Scholtmeijer K., van Kooten T.G., Dijkhuizen L., Wosten H.A.B. *Coating with genetic engineered hydrophobin promotes growth of fibroblasts on a hydrophobic solid*. Biomaterials (2002); 23: 4847-4854.
- [34] Sun T. Quing G., Su B., Jiang L. *Functional biointerface materials inspired from nature*. Chem. Soc. Rev. (2011); 40: 2909-2921.
- [35] Qin, M.; Wang, L.K.; Feng, X.Z.; Yang, Y.L.; Wang, R.; Wang, C.; Yu, L.; Shao, B.; Qiao, M.Q. *Bioactive surface modification of mica and poly(dimethylsiloxane) with hydrophobins for protein immobilization*. Langmuir (2007); 23: 4465-4471.

- [36] Wang, Z.; Lienemann, M.; Qiao, M.; Linder, M.B. *Mechanisms of protein adhesion on surface films of hydrophobin*. *Langmuir* (2010); 26: 8491-8496.
- [37] Corvis, Y.; Walcarius, A.; Rink, R.; Mrabet, N.T.; Rogalska, E. *Preparing catalytic surfaces for sensing applications by immobilizing enzymes via hydrophobin layers*. *Anal. Chem.* (2005); 77: 1622-1630.
- [38] Zhao, Z.X.; Qiao, M.Q.; Yin, F.; Shao, B.; Wu, B.Y.; Wang, Y.Y.; Wang, X.S.; Qin, X.; Li, S.; Chen, Q. *Amperometric glucose biosensor based on self-assembly hydrophobin with high efficiency of enzyme utilization*. *Biosens. Bioelectron.* (2007); 22, 3021-3027.
- [39] Zhao, Z.X.; Wang, H.C.; Qin, X.; Wang, X.S.; Qiao, M.Q.; Anzai, J.; Chen, Q. *Self-assembled film of hydrophobins on gold surfaces and its application to electrochemical biosensing*. *Colloids Surf. B Biointerfaces* (2009); 71. 102-106.
- [40] Hou, S.; Li, X.; Feng, X.Z.; Wang, R.; Wang, C.; Yu, L.; Qiao, M.Q. *Surface modification using a novel type I hydrophobin HGFI*. *Anal. Bioanal. Chem.* (2009), 394: 783-789.
- [41] Qin, M.; Hou, S.; Wang, L.; Feng, X.; Wang, R.; Yang, Y.; Wang, C.; Yu, L.; Shao, B.; Qiao, M. *Two methods for glass surface modification and their application in protein immobilization*. *Colloids Surf. B Biointerfaces* (2007); 60: 243-249.
- [42] Askolin S, Nakari-Setälä T, Tenkanen M. *Overproduction purification and characterization of the Trichoderma reesei hydrophobin HFBI*. *Appl. Microbiol. Biotechnol.* (2001); 57:124–130.
- [43] Wang Z., Feng S., Huang Y., Li S., Xu H., Zhang X., Bai Y., Qiao M. *Expression and characterization of a Grifola frondosa hydrophobin in Pichia pastoris*. *Protein Expr. Purif.* (2010); 72(1): 19-25.
- [44] Ballero M., E. Mascia A. Rescigno and E. S. *Use of Pleurotus for transformation of polyphenols in waste waters from olive presses into proteins*. *Micol. Italiana* (1990); 19: 39–41.
- [45] Puniya A., Shah K.G., Hire S.A., Ahire R.N., Rathod M.P., Mali R.S. *Bioreactor for solid-state fermentation of agro-industrial wastes*. *Indian J. Microbiol.*(1996); 36: 177–178.
- [46] Giardina P., Aurilia V., Cannio R., Marzullo L., Amoresano A., Siciliano R., Pucci P., Sannia G., *The gene, protein and glycan structures of laccase from Pleurotus ostreatus*. *Eur. J. Biochem.* (1996); 235: 508–515.
- [47] Marzullo L., Cannio R., Giardina P., Santini M., Sannia G., *Veratryl alcohol oxidase from Pleurotus ostreatus participates in lignin biodegradation and prevents polymerization of laccase-oxidized substrates*. *J. Biol. Chem.* (1995); 270: 3823–3827.
- [48] Axtell C., Johnston C.G., Bumpus J.A., *Bioremediation of soil contaminated with explosives at the Naval Weapons Station Yorktown*. *Soil Sediment Contam.* (2000); 9: 537–548.
- [49] Peñas M.M., Rust B., Larraya L.M., Ramírez L., Pisabarro A.G. *Differentially regulated, vegetative-mycelium-specific hydrophobins of the edible basidiomycete Pleurotus ostreatus*. *Appl Environ Microbiol.* (2002); 68(8): 3891-3898.
- [50] Peñas M.M., Asgeirsdóttir S.A., Lasa I., Culiánez-Macia F.A., Pisabarro A.G., Wessels J.G., Ramirez L. *Identification, characterization, and In situ detection of a fruit-body-specific of Pleurotus ostreatus*. *Appl. Environ. Microbiol.* (1998); 64(10): 4028-4034.
- [51] Asgeirsdóttir S.A., de Vries O.M.H., Wessels J.G.H. *Identification of three differentially expressed hydrophobins in Pleurotus ostreatus (oyster mushroom)*. *Microbiology* (1998); 144: 2961-2969.
- [52] Ma A, Shan L, Wang N, Zheng L, Chen L, Xie B., *Characterization of a Pleurotus ostreatus fruiting body-specific hydrophobin gene, Po.hyd*. *J Basic Microbiol.* (2007); 47(4): 317-324.

- [53] De Stefano L, Rea I, Armenante A, Giardina P, Giocondo M, Rendina I. *Self-Assembled Biofilm of Hydrophobins Protects the Silicon Surface in the KOH Wet Etch Process*. *Langmuir* (2007); 23:7920-7922.
- [54] De Stefano L, Rea I, Giardina P, Armenante A, Rendina I. *Protein-Modified Porous Silicon Nanostructures*. *Adv Mater* (2008); 20:1529–1533.
- [55] Sreerama N., Woody R.W. *Estimation of protein secondary structure from circular dichroism spectra: comparison of CONTIN, SELCON, and CDSSTR methods with an expanded reference set*. *Anal. Biochem.* (2000); 287:252-260.
- [56] Whitmore L., Wallace B.A. *Protein secondary structure analyses from circular dichroism spectroscopy: methods and reference databases*. *Biopolymers* (2008) 89:392-400.
- [57] Kirkland B. H, Keyhani N. O. *Expression and purification of a functionally active class I fungal hydrophobin from the entomopathogenic fungus Beauveria bassiana in E. coli*. *J Ind Microbiol Biotechnol* (2011); 38:327–335.
- [58] Biancalana M., Koide S. *Molecular mechanism of Thioflavin-T binding to amyloid fibrils*. *Biochim. Biophys. Acta* (2010); 1804:1405-12.
- [59] Chaniotakis N, Sofikiti N. *Novel semiconductor materials for the development of chemical sensors and biosensors: a review*. *Anal Chim Acta.* (2008); 615(1): 1-9.
- [60] Kane R.S., Stroock A.D. *Nanobiotechnology: Protein-Nanomaterial Interactions*. *Biotechnol. Prog.* (2007); 23: 316-319.
- [61] Buriak J. *High surface area silicon materials: fundamentals and new technology*. *Philos. Transact A Math. Phys. Eng. Sci.* (2006); 364: 217–225.
- [62] L. De Stefano, L. Rotiroti, I. Rendina, L. Moretti, V. Scognamiglio, M. Rossi, S. D'Auria, *Porous silicon-based optical microsensor for the detection of l-glutamine*. *Biosensors and Bioelectronics* (2006); 21: 1664–1667.
- [63] De Bock M., de Seny D., Meuwis M.A., Chapelle J.P., Louis E., Malaise M., Merville M.P., Fillet M. *Challenges for Biomarker Discovery in Body Fluids Using SELDI-TOF-MS*. *J Biomed Biotechnol.* (2010); 2010:906082.
- [64] Baggerly K.A., Morris J.S., Coombes K.R. *Reproducibility of SELDI-TOF protein patterns in serum: comparing datasets from different experiments*. *Bioinformatics* (2004); 20(5):777-85.
- [65] Greplova K., Pilny R., budinska E., Dubska L., Lakomy R., Vyzula R., Vojtesek B., Valik D. *When one chip is not enough: augmenting the validity of SELDI-TOF proteomic profiles of clinical specimen*. *Lab Chip* (2009); 9: 1014-1017.
- [66] Merchant, M. and Weinberger, S. R. *Recent advancements in surface-enhanced laser desorption/ionization-time of flight-mass spectrometry*. *ELECTROPHORESIS* (2000); 21: 1164–1177.
- [67] Asano T, Koizumi S, Takagi A, Hatori T, Kuwabara K, Fujino O, Fukunaga Y. *Identification of a novel biomarker candidate, a 4.8-kDa peptide fragment from a neurosecretory protein VGF precursor, by proteomic analysis of cerebrospinal fluid from children with acute encephalopathy using SELDI-TOF-MS* *BMC Neurol.* (2011);11(1):101.
- [68] Wang X., Shi, Wosten F., Hektor H.A.B., Poolman H.B., Robillard G.T. *The SC3 hydrophobin self-assembles into a membrane with distinct mass transfer properties*. *Biophys. J.* (2005); 88:434-443.



## Publications

**P1-** L. De Stefano, I. Rea, E. De Tommasi, I. Rendina, L. Rotiroti, M. Giocondo, **S. Longobardi**, A. Armenante, and P. Giardina. 2009. *Bioactive modification of silicon surface using self-assembled hydrophobins from Pleurotus ostreatus*. Eur. Phys. J. 30(2):181-5.

**P2-** L. De Stefano, I. Rea, E. De Tommasi, P. Giardina, A. Armenante, **S. Longobardi**, M. Giocondo, and I. Rendina, 2009. *Biological passivation of porous silicon by a self-assembled nanometric biofilm of proteins*, Journal of Nanophotonics Vol 3.

**P3-** A. Armenante, **S. Longobardi**, I. Rea, L. De Stefano, M. Giocondo, A. Silipo, A. Molinaro, P. Giardina. 2010. *The Pleurotus ostreatus hydrophobin Vmh2 and its interaction with glucans*. Glycobiology 20(5):594-602.

**P4-** **S. Longobardi**, L. De Stefano, C. Ercole; D. Picone, I. Rea, P. Giardina. 2010. *"Fungal hydrophobins, proteins as natural emulsifiers"*. Household and Personal Care TODAY.4:20-22.

**P5-** **S. Longobardi**, D. Picone, C. Ercole, R. Spadaccini, L. De Stefano, I. Rea, P. Giardina. *"Environmental conditions modulate the switch among different states of the hydrophobin Vmh2 from Pleurotus ostreatus"*. (Submitted to Biomacromolecules 09/2011).

**P6-** I. Rea, P. Giardina, **S. Longobardi**, F. Porro, V. Casuscelli, M. Gagliardi, I. Rendina, and L. De Stefano. *"Self-assembly of Glucose-Hydrophobin aggregates on silicon surface"* (submitted to journal of colloid and interfaces 2011).

**P7-** S.Houmadi, R Rodriguez, P. Giardina, S. Longobardi, M.C. Faurè, M. Giocondo, E. Lacaze. *"Determination of the structure of hydrophobin rodlets using atomic force microscopy in dynamic mode"* (submitted to Langmuir 10/2011).

## Comunications

**C1-** L. De Stefano, I. Rea, L. Rotiroti, I. Rendina, P. Giardina, A. Armenante, **S. Longobardi**, *"Bio/non-bio interfaces for a new class of protein microarrays"* XIII Conferenza Nazionale AISEM, Roma, Italia, 19-21 February, 2008.

**C2-** I. Rea, E. De Tommasi, I. Rendina, P. Giardina, A. Armenante, **S. Longobardi** and L. e Stefano, *"Ellipsometric characterization of self- assembled biological films on silicon based substrate"* European ottica society annual meeting EOS, Paris, France, 29 October-2 November, 2008.

**C3-** **S. Longobardi**, S. Albrizio, L. De Stefano, C. Ercole, L. Grumetto, D. Picone, P. Giardina. *"Film proteici di origine fungina: loro utilizzo per la riduzione del rischio di contaminazione degli alimenti da materiale di confezionamento"*. BIOPOLPACK - 1° Congresso nazionale sugli imballaggi in polimeri biodegradabili. Parma, Italia, 15-16 aprile 2010

**C4-** P. Giardina, **S. Longobardi**, D. Picone, C. Ercole, I. Rea, L. De Stefano. "*Hydrophobin from Pleurotus ostreatus, a multipurpose protein*". 7<sup>th</sup> International conference on Polymer and textile Biotechnology (IPTB). Milan, Italy, 2-4 March 2011.

### **Book chapters**

**B1-** L. De Stefano, I. Rea, I. Rendina, P. Giardina, **S. Longobardi**, M. Giocondo. 2011. "*Organic-Inorganic Interfaces for a New Generation of Hybrid Biosensors*". Biosensors for Health, Environment and Biosecurity / Book 1, ISBN 978-953-307-155-8.

**B2-** S. Houmadi, M. Giocondo, E. Bruno, M. P. De Santo, L. De Stefano, E. Lacaze, S. Longobardi, P. Giardina. "*Atomic Force Spectroscopies: a toolbox for probing the biological matter*". (Atomic Force Microscopy/ Book 1. ISBN 979-953-307-390-2).

### **Courses**

- "Corso teorico-pratico per operatori di Spettrometri di Massa per lo studio di molecole in soluzione". Napoli, 10-17 novembre 2008
- Seminario tecnico "Real Time PCR" dell'Applied Biosystem. Napoli, 23 febbraio 2009
- Italy-Japan Symposium: "New Trends in Enzyme Science and Technology". Naples, 28 October 2009
- "Prima scuola nazionale sui biosensori ottici e biofotonica". Ischia 25 settembre-1 ottobre 2010

### **Experience in foreign laboratories**

**April-May 2009:** Visiting PhD student in the laboratory of Dr. Emmanuelle Lacaze, Institut des NanoSciences de Paris (INSP) -Université Pierre et Marie Curie (Paris, France). The stage was focused on Atomic Force Microscopy.

**Appendix I**  
*Papers*

# Bioactive modification of silicon surface using self-assembled hydrophobins from *Pleurotus ostreatus*

L. De Stefano<sup>1,a</sup>, I. Rea<sup>1</sup>, E. De Tommasi<sup>1</sup>, I. Rendina<sup>1</sup>, L. Rotiroti<sup>1</sup>, M. Giocondo<sup>2</sup>, S. Longobardi<sup>3</sup>, A. Armenante<sup>3</sup>, and P. Giardina<sup>3</sup>

<sup>1</sup> Unit of Naples-Institute for Microelectronics and Microsystems, National Council of Research, Via P. Castellino 111, 80131, Naples, Italy

<sup>2</sup> Dept. of Organic Chemistry and Biochemistry, University of Naples "Federico II", Via Cintia 4, 80126, Naples, Italy

<sup>3</sup> LICRYL - INFM-CNR, Via P. Bucci, Cubo 33/B, 87036 Arcavacata di Rende, Cosenza, Italy

Received 16 January 2009 and Received in final form 22 June 2009

© EDP Sciences / Società Italiana di Fisica / Springer-Verlag 2009

**Abstract.** A crystalline silicon surface can be made biocompatible and chemically stable by a self-assembled biofilm of proteins, the hydrophobins (HFBs) purified from the fungus *Pleurotus ostreatus*. The protein-modified silicon surface shows an improvement in wettability and is suitable for immobilization of other proteins. Two different proteins were successfully immobilized on the HFBs-coated chips: the bovine serum albumin and an enzyme, a laccase, which retains its catalytic activity even when bound on the chip. Variable-angle spectroscopic ellipsometry (VASE), water contact angle (WCA), and fluorescence measurements demonstrated that the proposed approach in silicon surface bioactivation is a feasible strategy for the fabrication of a new class of hybrid devices.

**PACS.** 87.15.N- Properties of solutions of macromolecules – 89.90.+n Other topics in areas of applied and interdisciplinary physics

## 1 Introduction

Biological molecules are more and more used in a large class of research and commercial applications such as biosensors, DNA and protein microarrays, cell culturing, immunological assays, and so on. The fabrication of a new generation of hybrid biodevices, where a biological counterpart is integrated with a micro- or a nanoelectronic platform, depends on the bio-compatibilization treatments of the surfaces [1]. The design and the realization of bio/non-bio interfaces with specific properties, such as chemical stability, wettability, and biomolecules immobilization ability, are key features in the miniaturization of devices for genomic and proteomic research [2]. In particular, protein immobilization is a hot topic in biotechnology since commercial solutions, as in the case of DNA microarrays, are not still available. Proteins are, due to their composition, a class of very heterogeneous macromolecules with variable properties. For these reasons, it is extremely difficult to find a common surface suitable for different proteins with a broad range in molecular weight and physical-chemical properties such as charge and hydrophobicity. A further aspect is the orientation of the bound proteins, that could be of crucial relevance

for quantitative analysis, interaction studies, and enzymatic reactions [3]. Many different surfaces have been investigated in the last years, but a universal surface for all applications could not be identified [4–8]. Among others, silicon is a very attractive platform due to its wide use in all the micro- and nanotechnologies. Lots of studies about chemical procedures for the organic functionalization of silicon have been published in the last decade [9]. A completely different approach is to use a biological substrate to passivate the silicon surface: recently, a nanostructured self-assembled biofilm of amphiphilic proteins, the hydrophobins, was deposited by solution deposition on crystalline silicon and proved to be efficient as masking material in the KOH wet etch of the crystalline silicon [10]. HFBs are small (about 10 kDa) proteins that can be found in filamentous fungi, where they coat the spores and aerial structures. They mediate the attachment of fungal structures to hydrophobic surfaces [11–13]. In nature, HFBs self-assemble at the air/water interface and lower the surface tension of water. Furthermore, they shown self-assembling properties also at interfaces between oil and water, and between water and a hydrophobic solid [14]. HFBs are subdivided into classes I and II based on their hydrophobicity patterns, although the amino acid sequence similarity both within and between the classes is small. Class I HFB assemblies are insoluble even in hot solutions

<sup>a</sup> e-mail: luca.destefano@na.imm.cnr.it

of sodium dodecyl sulfate (SDS) and can only be dissolved in some strong acids, such as trifluoroacetic acid [11].

Some very recent applications of both class I and II hydrophobins in protein immobilization have been reported [12,15]. Inspired by these very promising results, we have studied the immobilization of a fluorescent protein and an enzyme on a class I hydrophobin biofilm when self-assembled on silicon surface.

## 2 Materials and methods

*Protein purification.* The HFB and the laccase POXC have been isolated from the culture broth of *P. ostreatus* (type: Florida ATCC no. MYA-2306). For HFBs production, mycelia have been grown at 28 °C in static cultures in 2 L flasks containing 500 mL of potato dextrose (24 g/l) broth with 0.5% yeast extract. After 10 days of fungal growth, the HFBs aggregates have been obtained by air bubbling of the culture broth by using a Waring blender. Foam has been then collected by centrifugation at 4000g. The precipitate has been freeze dried, treated with 100% trifluoroacetic acid for 2 h, and sonicated for 30 min. The sample has been dried again in a stream of air and then dissolved in 60% ethanol. The precipitate has been separated by centrifugation at 4000g. The homogeneity of the HFB sample has been ascertained by SDS-PAGE, by using a silver staining method. In particular, SDS-polyacrylamide gel electrophoresis (SDS-PAGE) was performed at 15% polyacrylamide concentration using the Bio-Rad Mini Protean III apparatus.  $\beta$ -galactosidase (120 kDa), bovine serum albumine (86.0 kDa), ovalbumin (47 kDa), carbonic anhydrase (34.0 kDa),  $\beta$ -lactoglobulin (26.0 kDa), lysozyme (20 kDa) were used as standards (Fermentas Inc., Glen Burnie, MD, USA). Mycelium growth and laccase purification have been carried out following the procedures described by Palmieri *et al.* [16].

*Hydrophobin self-assembly on silicon chip.* The organic and metallic contaminants of the silicon chip surface have been removed by a cleaning procedure, called RCA process [17]. RCA is based on a combination of two cleaning steps, one using solutions of ammonium hydroxide/hydrogen peroxide/deionized water, and the other using hydrochloric acid/hydrogen peroxide/deionized water, both at the temperature of 80 °C. The silicon samples, single side polished,  $\langle 100 \rangle$  oriented (chip size: 1 cm  $\times$  1 cm), after the RCA, have been washed in hydrofluoric acid solution for three minutes to remove the native oxide thin layer (1–2 nm). Then, a drop (80  $\mu$ L) of HFBs solutions (0.1 mg/mL in 80% ethanol) has been spotted on the chip. After 1 h, samples have been dried for 10 min on the hot plate (80 °C), and then washed by the solvent solution. All the chip have been handled and prepared in a clean room (ISO 5), humidity (50  $\pm$  5%) and temperature (22  $\pm$  1 °C) controlled.

*Laccase immobilization method.* A drop of the laccase solution has been deposited on HFB modified silicon surface, kept at 4 °C for 1 hour, and then rinsed over night

in 50 mM phosphate buffer, pH 7. After 16 hours, the silicon biochip has been washed in the same buffer at 25 °C till complete loss of laccase activity in the washing buffer. Then each chip has been dust-protected and kept at constant humidity conditions when not in use.

*BSA immobilization method.* Bovine serum albumin (BSA) has been labelled by rhodamine, following the Molecular Probes<sup>®</sup> procedure MP06161, and solubilised in water at three different concentration (3, 6, 12  $\mu$ M). To assess the protein binding on the chip surface, we have spotted 50  $\mu$ l of water solution containing the labeled protein on the chips covered by the HFBs biofilm. The immobilization has been carried at 4 °C overnight. After incubation, the samples have been rinsed three times in deionized water at room temperature.

*Enzyme assay.* Laccase activity has been assayed at 25 °C using 2,6-dimethoxyphenol (DMP) 10 mM in McIlvaine citrate-phosphate buffer, pH 5. Oxidation of DMP has been followed by the absorption increment at 477 nm ( $\epsilon_{477} = 14.8 \times 10^3 \text{ M}^{-1} \text{ cm}^{-1}$ ) using Beckman DU 7500 spectrophotometer (Beckman Instruments). Enzyme activity has been expressed in International Units (IU). Immobilized enzyme has been assayed by silicon dip in 10 ml of McIlvaine citrate-phosphate buffer, pH 5. The absorption increment at 477 nm has been followed withdrawing 200  $\mu$ l of reaction mixture each 30 s for 10 min. The total immobilised activity per unit of silicon (chip) has been calculated as  $U/\text{chip} = \Delta A_{\text{min}}^{-1} / \epsilon \cdot 10^4$ .

*Optical techniques.* Ellipsometric characterization of the hydrophobin biofilm deposited on the silicon substrate has been performed by a variable-angle spectroscopic ellipsometry model (UVISEL, Horiba-Jobin-Yvon). Ellipsometric parameters  $\Delta$  and  $\Psi$  have been measured at an angle of incidence of 65° over the range of 360–1600 nm with a resolution of 5 nm. Fluorescence images were recorded by a Leica Z16 APO fluorescence macroscopy system. Contact angle measurements have been performed by using a KSV Instruments LTD CAM 200 Optical Contact Angle Meter: each contact angle has been calculated as the average between the values obtained from three drops having the same volume (about 3  $\mu$ L), spotted on different points of the chip.

## 3 Results and discussion

In the following experiments, we have used purified protein samples, as is shown in Figure 1 where the result of the SDS-PAGE procedure is reported. The coating of a solid surface by solution deposition is not a finely controlled process, even if the covering substance has self-assembling properties, as is the case of HFB. For this reason, the HFB biofilms, self-assembled by deposition of equal concentration solutions, showed variable thicknesses ranging between 10 and 30 nanometers. This behaviour could be ascribed to different local aggregation of HFB in the solutions, due to the strong hydrophobic interactions among

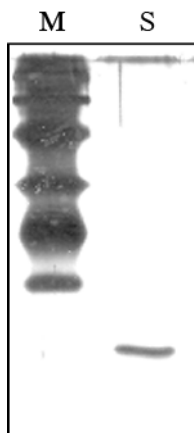


**Fig. 1.** SDS-PAGE of *P. ostreatus* hydrophobin. M: molecular weight markers. S: HFB sample.

the protein molecules [18,19]. In fact, during HFB deposition, solvent evaporation can determine local increases of protein concentration, thus favouring multimers and aggregates formation. In this step, there is no way to control the clustering and stacking of the proteins which constitutes the self-assembled biofilm. HFB solutions have been deposited on silicon just after the chips have been washed in the hydrofluoric acid which removes the native oxide: after this treatment the silicon surface is highly hydrogenated and, consequently, hydrophobic. The HFB biofilm self-assembled on the hydrophobic silicon shows a strong adhesion to the surface: the protein layers always exhibit great stability to basic solutions, even at high temperature, which generally denaturate the proteins. After 10 minutes washing in sodium hydroxide (NaOH) and SDS at 100 °C, a residual biofilm is still present, whose thickness is  $3.1 \pm 0.7$  nm, independently from the starting value. The biofilm characterization has been performed by VASE on 12 samples realized in the same experimental conditions; the optical model for experimental data fitting has been developed in our previous work [10]. We believe that this is the thickness of a monolayer of HFBs when self-assembled on hydrophobic silicon: this value is also consistent with a typical molecular size and comparable to atomic force microscopy measurements [20]. According to the above-described model, the washing step of the chip is strong enough to remove the proteins aggregates deposited on the HFB monolayer that directly interacts with the hydrophobic silicon surface. This behaviour points out the stronger interactions between the silicon surface and the HFB monolayer with respect to those between the HFB aggregates and the HFB monolayer. The presence of the biofilms does not alter the optical behaviour of the silicon surface as is shown in Figure 2, where the transmission curves of the biofilm is reported. The self-assembled layer is transparent in a very large interval of wavelengths: the transmittance is still the 80% at the wavelength of 290 nm.

The improvement in the silicon wettability is also a key feature in biodevices realization: the silicon surface, after RCA and HF washing, is hydrophobic, even if this kind of surface is not stable and undergoes a spontaneous

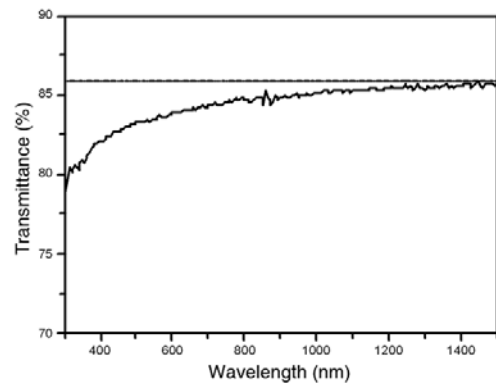


**Fig. 2.** Transmission curve of the HFB self-assembled biofilm on silicon.

oxidation on contact to air. This occurrence can constitute a severe limit in the fabrication of microchannels for microfluidics applications. The changing in silicon wettability has been monitored by water contact angle measurements.

In Figure 3A and B are reported the WCA results in case of the silicon surface, freshly washed in hydrofluoric acid, and after the deposition of the HFB biofilm. The dramatic increase in wettability of the silicon surface is well evident: in the first case, the WCA results in  $90^\circ \pm 1^\circ$ ; on the contrary, after the HFB deposition the WCA falls down to  $25^\circ \pm 2^\circ$  so that the surface is now clearly hydrophilic. The HFB modified silicon surface is highly stable and the WCA value does not change after months, even if stored at room temperature without particular saving condition.

The HFB modified silicon surface has been tested by BSA immobilization: solutions containing a rhodamine labelled BSA at different concentration, between 3 and 12  $\mu\text{M}$ , have been spotted on the HFB film. The labelled bioprobes have been spotted also on other bare silicon samples, as a negative control on the possible aspecific binding between the silicon and the probe. All the samples have been washed in deionized water to remove the excess of biological matter and observed by the fluorescence microscopy system. Under lamp illumination, we found that the fluorescence of silicon-HFB-BSA system is brighter than the negative control, as can be seen in Figure 4A and B, respectively. The fluorescence signal is also quite homogeneous on the whole surface, as confirmed by the intensity profile reported in Figure 4C. We have qualitatively tested the strength of the affinity bond between the HFB and the BSA, by washing the chip overnight in deionized water. Since the fluorescent intensities before and after the washing step do not differ, we can conclude that the HFB-BSA system is very stable. We have also realized a dose-response curve of fluorescence intensity as a function of BSA concentration, shown in Figure 4D, and we have estimated a saturation concentration equal to 6.05  $\mu\text{M}$  corresponding to 300  $\text{fmol}/\text{cm}^2$ .

Protein immobilization on the HFB film has been also verified and analyzed using an enzyme, POXC laccase. The enzymatic assay on the immobilized enzyme has been

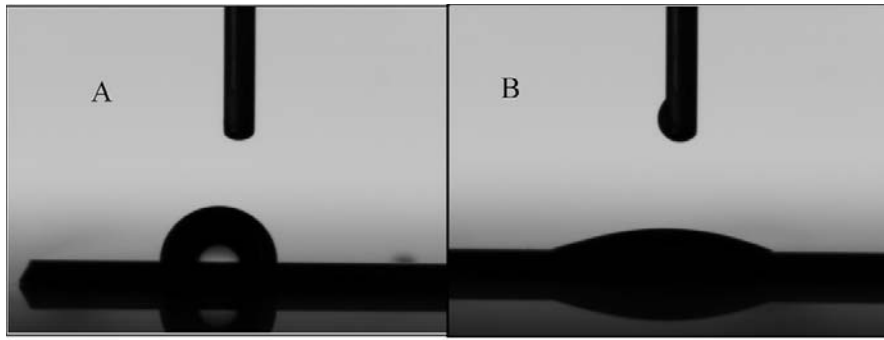


**Fig. 3.** Changing the wettability of c-Si: the hydrophobin nanolayer turns the hydrophobic surface of c-Si into a hydrophilic one. A: a water drop on the c-Si after washing in hydrofluoric acid forms a contact angle of  $90^\circ \pm 1^\circ$ . B: a water drop after the hydrophobin deposition forms a contact angle of  $25^\circ \pm 2^\circ$ .

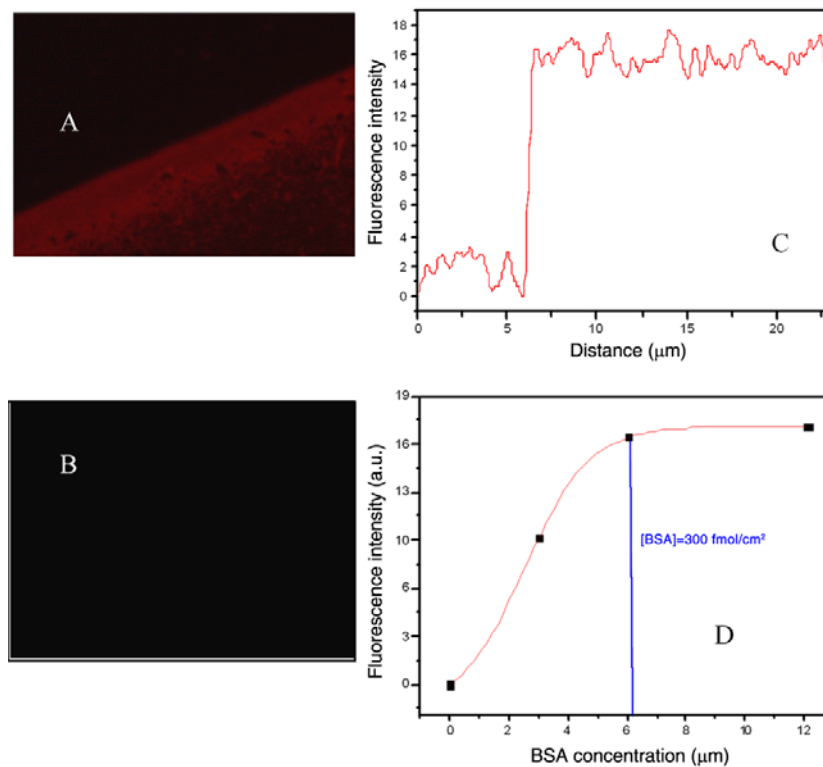


**Fig. 4.** A: Fluorescence image of labelled BSA spotted on a silicon chip covered by HFBS. B: Negative control sample: BSA spotted directly on silicon. C: Intensity profile of fluorescent BSA on HFBS biofilm inside and outside the drop. D: The dose-response curve of fluorescence intensity as a function of the BSA concentration.

performed by dipping the chip into the buffer containing the substrate and by following the absorbance change during several minutes. We have chosen to use a pH 5 buffer and DMP as a substrate, a good tradeoff between stability and activity of the enzyme. A  $30 \mu\text{l}$  drop of the enzyme solution (about 700 U/ml) has been deposited on protein-modified chips ( $1 \text{ cm} \times 1 \text{ cm}$ ) and, after several washing, an activity between 0.1 and 0.2 U has been determined on each chip, resulting in an immobilization yield of 0.5–1%. This value is comparable to the one (7%) obtained in optimized conditions for laccase immobilization on EUPERGIT C 250L<sup>©</sup> [21].

An equal volume of enzyme solution has been spotted on a bare silicon sample as negative control. After the

same washing step, we could not record any activity when the chip was immersed in the DMP buffer.

Taking into account the specific activity of the free enzyme ( $430 \text{ U mg}^{-1}$ ) and its molecular mass (59 kDa),  $0.5 \mu\text{g}$  of laccase corresponds to about 8 pmol ( $5 \times 10^{12}$  molecules) immobilized on each chip. A reasonable evaluation of the surface occupied by a single protein molecule can be based on crystal structures of laccases [22, 23]. This surface should be  $28 \times 10^{-12} \text{ mm}^2$ , considering the protein as a sphere with radius of  $3 \times 10^{-6} \text{ mm}$ . On this basis, the maximum number of laccase molecules on each chip should be  $3 \times 10^{12}$ . These data indicate that the number of active immobilized laccase molecules on each chip is of the same order of magnitude as the maximum expected. Laccase

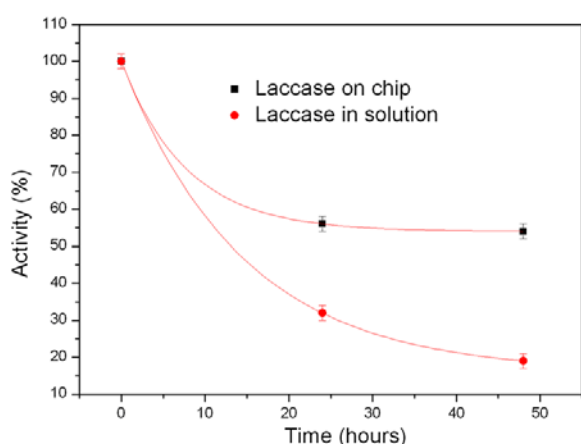


**Fig. 5.** Time-resolved profile of laccase activity of the immobilized enzyme.

assays have been repeated on the same chip after 24 and 48 hours in the same conditions and results are reported in Figure 5. About one half of the activity has been lost after one day, but no variation of the residual activity has been observed after the second day. Moreover, comparison of these data with those of the free enzyme, stored at the same temperature, showed that the immobilized enzyme is significantly more stable than the free form.

## 4 Conclusions

We have demonstrated the bio-modification of the silicon surface by using the self-assembling features of the HFB, an amphiphilic protein purified by the fungus *P. ostreatus*. The nanometric monolayer of proteins, casted on the silicon surface by solution deposition, is very stable from the chemical point of view, since it is still present after strong washing in NaOH and SDS at 100 °C. The biofilm turns a hydrophobic silicon surface into a hydrophilic one, which can be very useful in microfluidic integrated application. The HFB monolayer acts as a bioactive substrate to bind other proteins, such as BSA and laccase. It has been also demonstrated that the enzyme immobilization on the hydrophobin layer improves the enzyme stability.

The authors gratefully acknowledge dr. N. Malagnino of ST. Microelectronics in Portici (NA), Italy, for water contact angle measurements, Prof. P. Arcari (Dept. of Biochemistry and Medical Biotechnologies, University of Naples "Federico II") for fluorescent BSA, dr. F. Autore for the purification of POXC laccase and G. Armenante for technical support.

## References

1. V.V. Tsukruk, *Adv. Mater.* **13**, 95 (2001).
2. W. Xing, J. Cheng (Editors), *Frontiers in Biochip Technology* (Springer, 2006).
3. T. Cha, A. Guo, X.Y. Zhu, *Proteomics* **5**, 416 (2005).
4. P. Angenendt, J. Glokler, D. Murphy, H. Lehrach, D.J. Cahill, *Anal. Biochem.* **309**, 253 (2002).
5. P. Angenendt, J. Glokler, J. Sobek, H. Lehrach, D.J. Cahill, *J. Chromatogr. A* **1009**, 97 (2003).
6. M. Qin, L.K. Wang, X.Z. Feng, Y.L. Yang, R. Wang, C. Wang, L. Yu, B. Shao, M.Q. Qiao, *Langmuir* **23**, 4465 (2007).
7. R. Wang, Y.L. Yang, M. Qin, L.K. Wang, L. Yu, B. Shao, M.Q. Qiao, C. Wang, X.Z. Feng, *Chem. Mater.* **19**, 3227 (2007).
8. O. Gutmann, R. Kuehlewein, S. Reinbold, R. Niekrawietz, C.P. Steinert, B. de Heij, R. Zengerle, M. Daub, *Lab. Chip* **5**, 675 (2005).
9. J.M. Buriak, *Philos. Trans. R. Soc. London* **364**, 217 (2006).
10. L. De Stefano, I. Rea, P. Giardina, A. Armenante, M. Giocondo, I. Rendina, *Langmuir* **23**, 7920 (2007).
11. H.J. Hektor, K. Scholtmeijer, *Curr. Opin. Biotechnol.* **16**, 434 (2005).
12. M. Sunde, A.H.Y. Kwan, M.D. Templeton, R.E. Beever, J.P. Mackay, *Micron* **39**, 773 (2008).
13. M.B. Linder, G.R. Szilvay, T. Nakari-Setälä, M.E. Penttilä, *FEMS Microbiol. Rev.* **29**, 877 (2005).
14. S.O. Lumsdon, J. Green, B. Stieglitz, *Colloids Surf. B Biointerfaces* **44**, 172 (2005).
15. S. Hou, X. Li, X. Li, X. Feng, R. Wang, C. Wang, L. Yu, M.Q. Qiao, *Anal. Bioanal. Chem.* **394**, 783 (2009).
16. G. Palmieri, P. Giardina, L. Marzullo, B. Desiderio, G. Nitti, G. Sannia, *Appl. Microbiol. Biotechnol.* **39**, 632 (1993).
17. W. Kern (Editor), *Handbook of Semiconductor Cleaning Technology* (Noyes Publishing Park Ridge, NJ, 1993) Chapt. 1.
18. K. Kisko, G.R. Szilvay, U. Vainio, M.B. Linder, R. Serimaa, *Biophys. J.* **94**, 198 (2008).
19. A.H. Kwan, R.D. Winefield, M. Sunde, J.M. Matthews, R.G. Haverkamp, M.D. Templeton, J.P. Mackay, *Proc. Natl. Acad. Sci. U.S.A.* **103**, 3621 (2006).
20. L. Yu, B. Zhang, G.R. Szilvay, R. Sun, J. Jänis, Z. Wang, S. Feng, H. Xu, M.B. Linder, M. Qiao, *Microbiology* **154**, 1677 (2008).
21. M.E. Russo, P. Giardina, A. Marzocchella, P. Salatino, G. Sannia, *Enz. Microbiol. Biotechnol.* **42**, 521 (2008).
22. K. Piontek, M. Antorini, T. Choinowski, *J. Biol. Chem.* **277**, 37663 (2002).
23. M. Ferraroni, N.M. Myasoedova, V. Schmatchenko, A.A. Leontievsky, L.A. Golovleva, A. Scozzafava, F. Briganti, *BMC Struct. Biol.* **7**, 60 (2007).



# Biological passivation of porous silicon by a self-assembled nanometric biofilm of proteins

L. De Stefano<sup>1</sup>, I. Rea<sup>1</sup>, E. De Tommasi<sup>1</sup>, P. Giardina<sup>2</sup>, A. Armenante<sup>2</sup>, S. Longobardi<sup>2</sup>, M. Giocondo<sup>3</sup>, and I. Rendina<sup>1</sup>

<sup>1</sup>National Research Council - Institute for Microelectronic and Microsystems-Unit of Naples, Via P. Castellino 111, 80131 Naples, Italy

<sup>2</sup>Dept. of Organic Chemistry and Biochemistry - "Federico II" University of Naples, Via Cinthia, 4 - 80126 Naples, Italy

<sup>3</sup>Licryl – INFM-CNR, Via P. Bucci, Cubo 33/B, 87036 Arcavacata di Rende, Cosenza, Italy

E-mail: [luca.destefano@na.imm.cnr.it](mailto:luca.destefano@na.imm.cnr.it)

**Abstract.** Self-assembled monolayers are surfaces consisting of a single layer of molecules on a substrate: widespread examples of chemical and biological nature are alkylsiloxane, fatty acids, and alkanethiolate which can be deposited by different techniques on a large variety of substrates ranging from metals to oxides. In this paper, we demonstrate that a self-assembled biofilm of proteins can passivate porous silicon (PSi) based optical structures without affecting the transducing properties. Moreover, the protein coated PSi layer can also be used as a functionalized surface for proteomic applications.

## 1. Introduction

Self-Assembled Monolayers (SAM) are mono-molecular films formed on a solid surface by spontaneous organization of their constituents: thiol compounds on gold is one of the well-established combinations [1]. SAMs are very attractive alternative to the chemical passivation of surfaces based on deposition techniques, such as cathodic evaporation or sputtering, in particular when very thin film are required: repeatable and homogeneous films of tenths of nanometers are difficult to massively produce by standard microelectronic technologies. When the substrate is a porous material, such as mesoporous silica, zeolites or porous silicon, the SAM could sometimes be the only way to obtain a good quality coating of the internal surface. Among others porous materials, PSi can be considered a very attractive transducer for the monitoring of biochemical interactions, since on exposure to gaseous or liquid substances some physical parameters, such as dielectric constant, conductivity, and photoluminescence of PSi structures undergo strongly changes [2-5]. On the other hand, some troubles could arise from the chemical instability of the as-etched PSi surface: PSi is fabricated by electrochemical dissolution of doped silicon in a water based solution of hydrofluoric acid, so that being highly hydrogenated its surface tends to be slowly oxidized when in contact with air. Moreover, PSi is easily dissolved by aqueous alkaline solutions such as sodium hydroxide or potassium hydroxide. A common way to stabilize PSi devices is the silanization of oxidized PSi by using a chemical SAM, the aminopropyltriethoxysilane, which has been recently reported in literature [6]. Even if oxidized, PSi retains its sponge-like morphology and still shows high value of specific surface up to  $100 \text{ m}^2/\text{cm}^3$ . Nevertheless, the thermal or chemical oxidation of PSi could be a not desirable step since it implies a strong modification of some important physical parameters of PSi, first of all the refractive index value. In general, surface chemistry can be very effective but requires several reaction steps and, as any wet process, can be limited by the hydrostatic pressure which prevents the solution penetration in very small pores so that reducing the passivation rate of inner pores. We have recently demonstrated that a direct biological route to the passivation of semiconductor surface is possible: a self-assembled biofilm of hydrophobins (HFBs) effectively protects the silicon and PSi surface against alkaline dissolution [7, 8]. The HFBs are a family of small fungal proteins produced in the hyphal cell walls that can be purified by the culture medium. The HFBs self-assemble into thin and amphiphilic membranes at hydrophilic-hydrophobic interfaces, such as air-water or water-solid. HFBs are generally classified on the basis of the biofilm resistance: the class I HFBs form high insoluble assemblies, which can be dissolved only in strong acids, such as trifluoroacetic acid, whereas the class II biofilms can be dissolved in ethanol or in sodium dodecyl sulphate [9]. In this work, we demonstrate how the infiltration by adsorption of the class I hydrophobin from the fungus *Pleurotus ostreatus* in porous silicon monolayers and multilayers can tune their physical and chemical properties, enhancing their features in the field of biochemical sensing.

## 2. Materials and methods

For this study, we used a porous silicon film, which optically behaves as a Fabry-Perot interferometer, fabricated by the electrochemical etching of p<sup>+</sup>-type (100) crystalline silicon (resistivity 8-12 mΩ cm) in HF/EtOH (30:70) solution. The etching current had a value of 62 mA/cm<sup>2</sup> and was applied for 2.6 s. We also realized a multilayer structure, namely a porous silicon optical microcavity (PSMC), constituted by a  $\lambda/2$  Fabry-Perot optical resonator sandwiched between two Bragg reflectors of nine periods, each one realized by alternating layers with high and low refractive indices. The PSMC was obtained by electrochemical etch in a HF-based solution (50 wt. % HF : ethanol = 3 : 7) in dark and at room temperature. A current density of 39 mA/cm<sup>2</sup> for 1.1 s was applied to a highly doped p<sup>+</sup>-type standard silicon wafer, <100> oriented, 10 mΩ cm resistivity, 400 μm thick producing the high refractive index layer (with a porosity of 69 %) while a current density of 94 mA/cm<sup>2</sup> was applied for 1 s in the case of the low index layer (with a porosity of 76 %). The  $\lambda/2$  layer is a high refractive index one. This structure has a characteristic resonance peak at 1260 nm in the middle of a 125 nm broad stop band. The reflectivity optical spectra, due to a white light source illuminating the sample through an optical fiber, were measured over the range 600-1600 nm with a resolution of 0.2 nm by an optical spectrum analyzer (Ando model AQ6315A). Purification and preparation of the HFB proteins are described in the papers [7, 8] and references therein.

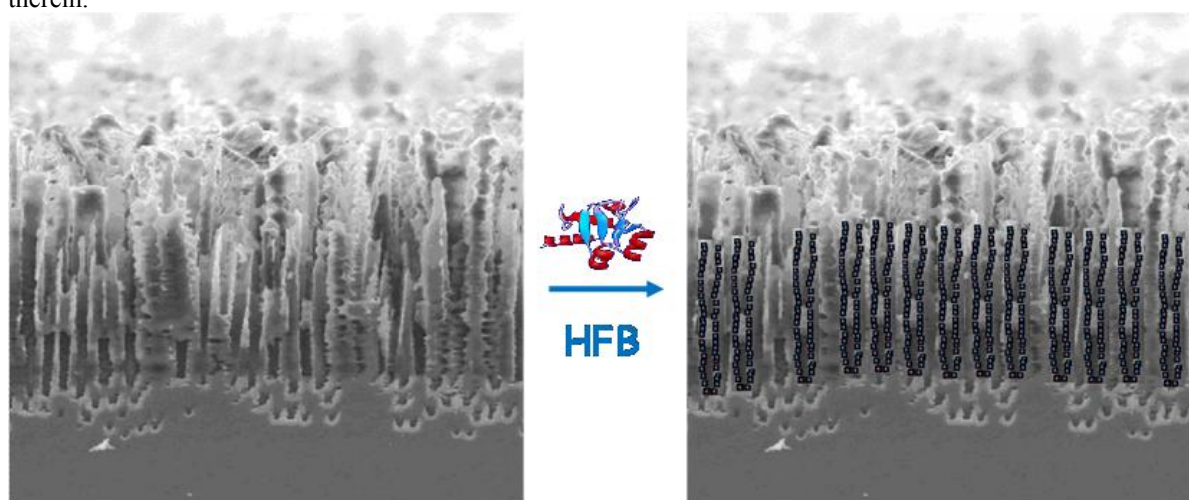


Figure 1. Schematic of HFB infiltration in porous silicon structures.

Ethanol-deionized water (60% V/V) solutions containing 0.11 mg/ml of hydrophobins were used to rinse porous silicon by immersion. The high ethanol concentration assures the HFB solution penetration in the hydrophobic porous silicon. Each sample has been rinsed for 1h, then dried for 10 min. on the hot plate at 80 °C and washed by the same solution used for the deposition.

Thicknesses and porosity of PSi layers have been estimated by variable angle spectroscopic ellipsometry. The ellipsometric parameters  $\Psi$  and  $\Delta$  have been measured at an incident angle of 65°, over the range 360-1600 nm with a resolution of 5 nm by a variable angle spectroscopic ellipsometer (mod. UVISEL Horiba-Jobin-Yvon)

## 3. Experimental results and discussion

It is well known that the main drawback in using PSi as an optical transducer for biochemical sensing is represented by its hydrogenated surface: Si-H bonds make the PSi surface highly hydrophobic, thus preventing the penetration of biological solution in the pores. Moreover, the as-etched PSi surface is chemically unstable: hydrogen tends to be substituted by oxygen thus determining the oxidation of the material. Silicon dioxide has a refractive index much lower than crystalline silicon so that oxidation can be really unwanted in the fabrication of high contrast optical devices such as Bragg mirrors or optical microcavity. The HFBs have hydrophobic domains which can strongly interact with the PSi hydrogenated surface so that a stable biofilm self-assembles on the inner surface of nanometric pores. The biofilm is so compact that oxygen cannot pass through this biologic barrier and

the oxidation process can not take place. From the optical point of view, the nanometric layer of proteins do not affect in a sensitive way the optical response of the device.

In order to demonstrate the effectiveness of the biological passivation in PSi multilayers, we have fabricated two twins optical microcavities, constituted by 20 layers of porous silicon having different porosities, and one has been infiltrated by HFBs, while the other one not. Then, we have exposed both the samples to an atmosphere saturated of water vapour for five days and the reflectivity spectra of both samples have been compared with their original ones. As it can be noted from the graphics reported in Figure 2, the reflectivity spectrum of the PSi bare microcavity (left graph) undergoes a irreversible blue-shift of 6 nm, which means that water can not infiltrate by capillary condensation in the nanometric pores and the PSi surface has been slightly oxidized [10]. On the contrary, the HFB infiltrated PSi optical microcavity shows a red-shift of 7 nm in its reflectivity spectrum (right graph): in this case, due to the presence of the proteins biofilm, the water vapour can condense in the nanometric pores of the PSi layer. The effect is repeatable and reversible so that a protein coated PSi microcavity can be used as an optical humidity sensor.

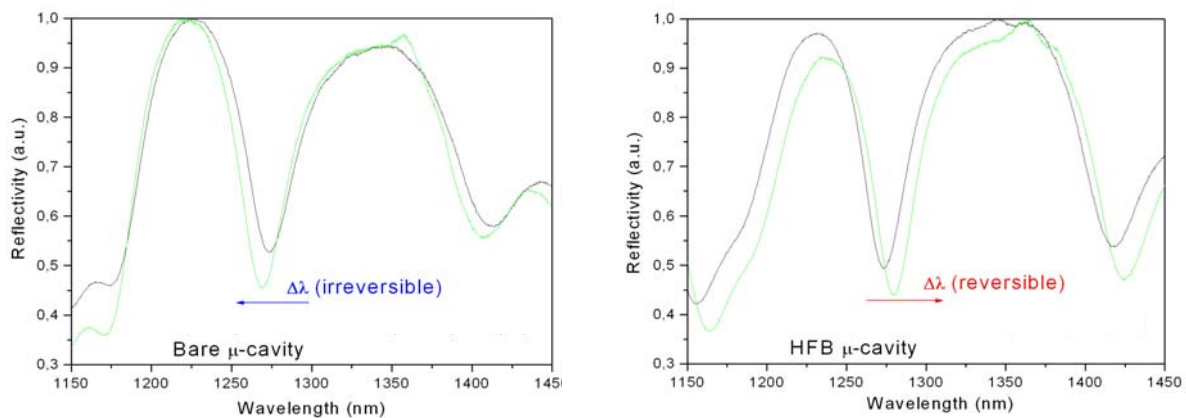


Figure 2. PSi optical microcavities on exposure to water vapors: a bare sample (left graph) is oxidized, while a HFB infiltrated sample (right graph) shows a reversible red-shift. Black and green lines are representative of PSMC optical spectrum before and after water vapors exposure, respectively.

Bare PSi is rapidly etched in alkaline solutions but also dissolution by biological molecules has been recently reported: DNA hybridization enhances the porous silicon corrosion by an oxidation-hydrolysis mechanism; bovine serum albumin (BSA), when adsorbed on PSi, strongly damages its nanostructures and partially lifts-off the film from the substrate [11, 12]. This is a severe limitation for PSi use in genomic and proteomic applications, like DNA optical microarrays. When self-assembled in biofilm, HFB can work as an active substrate for anchoring other proteins: the biofilm exposes the hydrophilic domains which can be used to not covalently bind the proteins. We have fabricated two twins film of PSi having the same porosities and the same thickness, then we have deposited, by adsorption from solution, a rhodamine labeled BSA, 3  $\mu$ M. Both samples have been incubated overnight at room temperature, then they have been rinsed in deionized water to remove the excess of biological matter. In Figure 3 we report the optical photograph of both the PSi chip, together with the fluorescent images captured by a fluorescence macroscopy (Leica Z16 APO). In the inset I, the optical images of the PSi chip are reported after the incubation of BSA and the rinsing in water: the A sample is the bare PSi, and the B is the protein coated sample. From these images, it is well evident that the porous silicon is seriously damaged on the A chip; while the PSi surface is completely preserved in the case of the HFB infiltrated sample. In the inset II, a particular of the fluorescent image on the A sample surface registered by the fluorescence microscope is reported: the rhodamine labeled BSA is scarcely present and the damaged surface is evident. on the contrary, the photo depicted in the inset III, shows a rhodamine labeled BSA distributed very homogeneously and the PSi surface is preserved, also in presence of an excess of BSA protein.

The qualitative results of optical and fluorescence imaging have been confirmed by the quantitative characterization performed by variable angle ellipsometric spectroscopy. We have deposited different concentrations of rhodamine labeled BSA on the same chip and we have measured the optical thickness, i.e. the refractive index times the physical thickness of the PSi sample for each deposition step, after the incubation in

the BSA solution. In the case of protein coated PSi layer the optical path remains almost constant, while in case of the bare PSi the value goes rapidly to zero, as it can be observed in Figure 4, which means that there is not more any porous layer on the chip.

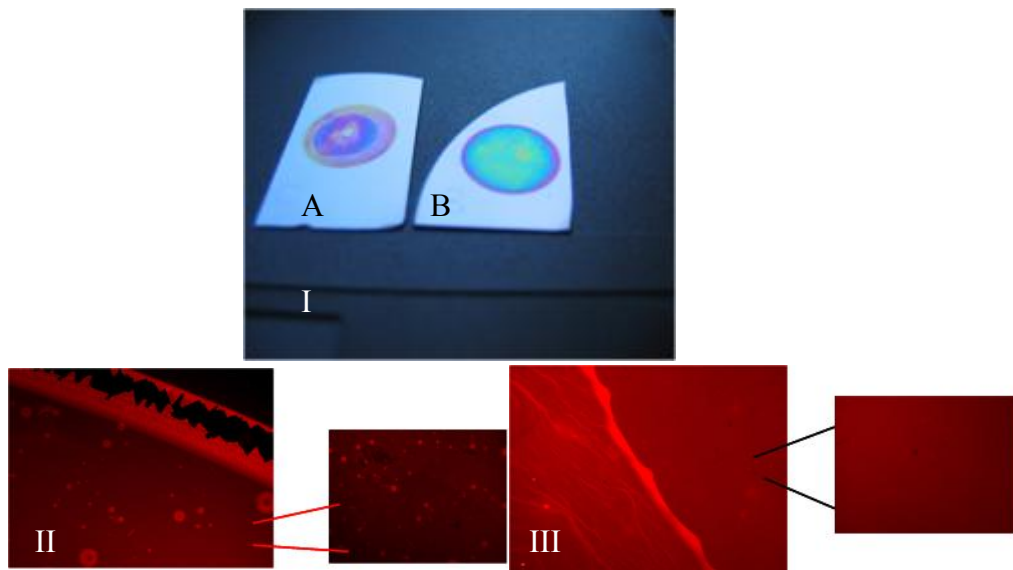
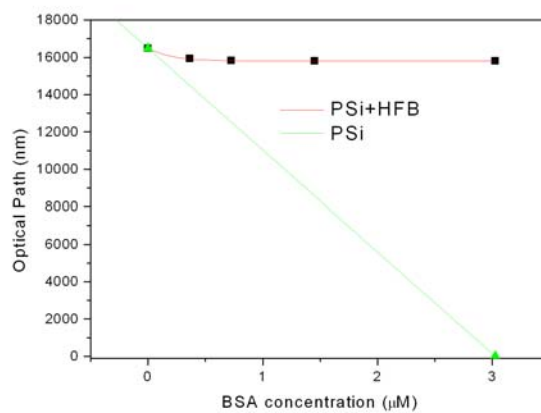


Figure 3. I: Optical images of two twins PSi chip on which BSA has been incubated overnight: A is a bare layer of PSi, while B is a protein coated chip. From the image is evident that PSi is seriously damaged in A sample while the B is perfectly stored. II: fluorescence images by macroscopy: in the A sample the rhodamine labeled BSA is scarcely present and the damaged surface is evident. III: in the B sample the rhodamine labeled BSA is



very homogeneous and the surface is preserved.

Figure 4. Ellipsometric determination of samples optical thicknesses after incubation in solutions with different concentration of BSA.

## 5. Conclusions

We have biologically modified PSi structures by infiltrating HFBs proteins by solution deposition technique. The biofilm coated devices shows high chemical stability on exposure to water vapours or when in contact with BSA, which normally cracks the PSi. In conclusion, we believe that the biological route to PSi surface passivation can be very effective and it constitutes a good alternative to chemical standard processes.

## References

- [1] M.J. Stevens, G.S. Grest, *Biointerphases* 2008, 3, 3.
- [2] Dancil K -P S, Greiner D P and Sailor M J 1999 *J. Am. Chem. Soc.* 121 (34) 7925-7930
- [3] De Stefano L, Moretti L, Rossi A M, Rocchia M, Lamberti A, Longo O, Arcari P and Rendina I *IEEE Trans. Nanotech.* 2004, 3 (1), 49-54.
- [4] L. De Stefano, L. Rotiroti, I. Rea, I. Rendina, L. Moretti, G. Di Francia, E. Massera, P. Arcari, A. Lamberti, C. Sangez, *Journal of Optics A: Pure and Applied Optics* 2006, 8, S540-S544.
- [5] L. De Stefano, M. Rossi, M. Staiano, G. Mamone, A. Parracino, L. Rotiroti, I. Rendina, M. Rossi, and S. D'Auria, *Journal of Proteome Research* 2006, 5, 1241-1245.
- [6] L. De Stefano, L. Rotiroti, I. Rea, I. Rendina, P. Arcari, A. Lamberti, C. Sanges, *Sensors* 2007, 7, 214-221.
- [7] L. De Stefano, I. Rea, P. Giardina, A. Armenante, M. Giocondo, I. Rendina, *Langmuir* 2007, 23, 7920.
- [8] L. De Stefano, I. Rea, P. Giardina, A. Armenante, I. Rendina, *Adv. Mat.* 2008, 20 (8), 1529-1533.
- [9] H.A.B. Wosten and M. L. de Vocht, *Biochimica and Biophysica Acta* 2000, 1469, 79.
- [10] L. Moretti, L. De Stefano, I. Rendina, *J. Appl. Phys.* 2007, 101, 024309.
- [11] C. Steinem, A. Janshoff, V.S.-Y. Lin, N.H. Volcker, M. Reza Ghadiri, *Tetrahedron* 2004, 60, 11259-11267.
- [12] L. Tay; N L. Rowell; D Poitras; J W. Fraser; D J. Lockwood; R Boukherroub, *Canadian Journal of Chemistry* 2004, 82, 1545-1553.



# The *Pleurotus ostreatus* hydrophobin Vmh2 and its interaction with glucans

Annunziata Armenante<sup>2</sup>, Sara Longobardi<sup>2</sup>, Ilaria Rea<sup>3</sup>,  
Luca De Stefano<sup>3</sup>, Michele Giocondo<sup>4</sup>, Alba Silipo<sup>2</sup>,  
Antonio Molinaro<sup>2</sup>, and Paola Giardina<sup>2,1</sup>

<sup>2</sup>Department of Organic Chemistry and Biochemistry, University of Naples “Federico II”, Via Cintia 4, 80126, Naples, Italy; <sup>3</sup>Unit of Naples-Institute for Microelectronics and Microsystems, National Council of Research, Via P. Castellino 111, 80131, Naples, Italy; and <sup>4</sup>CNR-INFM LICRYL-Liquid Crystals Laboratory, c/o Dipartimento di Fisica, Università della Calabria, 87036 Rende, Italy

Received on February 9, 2009; revised on December 22, 2009; accepted on January 19, 2010

**Hydrophobins are small self-assembling proteins produced by fungi. A class I hydrophobin secreted by the basidiomycete fungus *Pleurotus ostreatus* was purified and identified. The pure protein is not water soluble, whereas complexes formed between the protein and glycans, produced in culture broth containing amylose, are soluble in water. Glycan structure matched to cyclic structures of  $\alpha$ -(1-4) linked glucose containing from six to 16 monomers (cyclodextrins). Moreover, it was verified that not only pure cyclodextrins but also a linear oligosaccharide and even the simple glucose monomer are able to solubilize the hydrophobin in water. The aqueous solution of the protein—in the presence of the cyclic glucans—showed propensity to self-assembly, and conformational changes towards beta structure were observed on vortexing the solution. On the other hand, the pure protein dissolved in less polar solvent (60% ethanol) is not prone to self assembly, and no conformational change was observed. When the pure protein was deposited on a hydrophobic surface, it formed a very stable biofilm whose thickness was about 3 nm, whereas the biofilm was not detected on a hydrophilic surface. When the water-soluble protein—in the presence of the cyclic glucans—was used, thicker (up to 10-fold) biofilms were obtained on either hydrophilic or hydrophobic surfaces.**

**Keywords:** biotechnology/cyclodextrins/proteins/self-assembly

## Introduction

Hydrophobins are small proteins (about 100 amino acid residues) produced by fungi as soluble forms, self-assembling into an amphipathic membrane when they reach an interface

(e.g., medium–air or cell wall–air). Because of their properties, these proteins play a role in the formation of aerial hyphae, spores, in fruiting body and in the attachment of hyphae to hydrophobic surfaces during symbiotic or pathogenic interactions (Wösten 2001). The intriguing properties of these proteins make them of great interest to biotechnologists, as they have potentialities for numerous applications (Hektor and Scholtmeijer 2005). They could be used as coatings to increase biocompatibility of medical implants, to immobilize enzymes on surfaces, in cosmetic industry for hair-care products or in drug delivery.

At the molecular level, hydrophobins have low sequence identity but for the presence of eight cysteine residues forming a conserved four-disulfide bonding pattern (Sunde et al. 2008). Analyses of the known fungal genomes indicate that hydrophobins are encoded as gene families ranging from two to seven members, with the exception of *Coprinus cinereus* genome, which has 23 hydrophobin encoding genes. Hydrophobins have been split into two groups, class I and class II, based on the differences in their hydrophobicity patterns, spacing of amino acids between the cysteine residues and properties of the aggregates they form (Linder et al. 2005). Class I hydrophobins generate very insoluble assemblies, which can only be dissolved in strong acids (i.e., 100% trifluoroacetic acid (TFA)). Assemblies of class II can be more easily dissolved in ethanol or sodium dodecyl sulfate. Class II hydrophobins have been only detected in Ascomycetes, while those of class I have been identified in Ascomycetes and Basidiomycetes. One distinguishing feature of class I hydrophobins is the characteristic rodlet structure observed on the hydrophobic side of the amphipathic protein film. The morphology of isolated rodlets is reminiscent of amyloid fibrils, whereas the aggregates of class II hydrophobins lack the rodlet morphology, are non-amyloid and are needle like.

SC3 from *Schizophyllum commune* is one of the most characterized members of the class I hydrophobin family. SC3 contains approximately 20 mannose residues O-linked through threonine residues in the N-terminal region of the protein, a modification that increases the hydrophilicity of that region of the polypeptide chain (de Vocht et al. 1998). When SC3 has been induced to self-organize at the air/water or Teflon/water interface, a small, transient increase in  $\alpha$ -helical secondary structure has been observed, followed by an increase in  $\beta$ -sheet structure (Wang et al. 2002; Wang, Permentier, et al. 2004). More recently, the 3D structure in solution of another class I hydrophobin, EAS from *Neurospora crassa*, has been resolved (Kwan et al. 2006). EAS forms a  $\beta$ -barrel structure interrupted by some disordered regions and displays a complete segregation of charged and hydrophobic residues on its surface. On the

<sup>1</sup>To whom correspondence should be addressed: Fax: +39 081674313; e-mail: giardina@unina.it

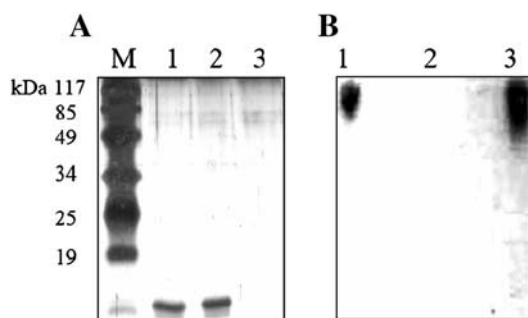


**Fig. 1.** SDS-PAGE of Hyd-w (lane 1), Hyd-et (lane 2) and the precipitate obtained from Hyd-et (lane 3). M,  $M_w$  markers. (A) Half of the gel stained by silver staining, (B) half of the gel stained by periodic acid.

basis of this structure, a model for the polymeric rodlet structure formation has been proposed.

Class II hydrophobins are more easily handled because they have less tendency to aggregate. The crystal structures of two class II hydrophobins, HFBI and HFBII of *Trichoderma reesei*, have been determined, and several other studies on these two proteins have been performed (Hakanpää, Linder, et al. 2006; Hakanpää, Szilvay, et al. 2006). The amino acid sequence of HFBII is 70% similar to HFBI, their 3D structures are similar and they form similar, hexagonally ordered films (Szilvay et al. 2007). The assemblies of HFBI have been recently shown to be more stable than those of HFBII, as the former can tolerate changes in temperature and pH and addition of ethanol better than the latter (Kisko et al. 2008). The differences in their behaviors could reflect different roles in fungal life.

Aside from these studies, very little is known about other hydrophobins, their characteristics and the films they form. It might be mainly due to the difficulties in extracting and handling these self-assembling proteins. A deeper knowledge of the properties and behaviors of other fungal hydrophobins, both in solution or assembled, is needed to generalize results obtained so far. We are contributing to this goal studying the hydrophobins secreted by the basidiomycete fungus *Pleurotus ostreatus*. It is a well-known edible mushroom, and its ligninolytic and biodegradative abilities have been widely reported (Cohen et al.

2002). Several hydrophobin encoding genes have been identified in *P. ostreatus*, and their expression in different growth stages or culture times has been studied (Peñas et al. 1998; Peñas et al. 2002), whereas very little is known on the encoded proteins, their structures and their potential applications.

In this paper, we analyze at molecular level the hydrophobin secreted by *P. ostreatus* mycelia, its behavior in solution and its interaction with glycans produced by the fungus or other oligo- and monosaccharides.

## Results

### Purification and analyses of the protein

*P. ostreatus* was grown in static cultures using potato dextrose broth (24 g/L) containing 0.5% yeast extract (PDY) till the mycelia completely covered the liquid surfaces. The amount of the lyophilized material, obtained after air bubbling into the liquid broths and centrifugation, ranged from 5 to 10 mg/L. After the TFA treatment, the dried material was dissolved in water (Hyd-w) and analyzed by sodium dodecyl sulfate polyacrylamide gel electrophoresis (SDS-PAGE), showing a unique protein band at about 10 kDa (Figure 1A). Since about 0.5–1 mg of proteins per liter of culture broth were determined by bicinchoninic acid (BCA) protein assay, nonprotein components have to be present in the dried material obtained after bubbling. Further treatment of this material with 60% ethanol extracted the hydrophobin in the ethanol solution (Hyd-et), as verified by SDS-PAGE (Figure 1A), leaving the nonprotein component as insoluble precipitate. The presence of glycans in Hyd-w and in the ethanol precipitate was demonstrated by the phenol-sulfuric acid test and by periodic acid staining of the SDS-PAGE (Figure 1B).

After glycan separation by precipitation in 60% ethanol, the protein was only soluble in the presence of ethanol, not in pure water. Therefore these glycans, when present, co-aggregate during air bubbling with hydrophobins, making the protein soluble in water.

However, if the hydrophobin was purified from *P. ostreatus* grown in malt extract (ME) cultural broth (a medium without amylose), the protein was not soluble in water but was soluble in 60% ethanol. In this condition no precipitate was formed,

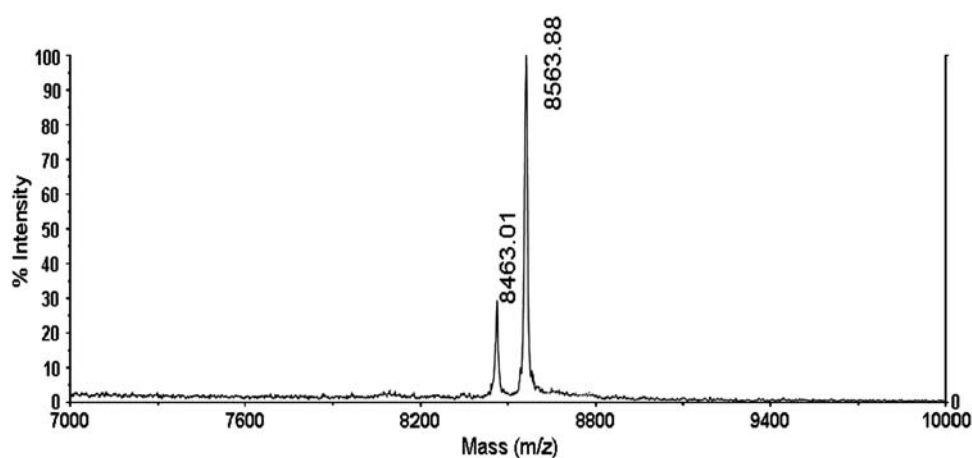


**Fig. 2.** MALDI-MS spectrum of Hyd-w (linear mode using sinapinic acid as matrix).

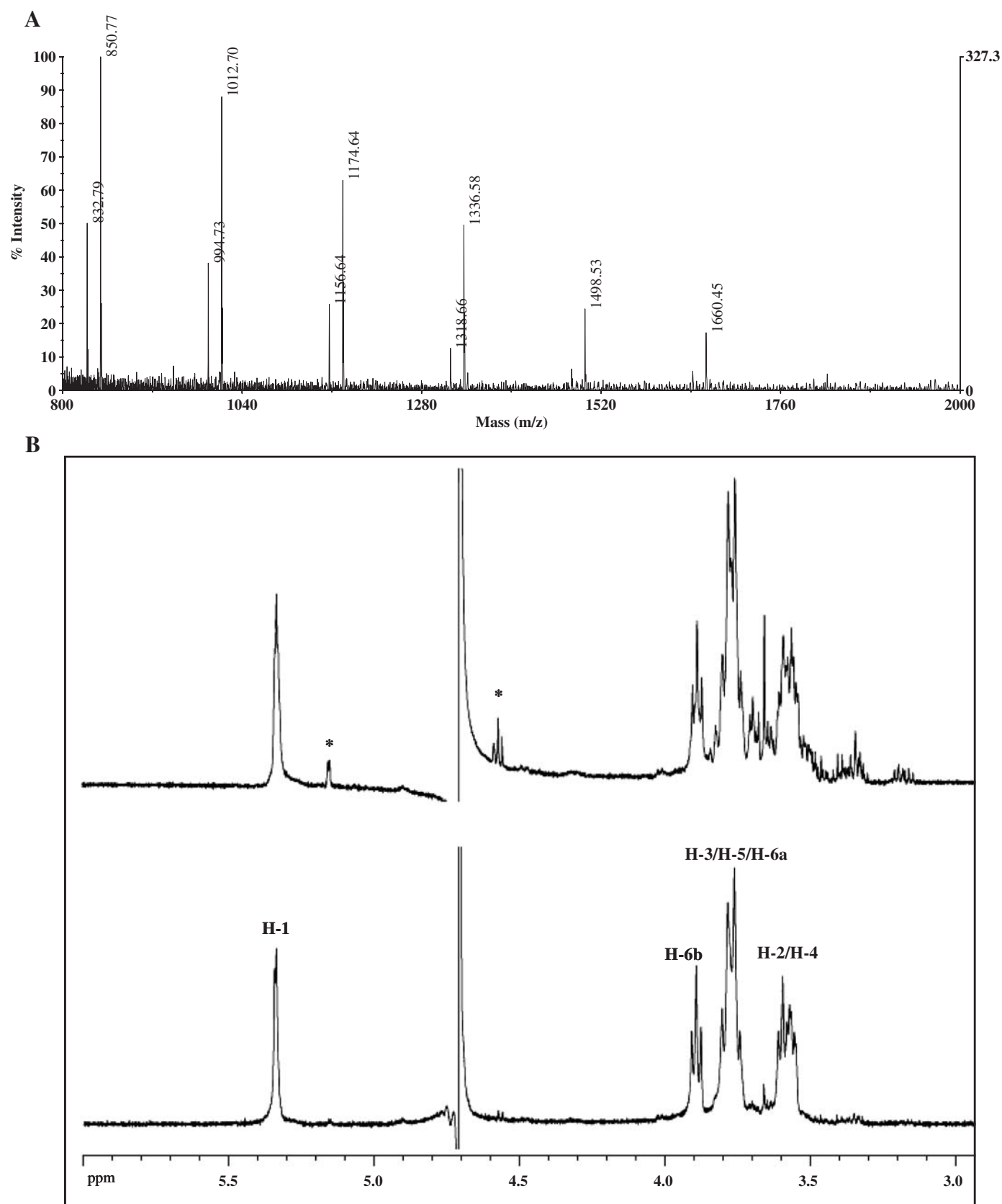


**Fig. 3.** (A) MALDI-MS spectrum (reflectron mode using DHB as matrix) of glycans from Hyd-w, after incubation at 110°C for 2 h at pH 3. Peaks corresponding to cyclic structures ( $162n + 23$ , sodium ion adduct) and peaks corresponding to linear structures ( $162n + 18 + 23$ ) are shown. (B) Comparison of the  $^1\text{H}$  NMR spectrum of the  $\alpha$ -(1 $\rightarrow$ 4) glucan before (bottom) and after (up) the acid hydrolysis. The anomeric signals of the reducing units are labeled (up), and the ring proton signals have been indicated (bottom).



indicating the absence of the glycan component in this sample. This evidence has been confirmed by the lack of any detectable band when the sample was loaded on periodic acid-stained SDS-PAGE.

#### Structural analyses

Matrix-assisted laser desorption/ionization mass spectrometry (MALDI-MS) spectra of the samples (Hyd-w and Hyd-et) showed two peaks at 8463 and 8564  $m/z$  (Figure 2), in which the relative intensity of the latter was higher than the former in all the protein purifications.

According to Penās et al. (2002), *P. ostreatus* hydrophobins undergo a proteolytic processing after signal peptide removal. The peak at 8564  $m/z$  can be attributed to Vmh2-1 (TrEMBL accession number Q8WZI2), starting from T25 and with the eight cysteine residues linked in four disulfide bridges, and the peak at 8463  $m/z$  to the same protein after further removal of the N-terminal threonine residue. Analysis of the MALDI-MS spectrum of the tryptic peptides, obtained by in situ hydrolysis, showed the presence of the expected peaks at 2002  $m/z$  (D26-K44) and 2103  $m/z$  (T25-K44), whereas the other expected peak at 6939  $m/z$  (corresponding to the peptide A45-L113) was not detected. The absence of this peak could be due to the difficult extraction of such a large peptide by the polyacrylamide gel.

The identity of the protein and its N-terminal processing was confirmed by liquid chromatography-MS-MS analysis. Fragmentation of the 2103 and 2002  $m/z$  peaks led to the sequences SCSTGSLQC (S29-C37) and CSTGSLQCCSSV (C30-V41) (Supplementary data, Fig. 1), respectively.

The protein was purified from fungal cultures grown at different times (5, 10, 15 or 20 days) and directly analyzed by MALDI-MS. A relative increase of the intensity of the peak corresponding to the form with D26 as N terminus, with respect to that with T25, was observed in older cultures. Furthermore, a peak at 8449  $m/z$ , probably corresponding to the form lacking also D26, was detected in the preparation from 15- and 20-day-old cultures.

The glycan component of Hyd-w was also subjected to chemical and spectroscopic analyses after purification by ethanol precipitation. Carbohydrate analysis by gas–liquid chromatography (GLC)-MS revealed exclusively the presence of 4-substituted D-glucose in pyranose form (4-D-Glcp); no terminal residues were detected, neither reducing nor non-reducing. The proton nuclear magnetic resonance ( $^1\text{H}$  NMR) spectrum of this glucan showed proton signals in the anomeric and ring sugar regions. The water-dissolved precipitate was fully assigned by 2D NMR spectroscopy that confirmed the presence of a single component, an  $\alpha$ -(1→4) glucan. It is worth noting that reducing ends were also undetectable by NMR.

The analysis of MALDI-MS spectra of such glucan showed the presence of several peaks whose molecular masses agreed with the theoretical values for cyclic glucans with degree of polymerization from 6 to 16. As a matter of fact, a cyclodextrin blend should have a mass of  $162n$ , whereas glucans in any noncyclic structure should have a molecular mass of  $162n + 18$ .

Incubation of the cyclic glucan at 110°C for 2 h at pH 3 led to partial hydrolysis of the cyclic glucans, as shown in the MS

spectrum reported in Figure 3A. In agreement, in the  $^1\text{H}$  NMR spectrum of this sample (Figure 3B), the presence of anomeric reducing signals was detectable.

No precipitate was obtained treating fresh PDY medium with the procedure described for hydrophobin purification. Moreover, the glycan component was absent in hydrophobin samples purified from *P. ostreatus* grown in ME cultural broth, as already mentioned above. Taking into consideration that amylose (( $\alpha$ -(1→4)-Glc) $_n$  glucan), a component of the PDY cultural broth coming from potato infusion, is absent in the ME culture broth, these results point out that the cyclic glucans are produced by the fungus grown in the presence of amylose.

#### Analyses of the protein–glucan interaction

A glucan/protein ratio of about 6 ( $w/w$ ) was determined for Hyd-w samples. Once cyclic glucans were removed by ethanol precipitation, the dried TFA-treated hydrophobin was not soluble either in the cyclic glucans aqueous solution, at the above reported ratio or in PDY broth. A water-soluble protein was re-obtained when the aqueous solution of the cyclic glucans was added to the Hyd-et solution, and the air-bubbling procedure (vortexing, centrifugation, lyophilization and TFA treatment) was performed. On the other hand, when the same procedure was performed using fresh PDY broth, no water-soluble protein was found. The presence of the protein in the aqueous solution was assessed by BCA assay, SDS-PAGE and MALDI-MS spectra. Hence, co-aggregation of the hydrophobin with the fungal cyclic glucans is needed to obtain the hydrophobin in aqueous solution.

In order to investigate the structural requirements of glucans for the hydrophobin solubilization in water, some commercial molecules were tested in comparison with the cyclic glucans produced by the fungus, following the protocol described above. When  $\alpha$ ,  $\beta$  or  $\gamma$  cyclodextrins were used, the presence of the protein in the aqueous solution was verified in all the samples. Moreover, the protein was solubilized even when maltohexaose, the linear form of the  $\alpha$  cyclodextrin, was tested. Afterwards, the ability of glucose to solubilize the hydrophobin was also proved and then analyzed in deeper details. In order to assess the glucose–hydrophobin interaction, a gel filtration chromatography was performed (Supplementary data, Fig. 2) using two different glucose/hydrophobin ratios (6 and 120  $w/w$ ). In both cases, the presence of glucose in the protein peak with a ratio of about 5  $w/w$  (corresponding to 200 ÷ 300 mol/mol) was verified. These results suggest that different types of glucans in comparable amounts can interact with the hydrophobin, allowing its water solubility. Among the glucans tested, just the amylose contained in the PDY broth was unable to solubilize the protein.

#### Analyses of hydrophobin aggregation

Since hydrophobins are prone to interfacial self assembly in response to external stimuli like agitation of the solution, we have investigated the hydrophobin behavior in water—in the presence of cyclic glucans—or ethanol solution by analyzing SDS-PAGE, protein concentration, circular dichroism (CD) and fluorescence spectra before and after vortexing.

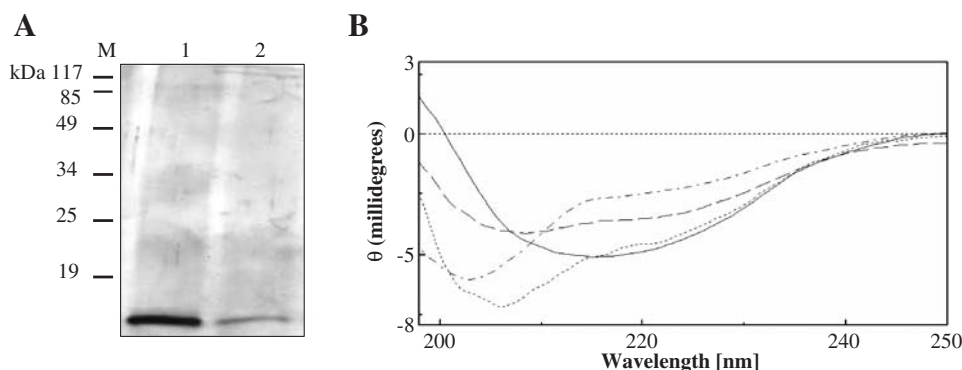


**Fig. 4.** (A) SDS-PAGE of Hyd-w (lane 1); Hyd-w after vortexing (lane 2). (B) CD spectra of Hyd-w (sample 1, dashed-dotted line; sample 2, dotted line; and sample 3, dashed line; each one at 0.15 mg/mL protein concentration) and sample 1 after vortexing (solid line).

A remarkable decrease of Hyd-w concentration was observed in the supernatant of vortexed solution. Protein concentration dropped down, as it can be inferred by the intensity of the SDS-PAGE band of the hydrophobin (Figure 4A).

CD spectra of Hyd-w slightly varied from sample to sample (Figure 4B) even when the same dried sample was apparently suspended in the same conditions. In all the samples, however, a significant contribution of random structure was noticed. Conformational changes with a large shift towards  $\beta$  structure were observed after vortexing (Figure 4B).

Significant changes of the secondary structure were also observed between 70°C and 80°C, registering CD spectra of Hyd-w at different temperatures in the range from 30°C to 90°C.

When the pure protein was dissolved in 60% ethanol (Hyd-et), no variation of band intensities on SDS-PAGE was observed after vortexing (Figure 5A). CD spectra of Hyd-et were recorded, showing a substantial contribution of  $\alpha$  helix to the secondary structure of the protein (Figure 5B). Interestingly, no change of the spectrum was detectable after vortexing these samples.

We also tried to suspend dried Hyd-et in 20% ethanol. The intensity of the SDS-PAGE band of this sample was much lower than that one obtained in 60% ethanol dissolving the same amount of protein (data not shown), and the corresponding CD

spectrum showed similar profile but at lower intensity (Figure 5B). No variation of these parameters was observed after vortexing, as for Hyd-et in 60% ethanol.

Furthermore, when the percentage of ethanol in Hyd-et solutions was decreased, protein bands on SDS-PAGE were observed up to 20% ethanol, while no band was present at 10% ethanol, yet again indicating that the protein aggregates in more polar solution.

The binding of thioflavin-T (ThT) to Hyd-w or Hyd-et was evaluated through the analyses of fluorescence spectra of samples before and after aggregation induced by vortexing. In Figure 6, the remarkable increase of the fluorescence intensity obtained for Hyd-w, not for Hyd-et, is shown thus confirming the formation of amyloid-like aggregates starting from the water solution of the hydrophobin.

#### Biofilm analyses

In order to analyze the Vmh2 aggregates, biofilms were formed on hydrophobic (silicon) or hydrophilic (oxidized silicon) surfaces using both Hyd-w or Hyd-et. The biofilm characterization has been performed by variable-angle spectroscopic ellipsometry (VASE) on at least six samples prepared in the same experimental conditions; the optical model for experimental data fitting has been developed in a

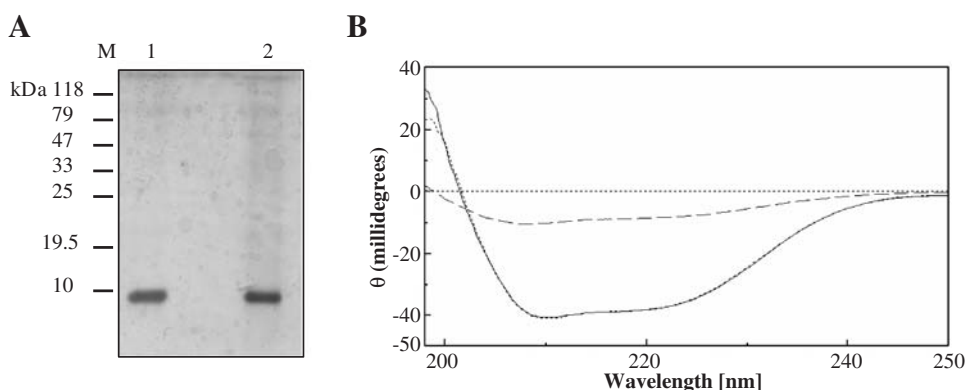


**Fig. 5.** (A) SDS-PAGE of Hyd-et (lane 1); Hyd-et after vortexing (lane 2). (B) CD spectra of Hyd-et in 60% ethanol (solid line), Hyd-et after vortexing (dotted line) and Hyd-et in 20% ethanol (dashed line).

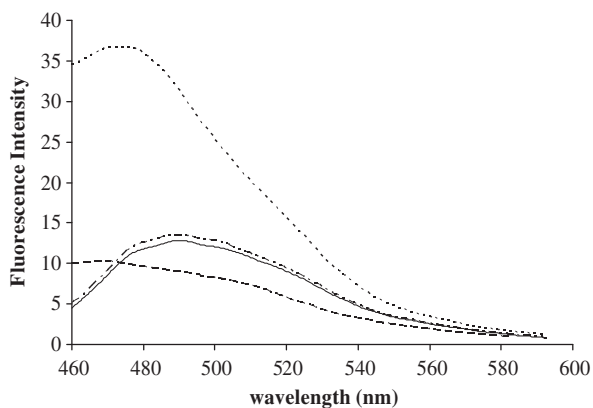


**Fig. 6.** Fluorescence spectra of Hyd-w and Hyd-et in the presence of ThT before and after vortexing: Hyd-w, dashed line; Hyd-w after vortexing, dotted line; Hyd-et, solid line; Hyd-et after vortexing, dashed-dotted line.

previous work (De Stefano et al. 2007). Hyd-et forms a very stable biofilm on silicon whose thickness is  $3.1 \pm 0.7$  nm, whereas Hyd-et did not stably interact with oxidized silicon; thus, the biofilm was not detectable. On the other hand, Hyd-w forms biofilms whose thickness was highly variable, sometimes significantly thicker than when Hyd-et was used on crystalline silicon. The Hyd-w biofilms thickness ranged from 3.5 to 30 nm on the silicon surface and from 6 to 38 nm on the oxidized silicon surface.

## Discussion

A hydrophobin secreted by the basidiomycete fungus *P. ostreatus* was purified and identified as Vmh2-1. Its encoding gene and cDNA had been previously isolated and sequenced by Penãs et al. (2002). The secreted protein undergoes a proteolytic processing, since the N terminus is either T25 or D26, whereas the expected signal peptide is M1-A21 according to the SignalP prediction program (<http://www.cbs.dtu.dk/services/SignalP>). Sequence analysis (hydropathy pattern and spacing between the cysteine residues) and robustness of the aggregates (dissolvable in 100% TFA) demonstrate that it belongs to class I hydrophobins.

Although hydrophobins are generally reported to share low sequence identity percentage (Sunde et al. 2008), comparison of the sequence of the often-used example of class I hydrophobin, SC3, with that of Vmh2 reveals 46% of identity on the whole sequence, increasing to 62% if the fragment starting from the first C of the disulfide pattern is considered (Supplementary data, Fig. 3). Actually, the main difference between the two sequences lies in the T stretch upstream of the first C of SC3 that is absent in Vmh2. This T stretch in SC3 is reported to be O-linked to mannose residues, thus further increasing the hydrophilicity of that region and, consequently, of the whole protein (de Vocht et al. 1998). The absence of this region in Vmh2 suggests a higher hydrophobicity of the *P. ostreatus* protein with respect to SC3. As a matter of fact, our results show that pure Vmh2 is not soluble in water. The two more studied class I hydrophobins, SC3 and EAS of *N. crassa*, can be dissolved in water up to 1 mg/mL (Mackay et al. 2001; Wang, Graveland-Bikker, et al. 2004), and class II

hydrophobins are reported to be even much more soluble (up to 10 mg/mL) (Kisko et al. 2008). Therefore, to the best of our knowledge, Vmh2 is the most hydrophobic hydrophobin characterized so far.

Analyses of protein samples purified from culture medium containing amylose have shown the presence of glycans in the hydrophobin aggregates. If the protein is dissolved in 60% ethanol, the glycan fraction precipitates, leaving the protein free in this solution. Since the free protein is not soluble in water, the interaction with glycans enables the protein to be water soluble.

The structure of the water-soluble glycans matched to  $\alpha$ -(1-4) linked glucose lacking of reducing ends, thus pointing towards cyclic structure containing from six to 16 monomers, namely  $\alpha$ ,  $\beta$  and  $\gamma$  cyclodextrins and higher homologues. On the basis of our results the cyclic glucans are produced by the fungus when grown in the presence of amylose. Enzymatic activities like 4- $\alpha$ -glucanotransferase (Takaha and Smith 1999) could be responsible for their synthesis. These enzymes are widely distributed in bacteria, yeasts, plants and mammals, and an increasing number of 4- $\alpha$ -glucanotransferases from different sources are known to be able to catalyze cyclization reactions to produce cycloamylose (Yanase et al. 2002).

When some commercial molecules were tested for their ability of restoring the hydrophobin water solubility, like the fungal cyclic glucans do, we ascertained that not only pure  $\alpha$ ,  $\beta$  and  $\gamma$  cyclodextrins but also the linear molecule maltohexaose and even the simple D-glucose monomer are able to solubilize the hydrophobin Vmh2 in water. Interaction between Vmh2 and glucose has been verified by the finding of a unique peak containing both the molecules eluted by gel filtration chromatography.

Even though the physical–chemical features of the binding are still unknown, it is evident that carbohydrates do mediate the interaction of the hydrophobin with water. The interaction between carbohydrate and hydrophobic regions of proteins is not surprising since they often bind to proteins by  $\pi$ -stacking interactions. It has been demonstrated that these interactions are facilitated by the formation of hydrogen bonds. However, CH/ $\pi$  stacking interaction, very common in the recognition sites of proteins that recognize carbohydrates, has origin in dispersion forces, which have an impact on the enthalpic term of the free energy (Vandenbussche et al. 2008).

By vortexing the aqueous solution of the Vmh2—in the presence of the fungal cyclic glucans—the protein self-assembles. The conformational changes observed for class I hydrophobins after self-assembling—increase of  $\beta$  sheet structure—have been demonstrated for Vmh2 by vortexing its water solution in the presence of glucans. On the other hand, when the pure protein is dissolved in less polar solvents (60% ethanol), the propensity to self-assemble is greatly reduced, and no conformational change has been observed upon vortexing the solution. Moreover, amyloid-like aggregates are formed by vortexing the hydrophobin water solution, as indicated by ThT binding, whereas no ThT binding was detected by vortexing the ethanol solution of Vmh2.

The behavior of the Vmh2 aggregates has also been investigated by analyzing the biofilms formed by the hydrophobin in different conditions and on different surfaces. We have previously reported that chemically and mechanically stable mono-



and multilayers formed by the *P. ostreatus* secreted hydrophobin (Vmh2 in the Hyd-et form, as described in this paper) (De Stefano et al. 2007, 2008; Houmadi et al. 2008) are obtained by deposition on crystalline silicon (De Stefano et al. 2007) or Porous Silicon (Psi) surfaces (De Stefano et al. 2008). This biofilm changes the wettability of both the silicon surface and the PSi structure. Formation and features of Langmuir Blodgett Vmh2 film have been also investigated and analyzed by atomic force microscopy after transfer onto silicon substrate, revealing the coexistence of a monolayer and rodlets (Houmadi et al. 2008). In this paper, biofilms that had been formed on hydrophobic or on hydrophilic surfaces by depositing the pure protein in ethanol or in water—in the presence of the fungal cyclic glucans—were analyzed by VASE. When the pure protein was deposited on the hydrophobic surface, crystalline silicon, a very stable biofilm was formed, whereas it could not be detected on a hydrophilic surface, the oxidized silicon. On the other hand, biofilms were obtained on both surfaces using Vmh2 dissolved in water. Their thicknesses were always higher but more variable than that obtained from the pure protein on crystalline silicon. Therefore, glucans seem to mediate also hydrophobin binding to hydrophilic surfaces.

Interaction between the most studied class I hydrophobin, SC3 from *S. commune*, and polysaccharides has been studied (Martin et al. 2000; Scholtmeijer et al. 2009). *S. commune* produces and excretes a high molecular weight polysaccharide, schizophyllan (Steiner et al. 1987). Martin et al. (2000) have demonstrated that this polysaccharide stabilizes small hydrophobin oligomers in solution, acting as hydrophilic stabilizer. Moreover, schizophyllan is necessary for SC3 assembly into films on hydrophilic surfaces, whereas the pure hydrophobin can assemble only on a hydrophobic surface.

More recently, Scholtmeijer et al. (2009) have demonstrated that schizophyllan, as well as some other polysaccharides, promotes formation of SC3 amyloid fibrils at the interface between the water and the air or a hydrophobic solid. According to the authors, the small hydrophobin oligomers found in the presence of the glucan could have a higher capacity to assemble at a hydrophobic–hydrophilic interface.

In the case of the more hydrophobic protein Vmh2, we have verified that oligomeric or monomeric glucans play a role as hydrophilic stabilizer, similar to that of the polysaccharide schizophyllan, allowing solubility of Vmh2 in water. Starting from these conditions, increase of  $\beta$ -sheet structures and formation of amyloid-like fibrils have been verified. Moreover, biofilms were obtained on hydrophilic surfaces using Vmh2 dissolved in water in the presence of the cyclic glucans. These results point out similarities in the behavior of the two hydrophobins in their relationships with glucans, although we do not know at the moment if in the case of Vmh2 the transition towards the amyloid form is favored by the presence of a polar solvent (water) or of the glucans.

## Materials and methods

### Fungal growth and protein purification

White-rot fungus, *P. ostreatus* (Jacq.:Fr.) Kummer (type: Florida) (ATCC no. MYA-2306), was maintained through periodic transfer at 4°C on potato dextrose agar (Difco, Detroit, MI) plates in the presence of 0.5% yeast extract (Difco). Mycelia were inoculated (by adding six agar circles

of 1 cm diameter) in 2-L flasks containing 500 mL of PDY or 2% ME and grown at 28°C in static cultures.

After 10 days of fungal growth, mycelia were removed by filtration, and hydrophobins released into the medium were aggregated by air bubbling using a Waring blender. Foam was then collected by centrifugation at 4000  $\times$  g. The precipitate was freeze dried, treated with TFA for 2 h and sonicated for 30 min. After centrifugation at 3200  $\times$  g for 20 min, the supernatant was dried again in a stream of air and then dissolved in water (Hyd-w) or 60% ethanol (Hyd-et). In the latter case, the solution was kept at 4°C overnight and then centrifuged at 3200  $\times$  g for 10 min.

Before use, the protein was always disassembled with pure TFA and dried, and then the monomeric protein was dissolved.

Protein concentration of Hyd-w was evaluated by BCA assay (Pierce, Rockford, IL) using bovine serum albumin as standard. Absorbance at 230 nm was measured to find out protein concentration in the presence of substances incompatible with the BCA protein assay. Concentration of Hyd-w evaluated by BCA assay was used as reference.

### Phenol-sulfuric acid test (Chaplin and Kennedy 1994)

The glycan solution (200  $\mu$ L) was mixed to 5% phenol (200  $\mu$ L) and sulfuric acid (1  $\mu$ L). This mixture was incubated for 10 min at room temperature and 20 min at 37°C, and then absorbance at 485 nm was determined. Standard curve was performed using from 2 to 200  $\mu$ g of glucose.

### SDS-PAGE

SDS-PAGE (Laemmli 1970) was performed at 15% polyacrylamide concentration using the Bio-Rad Mini Protean III apparatus (Bio-Rad Laboratories, Hercules, CA).  $\beta$ -Galactosidase (117 kDa), bovine serum albumin (85.0 kDa), ovalbumin (49 kDa), carbonic anhydrase (34.0 kDa),  $\alpha$ lactoglobulin (25.0 kDa) and lysozyme (19 kDa) were used as standards (Fermentas Inc., Glen Burnie, MD). The gels were stained by silver staining or by periodic acid staining (GelCode Glycoprotein Staining Kit, Pierce).

### Mass spectrometry

MALDI mass spectra were recorded on a Voyager DE Pro MALDI-TOF mass spectrometer (Applied Biosystems, Foster City, CA). The analyte solutions were mixed with sinapinic acid (20 mg/mL in 70% acetonitrile, TFA 0.1% v/v), 2,5-dihydroxybenzoic acid (DHB) (25 mg/mL in 70% acetonitrile) or  $\alpha$ -cyano-4-hydroxycinnamic acid (10 mg/mL in 70% acetonitrile, TFA 0.1%, v/v) as matrix, applied to the sample plate and air dried. The spectrometer was used in the linear or reflectron mode. Spectra were calibrated externally.

In situ hydrolysis was carried out on the silver-stained protein bands excised from a 15% polyacrylamide gel run under denaturing conditions (Cleveland et al. 1977). Excised bands were extensively washed with acetonitrile and then with 0.1 M ammonium bicarbonate. Protein samples were reduced by incubation in 10 mM dithiothreitol for 45 min at 56°C and carboxamidomethylated by using 55 mM iodoacetamide for 30 min, in the dark at room temperature. The gel particles were then washed with ammonium bicarbonate and acetonitrile. Enzymatic digestion was carried out with 15 mg/mL trypsin (Sigma-Aldrich, St.

Louis, MO) in 10 mM of ammonium bicarbonate, at 4°C for 2 h. The buffer solution was then removed, and a new aliquot of buffer solution was added for 18 h at 37°C. A minimum reaction volume, sufficient for complete rehydration of the gel, was used. Peptides were then extracted, washing the gel particles with 20 mM of ammonium bicarbonate and 0.1% trifluoroacetic acid in 50% acetonitrile at room temperature, and then lyophilized. Aliquots of the digests were concentrated and directly analyzed by MALDI-MS.

Peptides from in situ hydrolysis were analyzed by LCQ ion trap (Finnigan Corp., San Jose, CA) coupled to a 250 × 2.1 nm, 300 Å Phenomenex Jupiter C18 column on an HP 1100 HPLC (Agilent Technologies, Santa Clara, CA). Peptides were eluted at a flow rate of 0.5 mL/min with a 5–65% gradient of 95% acetonitrile, 5% formic acid and 0.05% TFA in 60 min.

#### *Carbohydrate analysis*

GLC and GLC-MS were all carried out as described (Leontein and Lönngren 1978; Molinaro et al. 2002). Monosaccharides were identified as acetylated *O*-methyl glycoside derivatives. After methanolysis (2 M HCl/MeOH, 85°C, 24 h) and acetylation with acetic anhydride in pyridine (85°, 30 min), the sample was analyzed by GLC-MS. Linkage analysis was carried out by methylation as described by Hakomori (1964). The sample was hydrolyzed with 2 M TFA (100°C, 2 h), carbonyl reduced with NaBD<sub>4</sub>, acetylated and analyzed by GLC-MS.

#### *NMR spectroscopy*

All spectra were recorded on a solution of 1 mg in 0.5 mL of D<sub>2</sub>O, at 300 K, at pD 7. NMR experiments were carried out using a Bruker DRX-600 spectrometer. Chemical shifts are in ppm with respect to the 0 ppm point of the manufacturer's indirect referencing method. Nuclear Overhauser enhancement spectroscopy was measured using data sets (t<sub>1</sub> × t<sub>2</sub>) of 2048 × 256 points, and 16 scans were acquired. A mixing time of 100 ms was used. Double quantum-filtered phase-sensitive correlation spectroscopy experiment was performed with 0.258 s acquisition time, using data sets of 2048 × 1024 points, and 64 scans were acquired. Total correlation spectroscopy experiments were performed with a spinlock time of 120 ms, using data sets (t<sub>1</sub> × t<sub>2</sub>) of 2048 × 256 points, and 16 scans were acquired. In all homonuclear experiments, the data matrix was zero-filled in the F1 dimension to give a matrix of 4096 × 2048 points and was resolution enhanced in both dimensions by a shifted sine-bell function before Fourier transformation. Heteronuclear single quantum coherence was measured in the <sup>1</sup>H-detected mode via single quantum coherence with proton decoupling in the <sup>13</sup>C domain, using data sets of 2048 × 256 points, and 64 scans were acquired for each t<sub>1</sub> value. Experiments were carried out in the phase-sensitive mode according to the method of States et al. (1982).

#### *Analysis of hydrophobin water solubility*

PDY broth or an aqueous solution of the previously separated glycans (0.6 mg/mL), were added to Hyd-et or to Hyd-et dried after TFA treatment, and the procedure used for hydrophobin

purification (vortexing, centrifugation, lyophilization and TFA treatment) was performed. Alternatively, Hyd-et was diluted up to 4% ethanol, and then aqueous solutions (0.6 mg/mL) of PDY broth, or of the cyclic glucans, or of the cyclodextrins (α, β, or γ) or of maltohexaose, or of D-glucose (Sigma-Aldrich) were added. Samples were then vortexed for 10 min, the aggregates lyophilized, TFA treated and solubilized in water.

#### *Gel filtration chromatography*

One milliliter of a solution containing hydrophobin (0.1 mg) solubilized in the presence of glucose (0.6 or 12 mg) was subjected to size exclusion chromatography on Toyopearl HW-40S (Tosoh Bioscience GmbH, Montgomeryville, PA). The column (1 × 40 cm) was eluted with water at a flow rate of 10 mL/h, and the absorbance of the eluate at 230 and 280 nm was recorded. Protein and sugar contents were determined by BCA assay and by phenol-sulfuric acid test, respectively.

#### *Circular dichroism and fluorescence spectroscopies*

Far-UV CD spectra were recorded on a Jasco J715 spectropolarimeter equipped with a Peltier thermostatic cell holder (Jasco model PTC-348) in a quartz cell (0.1-cm light path) from 190 to 250 nm. The temperature was kept at 20°C, and the sample compartment was continuously flushed with nitrogen gas. The final spectra were obtained by averaging three scans, using a bandwidth of 1 nm, a step width of 0.5 nm and a 4-s averaging per point. The spectra were then corrected for the background signal using a reference solution without the protein.

CD spectra of the protein were also recorded by varying the temperatures from 30°C to 90°C at a rate of 1°C/min with 10°C step.

Fluorescence spectra were recorded at 25°C with a Perkin-Elmer LS50B fluorescence spectrometer. Slit widths were set at 10 nm in both the excitation and emission monochromators. ThT (Sigma-Aldrich, 100 μM final concentration) was added to Hyd-w and Hyd-et before and after vortexing for 30 min. Samples were excited at 435 nm, and emission was monitored from 460 to 600 nm. The spectra were then corrected by subtracting the ThT spectrum.

#### *Biofilm on silicon chip*

Silicon samples, single side polished, <100> oriented (chip size: 1 cm × 1 cm), after standard cleaning procedure, were washed in hydrofluoric acid solution for 3 min to remove the native oxide thin layer (1–2 nm) due to silicon oxidation. To obtain oxidized silicon, samples were thermally oxidized in O<sub>2</sub> atmosphere, at 1100°C for 1 h, resulting in an oxide thickness of about 80 nm. A drop (80 μL) of Hyd-et solutions (0.1 mg/mL in 80% ethanol) was spotted on the chip. After 1 h, samples were dried for 10 min on the hot plate (80°C) and then washed by the solvent solution and then by 2% SDS at 100°C for 10 min. Ellipsometric characterization of the hydrophobin biofilm was performed by a variable-angle spectroscopic ellipsometry model (UVISEL, Horiba-Jobin-Yvon). At least six different experiments were performed in each condition.

## Supplementary data

Supplementary data for this article is available online at <http://glycob.oxfordjournals.org/>.

## Funding

This work was supported by the European Commission, Sixth Framework Program (QUORUM contract NMP-2004-032811).

## Acknowledgements

The authors gratefully acknowledge Professor Gennaro Marino, Professor Delia Picone and Professor Leila Birolo for the helpful discussions.

## Abbreviations

BCA, bicinehoninic acid; CD, circular dichroism; DHB, 2,5-dihydroxybenzoic acid; GLC, gas-liquid chromatography; <sup>1</sup>H NMR, proton nuclear magnetic resonance; Hyd-et, hydrophobin dissolved in ethanol; Hyd-w, hydrophobin dissolved in water; MALDI, matrix-assisted laser desorption/ionization; ME, malt extract; MS, mass spectrometry; PDY, potato dextrose (24 g/L) broth supplemented with 0.5% yeast extract; SDS-PAGE, SDS-polyacrylamide gel electrophoresis; TFA, trifluoroacetic acid; ThT, thioflavin-T; VASE, variable-angle spectroscopic ellipsometry.

## References

Chaplin MF, Kennedy JF. 1994. *Carbohydrate Analysis: A Practical approach*. 2nd ed, Oxford (UK): IRL press.

Cleveland DW, Fischer SG, Kirschner MW, Laemmli UK. 1977. Peptide mapping by limited proteolysis in sodium dodecyl sulfate and analysis by gel electrophoresis. *J Biol Chem.* 252(3):1102–6.

Cohen R, Persky L, Hadar Y. 2002. Biotechnological applications and potential of wood-degrading mushrooms of the genus *Pleurotus*. *Appl Microbiol Biotechnol.* 8(5):582–94.

De Stefano L, Rea I, Armenante A, Giardina P, Giocondo M, Rendina I. 2007. Self-assembled biofilm of hydrophobins protects the silicon surface in the KOH wet etch process. *Langmuir.* 23:7920–7922.

De Stefano L, Rea I, Giardina P, Armenante A, Rendina I. 2008. Protein-modified porous silicon nanostructures. *Adv Mater.* 20:1529–1533.

de Vocht ML, Scholtmeijer K, van der Vegte EW, de Vries OM, Sonveaux N, Wösten HA, Ruysschaert JM, Hadziioannou G, Wessels JG, Robillard GT. 1998. Structural characterization of the hydrophobin SC3, as a monomer and after self-assembly at hydrophobic/hydrophilic interfaces. *Biophys J.* 4(4):2059–68.

Hakanpää J, Linder M, Popov A, Schmidt A, Rouvinen J. 2006. Hydrophobin HFBII in detail: ultrahigh-resolution structure at 0.75 Å. *Acta Crystallogr D Biol Crystallogr.* 62:356–67.

Hakanpää J, Szilvay GR, Kaljunen H, Maksimainen M, Linder M, Rouvinen J. 2006. Two crystal structures of *Trichoderma reesei* hydrophobin HFBII—the structure of a protein amphiphile with and without detergent interaction. *Protein Sci.* 15(9):2129–40.

Hakomori S. 1964. A rapid permethylation of glycolipid, and polysaccharide catalyzed by methylsulfonyl carbanion in dimethyl sulfoxide. *J Biochem (Tokyo)* 55:205–208.

Hektor HJ, Scholtmeijer K. 2005. Hydrophobins: proteins with potential. *Curr Opin Biotechnol.* 16(4):434–9.

Houmadi S, Ciuchi F, De Santo MP, De Stefano L, Rea I, Giardina P, Armenante A, Lacaze E, Giocondo M. 2008. Langmuir Blodgett film of hydrophobin protein from *Pleurotus ostreatus* at the air-water interface. *Langmuir.* 24(22):12953–7.

Kisko K, Szilvay GR, Vainio U, Linder MB, Serimaa R. 2008. Interactions of hydrophobin proteins in solution studied by small-angle X-ray scattering. *Biophys J.* 94(1):198–206.

Kwan AH, Winefield RD, Sunde M, Matthews JM, Haverkamp RG, Templeton MD, Mackay JP. 2006. Structural basis for rodlet assembly in fungal hydrophobins. *Proc Natl Acad Sci USA.* 103(10):3621–6.

Laemmli UK. 1970. Cleavage of structural proteins during the assembly of the head of bacteriophage T4. *Nature (London)* 227:680–685.

Leontin K., Lönngrén J. 1978. Determination of the absolute configuration of sugars by gas-liquid chromatography of their acetylated 2-octyl glycosides. *Methods Carbohydr. Chem.* 62:359–362.

Linder MB, Szilvay GR, Nakari-Setälä T, Penttilä ME. 2005. Hydrophobins: the protein-amphiphiles of filamentous fungi. *FEMS Microbiol Rev.* 29(5):877–96.

Mackay JP, Matthews JM, Winefield RD, Mackay LG, Haverkamp RG, Templeton MD. 2001. The hydrophobin EAS is largely unstructured in solution and functions by forming amyloid-like structures. *Structure.* 9:83–91.

Martin GG, Cannon GC, McCormick CL. 2000. Sc3p hydrophobin organization in aqueous media and assembly onto surfaces as mediated by the associated polysaccharide schizophyllan. *Biomacromolecules.* 1(1):49–60.

Molinaro A, De Castro C, Lanzetta R, Evidente A, Parrilli M, Holst O. 2002. Lipopolysaccharides possessing two L-glycero-D-manno-heptopyranosyl- $\alpha$ -(1 $\rightarrow$ 5)-3-deoxy-D-manno-oct-2-ulopyranosonic acid moieties in the core region. The structure of the core region of the lipopolysaccharides from *Burkholderia caryophylli*. *J. Biol. Chem.* 277:10058–10063.

Peñas MM, Asgeirsdóttir SA, Lasa I, Culiñez-Macià FA, Pisabarro AG, Wessels JG, Ramírez L. 1998. Identification, characterization, and in situ detection of a fruit-body-specific hydrophobin of *Pleurotus ostreatus*. *Appl Environ Microbiol.* 64(10):4028–34.

Peñas MM, Rust B, Larraya LM, Ramírez L, Pisabarro AG. 2002. Differentially regulated, vegetative-mycelium-specific hydrophobins of the edible basidiomycete *Pleurotus ostreatus*. *Appl Environ Microbiol.* 68(8):3891–8.

Scholtmeijer K, de Vocht ML, Rink R, Robillard GT, Wösten HA. 2009. Assembly of the fungal SC3 hydrophobin into functional amyloid fibrils depends on its concentration and is promoted by cell wall polysaccharides. *J Biol Chem.* 284(39):26309–14.

States DJ, Haberkorn RA, Ruben DJ. 1982. A two-dimensional nuclear overhauser experiment with pure absorption phase in four quadrants. *J Magn. Reson.* 48:286–292.

Steiner W, Lafferty RM, Gomes I, Esterbauer H. 1987. Studies on a wild strain of *Schizophyllum commune*: cellulase and xylanase production and formation of the extracellular polysaccharide schizophyllan. *Biotechnol Bioeng.* 30(2):169–78.

Sunde M, Kwan AH, Templeton MD, Beever RE, Mackay JP. 2008. Structural analysis of hydrophobins. *Micron.* 39(7):773–84.

Szilvay GR, Paananen A, Laurikainen K, Vuorimaa E, Lemmetyinen H, Peltonen J, Linder MB. 2007. Self-assembled hydrophobin protein films at the air-water interface: structural analysis and molecular engineering. *Biochemistry.* 46(9):2345–54.

Takaha T, Smith SM. 1999. The functions of 4- $\alpha$ -glucanotransferases and their use for the production of cyclic glucans. *Biotechnol. Genet. Eng. Rev.* 16:257–280.

Vandenbussche S, Díaz D, Fernández-Alonso MC, Pan W, Vincent SP, Cuevas G, Cañada FJ, Jiménez-Barbero J, Bartik K. 2008. Aromatic-carbohydrate interactions: an NMR and computational study of model systems. *Chemistry.* 15:7570–7578.

Wang X, de Vocht ML, de Jonge J, Poolman B, Robillard GT. 2002. Structural changes and molecular interactions of hydrophobin SC3 in solution and on a hydrophobic surface. *Protein Sci.* 11(5):1172–81.

Wang X, Graveland-Bikker JF, de Kruijff CG, Robillard GT. 2004. Oligomerization of hydrophobin SC3 in solution: from soluble state to self-assembly. *Protein Sci.* 13(3):810–21.

Wang X, Permentier HP, Rink R, Kruijtz JA, Liskamp RM, Wösten HA, Poolman B, Robillard GT. 2004. Probing the self-assembly and the accompanying structural changes of hydrophobin SC3 on a hydrophobic surface by mass spectrometry. *Biophys J.* 87(3):1919–28.

Wösten HA. 2001. Hydrophobins: multipurpose proteins. *Annu Rev Microbiol.* 55:625–46.

Yanase M, Takata H, Takaha T, Kuriki T, Smith SM, Okada S. 2002. Cyclization reaction catalyzed by glycogen debranching enzyme and its potential for cycloamylose production. *Appl Environ Microbiol.* 68(9):4233–9.



# Fungal hydrophobins, proteins as natural emulsifiers

SARA LONGOBARDI<sup>1</sup>, LUCA DE STEFANO<sup>3</sup>, CARMINE ERCOLE<sup>2</sup>, DELIA PICONE<sup>2</sup>, ILARIA REA<sup>3</sup>, PAOLA GIARDINA<sup>1\*</sup>

\*Corresponding author

<sup>1</sup> University of Naples "Federico II", Dipartimento di Chimica Organica e Biochimica, Complesso Universitario Monte S. Angelo via Cintia 4, Napoli, 80126, Italy

<sup>2</sup> University of Naples "Federico II", Dipartimento di Chimica, Complesso Universitario Monte S. Angelo, via Cintia 4, Napoli, 80126, Italy

<sup>3</sup> Institute for Microelectronics and Microsystems, Unit of Naples, National Council of Research, Via P. Castellino 111, Napoli, 80131, Italy

**ABSTRACT:** Hydrophobins are proteins produced by filamentous fungi that exhibit very peculiar properties. Their behaviour in solution resembles that of typical surfactants characterized by self-assembling into an amphiphilic membrane. Actually the hydrophobin self-assembly at the cell-wall-air interface plays a key role in the formation of aerial hyphae and fruiting bodies by establishing a water-repellent layer. The interest in this class of proteins is increasing because of their multiple and attractive potential applications. Just to give an example, hydrophobins can be used to stabilize emulsions, and this property might be extremely useful for pharmaceutical applications and in the food industry. We have purified and characterized the hydrophobin that is secreted in the cultural broth by the mycelia of the edible fungus *Pleurotus ostreatus*. Higher amounts of the same protein have been obtained from the fungal mycelia and by recombinant expression in *E. coli*. In this paper the emulsifying properties of the protein are also discussed.

Amphiphiles are molecules characterized by distinct hydrophilic and hydrophobic parts. This characteristic provides them with properties such as a high tendency to migrate to hydrophobic-hydrophilic interfaces (such as the air-water interface) and the ability to encapsulate and dissolve hydrophobic molecules into aqueous media. The most common amphiphiles is soap, which is used to solubilise dirt. In biology, amphiphiles play extremely important roles, and the most crucial one is the formation of membranes by amphiphilic phospholipids.

Amphiphiles reduce the surface tension of water: in a drop of water the external molecules encounter an environment, e.g., air or a solid surface, different from that experienced from the internal ones. Since the water molecules at the interface/surface cannot make favourable contacts among them, the system tries to minimize the number of water molecules interacting with the surroundings. The spherical shape of a water drop on a hydrophobic support is a consequence of that, being the lowest ratio of surface molecules to bulk molecules in a sphere. The amphiphiles can favourably interact with water on one side and with air or the hydrophobic surface on the other side, thus they migrate to the interfaces, e.g., solid and water or air and water, and allow the drop to spread out. Since amphiphiles migrate to the surface, they are called surface active molecules and the

spreading of a water drop is a convenient way of measuring surface activity.

Biosurfactants are surface-active substances synthesized by living cells. Some proteins can be considered as biosurfactants, although very different from regular detergents from a structural point of view. Proteins are globular, and rather rigid macromolecules, when compared with detergents, that are generally small, elongated, and flexible molecules with long hydrocarbon tails and hydrophilic head groups. Hydrophobins are among the most surface active proteins known. They are produced by filamentous fungi, and endowed with very special properties (1, 2). They are able to reduce the surface tension from  $70 \text{ mN m}^{-1}$  to approximately  $30 \text{ mN m}^{-1}$  (3). Their behaviour as surfactants can be explained from a structural point of view. On one side of their molecular surface, some exposed hydrophobic aliphatic side chains form a flat hydrophobic patch, whilst polar or charged residues are confined to the other side (4, 5). Hydrophobins are produced as soluble proteins and when they reach an interface (e.g. medium-air or cell wall-air) they self-assemble into an amphiphilic membrane. Several features of fungal development have been attributed to these proteins (6, 7). For example, the self-assembly of hydrophobins seems to play an essential role in the formation of aerial hyphae and fruiting bodies. Assembly at the medium-air interface results in the reduction of the surface tension, allowing hyphae to break the water-air interface (8). Self-assembly at the cell wall-air interface results in the coating of aerial hyphae and fruiting bodies with a water-repellent layer (9, 10). Hydrophobins are also involved in the attachment of hyphae to hydrophobic surfaces (11); for example, during symbiotic or pathogenic interactions hydrophobins self-assemble into an amphiphilic layer between the fungal wall and the hydrophobic surface of the host (12, 13).

Because of the multiple attractive potential applications of this class of proteins, multinational companies as BASF, Unilever or L'Oreal have increasingly addressed their attention to them, as demonstrated by the conspicuous number of patents. For example hydrophobins can be a good additive to hair care products in the cosmetic industry. They can prolong the residence time of those products that do not firmly adhere and are easily removed upon shampooing (i. e. WO/2003/053383 Cosmetic use of at least a hydrophobin for treating keratinous materials). Hydrophobins can be used to stabilize emulsions in creams and ointments (i.e. WO/2007/006765 Aqueous monomer emulsions containing hydrophobin). This property might also be beneficial for

pharmaceutical applications (WO/2010/060811 Surface active proteins as excipients in solid pharmaceutical formulations) and applications in the food industry (WO/2008/116733 Aerated food products being warm containing soluble and/or insoluble solids and methods for producing them), which both require stable emulsions for certain formulations and ingredients. Recently, Akanabi et al. (14) show that the fungal hydrophobin SC3 can be used to make suspension of water insoluble drugs, resulting in a constant longer lasting drug level in the body. Standardized emulsion testing under realistic laundry conditions demonstrates that tiny amounts of hydrophobin can boost the emulsifying power of an appropriate technical surfactant (15). Before considering the use of hydrophobins as an additive, especially for the food industry, their production levels and price should be affordable. If this is the case, the advantage of hydrophobins is that several of them can be considered food-grade surfactants. Hydrophobins from edible fungi, for example, are already consumed in large amounts by people eating these common mushrooms.

Adequate production levels of hydrophobins would also make possible their use in anti-fouling applications to modify surfaces which are usually significant in size. For example, window panes and cars suffer from fouling, and the growth of unwanted organisms on ships represents a significant problem for the marine shipping industry (16).

Hydrophobins have been split in two groups, class I and class II, based on structural differences and properties of the aggregates they form (17). Class I hydrophobins form highly insoluble aggregates that have the appearance of distinct rodlets and, similarly to amyloid fibrils, are characterized by  $\beta$ -structure. These aggregates can be dissolved in 100 percent trifluoroacetic acid (TFA) whereas class II hydrophobins form polymers that are soluble in some organic solvents and lack the rodlet appearance of class I hydrophobins (1).

Basidiomycete fungi produce only class I hydrophobins, while ascomycetes produce both class I and II proteins.

A better understanding of hydrophobin self-assembly process as well as of their behaviour in solution is needed, in order to meet the full exploitation of these proteins. Comparison of the known properties of the few studied proteins with other ones of the same class will advance this knowledge, allowing an outline of the molecular mechanisms underlying these properties. Differences between the proteins belonging to the two diverse classes and among those within the same class, can be fruitfully used to select the molecule that is suitable for a specific application. This will further improve their potentiality. The basidiomycete *Pleurotus ostreatus* (Figure 1) is a commercially relevant edible mushroom, also used for the bioconversion of wastes and as a source of enzymes for industrial applications. We are studying a Class I hydrophobin (named Vmh2) produced by the mycelium of this fungus. A simple protein purification procedure has been set up; hydrophobins released in the medium are aggregated by aeration, then captured by precipitation. The precipitate is then dissolved in TFA. After TFA evaporation, the protein is solubilised in 60 percent ethanol. This procedure results in a protein production with a yield of about 0.5-1 mg/l of culture broth (18).

Pure Vmh2 is not water soluble, whereas complexes formed between the protein and glucans are soluble in water. It has been demonstrated that glucose is also able to solubilise the hydrophobin in water. The protein in aqueous solution shows high propensity to self-assembly. Conformational changes towards  $\beta$ -structure upon vortexing the solution are observed by circular dichroism spectroscopy. Similar changes occur upon temperature increase: a major change of structure has been detected at about 80°C. On the other hand the pure protein dissolved in less polar solvent (60 percent ethanol) is not prone to self assembly and no conformational change has been observed (18). The protein is very stable at high temperature and in a broad pH range.

We are seeking for procedures to improve the protein yield. A simple procedure to purify the hydrophobin from the *P. ostreatus* vegetative mycelia has been set up, obtaining an at least tenfold higher protein yield. Protein expression in easily cultivable and handling hosts can allow higher productivity in shorter time and reduce the costs of production. The versatility and scaling-up possibilities of the recombinant protein production opened up new commercial opportunities for its industrial uses. For these reasons, recombinant expression of the *P. ostreatus* hydrophobin in *E. coli* has been achieved and the properties of the recombinant protein compared with those of the extractive one, showing similar behaviours (unpublished data). We are also setting up recombinant expression of the protein in yeast.

Biofilms formed by the extractive protein on different surfaces have been characterized. Chemically and mechanically stable monolayers of the self-assembled protein have



Figure 1. The basidiomycete edible fungus *Pleurotus ostreatus*.



been obtained. On a hydrophobic surface the pure protein forms a very stable biofilm (19) whose thickness was about 3nm, whereas the biofilm has not been detected on a hydrophilic surface (18, 20). On the other hand, the water-soluble protein -in the presence of glucans- forms thicker (up to ten fold) biofilms either on hydrophilic and hydrophobic surfaces. The hydrophobin modified hydrophobic surface shows a great improvement in wettability. In Figure 2 it is shown that the contact angle of a water drop (90° on the untreated hydrophobic surface) falls down to 25° after hydrophobin deposition, and the surface becomes clearly hydrophilic (20). The hydrophobin solution has been also infiltrated in the nanometric sponge-like matrix of the porous silicon, a material widely used in biomedical and biotechnological applications, increasing its chemical stability and changing its wettability (21).

Moreover, recent results demonstrate the emulsification capacity of the hydrophobin solution with three different oils: olive, peanut, and almond oil. The hydrophobin solutions (0.1 mg/ml) in 20 percent ethanol was vortexed in the presence of each one of the three oils. In Figure 3 the emulsions obtained in the presence or absence of the hydrophobin are shown. These emulsions were stable at least for two days, and even longer (up to 7 days) in the cases of the peanut and almond oils. These data indicate the potentiality of the use of the *P. ostreatus* hydrophobin as emulsion stabilizer. It is worth noting that this hydrophobin can be considered a food-grade surfactant, since its source, *P. ostreatus*, is an edible fungus consumed in large amounts.

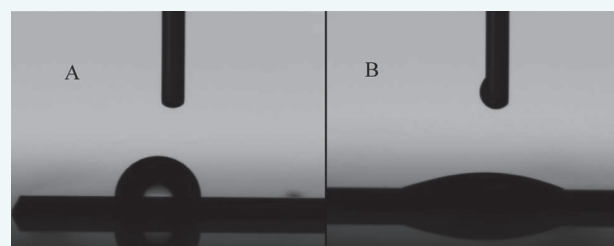


Figure 2. The hydrophobin layer turns a hydrophobic surface (A) into a hydrophilic one (B). The contact angle of a water drop changes from 90° to 25° after the hydrophobin deposition.

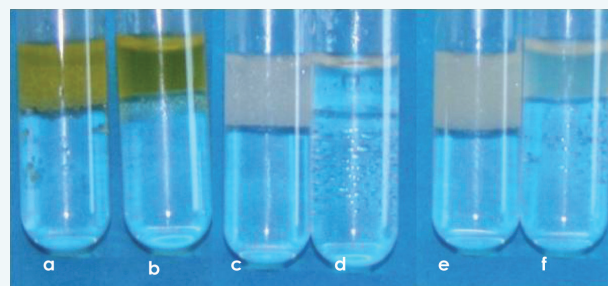


Figure 3. Emulsions of olive, peanut, and almond oils in the presence (a, c, e, respectively) or absence (b, d, f, respectively) of the hydrophobin.

REFERENCES AND NOTES

1. M.B. Linder, G.R. Szilvay et al., *FEMS Microbiol. Rev.*, **29**, pp. 877-896 (2005).
2. M.B. Linder, *Curr. Op. . Colloid & Interface Sci.*, **14**, pp. 356-363 (2009).
3. A.R. Cox, F. Cagnol et al., *Langmuir*, **23**, pp. 7995-8002 (2007).
4. J. Hakanpaa, A. Paananen et al., *J. Biol. Chem.*, **279**, pp. 534-539 (2004).
5. A.H.Y. Kwan, R.D. Winefield et al., *Proc. Natl. Acad. Sci. USA*, **103**, pp. 3621-3626 (2006).
6. J.G. Wessels, *Adv. Microb. Physiol.*, **38**, pp. 1-45 (1997).
7. H.A.B. Wosten, *Annu. Rev. Microbiol.*, **55**, pp. 625-646 (2001).
8. H.A.B. Wosten, M.A. van Wetter et al., *Curr. Biol.*, **9**, pp. 85-88 (1999).
9. M.A. van Wetter, F.H.J. Schuren et al., *FEMS Microbiol. Lett.*, **140**, pp. 265-269 (1996).

10. P.W.J de Groot, P.J. Schaap et al., *J Mol Biol.*, **257**, pp. 1008-1019 (1996).
11. H.A.B. Wosten, F.H. Schuren et al., *EMBO J.*, **13**, pp. 5848-5854 (1994).
12. N.J. Talbot, M.J. Kershaw et al., *Plant Cell*, **8**, pp. 985-999 (1996).
13. D.J. Ebbole, *Trends Microbiol.*, **5**, pp. 405-408 (1997).
14. M.H.J. Akanbi, E. Post et al., *Colloids Surf. B Biointerfaces*, **75**, pp. 526-531 (2010).
15. W. Wohlleben, T. Subkowski et al., *Eur Biophys J.*, **39**, pp. 457-468 (2010).
16. H.J. Hektor, K. Scholtmeijer, *Curr. Opin. Biotechnol.*, **16**, pp. 434-439 (2005).
17. M. Sunde, A.H. Kwan et al., *Micron.*, **39**, pp. 773-784 (2008).
18. A. Armenante, S. Longobardi et al., *Glycobiology*, **20**, pp. 594-602 (2010).
19. L. De Stefano, I. Rea et al., *Langmuir*, **23**, pp. 7920-792 (2007).
20. L. De Stefano, I. Rea et al., *Eur. Phys. J.*, **30**, pp. 181-185 (2009).
21. L. De Stefano, I. Rea et al., *Adv. Mater.*, **20**, pp. 1529-1533 (2008).

**Environmental conditions modulate the switch among  
different states of the hydrophobin Vmh2 from *Pleurotus  
ostreatus***

Journal:	<i>Biomacromolecules</i>
Manuscript ID:	bm-2011-01663f
Manuscript Type:	Article
Date Submitted by the Author:	23-Nov-2011
Complete List of Authors:	Longobardi, Sara; University of Naples "Federico II", Department of Organic Chemistry and Biochemistry Picone, Delia; University of Naples "Federico II", Department of Chemistry , Italy Ercole, Carmine; University of Naples "Federico II", Department of Chemistry , Italy Spadaccini, Roberta; University of Sannio, Department of Biological and Environmental Sciences De Stefano, Luca; CNR, Institute for Microelectronics and Microsystems, Rea, Ilaria; CNR, Institute for Microelectronics and Microsystems, Giardina, Paola; University of Naples "Federico II", Department of Organic Chemistry and Biochemistry

SCHOLARONE™  
Manuscripts

1  
2  
3  
4  
5  
6  
7  
8  
9  
10  
11  
12  
13  
14  
15  
16  
17  
18  
19  
20  
21  
22  
23  
24  
25  
26  
27  
28  
29  
30  
31  
32  
33  
34  
35  
36  
37  
38  
39  
40  
41  
42  
43  
44  
45  
46  
47  
48  
49  
50  
51  
52  
53  
54  
55  
56  
57  
58  
59  
60

# Environmental conditions modulate the switch among different states of the hydrophobin Vmh2 from *Pleurotus ostreatus*

Sara Longobardi<sup>1</sup>, Delia Picone<sup>2</sup>, Carmine Ercole<sup>2</sup>, Roberta Spadaccini<sup>3</sup>, Luca De Stefano<sup>4</sup>, Ilaria  
Rea<sup>4</sup>, Paola Giardina<sup>1\*</sup>

<sup>1</sup>Department of Organic Chemistry and Biochemistry, University of Naples “Federico II”, Italy

<sup>2</sup>Department of Chemistry, University of Naples “Federico II”, Italy

<sup>3</sup>Department of Biological and Environmental Sciences, University of Sannio, Italy

<sup>4</sup>Institute for Microelectronics and Microsystems, CNR, Naples, Italy

TITLE RUNNING HEAD: Vmh2 hydrophobin from *P. ostreatus*.

CORRESPONDING AUTHOR: Paola Giardina, Department of Organic Chemistry and Biochemistry,  
University of Naples “Federico II” Via Cintia 4, 80126, Naples, Italy. Tel: +39 081674319. Fax: +39 081674313;  
E-mail: [giardina@unina.it](mailto:giardina@unina.it)

## ABSTRACT

1  
2  
3  
4  
5  
6  
7 Fungal hydrophobins are amphipathic, highly surface-active and self-assembling proteins. The class I  
8 hydrophobin Vmh2 from the basidiomycete fungus *Pleurotus ostreatus* seems to be the most  
9 hydrophobic hydrophobin characterized so far. Structural and functional properties of the protein as a  
10 function of the environmental conditions have been determined. At least three distinct phenomena can  
11 occur, being modulated by the environmental conditions. 1- When the pH increases or in the presence of  
12  $\text{Ca}^{2+}$  ions, an **assembled state,  $\beta$ -sheet rich**, is formed; 2- when the solvent polarity increases the protein  
13 shows an increased tendency to reach hydrophobic/hydrophilic interfaces, with no detectable  
14 conformational change; 3- a reversible conformational change and reversible aggregation occurs at high  
15 temperature. Modulation of the Vmh2 conformational/aggregation features by changing the  
16 environmental conditions can be very useful in view of the potential protein applications.  
17  
18  
19  
20  
21  
22  
23  
24  
25  
26  
27  
28  
29  
30  
31  
32  
33  
34  
35  
36  
37

38 **KEYWORDS.** Fungal hydrophobins, Self-assembly; Recombinant proteins; Conformational changes;  
39  
40 Biosurfactants  
41  
42  
43  
44  
45  
46  
47  
48  
49  
50  
51  
52  
53  
54  
55  
56  
57  
58  
59  
60

## INTRODUCTION

1  
2  
3 Hydrophobins are a family of small fungal proteins (about 100 amino acids) that have unusual  
4 biophysical properties. They are amphipathic, highly surface-active and self-assembling proteins.  
5  
6  
7 Because of their features, they are able to coat both hydrophobic and hydrophilic solid surfaces and  
8  
9 reverse the hydrophobic character of these surfaces<sup>1</sup>. Due to these peculiar characteristics, some of their  
10  
11 biological functions are linked to the reduction of the surface tension of water, that allows fungi to  
12  
13 escape an aqueous environment, and to facilitate dispersal of the spores by their hydrophobization.  
14  
15  
16 Furthermore several hydrophobins are involved in the attachment of pathogenic fungi to plant  
17  
18 surfaces<sup>1,2</sup>.

20  
21 The sequence similarity between different hydrophobins is quite low except for the characteristic  
22  
23 pattern of eight cysteine residues that form four intramolecular disulfide bonds. Hydrophobins are  
24  
25 classified into two classes based on physical properties and sequence similarity. The membranes formed  
26  
27 by Class II hydrophobins are soluble in SDS, while Class I hydrophobins can form highly insoluble  
28  
29 membranes that can resist in boiling 2% (w/v) sodium dodecylsulfate (SDS), and have a characteristic  
30  
31 rodlet morphology<sup>3</sup>. Rodlets are about 10-nm wide, and share many of the structural characteristic of  
32  
33 amyloid fibrils; their formation is accompanied by conformational change to an ordered  $\beta$ -structure, able  
34  
35 to bind to the dye thioflavin T (ThT)<sup>4</sup>.

36  
37  
38  
39  
40 Many industrial applications of hydrophobins have been discussed<sup>2-5</sup>. For example, a hydrophobin  
41  
42 coating can be used in biosensor technology, being an intermediate to attach cells, proteins, or other type  
43  
44 of molecules to hydrophobic surfaces<sup>6,7</sup>. For nano-technological applications, hydrophobins might be  
45  
46 used to pattern different molecules on a surface with nanometre accuracy<sup>8,9</sup>.

47  
48  
49 Taking into consideration the use of hydrophobins in large scale applications, they could find use in  
50  
51 anti-fouling applications<sup>5</sup> -replacing existing applications for dirt repellent-, or as an alternative to  
52  
53 surfactants such as emulsifiers or foaming agents in different branches of industry<sup>10,11</sup>. The capacity for  
54  
55 emulsification of a standard surfactant can be boosted by the addition of tiny amounts of hydrophobin,  
56  
57 under conditions that mimic a laundry process<sup>12</sup>. It has been demonstrated that the fungal hydrophobin  
58  
59  
60

1 SC3 can be used to make suspension of water insoluble drugs, resulting in a constant longer lasting drug  
2 level in the body<sup>13</sup>. Valo et al.<sup>14</sup> have synthesized protein coated nanoparticles for drug delivery  
3 purposes, using the hydrophobin HFBII.  
4  
5

6  
7 An advantage of using hydrophobins in the food or pharmacy industry is that several of them can be  
8 considered food-grade surfactants. Hydrophobins from edible fungi, for example, are already consumed  
9 in large amounts by people eating these common mushrooms. However, production levels and costs of  
10 hydrophobins should be improved before some of these applications could be affordable for general use.  
11  
12

13  
14 A high production level of a Class II hydrophobin (600 mg/l) was obtained by constructing a  
15 *Trichoderma reesei* HFBI-overproducing strain<sup>15</sup>. Recently BASF succeeded in a production process of  
16 a recombinant Class I hydrophobin up-scaled to pilot plant production in kilogram scale<sup>12</sup>. Further  
17 knowledge of the structural properties of Class I hydrophobins, the process of rodlet formation, and the  
18 characteristics of the films they form is helpful to optimize their production and use. Unfortunately  
19 difficulties in extracting and handling these very peculiar proteins make these studies still limited and  
20 performed on only few proteins.  
21  
22

23  
24 As far as the extensively studied Class I hydrophobin, SC3 from *Schizophyllum commune*, is concerned,  
25 it spontaneously self-assembles via an  $\alpha$ -helical intermediate state into a stable  $\beta$ -sheet end  
26 configuration at a water-air interface. In contrast, upon contact with hydrophobic solids (e.g., Teflon) in  
27 water, SC3 is arrested in the intermediate  $\alpha$ -helical configuration. The transition to the stable  $\beta$ -sheet  
28 end form is promoted by high protein concentration, the presence of cell wall polysaccharides and the  
29 combination of heat and detergents<sup>16</sup>.  
30  
31

32  
33 Conditions inducing self-association of other Class I recombinant hydrophobins, H\*Protein A and B,  
34 have been also analyzed (pH>6, temperature $\gg$ 5°C, concentration>0.2mg/ml)<sup>12</sup>. Morris et al. studied the  
35 effect of some additives (alcohols, detergents, ionic liquids) on rodlet formation of two recombinant  
36 hydrophobins, EAS and DewA<sup>17</sup>. They observed that the rate of rodlet formation is slowed as the  
37 surface tension of the solution is decreased, regardless of the nature of the additive.  
38  
39  
40  
41  
42  
43  
44  
45  
46  
47  
48  
49  
50  
51  
52  
53  
54  
55  
56  
57  
58  
59  
60

1 A Class I hydrophobin secreted by the basidiomycete fungus *Pleurotus ostreatus* has been recently  
2 purified and identified as Vmh2<sup>18</sup>. According to Peñas et al.<sup>19</sup>, this protein is specific to vegetative  
3 mycelium, it is produced throughout the culture time, and it is found both as cell wall-associated protein,  
4 and in the bulk medium. The pure protein is not soluble in water, but in ethanol solution, whereas  
5 complexes formed between the protein and glucans, produced in culture broth containing amylose, are  
6 soluble in water. It has been verified that glucose is also able to solubilize the hydrophobin in water<sup>18</sup>.  
7 The aqueous solution of the protein -in the presence of glucans- showed propensity to self-assembly,  
8 whilst the pure protein dissolved in less polar solvent (60% ethanol) is not prone to self assembly.  
9  
10 Langmuir-Blodgett films of Vmh2 deposited on silicon substrates were investigated by atomic force  
11 microscopy (AFM). Compact and uniform monomolecular layers coexisting with protein aggregates,  
12 under the typical rodlet form, were observed<sup>20</sup>.  
13  
14  
15  
16  
17  
18  
19  
20  
21  
22  
23  
24  
25

26 Vmh2 seems to be the most hydrophobic hydrophobin characterized so far since both SC3 and EAS  
27 from *Neurospora crassa*, can be dissolved in water up to 1 mg/ml<sup>21</sup> whereas class II hydrophobins are  
28 reported to be even much more soluble (up to 100 mg/ml)<sup>3</sup>. In this paper we describe how to set up  
29 protein production by Vmh2 extraction from *P. ostreatus* mycelia and how to produce recombinant  
30 protein in *E. coli*. Structural and functional characteristics of the protein as a function of the  
31 environmental conditions have been determined. Our data show that the Vmh2 unique  
32 conformational/aggregation features can be easily modulated.  
33  
34  
35  
36  
37  
38  
39  
40  
41  
42  
43  
44  
45  
46  
47  
48  
49  
50  
51  
52  
53  
54  
55  
56  
57  
58  
59  
60

## EXPERIMENTAL PROCEDURES

1  
2  
3 *Extraction from P. ostreatus mycelium* - White-rot fungus, *P. ostreatus* (Jacq.:Fr.) Kummer (type:  
4  
5 Florida) (ATCC no. MYA-2306) was maintained through periodic transfer at 4°C on potato dextrose  
6  
7 agar (Difco) plates in the presence of 0.5% yeast extract. Mycelia were inoculated in 2 l flasks  
8  
9 containing 500 ml of potato-dextrose broth (24 g/l) supplemented with 0.5% yeast extract (PDY broth)  
10  
11 grown at 28 °C in static or in shaken (150 rpm) mode. After 10 days of fungal growth, mycelia were  
12  
13 separated by filtration through gauze.  
14  
15

16  
17 Mycelia were treated twice with 2% SDS in a boiling water bath for 10 min, washed several times  
18  
19 with water and once with 60% ethanol to completely remove the detergent. The residue was freeze-dried  
20  
21 and treated with 100% trifluoroacetic acid (TFA) in a water bath sonicator (Bandelin Sonorex Digitec)  
22  
23 for 10 minutes. The supernatant was dried in a stream of air, dissolved in 60% ethanol and centrifuged  
24  
25 (10 min at 3200 x g). The new supernatant was lyophilized and extracted three times with chloroform-  
26  
27 methanol 2:1 v/v (10 min in bath sonicator and 10 min incubation at 65°C). The precipitate was again  
28  
29 freeze-dried, treated with TFA for 30 min in bath sonicator, dried in a stream of air and dissolved in  
30  
31 60% ethanol. The sample was diluted ten times in water, the pH adjusted at 7 by addition of NH<sub>3</sub>,  
32  
33 incubated at 80°C for 10 minutes and vortexed to induce hydrophobin aggregation. The precipitate  
34  
35 obtained after centrifugation (10 min at 3200 xg), was treated with TFA as above described and re-  
36  
37 dissolved in 60% ethanol.  
38  
39  
40  
41

42  
43 *Production and purification of the recombinant hydrophobin in E. coli* - RNA was extracted from  
44  
45 shaken cultures of *P. ostreatus* grown in PDY broth, using a RNeasy kit as described by the  
46  
47 manufacturer (Qiagen). DNase I treated total RNA was used as a template for RT-PCR using  
48  
49 Superscript II (Invitrogen). cDNA was synthesized and amplified with this template using the designed  
50  
51 primers: Vmh2fw Nco 5' CATGCCATGGATACTCCCAGTTGCTCAAC 3' and Vmh2rv Xho 5'  
52  
53 CCGCTCGAGTCACAGGCTAATATTGATGGG 3'. The sequences of these primers correspond to the  
54  
55 N terminal and C-terminal ends of mature Vmh2 (from D26 to L111 of the sequence whose TrEMBL  
56  
57 accession number is Q8WZI2). The PCR reaction was carried out in 50 µl of solution containing: 2.5 µl  
58  
59  
60



1 cDNA, 5  $\mu$ l Buffer Taq 10X, 5  $\mu$ l 25mM MgCl<sub>2</sub>; 1  $\mu$ l 10 mM dNTP, 5  $\mu$ l 100  $\mu$ M Vmh2fw Nco, 5  $\mu$ l  
2  
3 100  $\mu$ M Vmh2rev Xho, 1  $\mu$ l *Taq* DNA Polymerase (5 U/ $\mu$ l).  
4

5 The cycling program started with a 5-min denaturation step at 94°C, followed by 35 cycles of 1 min  
6 denaturation at 94°C, 45 sec of annealing at 54°C, 45 sec of extension at 72°C, followed by 10min of  
7 extension at 72°C. After confirming the sequence, the *vmh2* hydrophobin cDNA was cloned in a pET-  
8 derived plasmid vector as a fusion with a 6His-glutathione S-transferase (GST) tag with a TEV (tobacco  
9 etch virus) protease cleavage site. For this end the amplified DNA was digested with *NcoI* and *XhoI* and  
10 cloned into the vector downstream the His-Tag sequence and the GST coding sequence, thus generating  
11 a fusion protein His tag-GST-Vmh2. The resulting vector was transformed into the *E. coli* BL21 DE3  
12 (Novagen). Expression of the fusion protein was induced by adding isopropyl-b-D-  
13 thiogalactopyranoside (IPTG, Sigma) up to 1 mM final concentration at an early exponential-phase  
14 culture. After expression induction at 37°C for 3 hours, the bacteria were harvested by centrifugation,  
15 resuspended in 50mM Tris-HCl buffer pH 8.4, 5mM EDTA, and disrupted by sonication in Microson  
16 Ultrasonic Homogenizer XL2000, at 12 W, with 20 cycles (30" ON e 30" OFF). The soluble fraction  
17 was discarded, and the insoluble pellet with the inclusion bodies was washed in denaturing buffer  
18 containing 0.1 M Tris-HCl pH 8.4, 2% Triton, 2M urea, 10 mM EDTA, sonicated and centrifuged three  
19 times at 24000 xg for 20 min. This pellet was further washed in 50mM Tris-HCl buffer pH 8.4, 5mM  
20 EDTA, sonicated for 10 min, centrifuged twice at 24000 xg for 20 min, dissolved in 0.1 M Tris-HCl  
21 buffer pH 8.4, 10 mM EDTA, 8 M urea, 10 mM DTT. Several attempts were then performed to reduce  
22 urea concentration. Kirkland and Keyhani suggested a general protocol to purify recombinant  
23 hydrophobins from inclusion bodies by dialysis of the sample at decreasing urea concentrations<sup>22</sup>. This  
24 refolding strategy did not work in our case, because of rVmh2 aggregation and its interaction with the  
25 dialysis bag. This event was only avoided when the sample was slowly diluted in 0.1 M Tris-HCl, pH  
26 8.4 up to 0.4 M urea (1:20 vol/vol). After TEV addition (0.25  $\mu$ M, final concentration), a precipitate was  
27 formed during the incubation. This precipitate was separated by centrifugation, washed several times in  
28 water, lyophilized, treated with TFA as above described and dissolved in 60% ethanol. The sample was  
29  
30  
31  
32  
33  
34  
35  
36  
37  
38  
39  
40  
41  
42  
43  
44  
45  
46  
47  
48  
49  
50  
51  
52  
53  
54  
55  
56  
57  
58  
59  
60

1 diluted ten times in water, the pH adjusted at 7 by addition of  $\text{NH}_3$ , incubated at  $80^\circ\text{C}$  for 10 minutes  
2 and vortexed to induce hydrophobin aggregation. The precipitate obtained after centrifugation (10 min at  
3 3200 xg), was again treated with TFA and re-dissolved in 60% ethanol.  
4  
5

6  
7 *Protein concentration determination* - Protein concentration were evaluated using the PIERCE 660  
8 nm Protein Assay kit, because of its compatibility with 50% organic solvent. Bovine serum albumin was  
9 used as standard.  
10  
11

12  
13 *SDS-PAGE* - SDS-polyacrylamide gel electrophoresis (SDS-PAGE) was performed using the standard  
14 method and 15% acrilamide concentration. Molecular weight markers from Fermentas were used as  
15 standards. The gels were stained by Coomassie blue or silver staining.  
16  
17  
18

19  
20 *HPLC*- For chromatography analyses a HPLC system (HP 1100 series Agilent Technologies)  
21 equipped with an analytical reverse phase Vydac C8 column (4.6x150 mm,  $5\mu\text{m}$ ) was used. Solvent A  
22 was composed of 0.1% TFA and 10% isopropanol; solvent B was composed of 0.1% TFA in 90 %  
23 acetonitrile and 10% isopropanol. A linear gradient of solvent B from 30 to 95% in 45 minutes at a flow  
24 rate of 1 ml/min was employed. UV absorbance of the eluent was monitored at 220 nm.  
25  
26  
27  
28  
29  
30  
31  
32

33 *Ellman's reaction*- To determine protein free thiol content, Ellman's method was performed. The  
34 protein solution (100  $\mu\text{l}$ ) was mixed with 10 mM DTNB (5,5'-Dithio-bis(2-nitrobenzoic acid))(900  $\mu\text{l}$ )  
35 in 40% ethanol. The absorbance was monitored at 410 nm for 15 min. Cystein solution (100mM) was  
36 used as standard.  
37  
38  
39  
40  
41  
42

43 *Spectroscopy techniques* - Far-UV CD spectra were recorded on a Jasco J715 spectropolarimeter  
44 equipped with a Peltier thermostatic cell holder, in a quartz cell (0.1 cm light path) from 190 to 250 nm.  
45 The temperature was kept at  $20^\circ\text{C}$  and the sample compartment was continuously flushed with nitrogen  
46 gas. The final spectra were obtained by averaging three scans, using a bandwidth of 1 nm, a step width  
47 of 0.5 nm, and a 4 sec averaging per point. The spectra were then corrected for the background signal  
48 using a reference solution without the protein.  
49  
50  
51  
52  
53  
54  
55

56  
57 Fluorescence spectra were recorded at  $25^\circ\text{C}$  with a Perkin-Elmer LS50B fluorescence spectrometer.  
58 Slit widths were set at 10 nm in both the excitation and emission monochromators. Thioflavin T (ThT,  
59  
60

1 Sigma, 100  $\mu\text{M}$  final concentration) was added to the samples. Samples were excited at 435 nm and  
2 emission was monitored from 460 to 600 nm. Spectra were corrected by subtraction of the ThT  
3 spectrum. Turbidimetry analyses were performed evaluating the absorbance values at 405 nm of the  
4  
5  
6  
7 solutions incubated for 10 min in the analyzed conditions<sup>23</sup>.  
8

9  
10 *Mass spectrometry* - MALDI mass spectra were recorded on a Voyager DE Pro MALDI-TOF mass  
11 spectrometer (Applied Biosystems). The analyte solutions were mixed with sinapinic acid (20 mg/ml in  
12  
13 70% acetonitrile, TFA 0.1% v/v), as matrix, applied to the sample plate and air-dried. The spectrometer  
14  
15 was used in the linear or reflectron mode. Spectra were calibrated externally.  
16  
17

18  
19 *Vmh2 biofilms* – A Vmh2 solution (0.3 mg ml<sup>-1</sup> in 60% ethanol) was diluted three-fold in 60%  
20 ethanol, or in 20% ethanol, or in 60% ethanol at pH 6, and Teflon chips were introduced in the glass  
21  
22 tubes containing the solutions. After 24 hr, the chips were removed, air dried, and washed in water.  
23  
24

25  
26 Silicon samples, single side polished, <100> oriented (chip size: 1cmx1cm), after standard cleaning  
27 procedure were washed in hydrofluoric acid solution for three minutes to remove the native oxide thin  
28  
29 layer (1-2 nm) due to silicon oxidation. A drop (80  $\mu\text{L}$ ) of Vmh2 solutions (0.1 mg/ml in 60% ethanol)  
30  
31 was spotted on the chip. After 1 h, samples were dried for 10 min on the hot plate (80°C), and washed  
32  
33 by the solvent solution. This procedure was repeated once again and then the chips were washed by 2%  
34  
35 SDS at 100 °C for 10 min. Ellipsometric characterization of the hydrophobin biofilm was performed by  
36  
37 a variable-angle spectroscopic ellipsometer (UVISEL, Horiba-Jobin-Yvon).  
38  
39

40  
41  
42 Wettability of surfaces has been measured by sessile drop technique. Water Contact Angles (WCA)  
43  
44 have been determined by a OCA 30 – DataPhysics coupled with a drop shape analysis software. Five  
45  
46 measurements were analyzed for each sample.  
47  
48  
49  
50  
51  
52  
53  
54  
55  
56  
57  
58  
59  
60

## RESULTS

1  
2  
3 *Hydrophobin extraction from P. ostreatus mycelia* - The main problem faced with the purification of  
4 the *P. ostreatus* hydrophobins was the removal of non proteic contaminants. As a matter of fact, samples  
5 prepared in different ways, showed an unique band on SDS-PAGE at a Mw corresponding to that of the  
6 hydrophobin (about 10 kDa) (Fig.1), but other analyses (i.e. UV absorption spectra, 1D <sup>1</sup>H-NMR)  
7 indicated the presence of other additional compounds. Several chromatography steps in different  
8 conditions were tried, but very low yields were always obtained, probably because of the high propensity  
9 of the protein to aggregate. Definitely better results were obtained when hydrophobins were directly  
10 solubilized by TFA treatment of the SDS rinsed intact mycelia and extensively washed in a 2:1  
11 chloroform/methanol mixture. Once conditions inducing conformational transition and aggregation were  
12 known (see below), the final protocol was set up, including an aggregation step (by water dilution, pH  
13 adjustment, incubation at 80°C and vortexing). A rather high amount of protein (about 0.1 g per litre of  
14 culture) was obtained.

15  
16  
17  
18  
19  
20  
21  
22  
23  
24  
25  
26  
27  
28  
29  
30  
31 Hydrophobins extraction was performed from vegetative mycelia grown in both static or shaken  
32 cultures. MALDI-MS spectra of the samples extracted from mycelia grown in shaken cultures showed a  
33 peak at 8564 m/z, corresponding to the same peak already attributed to Vmh2 purified from *P. ostreatus*  
34 cultural broth (Fig. 1 of Supporting information; TrEMBL accession number Q8WZI2, starting from  
35 T25)<sup>18</sup>. On the other hand MALDI-MS spectra of samples extracted from mycelia grown in static  
36 cultures showed an additional peak at 8758 m/z probably due to the presence of another hydrophobin  
37 induced in the static growth conditions and bound to the mycelia cell wall. No further investigation has  
38 been performed on these samples, whereas samples extracted from mycelia grown in shaken cultures  
39 were further characterized.

40  
41  
42  
43  
44  
45  
46  
47  
48  
49  
50  
51  
52 *Production and purification of the recombinant hydrophobin in E. coli (rVmh2)* - Recombinant  
53 expression of *vmh2* cDNA was performed using a construct designed to increase protein solubility.  
54 rVmh2 N-terminus was fused to glutathione S-transferase (GST) and to His-6 tag, linked through a  
55 sequence coding for a specific protease (TEV protease) site. The recombinant protein was found in  
56  
57  
58  
59  
60

inclusion bodies. Hence it was dissolved in 8M urea and slowly diluted up to 0.4 M urea. However, after removal of the GST tag (after incubation with the TEV protease), rVmh2 spontaneously precipitated in the buffer. The typical yield of rVmh2 was about 50 mg/l of culture.

*Comparison of recombinant and extractive Vmh2* - The chromatographic behavior of the two proteins was compared by means of a high resolution technique, a reverse phase HPLC on a C8 column. Even if the protein yield was very low, detectable peaks were obtained in highly apolar conditions. A peak eluting at 25 min was observed for both samples (Fig. 1A and B).

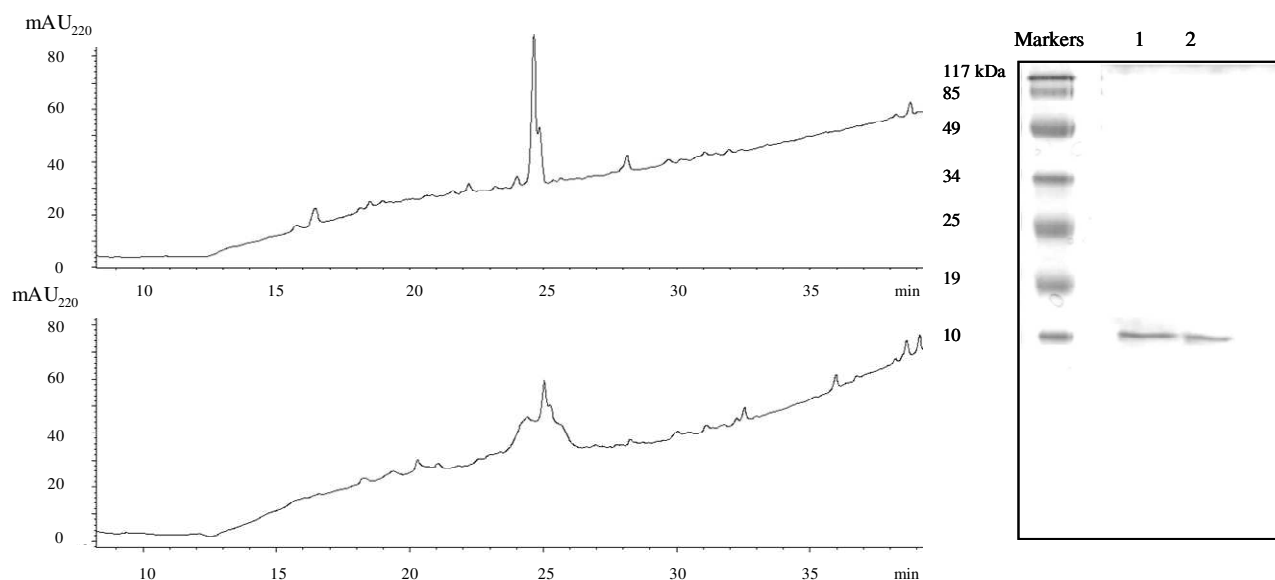


Figure 1 HPLC profiles of rVmh2 (A) and Vmh2 from *P. ostreatus* mycelia (B); SDS-PAGE of rVmh2 (lane 1) and Vmh2 (lane 2) (C)

The electrophoretic mobility in SDS PAGE of the recombinant and mycelia extractive proteins was the same, as shown in Fig. 1C. The shape of the extractive protein peak was broader than that of the recombinant one, probably because of the presence of different forms of the mycelium protein.

The presence of free Cys in the purified proteins was analysed by the Ellmann assay, and no free SH group was detected in both extractive and recombinant purified proteins.

1  
2  
3  
4  
5  
6  
7  
8  
9  
10  
11  
12  
13  
14  
15  
16  
17  
18  
19  
20  
21  
22  
23  
24  
25  
26  
27  
28  
29  
30  
31  
32  
33  
34  
35  
36  
37  
38  
39  
40  
41  
42  
43  
44  
45  
46  
47  
48  
49  
50  
51  
52  
53  
54  
55  
56  
57  
58  
59  
60

Absorbance spectra of both samples are shown in Fig. 2. It is worth noting the peculiar resolution of the spectra with a maximum at about 260 nm, due to the unique aromatic residue in the protein (F96 in the sequence whose TrEMBL accession number is Q8WZI2).

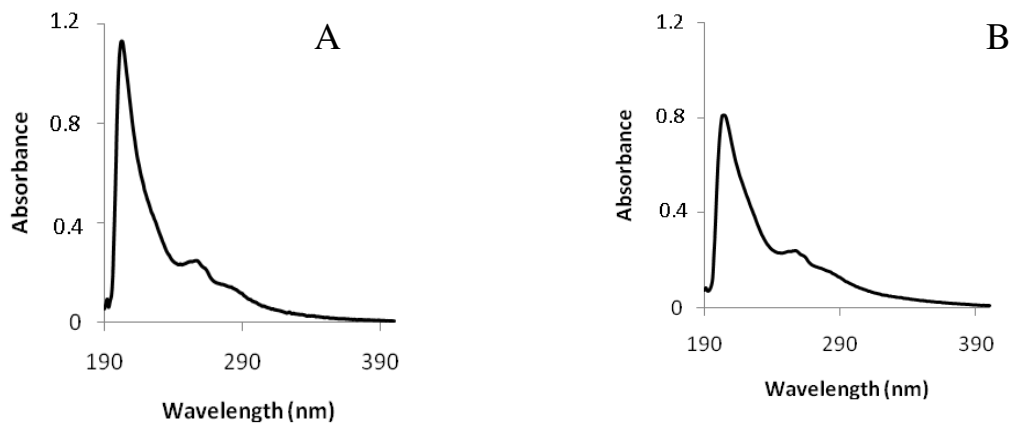


Figure 2: Absorbance spectra of rVmh2 (A) and Vmh2 (B) in 60% ethanol

CD spectra of the two proteins dissolved in 60% ethanol indicate a prevailing  $\alpha$  helix structure (Fig. 3). These solutions are stable at 4°C and no variation of their spectra was observed over 1 month.

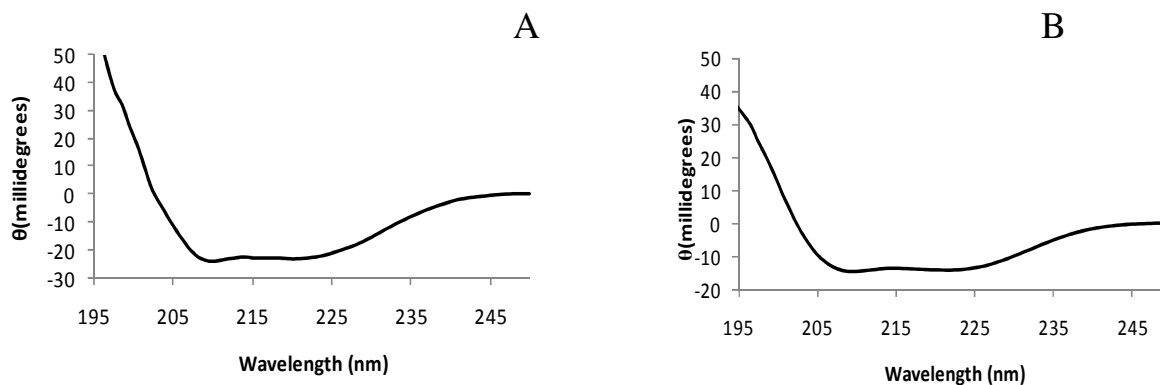


Figure 3. CD spectra of rVmh2 (A) and Vmh2 (B) in 60% ethanol

*Vmh2 characterization: Effect of pH, temperature, salts* - Experiments were carried out in order to evaluate the protein behavior in different conditions, as pH, temperature, ionic strength or solvent

polarity. In all these conditions Vmh2 and rVmh2 always showed analogous behaviors, therefore results obtained using Vmh2 are just shown. However the representative data obtained with rVmh2 are reported as Supplementary information (Fig. 2-5).

When the pH was adjusted at 6 or 8 by addition of few micro-liters of 2M  $\text{NH}_3$  to the 60% ethanol solution, CD spectra showed a shift ascribable to a conformation with a higher contribution of  $\beta$  structure. Turbidimetry analyses (absorbance measurements at 405 nm) were performed in order to evaluate the correlation of these conformational changes to protein aggregation. Results shown in Fig. 4, pointed out that the aggregation process occurs at pH values above 4. Moreover, the protein was undetectable (by CD and protein concentration assay) when samples are centrifuged after 6 hr at pH 6.

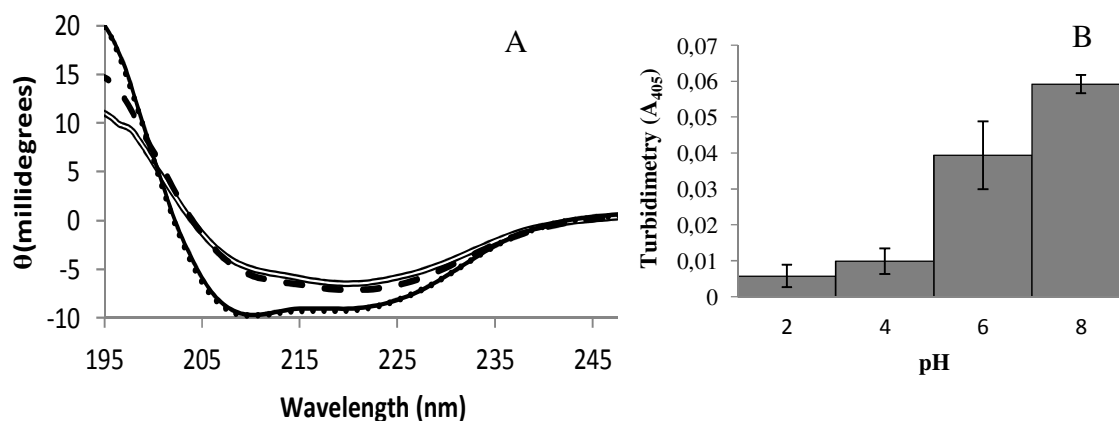


Figure 4. pH effect on the Vmh2 conformation. A: CD spectra at different pHs ( — pH 2, ..... pH 4, - - pH 6, = = pH 8); B: turbidimetry analysis of these samples.

The effect of the presence of monovalent or bivalent cations on Vmh2 was also evaluated (Fig 5). Calcium ions at concentration higher than 10 mM induced conformational changes similar to those obtained at pH higher than 4. Results obtained from turbidimetry, CD and protein concentration analyses, carried out on samples in  $\text{CaCl}_2$ , again suggested that the conformational change was associated to protein aggregation. On the other hand, no conformational change and turbidimetry increase were observed in the presence of magnesium ions, so indicating a specific interaction of the

protein with calcium ions. Moreover the presence of 10 mM NaCl did not affect the conformation and self-assembly of the protein, on the contrary inhibited the conformational changes observed at pH 6.

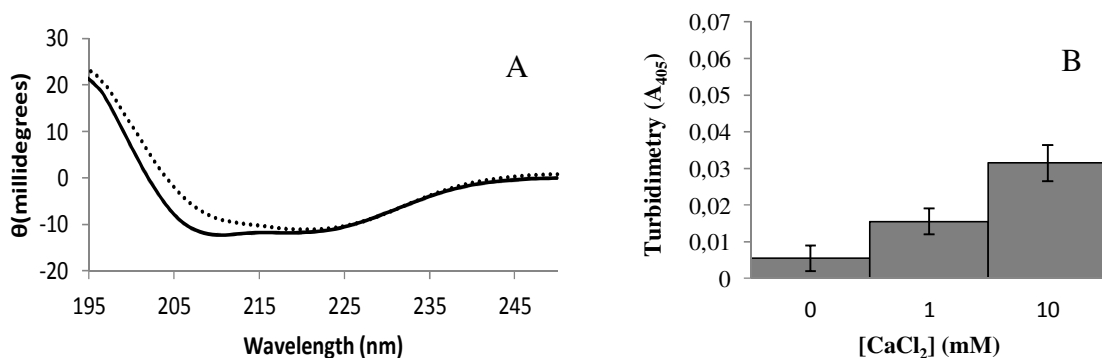


Figure 5. A: CD spectra of Vmh2 in 60% ethanol (—) and upon addition (····) of 10 mM  $\text{CaCl}_2$ ; B: turbidimetry analysis of samples at different  $\text{CaCl}_2$  concentrations.

As far as the effect of temperature on the protein structure is concerned, a different variation of the CD spectra occurred at 80°C (Fig. 6), showing in this case a higher contribution of random conformation. **This partial unfolding** is reversible, as a fact when the temperature is again lowered at 25°C, spectra very similar to the original ones were recorded. Turbidimetry analysis indicates the formation of aggregates, but confirms the reversibility of the process. This reversible conformational change **is expected to reduce** the affinity of contaminants for the protein and indeed was used as a purification step.

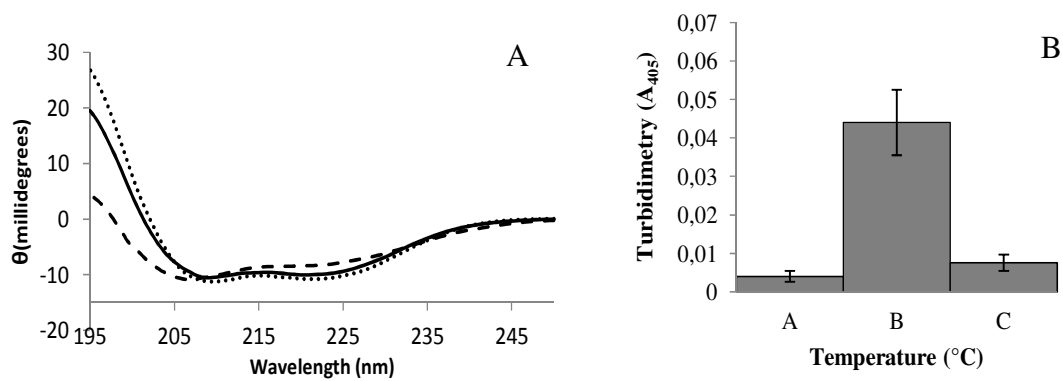




Figure 6 A: Temperature effect on Vmh2 conformation. CD spectra in 60% ethanol at 25°C (—), after 10 min incubation at 80°C (---), after 10 min incubation at 80°C and 10 min at 25°C (·····); B: turbidimetry analysis of the sample at 25°C (a), at 80°C (b), at 25°C after 80°C incubation (c).

Fluorescence analyses in the presence of ThT were performed to further analyze the protein aggregates, since ThT has become a very widely used standards for identification of amyloid and amyloid-like fibrils both *in vivo* and *in vitro*. A high increase of ThT fluorescence intensity was observed for the Vmh2 solutions at pH 6 or in the presence of calcium ions, while no increase was observed in the presence of NaCl or at 80 °C (Fig. 7). Therefore changes of the protein conformation (pH≥6 or [Ca<sup>2+</sup>]≥10mM) are linked to protein aggregation (turbidimetry increase) and the increase of ThT fluorescence intensity indicates the formation of an amyloid like, β-sheet state.

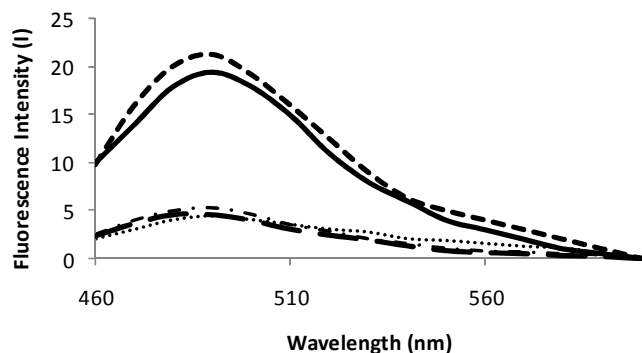
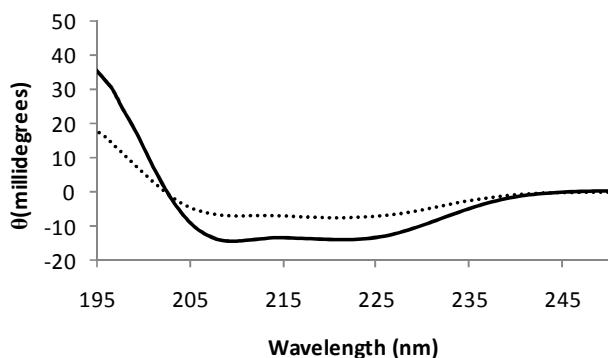


Figure 7: Fluorescence spectra of Vmh2 in the presence of 100 μM ThT in different conditions. pH 4 (---), pH 6 (—), presence of 10 mM CaCl<sub>2</sub> (- · - ·), pH 6 in the presence of 10 mM NaCl (- · · ·), after 10 min incubation at 80°C (·····). Spectra were corrected by subtraction of the ThT spectrum.

*Vmh2 characterization: Effect of solvent* - Vmh2 was usually dissolved in 60% ethanol at a concentration of 0.1÷0.2 mg/ml. If the protein was solubilized in 40% ethanol, no significant variation of its concentration was observed, whilst at 20% ethanol the amount of dissolved protein was about one third of that in 60% ethanol. Moreover, when Vmh2 was dissolved in 10% ethanol or in pure water, the

1 protein concentration was at level of the lowest detection limit of the assay (about  $25 \mu\text{g mL}^{-1}$ ). Similar  
2 results were also obtained by sample dilution. Again the concentration of the protein diluted in 20%  
3 ethanol, as well as the intensity of its CD spectrum, was about one third with respect to that diluted in  
4 60% ethanol. It is worth noting that CD spectra in 60 or 20% ethanol showed very similar profiles (Fig.  
5 8).  
6  
7  
8  
9  
10



11  
12  
13  
14  
15  
16  
17  
18  
19  
20  
21  
22  
23  
24  
25  
26 Figure 8: CD spectra of Vmh2 in 60% ethanol (—) and 20% ethanol (·····).  
27  
28  
29

30 Therefore in this condition the protein maintains a  $\alpha$  helix structure, but it is less soluble.  
31  
32 Turbidimetry analyses showed the absence of sizeable aggregates in both conditions (20 and 60%  
33 ethanol) and no increase of the fluorescence intensity in the presence of ThT was observed. Moreover  
34 protein solutions in 20% ethanol are stable, as a matter of fact no difference of concentration or CD  
35 spectra was noticed in samples after either vortexing or 24 hr incubation followed by centrifugation.  
36  
37 Other solvents, isopropanol, trifluoroethanol (TFE) or acetonitrile, a non-alcoholic solvent, were chosen  
38 and used to investigate on the parameters affecting the Vmh2 behavior. In Table 1, literature data about  
39 surface tension and dielectric constant of the 20% and 60% solvent/water mixtures are reported<sup>24-29</sup>. It is  
40 shown that the surface tension of 60% ethanol is comparable to that of 20% isopropyl alcohol or TFE,  
41 which in turn are close to each other. On the other hand the dielectric constants of all the mixtures are  
42 linked mainly to the mixture percentage and not to the specific solvent.  
43  
44  
45  
46  
47  
48  
49  
50  
51  
52  
53  
54  
55  
56  
57  
58  
59  
60

	% (vol/vol)	Surface tension (mN m <sup>-1</sup> )	Dielectric constant	References
ethanol	20	56	70	24, 25
ethanol	60	27	46	
isopropanol	20	32	67	24, 26
isopraponol	60	23	42	
TFE	20	31	70	27
TFE	60	25	49	
acetonitrile	20	42	70	28, 29
acetonitrile	60	33	51	

Table 1 Dependence of the surface tension and dielectric constant at 25°C on the concentration of concentration of ethanol, isopropanol, TFE, acetonitrile in water, using published data.

In order to verify if the Vmh2 behavior is correlated with the surface tension or dielectric constant values of the solvents, solubility and CD spectra of the protein dissolved in 20 or 60% isopropyl alcohol, TFE or acetonitrile were determined. The concentration of the protein in 20% solvent, as well as the intensity of the CD spectra, were about one third of that in 60%, whilst the profiles of the CD spectra were similar (Fig.6 of Supplementary information). Since these results are comparable to those obtained using ethanol, we can infer that i) Vmh2 solubility is linked to the value of the dielectric constant (polarity) of the media rather than that of their surface tension; ii) its  $\alpha$ -helical conformation is not strictly related to the presence of alcohols.

Overall, taking into consideration the results obtained in the presence of 20% co-solvent (concentration decrease, no increase of turbidimetry, no conformational variation, no increase of ThT fluorescence intensity) the increased solvent polarity seems to increase the protein tendency to reach hydrophilic/hydrophobic interfaces, rather than the formation of the assembled  $\beta$ -sheet state, as occurs at high pH or in the presence of calcium chloride.

Moreover it has been verified the emulsifying capability of Vmh2 in 20% ethanol. Stable emulsions (at least for 7 days) were obtained by mixing the hydrophobin with almond or peanut oils at pH 2 or 4, whilst a complete separation of the two phases was observed just after some hours at pH 6 or 8.

*Biofilm formation* - In order to confirm the propensity of Vmh2 to reach hydrophobic/hydrophilic interface when solvent polarity increases, the WCA of Teflon chips immersed in solution of Vmh2 were determined. Indeed, the WCA change can be related to the amount of protein migrated to the hydrophobic surface. Results in 20% or 60% ethanol, at pH4 or 6, are shown in Table 2.

	bare Teflon	60% ethanol pH 4	20% ethanol pH 4	60% ethanol pH 6	20% ethanol pH 6
WCA	100±1	95±4	66±1	90±2	98±4

Table 2 Water contact angles (WCA) of Teflon chips dried after 24 hr incubation in the presence of Vmh2 in 20% or 60% ethanol, at pH 4 or 6, compared to bare Teflon.

Very slight WCA changes were observed in 60% ethanol either at pH 4 or 6 and in 20% ethanol at pH 6, whilst a significant decrease of WCA was observed in the more polar solution (20% ethanol) at pH 4. Therefore if Vmh2 forms self-assembled  $\beta$ -sheet state (pH 6), it will not reach the hydrophobic surface, whatever was the solvent polarity. On the other hand, when Vmh2 does not form self-assembled  $\beta$ -sheet state (pH 4) the increased solvent polarity (20% ethanol) leads to increase the protein tendency to reach hydrophilic/hydrophobic interfaces.

Very stable and uniform protein biofilms were formed by deposition on silicon surfaces of both Vmh2 or rVmh2. These films were washed in harsh conditions, and characterized by VASE using the optical model for experimental data fitting developed in a previous work<sup>30</sup>. Their thickness was  $5\pm 1$  nm and the water contact angle on the silicon surfaces decreased from  $90^\circ\pm 2^\circ$  to about  $28^\circ\pm 1^\circ$ , thus indicating a drastic change of the surface wettability.

## DISCUSSION

1  
2  
3 The class I hydrophobin secreted in the cultural broth by the basidiomycete fungus *Pleurotus*  
4 *ostreatus*, previously purified and identified as Vmh2, represents still the most hydrophobic  
5 hydrophobin characterized so far, being very scarcely soluble in water and soluble in less polar solvents  
6 (i.e. ethanol, at least 40%)<sup>18</sup>. In this paper we report the purification of the same protein from the  
7 mycelial mat, obtaining hundred milligrams per litre of culture broth, and the expression in *E. coli* of the  
8 recombinant Vmh2 (rVmh2), even if with a lower yield. Vmh2 and rVmh2 behave very similarly under  
9 all the different conditions analyzed, thus suggesting that there is no structural difference between them.  
10  
11  
12  
13  
14  
15  
16  
17  
18

19 CD spectra show that the protein in 60% ethanol adopts mainly a  $\alpha$ -helix conformation. A similar  
20 conformation has been observed for another class I hydrophobin, SC3, only when assembled on a  
21 hydrophobic colloidal Teflon surface<sup>4,31-32</sup>. The  $\alpha$ -helix is a stable conformation of Vmh2 in solution, as  
22 a matter of fact no change of the CD spectrum was detectable even when the protein solution is agitated,  
23 thus continuously introducing new hydrophobic:hydrophilic interface, as already previously reported<sup>18</sup>.  
24  
25  
26  
27  
28  
29  
30

31 Vmh2 conformation is affected by temperature in a reversible way, since at high temperature an  
32 increased contribution of random conformation is observed, but the  $\alpha$ -helix structure is recovered  
33 coming back to room temperature. This behavior, together with the absence of ThT fluorescence  
34 increase, excludes the formation of Vmh2 stable aggregates, which can only be reversed in the presence  
35 of TFA, and points to the presence of a different form of reversible aggregates.  
36  
37  
38  
39  
40  
41  
42

43 On the other hand, by increasing the pH of the solution ( $\text{pH} \geq 6$ ), Vmh2 undergoes a conformational  
44 change, forming a self-assembled  $\beta$ -sheet rich state. A significant increased association at alkaline pH  
45 has been also demonstrated for SC3<sup>20</sup>. Analogous behavior was observed in the presence of  $\text{Ca}^{2+}$ , while  
46 a monovalent cation,  $\text{Na}^+$ , has a quite opposite effect, inhibiting the conformational change and self-  
47 assembly occurring at pH 6. The recombinant class I hydrophobin H\*protein A, studied using other  
48 techniques such as analytical ultracentrifugation, has showed propensity to self-assembly in the same  
49 conditions of Vmh2<sup>12</sup>. It has been suggested that the formation of large agglomerates can be triggered by  
50 bivalent cations bridging and prevented by charge screening with monovalent cations. However it is  
51  
52  
53  
54  
55  
56  
57  
58  
59  
60

1  
2  
3  
4  
5  
6  
7  
8  
9  
10  
11  
12  
13  
14  
15  
16  
17  
18  
19  
20  
21  
22  
23  
24  
25  
26  
27  
28  
29  
30  
31  
32  
33  
34  
35  
36  
37  
38  
39  
40  
41  
42  
43  
44  
45  
46  
47  
48  
49  
50  
51  
52  
53  
54  
55  
56  
57  
58  
59  
60

worth noting that we observe conversion into the  $\beta$ -sheet rich, assembled form, not triggered by migration to hydrophobic:hydrophilic interface as suggested by Morris et al.<sup>17</sup>, since Vmh2 self-assembles without agitation of the protein solution.

Furthermore, an intriguing effect of solvents on the Vmh2 behavior has been more carefully analyzed. In solutions characterized by low solvent dielectric constants (range from 40 to 50) and low pH, Vmh2 assumes the stable  $\alpha$ -helical conformation. When the solvent polarity values increase (up to  $\approx 70$ ), no conformational transition is observed, but its solubility is decreased. This is due to an increased tendency to reach hydrophobic surfaces, not necessarily correlated with  $\beta$ -sheet state formation. This process is reported here for the first time, and points to a mechanism similar to the one described by Morris and coauthors<sup>17</sup>, who reported that the Class I hydrophobins EAS and DewA do not change their conformation, when the apolar solvent percentage increases, but reduce the rodlet assembly rate (induced by solution agitation). They suggest that additives (i.e. alcohols) in an aqueous environment can be adsorbed onto the relatively large exposed surface hydrophobic areas of hydrophobin molecules, thus reducing protein-protein interactions. This hypothesis can explain the solubility increase observed for the more hydrophobic hydrophobin Vmh2 in the presence of apolar solvents and its increased tendency to reach hydrophobic:hydrophilic interfaces in more polar solutions. However, it is important to highlight that, in the case of Vmh2, conversion into the assembled form is always associated with the switch towards a  $\beta$ -conformation, even in the absence of new air:water interfaces. Therefore a reasonable explanation of the Vmh2 behaviour could be the stabilization of the  $\alpha$ -helix conformation in the presence of apolar solvents or  $\text{Na}^+$  ions, and an induction of the self-assembled  $\beta$ -sheet state, in the presence of  $\text{Ca}^{2+}$  or by increasing the negative charge of the molecules at  $\text{pH} \geq 6$  (calculated  $\text{pI} = 3.9$ ).

Overall our data suggest that distinct phenomena are modulated by the environmental conditions.

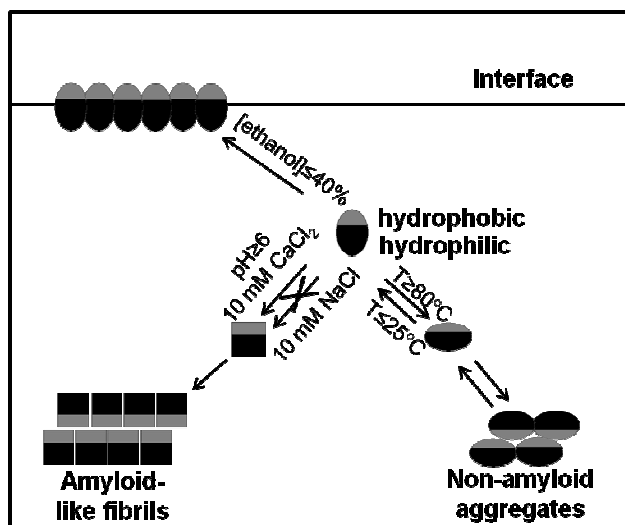
Starting from the helical structure observed in low polarity solvents, the following events can occur:

1- **Irreversible** conformational change towards a  $\beta$ -structure followed by **self-assembling** when the pH increases above 6 or in the presence of  $\text{Ca}^{2+}$  ions.

1 2- Increased tendency to reach hydrophobic/hydrophilic interfaces when the solvent polarity increases,  
2  
3 with no detectable conformational change.

4  
5 3- Reversible conformational change **towards a disordered structure** and reversible aggregation at high  
6  
7 temperature.

8  
9 A schematic representation of the behavior of Vmh2 by changing the environmental conditions is  
10  
11 shown in Fig 9.



12  
13  
14  
15  
16  
17  
18  
19  
20  
21  
22  
23  
24  
25  
26  
27  
28  
29  
30  
31  
32 Fig. 9 Schematic representation of the Vmh2 self-assembling mechanisms.

33  
34  
35  
36  
37 In conclusion the unique conformational/aggregation features of Vmh2 can be easily modulated by  
38  
39 changing the environmental conditions. Further studies will be necessary to give details on the protein  
40  
41 aggregation state at the interface. On the other hand, to the best of our knowledge, phenomena like those  
42  
43 occurring to Vmh2 (points 2 and 3) are clearly described here for the first time and are worth of further  
44  
45 investigation. Moreover, the availability of a simple, handy protocol for recombinant protein expression  
46  
47 and purification will open the way for a deeper analysis of the structure/function relationship of this  
48  
49 interesting protein.  
50  
51  
52  
53  
54  
55  
56  
57  
58  
59  
60

1 ACKNOWLEDGMENT The authors thank Emanuele Orabona and Fabrizio Porro for their support  
2  
3 in the biofilm characterizations. This work was supported by grant from the Ministero dell'Università e  
4  
5 della Ricerca Scientifica (Progetti di Rilevante Interesse Nazionale, PRIN 20088L3BP3)  
6  
7

8  
9 SUPPORTING INFORMATION AVAILABLE

10  
11 Figure 1. pH effect on the rVmh2 conformation. A: CD spectra at different pHs (— pH 2, ..... pH  
12  
13 4, -- pH 6, == pH 8); B: turbidimetry analysis of these samples.  
14  
15  
16

17  
18 Figure 2. A: CD spectra of rVmh2 in 60% ethanol (—) and upon addition (.....) of 10 mM CaCl<sub>2</sub>;  
19  
20 B: turbidimetry analysis of samples at different CaCl<sub>2</sub> concentrations.  
21  
22

23  
24 Figure 3 A: Temperature effect on rVmh2 conformation. CD spectra in 60% ethanol at 25°C (—),  
25  
26 after 10 min incubation at 80°C (--), after 10 min incubation at 80°C and 10 min at 25°C (.....); B:  
27  
28 turbidimetry analysis of the sample at 25°C (a), at 80°C (b), at 25°C after 80°C incubation (c).  
29  
30

31  
32 Figure 4: Fluorescence spectra of rVmh2 in the presence of 100 μM ThT in different conditions. pH 4  
33  
34 (--), pH 6 (—), presence of 10 mM CaCl<sub>2</sub> (---), pH 6 in the presence of 10 mM NaCl (-·-·),  
35  
36 after 10 min incubation at 80°C (.....). Spectra were corrected by subtraction of the ThT spectrum.  
37  
38

39  
40 Fig.5: CD spectra of Vmh2 in 60% (—) or 20% (.....) acetonitrile (A), isopropanol (B), and  
41  
42 trifluoroethanol (C).  
43  
44  
45  
46  
47  
48  
49  
50

51 This material is available free of charge via the Internet at <http://pubs.acs.org>.  
52  
53  
54  
55  
56  
57  
58  
59  
60



## FIGURE CAPTIONS

1  
2  
3 Figure 1: HPLC profiles of rVmh2 (A) and Vmh2 from *P. ostreatus* mycelia (B); SDS-PAGE of rVmh2  
4 (lane 1) and Vmh2 (lane 2) (C)

5  
6  
7  
8  
9 Figure 2: Absorbance spectra of rVmh2 (A) and Vmh2 (B) in 60% ethanol

10  
11  
12 Figure 3. CD spectra of rVmh2 (A) and Vmh2 (B) in 60% ethanol

13  
14  
15 Figure 4. pH effect on the Vmh2 conformation. A: CD spectra at pH ( — pH 2, ..... pH 4, - - pH  
16 6, = pH 8); B: turbidimetry analysis of these samples.

17  
18  
19  
20  
21 Figure 5. A: CD spectra of Vmh2 in 60% ethanol ( — ) and upon addition ( ..... ) of 10 mM CaCl<sub>2</sub>;  
22  
23 B: turbidimetry analysis of samples at different CaCl<sub>2</sub> concentrations.

24  
25  
26 Figure 6 A: Temperature effect on Vmh2 conformation. CD spectra in 60% ethanol at 25°C ( — ),  
27  
28 after 10 min incubation at 80°C ( - - ), after 10 min incubation at 80°C and 10 min at 25°C ( ..... ); B:  
29  
30 turbidimetry analysis of the sample at 25°C (a), at 80°C (b), at 25°C after 80°C incubation (c).

31  
32  
33  
34 Figure 7: Fluorescence spectra of Vmh2 in the presence of 100 μM ThT in different conditions.

35  
36  
37 pH 4 ( - - ), pH 6 ( — ), presence of 10 mM CaCl<sub>2</sub> ( - - - ), pH 6 in the presence of 10 mM NaCl  
38  
39 ( - - - - ), after 10 min incubation at 80°C ( ..... ). **Spectra were corrected by subtraction of the ThT**  
40  
41 **spectrum.**

42  
43  
44 Figure 8: CD spectra of Vmh2 in 60% ethanol ( — ) and 20% ethanol ( ..... ).

45  
46  
47 Fig. 9 Schematic representation of the Vmh2 self-assembling mechanisms.

## TABLES.

1  
2  
3 Table 1 Dependence of the surface tension and dielectric constant at 25°C on the concentration of  
4  
5 concentration of ethanol, isopropanol, TFE and acetonitrile in water, using published data  
6  
7

8  
9 Table 2 Water contact angles (WCA) of Teflon chips dried after 24 hr incubation in the presence of  
10  
11 Vmh2 in 60% ethanol, in 20% ethanol, or at pH 6, compared to bare Teflon.  
12  
13  
14  
15  
16  
17  
18  
19  
20  
21  
22  
23  
24  
25  
26  
27  
28  
29  
30  
31  
32  
33  
34  
35  
36  
37  
38  
39  
40  
41  
42  
43  
44  
45  
46  
47  
48  
49  
50  
51  
52  
53  
54  
55  
56  
57  
58  
59  
60

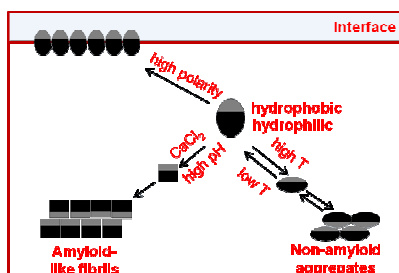
## REFERENCES

- 1  
2  
3 (1) Linder, M. *Curr. Opin. Colloid Interface Sci.* **2009**, *14*, 356–363.
- 4  
5  
6 (2) Wösten, H. A. B. *Annu. Rev. Microbiol.* **2001**, *55*, 625–46.
- 7  
8  
9 (3) Linder, M. B., Szilvay, G. R., Nakari-Setälä, T., Penttilä, M. E. *FEMS Microbiol Rev.* **2005**, *29*, 877-  
10 896.
- 11  
12  
13 (4) Sunde, M., Kwan, A. H., Templeton, M. D., Beever, R. E., Mackay, J. P. *Micron* **2008**, *39*, 773-84.
- 14  
15  
16 (5) Hektor, H. J., Scholtmeijer, K. *Curr Opin Biotechnol.* **2005**, *16*, 434–439.
- 17  
18  
19 (6) Zhao, Z.X., Qiao, M.Q., Yin, F., Shao, B., Wu, B. Y., Wang, Y. Y., Wang, X. S., Qin, X., Li S.,  
20 Yu, L., Chen, Q. *Biosens Bioelectron.* **2007**, *22*, 3021-3027.
- 21  
22  
23 (7) Zhao, Z. X., Wang, H. C., Qin, X., Wang, X. S., Qiao, M. Q., Anzai, J., Chen, Q. *Colloids Surf B*  
24 *Biointerfaces.* **2009**, *71*, 102-106.
- 25  
26  
27 (8) Hou, S., Yang, K., Qin, M., Feng, X. Z., Guan, L., Yang, Y., Wang, C. *Biosens Bioelectron.* **2008**,  
28 24, 918-922.
- 29  
30  
31 (9) Li, X., Hou, S., Feng, X., Yu, Y., Ma, J., Li, L. *Colloids Surf B Biointerfaces* **2009**, *74*, 370-374.
- 32  
33  
34 (10) Cox, A. R., Cagnol, F., Russell, A. B., Izzard, M. J. *Langmuir* **2007**, *23*, 7995-8002.
- 35  
36  
37 (11) Cox, A. R., Aldred, D. L., Russell, A. B. *Food Hydrocolloids* **2009**, *23*, 366–376.
- 38  
39  
40 (12) Wohlleben, W., Subkowski, T., Bollschweiler, C., von Vacano, B., Liu, Y., Schrepp, W., Baus,  
41 U. *Eur Biophys J.* **2010**, *39*, 457-468.
- 42  
43  
44 (13) Haas Jimoh Akanbi, M., Post, E., Meter-Arkema, A., Rink, R., Robillard, G. T., Wang, X.,  
45 Wösten, H. A., Scholtmeijer, K. *Colloids Surf B Biointerfaces* **2010**, *75*, 526-531.
- 46  
47  
48 (14) Valo, H. K., Laaksonen, P. H., Peltonen, L. J., Linder, M. B., Hirvonen, J. T., Laaksonen, T. J.  
49 *ACS Nano* **2010**, *4*, 1750-1758.
- 50  
51  
52  
53  
54  
55  
56  
57  
58  
59  
60

- 1  
2  
3  
4  
5  
6  
7  
8  
9  
10  
11  
12  
13  
14  
15  
16  
17  
18  
19  
20  
21  
22  
23  
24  
25  
26  
27  
28  
29  
30  
31  
32  
33  
34  
35  
36  
37  
38  
39  
40  
41  
42  
43  
44  
45  
46  
47  
48  
49  
50  
51  
52  
53  
54  
55  
56  
57  
58  
59  
60
- (15) Askolin, S., Nakari-Setälä, T., Tenkanen, M. *Appl Microbiol Biotechnol.* **2001**, *57*, 124-130.
- (16) Scholtmeijer, K., de Vocht, M. L., Rink, R., Robillard, G. T., Wösten, H.A. *J Biol Chem.* **2009**, *284*, 26309-26314.
- (17) Morris, V. K., Ren, Q., Macindoe, I., Kwan, A. H., Byrne, N., Sunde, M. *J Biol Chem.* **2011**, *286*, 15955-15963.
- (18) Armenante, A., Longobardi, S., Rea, I., De Stefano, L., Giocondo, M., Silipo, A., Molinaro, A., Giardina, P. *Glycobiology.* **2010**, *20*, 594–602.
- (19) Peñas, M. M., Rust, B., Larraya, L. M., Ramírez, L., Pisabarro, A.G. *Appl Environ Microbiol.* **2002**, *68*, 3891-3898.
- (20) Houmadi S., Ciuchi, F., De Santo, M. P., De Stefano, L., Rea, I., Giardina, P., Armenante, A., Lacaze, E., Giocondo, M. *Langmuir.* **2008**, *24*, 12953-12957.
- (21) Wang, X., Graveland-Bikker, J. F., De Kruif, C. G., Robillard, G. T. *Protein Science* **2004**, *13*, 810–821.
- (22) Kirkland, B. H., Keyhani, N. O. *J Ind Microbiol Biotechnol.* **2011**, *38*, 327-35.
- (23) Murphy, R. M., Pallitto, M. M. *J. Struct. Biol.* **2000**, *130*, 109–122.
- (24) Vazquez, G., Alvarez, E., Navaza, J. M. *J. Chem. Eng. Data* **1995**, *40*, 611-614.
- (25) Yilmaz, H. *Turk. J. Phys.* **2002**, *26*, 243-246.
- (26) Park, J. G., Lee, S. H., Ryu, J. S., Hong, Y. K., Kim, T. G., Busnaina, A. A. *J. Electrochem. Soc.*, **2006**, *153*, G811-G814.
- (27) Gente, G., La Mesa, C. *J. Sol. Chem.* **2000**, *29*, 1159-1172.
- (28) Gagliardi, L. G., Castells, C. B., Rafols, C., Roses, M., Bosch, E. *J. Chem. Eng. Data* **2007**, *52*, 1103-1107.
- (29) Rafati, A.A., Bagheri, A., Najafi M. *J. Chem. Thermodynamics* **2011**, *43*, 248–254.

- 1  
2  
3  
4  
5  
6  
7  
8  
9  
10  
11  
12  
13  
14  
15  
16  
17  
18  
19  
20  
21  
22  
23
- (30) De Stefano, L., Rea, I., Armenante, A., Giardina, P., Giocondo, M., Rendina, I. *Langmuir* **2007**, *23*, 7920–7922.
- (31) de Vocht, M. L., Scholtmeijer, K., van der Vegte, E. W., de Vries, O. M., Sonveaux, N., Wösten, H. A., Ruyschaert, J. M., Hadziioannou, G., Wessels, J. G., Robillard, G. T. *Biophys J.* **1998**, *74*, 2059-2068.
- (32) de Vocht, M. L., Reviakine, I., Ulrich, W. P., Bergsma-Schutter, W., Wösten, H. A., Vogel, H., Brisson, A., Wessels, J. G., Robillard, G. T. *Protein Sci.* **2002**, *11*, 1199-1205.

## Table of Contents Graphic



10 20 30 40 50 60 70 80  
 TDTFSCSTGSLQCCSSVQKATDPLASLLIGLLGIVLGPLDLLVGVTCSPITVIGVGGTSC TQQTVCC TGN SFNGLIAIGC  
 SPINISL

Figure 1. Sequence of the mature Vmh2 (TrEMBL accession number Q8WZI2, starting from T25)

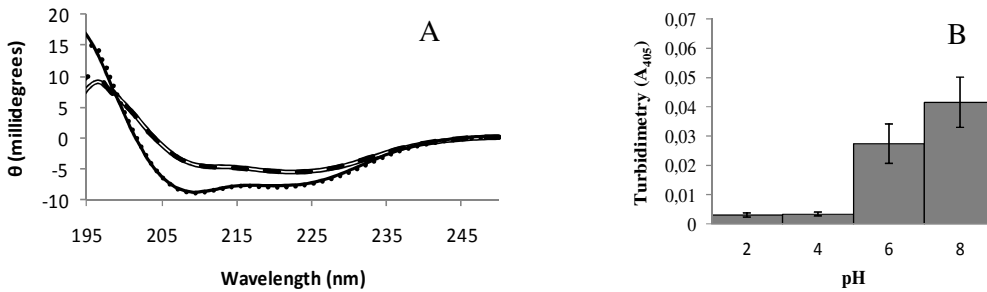


Figure 2. pH effect on the rVmh2 conformation. A: CD spectra at pH (— pH 2, .....pH 4, - - pH 6, = = pH 8); B: turbidimetry analysis of these samples.

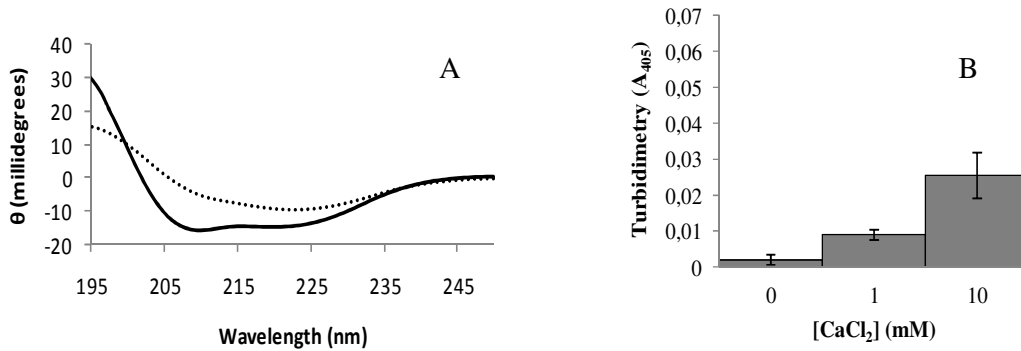


Figure 3. A: CD spectra of rVmh2 in 60% ethanol (—) and upon addition (.....) of 10 mM  $CaCl_2$ ; B: turbidimetry analysis of samples at different  $CaCl_2$  concentrations.

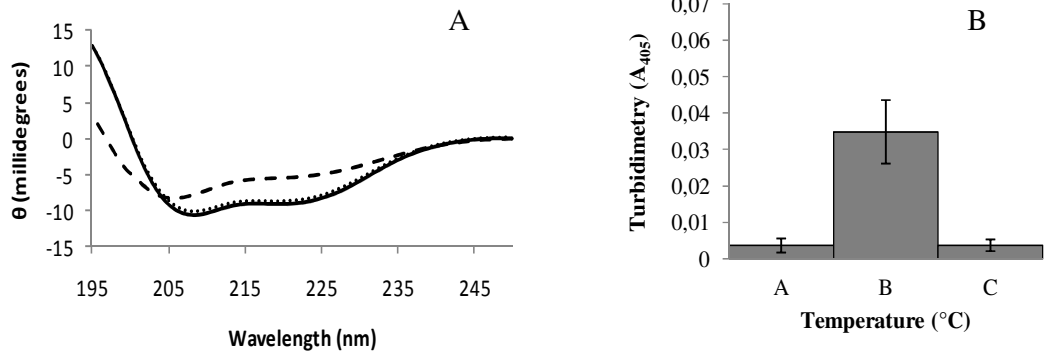


Figure 4. A: Temperature effect on rVmh2 conformation. CD spectra in 60% ethanol at 25°C (—), after 10 min incubation at 80°C (---), after 10 min incubation at 80°C and 10 min at 25°C (.....); B: turbidimetry analysis of the sample at 25°C (a), at 80°C (b), at 25°C after 80°C incubation (c).

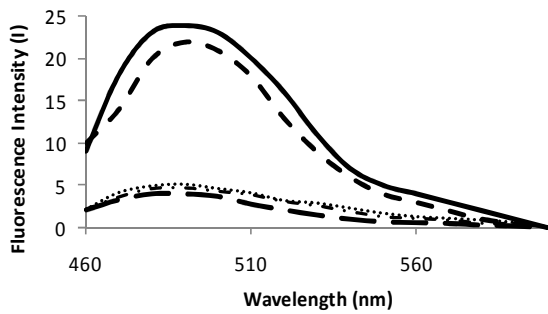


Figure 5. Fluorescence spectra of rVmh2 in the presence of 100  $\mu$ M ThT in different conditions. pH 4 (---), pH 6 (—), presence of 10 mM  $CaCl_2$  (.....), pH 6 in the presence of 10 mM NaCl (- · - ·), after 10 min incubation at 80°C (.....).

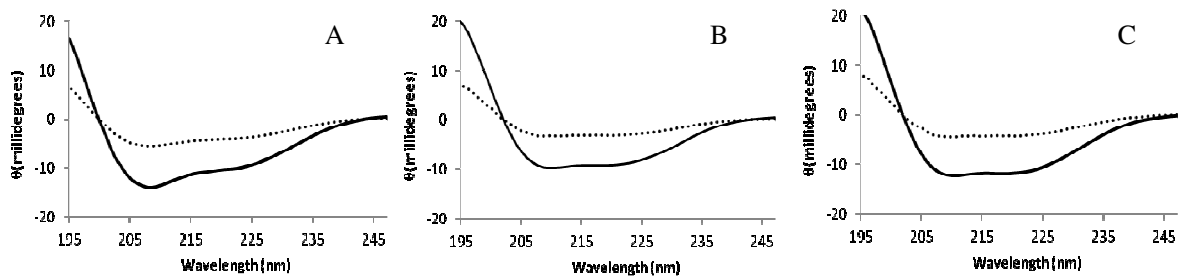


Fig.6 CD spectra of Vmh2 in 60% (—) or 20% (.....) acetonitrile (A), isopropanol (B), and trifluoroethanol (C).

# Hydrophobin bind glucose in nanometric self-assembled biofilms

Ilaria Rea<sup>1</sup>, Paola Giardina<sup>2</sup>, Sara Longobardi<sup>2</sup>, Fabrizio Porro<sup>3</sup>, Valeria Casuscelli<sup>3</sup>, Massimo Gagliardi<sup>1</sup>, Ivo Rendina<sup>1</sup>, and Luca De Stefano<sup>1\*</sup>

<sup>1</sup>Unit of Naples-Institute for Microelectronics and Microsystems, National Council of Research,  
Via P. Castellino 111, 80131, Naples, Italy

<sup>2</sup>Department of Organic Chemistry and Biochemistry, University of Naples "Federico II",  
Via Cintia 4, 80126, Naples, Italy

<sup>3</sup>STMicroelectronics, Via Remo di Feo 1, 80022, Arzano, Naples, Italy

## Abstract

The hydrophobins are small proteins secreted by fungi, which self-assemble into amphipatic membranes at air-liquid or liquid-solid interface. The physical and chemical properties of some hydrophobins, both in solution and as biofilm, are affected by poly or oligosaccharides. We have studied the interaction between glucose and the hydrophobin Vmh2 from *Pleurotus ostreatus*. Stable biofilms containing Vmh2 and glucose were obtained by drop deposition, and were investigated by variable angle spectroscopic ellipsometry, atomic force microscopy (AFM), and water contact angle (WCA). The evaluated amount of protein on the surface was halved in the presence of glucose. AFM highlighted the presence of nanometric rodlet-like aggregates on the biofilm surface, slightly different from those obtained in the absence of glucose. The wettability of silicon surface covered by the organic layer of glucose-Vmh2 strongly changed: WCA decreases from 90° down to 17°. On the whole, this is a simple method for sugar immobilization, which can be very useful for several biotechnological applications.

**Keywords:** Surface modification, Protein biofilm, ellipsometry, Atomic force microscopy

---

\* Corresponding author: Tel: +390816132375; fax: +390816132598; Email address: luca.destefano@na.imm.cnr.it



## 1. Introduction

How proteins are adsorbed and organized at liquid-solid interface is a key issue in biosensors and biomaterials applications, since the properties of the biological layer strongly depends on a complex of physical and chemical phenomena which drive the proteins deposition [1]. Mass transport, binding mechanisms, and solution composition have been extensively studied and lot of experimental techniques have been proposed to characterize the adsorption process [2]. Proteins functionalized surfaces are a hot point in life sciences and are becoming more and more popular also in the medical field: protein based microarrays and biosensors, proteins delivery in human body and proteins mediated tissue engineering, all these applications require that their structures are preserved once adsorbed on a surface and their bioactivity is unchanged or even increased [3].

Hydrophobins are small proteins constituted by about 100 amino acid residues which are produced by fungi as soluble forms [4]. They are able to self-assemble into amphipatic membranes at air-liquid or solid-liquid interfaces. Beyond their natural functions, hydrophobins show very peculiar chemical-physical properties which are of interest for biotechnologists since they could be used in relevant industrial applications [5]. In particular, the chemical stability of the nanometric hydrophobin biofilm could be very attractive for surface functionalization as an alternative to classic passivation methods.

Hydrophobins are divided in two classes on the basis of the stability of the assembled biofilm: the class I hydrophobins forms high insoluble assemblies, which can be dissolved in strong acids, whereas class II biofilms can be dissolved in ethanol or in sodium dodecyl sulphate. One distinguishing feature of class I hydrophobins is their ability to form nanometric rodlets, similar to amyloid fibrils, which are very stable protein aggregate with  $\beta$  structure. Moreover, the class I hydrophobin biofilm is not only high resistant to aggressive chemicals, but it could also play the role of active substrate for binding other biomolecules or organic substances [6, 7]. In particular, interaction between sugars and some class I hydrophobins has been studied: Scholtmeijer et al. [8] have demonstrated that some polysaccharides promote rodlets formation of the class I hydrophobin SC3 at the interface between the water and the air or a hydrophobic solid. Furthermore, it has been proved that growth of amyloid fibrils, related to severe diseases, can be accelerated by glycosaminoglycans and proteoglycans [9,10]. The mechanism by which these sugars stimulate amyloid formation and the nature of carbohydrates-proteins interaction are largely unknown, even if the binding of polysaccharides to proteins has been observed. Moreover, carbohydrates play a vital role in biological functions such as cell-cell recognition, immunological response, metastasis and fertilization. The introduction of bio-functionalities by integration of carbohydrates in a protein modified surface could pave a new way to bio-nanotechnology. Carbohydrate functionalized surfaces can be used to detect bacteria, to bind to specific lectins, to deliver glycomimetic drug molecules into cells and to probe cellular activities as biosensors [11]. In a recent paper we described the interaction between the class I hydrophobin Vmh2 of *Pleurotus ostreatus* and glucans (glucose based cyclic and linear polysaccharides, and glucose monomers) in aqueous solutions [12]. Purified, TFA treated Vmh2 is not water soluble but can be solubilized in 60% ethanol. In contrast, complexes formed between Vmh2 and glucans are soluble in water after TFA-treatment. In this work we have focused our research on glucose-Vmh2 interactions in order to better understand the influence of sugar on protein self-assembly and throw the basis for multiple potential applications in biomaterial, biosensor and device fields.

## 2. Materials and Methods

### *Preparation of Vmh2 samples*

The class I hydrophobin Vmh2 secreted by the fungus *Pleurotus ostreatus* was purified as previously described in ref. [12]. We prepared two types of samples: the first one, in the following cited as Vmh2P, by dissolving the pure protein after the TFA treatment in an ethanol-deionized water (60:40 v/v) solution; the second one, in the following cited as Vmh2G, by dissolving Vmh2 after the TFA treatment in a water-glucose (0.6 mg/ml; Sigma-Aldrich) solution. The concentration of Vmh2G and Vmh2P was evaluated using the PIERCE 660 nm Protein Assay kit, since it is compatible with both glucose and organic solvents. Concentrazioni usate

### *Spectroscopy techniques*

Circular Dichroism (CD) spectra of the protein solutions were recorded by a Jasco J715 spectropolarimeter equipped with a Peltier thermostatic cell holder (Jasco model PTC-348), in a quartz cell from 190 to 250 nm. The temperature was kept at 25° C and the sample compartment was continuously flushed with nitrogen gas. The spectra were obtained using a bandwidth of 1 nm, a step width of 0.5 nm, and 4 s averaging per point. The spectra were corrected for the background signal using a reference solution without the protein. The content of the secondary structure was calculated from the spectra using the CONTIN method and the reference set 4 [13] available on the Dichroweb server [14].

Fluorescence spectra were recorded at 25°C with a Perkin-Elmer LS50B fluorescence spectrometer. Slit widths were set at 10 nm in both the excitation and emission monochromators. Thioflavin T (ThT) (Sigma-Aldrich, St. Louis, MO, 100 µM final concentration) was added to the sample (0.15 mg ml<sup>-1</sup>), afterwards excited at 435 nm and emission was monitored from 460 to 600 nm.

### *Biofilm preparation*

Highly doped p<sup>+</sup> silicon wafers, <100> oriented, 0.003 Ω cm resistivity, 400 µm tick, were cut into 10 mm x 10 mm square pieces. The silicon substrates were cleaned using the standard RCA process [15] and dried in a stream of nitrogen gas. Two sets of five samples were prepared by spotting on one set the Vmh2P solution and on the other, the Vmh2G one, both at 0.2 mg ml<sup>-1</sup>. Silicon chips were coated in both cases by 150 µl of solution for 1 h, dried for 10 min on a hot plate at 80°C, and then washed with the respective solvents. The incubation process was repeated two times. Then, the samples were treated for 10 min at 100°C in 2% SDS and again washed in deionized water.

La parte successiva non so se può andare sotto *Spectroscopy techniques* e se deve essere modificata

Spectroscopic ellipsometry measurements were performed by a Jobin Yvon UVISEL-NIR phase modulated spectroscopic ellipsometer apparatus, at an angle of incidence of 65° over the range 320-1600 nm with a resolution of 5 nm. The instrument measures the parameters  $I_s$  and  $I_c$  which are related to standard ellipsometric angles  $\Delta$  and  $\Psi$  through the following equations:

$$I_s = \sin^2 \Psi \sin \Delta \quad (1)$$

$$I_c = \sin^2 \Psi \cos \Delta \quad (2)$$

The optical properties (refractive index and extinction coefficient), the thickness and the composition of the films assembled on silicon were determined from the ellipsometric data analysis using Delta Psi software [16].

A NanoScope V Multimode AFM (Digital Instruments/Veeco) was used for the imaging of biofilms. All samples were imaged in air in tapping mode. The scan frequency was typically 1 Hz per line and images were flattened to a second order polynomial.

Sessile drop technique has been used for Water Contact Angle (WCA) measurements on a OCA 30 – DataPhysics coupled with a drop shape analysis software. Five measurements were analyzed for both set of samples Vmh2P and Vmh2G.

### 3. Results and Discussion

#### *Glucose-Vmh2 interaction in solution*

The presence of carbohydrates, i.e. cyclodextrins, maltohexaose, and glucose, strongly changes the Vmh2 solubility in water [12]: a concentration of pure Vmh2, which we measured as  $0.20 \pm 0.03 \text{ mg ml}^{-1}$  when dissolved in 60% ethanol-water solution, cannot be revealed by the same test, i.e. the protein concentration is less than the detection limit of the assay ( $25 \text{ } \mu\text{g ml}^{-1}$ ), when dissolved in pure water. The same amount of Vmh2, this time in glucose-water solution, resulted in a protein concentration of  $0.15 \pm 0.03 \text{ mg ml}^{-1}$ . Moreover, the existence of a glucose-Vmh2 complex in solution, with a ratio of about 5 (w/w, corresponding to  $200 \div 300 \text{ mol/mol}$ ), has been previously demonstrated [12]. We have also verified by the same method that other hexoses, like mannose or galactose, can solubilise Vmh2, whereas pentoses (i.e. xylose) or polyols (i.e. sorbitol or glycerol) have not the same effect. Therefore, a hexose molecule seems to have the structural requisite to solubilise Vmh2 in water. Further information on Vmh2-glucose interaction comes from the CD spectra recorded for both samples, Vmh2P (the pure protein in 60% ethanol) and Vmh2G (the protein in water supplemented with  $0.6 \text{ mg ml}^{-1}$  glucose), reported in Fig. 1.

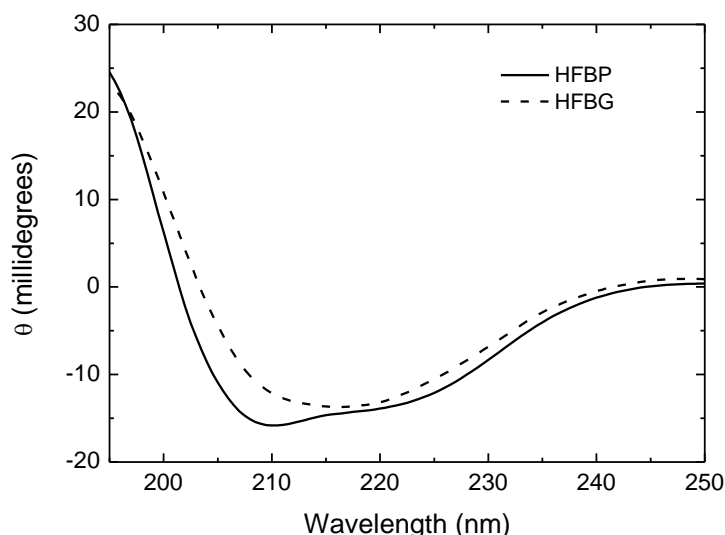


**Figure 1.** CD spectra of pure hydrophobin (solid line) and glucose (dash line) solutions.

Deconvolution of the Vmh2P CD spectrum estimated a relative contribution of  $\alpha$ -helix and  $\beta$  structure of 30% and 20%, respectively. It is worth noting that this spectrum remained identical at least up to 20 days, even after vortexing, and that was not possible to observe any protein aggregation. On the other hand, data relative to Vmh2G showed a higher contribution of  $\beta$ -sheet structure (34%) with respect to the  $\alpha$ -helix (10%). The Vmh2G solution was stable at least for some days. The absence of insoluble aggregates in this solution was verified ruling out any variation of the protein concentration after centrifugation. On the other hand, Vmh2G quickly aggregated after vortexing. As a matter of fact, a slight decrease of the intensity of the CD spectrum just after vortexing was observed, whilst no protein was detectable after centrifugation of this sample.

The binding of ThT to proteins generally indicates the formation of amyloid-like fibrils. This binding can be evaluated through the analyses of fluorescence spectra of samples. As previously reported [12], no variation of the ThT fluorescence spectrum of Vmh2P was observed either before or after vortexing. On the other hand Vmh2G showed a remarkable high fluorescence intensity in the presence of ThT even before vortexing, and a slight increase of the fluorescence intensity after vortexing (Fig. 2).

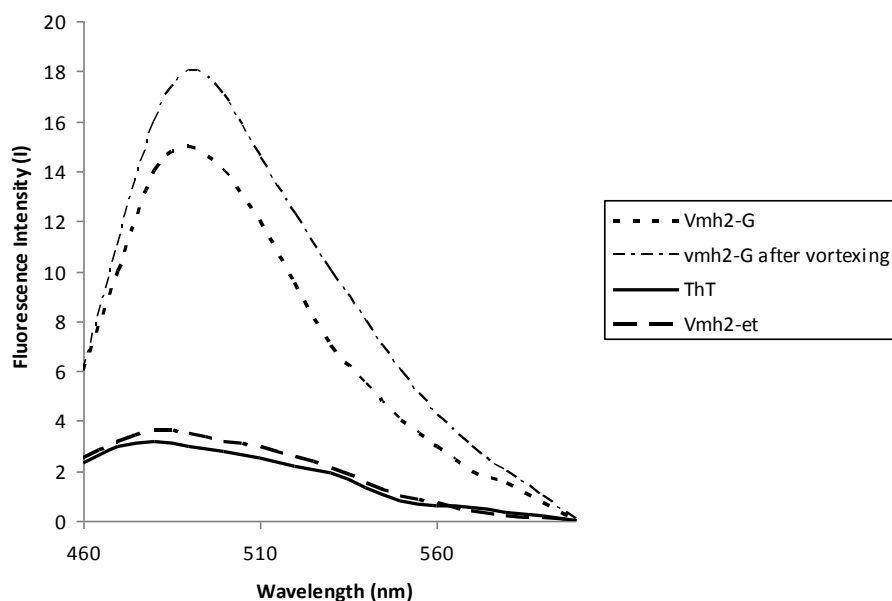


**Figure 2.** Fluorescence intensities in the presence of ThT.

Therefore, Vmh2G adopts in solution a structure able to bind ThT. This structure could be constituted by small oligomers or even monomers of hydrophobin, as suggested by the work of Biancalana et al. [17]: their results demonstrated that the minimal ThT binding site can be formed by four consecutive  $\beta$  strands organized in an aromatic-hydrophobic groove.

*Hydrophobin biofilms self-assembled on silicon.*

VASE is really a powerful technique for the characterization of hybrid organic-inorganic interfaces: physical, chemical and morphological features can be obtained by a single, non invasive measurement. From the ellipsometric data, the thickness and the composition of the biological films self-assembled on silicon surface can be precisely estimated. Before the ellipsometric characterization of the Vmh2G biofilm, we studied the optical parameters (i.e., the refractive index  $n$  and the extinction coefficient  $k$ ) of pure hydrophobin and pure glucose once deposited on the same substrate). As described in the Experimental section, the Vmh2P biofilm was prepared rinsing the surface at 100°C in 2% SDS after the sample deposition. In case of the glucose sample, we did not wash the silicon chip since the sugar is easily removed from the support surface by a quick dip in deionized water at room temperature. In Figure 3 (A) and 3 (B),  $n$  and  $k$ , as functions of the wavelength, are reported for pure hydrophobin and for glucose, respectively.

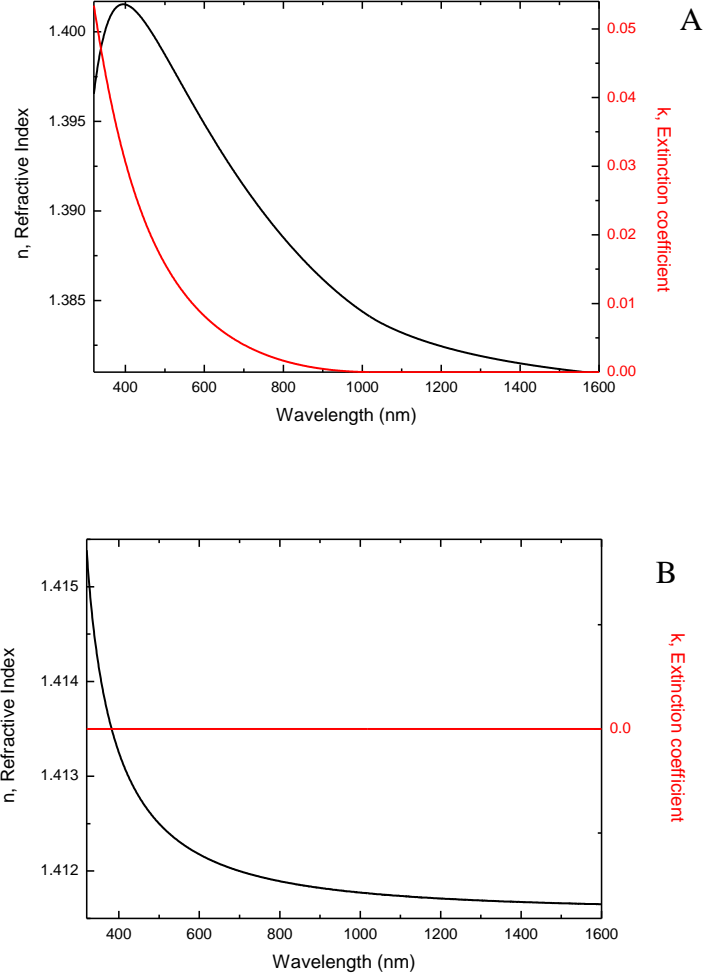


**Figure 3.** Dispersion of the refractive index and extinction coefficient of (A) hydrophobin and (B) glucose deposited on silicon.

The curves have been determined by fitting the experimental results using the Tauc-Lorentz model, firstly proposed in 1996 by Jellison and Modine [18] as a new parameterization of the optical functions of amorphous materials. The imaginary part of the dielectric function is based on the Lorentz oscillator model and the Tauc joint density of states:

$$\varepsilon_2 = \begin{cases} \frac{1}{E} \frac{AE_0C(E - E_g)^2}{(E^2 - E_0^2)^2 + C^2E^2} & E > E_g \\ 0 & E \leq E_g \end{cases} \quad (3)$$

The real part of the dielectric function is given by Kramers-Kronig integration:

$$\varepsilon_1 = \varepsilon_\infty + \frac{2}{\pi} P \int_{E_g}^{\infty} \frac{\xi \varepsilon_2(\xi)}{\xi^2 - E^2} d\xi \quad (4)$$

These equations include five fitting parameters: the peak transition energy  $E_0$ , the broadening term  $C$ , the optical energy gap  $E_g$ , the transition matrix element related  $A$ , and the integration constant  $\varepsilon_\infty$ . The values of the fitting parameters, determined from the analysis of the experimental spectra, are reported in Table 1 together with the statistical parameter  $\chi^2$ . In the interval of wavelengths considered, refractive index values of glucose are slightly higher than those of Vmh2 and it does not absorb light: these differences allow VASE the quantification of both substances when present in a composite membrane. In case of the Vmh2 biofilm, the absorption coefficient  $\alpha$ , related to the

extinction coefficient  $k$  by the relationship  $\alpha = \left(\frac{4\pi}{\lambda}\right)k$ , is in good agreement with that determined by UV-VIS spectroscopic analysis (data not shown here).

Material	$E_g$ (eV)	$A$ (eV)	$E_0$ (eV)	$C$ (eV)	$\epsilon_\infty$	$\chi^2$
Vmh2P	$1.20 \pm 0.07$	$1.785 \pm 0.09$	$5.5 \pm 0.2$	$5.0 \pm 0.2$	$1.766 \pm 0.02$	0.05
Glucose	$3.9 \pm 0.3$	$37 \pm 6$	$1.468 \pm 0.2$	$0.9 \pm 0.1$	$1.97 \pm 0.04$	2.8

**Table 1.** Fitting parameters obtained from the fit to the ellipsometric spectra of hydrophobin and glucose films on silicon.

The composite Vmh2G film self-assembled on silicon was analyzed in comparison to the pure Vmh2P film. The Figures 4 (A) and 4 (B) show the  $I_s$  and  $I_c$  experimental spectra in case of Vmh2P and Vmh2G films self-assembled on silicon together with the calculated spectra and the models used to fit them.

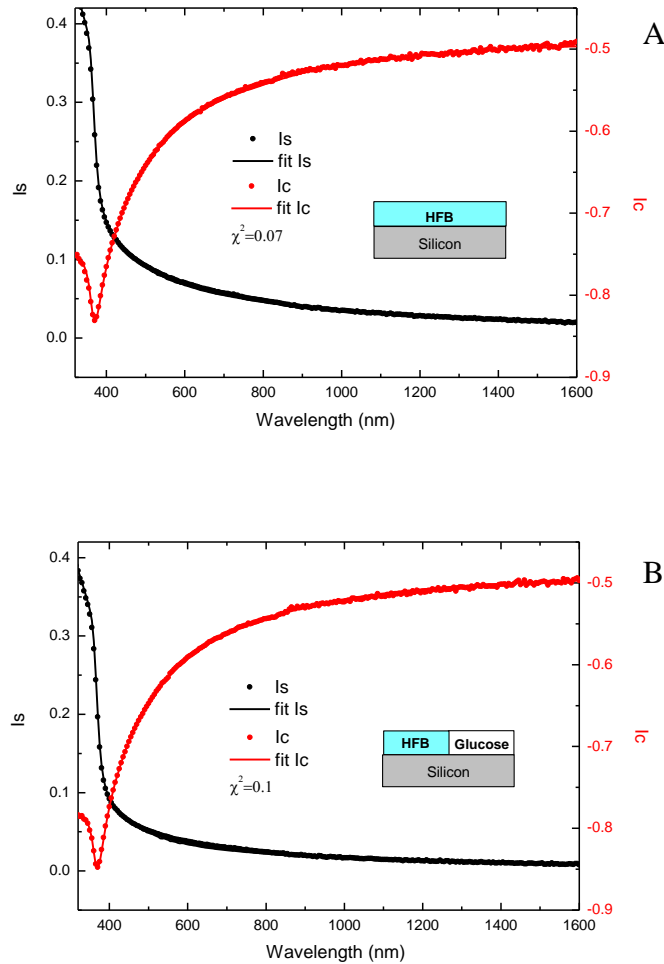


**Figure 4.** Measured and calculated spectra ( $I_s$ ,  $I_c$ ) of (A) hydrophobin and (B) glucose-hydrophobin biofilms self-assembled on a silicon substrate.

The Vmh2P sample has been modeled by a simple homogeneous layer; the fitting parameter is the film thickness. The Vmh2G biofilm can be considered as a mixture of two constituents, the glucose and the pure protein: in this case the biological layer has been modeled using the Bruggeman Effective Medium Approximation (EMA) [19]; the fitting parameters are now the thickness and the content of glucose in the biofilm, considered as host in the protein matrix. The results of this

analysis are reported in Table 2; each value has been obtained as the average on five different measurements. By this optical method, a glucose content of 24% in the glucose-hydrophobin biofilm has been found, showing a layer thickness of 1.5 nm, which is smaller than the thickness of the pure hydrophobin self-assembled on silicon.

Biofilm	d (nm)	Glucose amount (%)
Vmh2P	3.91 ± 0.06	-----
Vmh2G	1.5 ± 0.1	24 ± 2

**Table 2.** Thickness and glucose amount of the two biofilms considered. The values have been obtained as arithmetic mean of those determined by spectroscopic ellipsometry on different samples.

Surface coverage, expressed as the relative surface concentration  $\Gamma$  ( $\mu\text{g}/\text{cm}^2$ ) of Vmh2P and Vmh2G-biofilms self-assembled on silicon, can be also calculated from ellipsometric data by using the Cuypers formula [20]:

$$\Gamma = 0.1d \frac{M}{A} \frac{n_f^2 - 1}{n_f^2 + 2} \quad (5)$$

where  $A$  is the molar refractivity ( $\text{cm}^3/\text{mol}$ ),  $M$  is the molecular weight, and  $d$  and  $n_f$  are the thickness and the refractive index of the biofilm (determined by spectroscopic ellipsometry). In Table 3 we have reported the parameters used to calculate  $\Gamma$  and the values of  $\Gamma$ ; the refractive indexes have been extrapolated by the ellipsometric data using the formula (4) applied to each substance. In case of glucose-hydrophobin biofilm, we have considered a molecular complex constituted by two hundred and fifty units of glucose and one unit of hydrophobin, as suggested by results obtained in ref. [12]. The value of the relative surface concentration of the Vmh2P biofilm, reported in Table 3, is about twice than that calculated in case of Vmh2G, due to the very different thicknesses estimated for both these biofilms. Even if we do not have any information on the molecules disposition in the Vmh2G layer, these results suggest that in this case a larger portion of the surface is covered by the smaller glucose molecules, which are still engaged in the biofilm formation (i.e. they cannot be washed away), so that an average decrease of the determined thickness is observed (1.5 nm) with respect to the case of Vmh2P (3.91 nm).

Sample	$n_f$ (@ $\lambda=1\mu\text{m}$ )	A ( $\text{cm}^3/\text{mol}$ )	M (g/mol)	M/A ( $\text{g}/\text{cm}^3$ )	$\Gamma$ ( $\mu\text{g}/\text{cm}^2$ )
Vmh2P	1.384	2104	8572	4.0746	0.0372 ± 0.0006
Vmh2G	1.391	12316	53612	4.3530	0.015 ± 0.001

**Table 3.** Physical-chemical properties of the two self-assembled biofilms:  $n_f$ , film refractive index;  $A$ , molar refractivity;  $M$ , molecular weight;  $\Gamma$ , relative surface concentration.

The higher density of the pure hydrophobin film has been also confirmed by the AFM characterization. In Figure 5 (A) and 5 (B) we show the AFM images (height, phase, and 3D-height) of silicon surfaces coated by Vmh2P and Vmh2G biofilms, respectively. The formation of a homogeneous biofilm can be observed in both cases in the 3D-height images. The AFM pictures also reveal the presence of rodlets-like structures on top of the biofilm surfaces. In case of pure hydrophobin a larger number of longer rodlets can be individuated with respect to the glucose-hydrophobin biofilm.

(A) Vmh2P



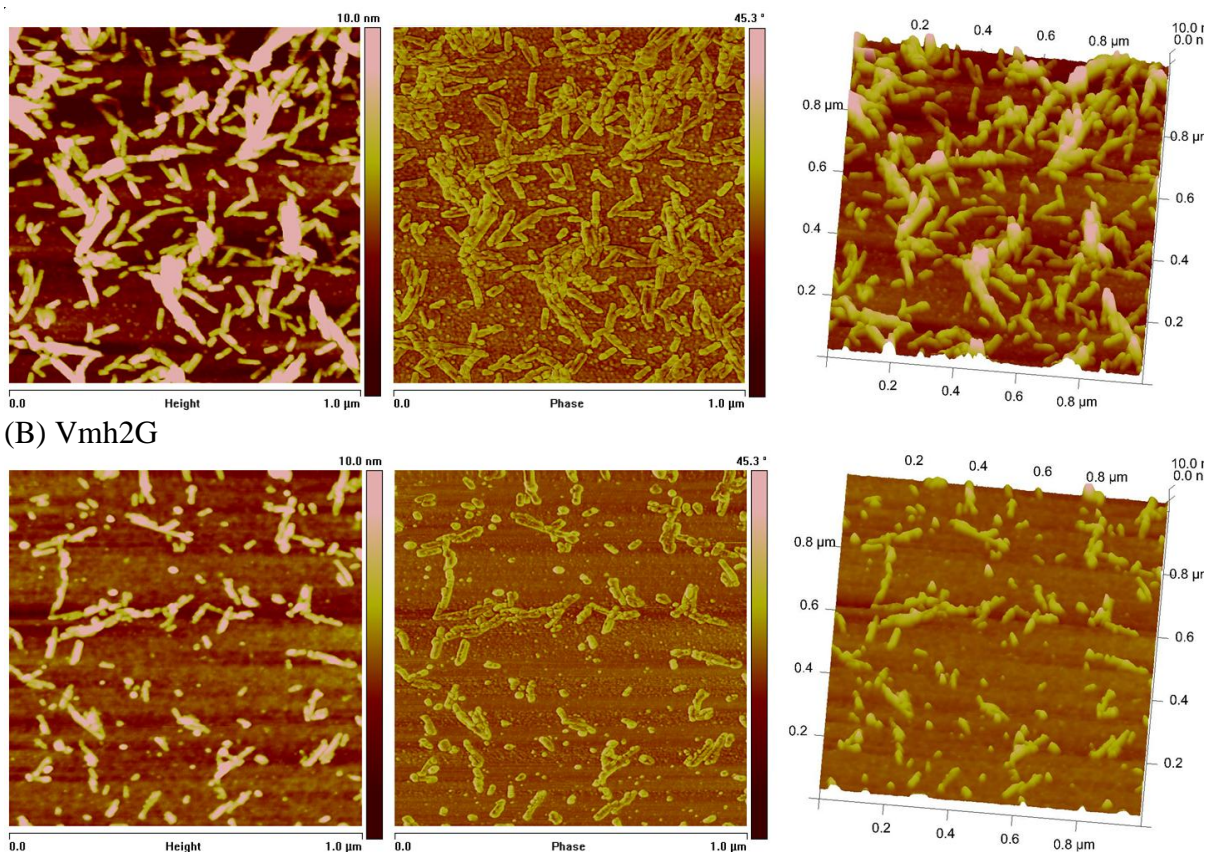


**Figure 5.** Atomic force microscope images of silicon coated by (A) Vmh2P and (B) Vmh2G biofilms.

The average values of the aggregates height, width, and length have been reported in Table 4 together with the mean roughness of the biofilms.

Biofilm	Rodlet average height (nm)	Rodlet average width (nm)	Rodlet average length (nm)	Mean roughness (nm)
Vmh2P	$4.11 \pm 0.08$	$23.9 \pm 0.6$	$64 \pm 3$	3.32
Vmh2G	$3.6 \pm 0.2$	$23.8 \pm 0.5$	$40 \pm 2$	1.38

**Table 4.** AFM analysis for hydrophobin and glucose-hydrophobin coated silicon.

Changes in surface wettability due to the presence of the biological films self-assembled on silicon have been verified by water contact angle measurements. The values of the WCA are the average of five determinations on duplicate samples.

The silicon surface, after the removal of the native oxide layer in hydrofluoric acid, is characterized by a WCA of  $(90.0 \pm 0.3)^\circ$  (Figure 6 (A)), so that it can be defined as hydrophobic. The presence of the Vmh2P biofilm lowers the WCA down to  $(44 \pm 1)^\circ$  (Figure 6 (B)): this interface is more hydrophilic due to the assembly of the protein into a film with apolar groups disposed towards the hydrophobic silicon and the polar groups on the other side. When the Vmh2G biofilm is considered, a WCA of  $(17.5 \pm 0.5)^\circ$  has been measured (Figure 6 (C)): the presence of polar sugar groups in the structure of the composite biofilm further increases the wettability of the resulting surface [8].



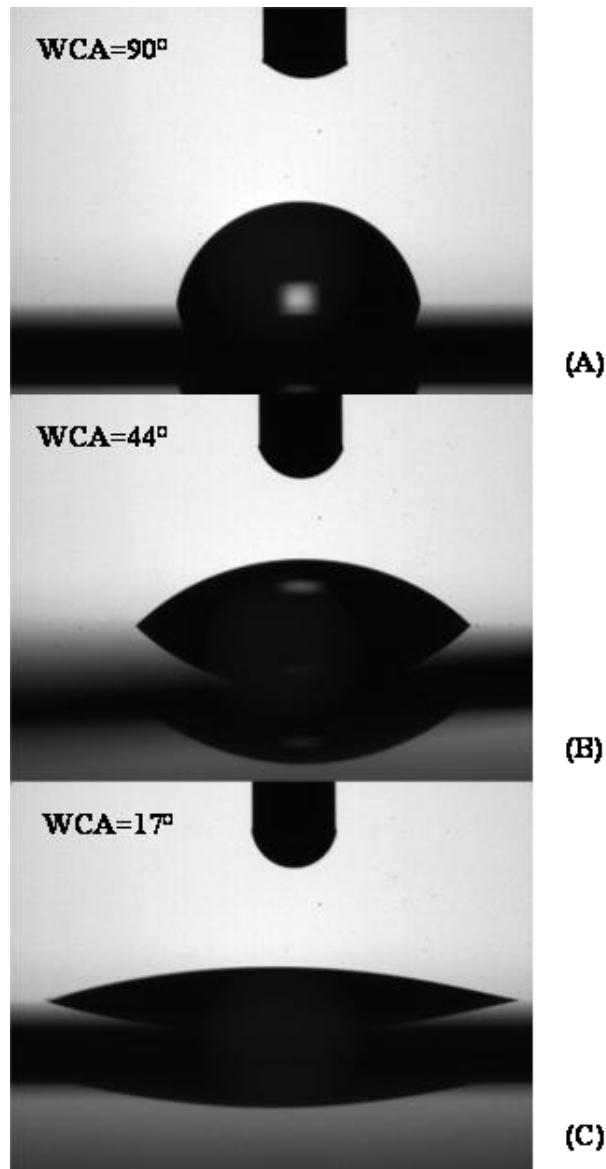


**Figure 6.** Water contact angle measurements on (A) bare silicon, (B) hydrophobin coated silicon, and (C) glucose-hydrophobin coated silicon.

#### 4. Conclusions

In this work we have analyzed glucose-Vmh2 interaction in solution and characterized the biofilm self-assembled at the water-silicon interface after drop deposition. Vmh2 adopts a  $\beta$  conformation in water solution in the presence of glucose that is able to bind ThT, differently from the pure protein in 60% ethanol. A chemically stable, nanometric biofilm is produced by deposition of the Vmh2 water solution in presence of the sugar. The glucose molecules are still coordinated with Vmh2 in the self-assembled biofilm which-strongly modifies the wettability of the hybrid organic-inorganic interface.

This simple method for sugar immobilization can be very useful for several applications, such as bacterial detection systems. Invasive strains of the pathogenic bacterium *Escherichia coli* express high level of mannose-binding proteins on their pili. These proteins have been exploited in the development of detection systems, based on multivalent presentation of carbohydrate ligands [22]. Our studies on the stable immobilization of hexoses on a silicon chip can be the basis for future biosensors; investigations regarding this issue are currently in progress.

**Acknowledgement**

The authors gratefully thank Dr. F. Villani and Dr. A. De Girolamo of ENEA – Portici Research Centre for the water contact angle measurements. Thanks are also due to Dr. S. Pergolini (2Mstrumenti) for useful discussions on AFM images. This work was partially supported by CNR and MIUR, Italy.

## References

1. Dekker M., Physical chemistry or biological interfaces. **1999**. New York: Baszkin A, Norde W, Eds.
2. Voros J., *Biophys. J.* **2004** 87:553-61.
3. Norde W., *Colloids and Surfaces B: Biointerfaces* 2008 61:1-9.
4. Wösten H.A., *Ann. Rev. Microbiol.* **2001** 55:625-46.
5. Hektor H.J.; K. Scholtmeijer, *Curr. Opin. Biotechnol.* **2005** 16:434-9.
6. De Stefano L., I. Rea, A. Armenante, P. Giardina, M. Giocondo, I. Rendina, *Langmuir* **2007** 23:7920-2.
7. De Stefano L., I. Rea, E. De Tommasi, P. Giardina, A. Armenante, S. Longobardi, *J. Nanophoton.* **2009** 3:031985.
8. Scholtmeijer K., M.L. de Vocht, R. Rink, G.T. Robillard, H.A.B. Wösten, *J. Biol. Chem.* **2009** 284:26309-14.
9. Relini A., S. De Stefano, S. Torrassa, O. Cavalleri, R. Rolandi, A. Gliozzi, *J. Biol. Chem.* **2008** 283:4912-20.
10. Bellotti V., F. Chiti, *Curr. Opin. Struct. Biol.* **2008** 18:771-9.
11. Gorityala B.K., J. Ma, X. Wang, P. Chen, X.W. Liu, *Chem. Soc. Rev.* **2010** 39:2925-34.
12. Armenante A., S. Longobardi, I. Rea, L. De Stefano, M. Giocondo, A. Silipo, *Glycobiology* **2010** 20:594-602.
13. Sreerama N., R.W. Woody, *Anal. Biochem.* **2000** 287:252-260.
14. Whitmore L., B.A. Wallace, *Biopolymers* **2008** 89:392-400.
15. Handbook of Semiconductor Cleaning Technology; Kern, W., Eds.; Noyes Publications, Park Ridge, NJ, **1993**; Chapter 1.
16. Delta Psi Software Manual Ver. 2.4.3. 158 HORIBA JOBIN YVON.
17. Biancalana M., S. Koide, *Biochim Biophys Acta* **2010** 1804:1405-12.
18. Jellison G.E. Jr, F.A. Modine, *Appl. Phys. Lett.* **1996** 69:371-4
19. Aspnes D.E., J.B. Theeten, *Phys. Rev. B* **1979** 20:3292-302.
20. Cuypers P.A., J.W. Corsel, M.P. Janssen, J.M.M. Kop, W.T. Hermens, H.C. Hemker, *J. Biol. Chem.* **1983** 258:2426-31.
21. Wosten H.A.B., F.H.J. Schuren, J.G.H. Wessels, *EMBO J.* **1994** 13:5848-54.
22. Laurino P., R. Kikkeri, N. Azzouz, P.H. Seeberger, *Nano Lett.* **2011** 11:73-78.

# Self-assembly of hydrophobin protein rodlets studied with atomic force spectroscopy in dynamic mode

S. Houmadi<sup>a,b</sup>, Raul D. Rodriguez<sup>a,c</sup>, S. Longobardi<sup>d</sup>, P. Giardina<sup>d</sup>, M. C. Fauré<sup>a</sup>, M. Giocondo<sup>b</sup> and E. Lacaze<sup>a</sup>

<sup>a</sup>*Institut des Nano-Sciences de Paris (INSP), UMR-CNRS 7588, Université Pierre et Marie Curie-Paris 6, 4 place Jussieu 75005 PARIS, France.*

<sup>b</sup>*CNR-IPCF - UOS di Cosenza. c/o Dipartimento di Fisica, Università della Calabria, 87036 Rende, Italy.*

<sup>c</sup>*Institute of Physics, Chemnitz University of Technology, 09107 Chemnitz, Germany*

<sup>d</sup>*Dipartimento di Chimica Organica e Biochimica, Università di Napoli Federico II, Via Cintia 4, 80126 Napoli, Italy.*

houmadi3@yahoo.fr, raulmet@gmail.com, sara.longobardi1983@libero.it, giardina@unina.it,

marie-claude.faure@univ-paris5.fr, michele.giocondo@cnr.it, Emmanuelle.Lacaze@insp.jussieu.fr

Corresponding author. E-mail: Emmanuelle.Lacaze@insp.jussieu.fr Tel: +33144274654. Fax: +33143542878

## ABSTRACT.

Self-assembling fungal proteins, the hydrophobins, form layers which have been demonstrated to control and reverse the hydrophobicity of the surface onto which they attach, leading to applications in issues such as biosensor development. We have investigated the self-assembling properties of the class I hydrophobin Vmh2 isolated from the fungus *Pleurotus Ostreatus*. Different hydrophobin films including monolayers, bilayers and aggregates under the form of rodlets have been prepared by Langmuir technique and studied at the nanoscale. Local wettability and visco-elasticity of hydrophobin assemblies were obtained from atomic force spectroscopy experiments in dynamic mode performed at different relative humidity (RH) values. It was found that hydrophobins assembled either in rodlets or in bilayer films, display similar hydrophobicity and viscoelasticity in contrast to the case of monolayers. The comparison with monolayers properties evidences a rearrangement of the bilayers adsorbed onto solid substrates. It is shown that this rearrangement leads to formation of a stable hydrophobic film, not exposing the protein flexible loop at the air/interface and that the rodlets structure consists in fragments of restructured bilayers. These findings should now serve future developments and applications of hydrophobin films beyond the archetypal monolayer.

## KEYWORDS.

Langmuir films, Hydrophobin proteins, Rodlets, AFM, AFS, Capillarity, Viscoelasticity.

## Introduction

Hydrophobins are amphiphilic proteins produced exclusively by fungi<sup>1</sup>. They form an amphipathic layer which self-assembles at hydrophobic and hydrophilic surfaces and are the most surface active proteins known<sup>2, 3</sup>. It has been shown that hydrophobicity of surfaces can be reversed using hydrophobin films<sup>2, 4-8</sup>. Recently, research on these proteins has focused on utilizing their physical properties for biotechnological applications<sup>3, 9, 10</sup>. In biosensor design hydrophobins allow the subsequent attachment of cells or proteins<sup>6, 11</sup>. Hydrophobins are divided into two groups, class I and class II hydrophobins. It is well-known that at the air-water interfaces, molecules of class I self-assemble to form anisotropic aggregates, the so-called rodlets<sup>12</sup>. Rodlets may also be formed in vitro on both hydrophobic and hydrophilic surfaces<sup>13</sup>. They are extremely stable and can be dissolved only in pure trifluoro acetic acid. This property makes them useful for application in nanotechnology<sup>14</sup>. The formation of the rodlet-like film is accompanied by beta-sheet structure formation<sup>15</sup>. Models proposed to account for the formation of rodlets interpret them as corresponding to a monolayer<sup>13, 16, 17</sup>. However, in a previous paper, we have demonstrated the coexistence of rodlets and monolayers<sup>18</sup> in the same film suggesting the hypothesis of a hydrophilic double-layer structure for the rodlets possibly stabilized by the presence of the surrounding monolayer. Our aim in this work is to advance in the understanding of the structural conformation taken by self-assembled class I hydrophobins that are purified from the basidiomycete fungus *Pleurotus Ostreatus* and identified as Vmh2<sup>19</sup>. We have investigated physical properties of different films prepared by Langmuir-Schaefer (LS), Langmuir-Blodgett (LB) methods and bilayer films obtained by a combination of both methods, using Atomic Force Microscopy (AFM) and Atomic Force Spectroscopy (AFS) in dynamic mode. The relevance of this latter technique is here evidenced by providing new insights about wetting properties and viscoelasticity of the films, leading to new assumptions concerning internal structure and terminal groups of hydrophobin films as well as rearrangement during films and rodlets formation.

## Materials and Methods.

### Hydrophobin Purification.

The Vmh2 hydrophobin protein was purified from the fungus *Pleurotus Ostreatus* as described in the reference [19]. Briefly, mycelia were grown at 28°C in static cultures in potato dextrose (24 g/L) broth with 0.5% yeast extract. Hydrophobins released into the medium were aggregated by air bubbling. Foam was then collected by centrifugation at 4000 x g. The precipitate was freeze dried, treated with trifluoroacetic acid (TFA). The sample was dried, dissolved in 60% ethanol and centrifuged.

### LB/LS films.

The Langmuir films were prepared in a Nima Tech 632D1D2 LB system trough and a home-built trough using ultrapure water, at 5.5 pH and  $T = 18.0 \pm 0.5$  °C for the subphase<sup>18</sup>. Once Vmh2 deposited at the air/water interface, the monolayer was compressed up to the transfer pressure of 36 mN/m<sup>18</sup>. We compressed the layers at the air-water interface five times to obtain coexistence between rodlets and monolayer but only once to obtain homogeneous monolayers. The LB monolayers were transferred at constant pressure of 36 mN/m onto hydrophilic SiO<sub>2</sub> substrates by vertical lifting at a rate of 10 mm/min. Transfer was similar for coexisting rodlets and monolayers. Silanized silicon wafers were used for the LS transfer that allows by horizontal lifting method to deposit films with the hydrophilic side in contact with air (LS film). SiO<sub>2</sub> wafers were silanized using octadecyltriethoxysilane (OTE), according to the procedure described by Malham et al.<sup>20</sup>. In order to obtain a bilayer with hydrophilic surface in contact with air, a monolayer (compressed once) was deposited using LS technique onto an already-prepared Vmh2 LB film (this bilayer is named hereinafter LB+LS). Conversely, in order to obtain a bilayer with hydrophobic surface in contact with air, a monolayer (compressed once) was deposited

using vertical lifting onto Vmh2 LS film (this bilayer is named hereinafter LS+LB).

### **Contact Angle Measurements.**

Contact angles of water on samples were measured on a home-built instrument. Each surface, placed on a horizontal holder, was brought into contact with a droplet of ultrapure water hanging from the vertical needle of a 10  $\mu$ L microsyringe. Video acquisition was performed using a CCD camera and a long working-distance objective on 3 to 5 different locations.

### **Atomic Force Microscopy (AFM), Spectroscopy and Imaging.**

AFM measurements were obtained in tapping mode using two apparatus from Veeco Instruments: Nanoscope Dimension 3100 and MultiMode. Oxidized silicon cantilevers purchased from NanoSensors were used with tips radius of the order of 10nm. The AFM measurements were performed in ambient conditions (i.e. 40 % RH) as well as in controlled RH. Humidity control was achieved by placing the microscope inside a glass chamber and using a home-made humidifier to vary the ratio of dry/wet nitrogen flowing into the chamber. RH was measured with a precision of  $\pm 0.5\%$  RH. To avoid local gradients of water vapor, the system was left to stabilize for at least half an hour before each measurement. Prior to the AFS measurements (with no sample beneath) the AFM cantilever was excited at its resonance frequency (around 150 kHz) and the phase-distance curves on the sample were conducted at this same frequency. To ensure the appropriate comparison between AFS data, we checked that the AFM tip underwent no changes during the entire experiment: AFM tips were tested against a SiO<sub>2</sub> surface used as a reference. Phase distance curves on the SiO<sub>2</sub> surfaces were compared before and after each measurement done on the Vmh2 film ; phase data that showed differences on the SiO<sub>2</sub> were taken as due to a modified (i.e. : blunted) tip and discarded.

## **Results and Discussion**

Using Langmuir method, we formed hydrophobin layers at the air/water interface, compressed only once, which were then transferred by LB technique on a hydrophilic SiO<sub>2</sub> substrate for one film (LB film) and by LS technique on a hydrophobic silanized SiO<sub>2</sub> substrate for the other film (LS film). In both LB and LS depositions, Vmh2 molecules formed homogenous films as shown in Fig. 1A and 1B from AFM imaging. The similarity of topography between both films suggests that LS transfer does not disrupt more the hydrophobin interfacial film than LB transfer, as already reported for HGFI class I hydrophobin<sup>21</sup>. From detailed AFM analysis, same low roughness RMS of 0.25 nm has been found. Possibly due to some inhomogeneity of the substrate, rarely, holes could be found in the LB and LS layers, allowing measurement of thickness by AFM. Same value of  $2.5 \pm 0.4$  nm has been found for LB and LS layers (fig. 1). 2.5nm corresponds to the hydrophobin size in solution<sup>3</sup>, it is thus associated with monolayer films. On the other hand, as already reported<sup>20,18</sup>, films prepared by repeating compression-expansion cycles at the air-water interface and then deposited on SiO<sub>2</sub> substrates showed rod-like aggregates characteristic of class I hydrophobins (see Fig. 1C taken from [18]). These rodlets appear to coexist with the hydrophobin monolayer. Moreover they appear 2.5 nm higher than the surrounding monolayer. This shows that rodlet's height is of 5 nm which may imply two different possibilities: 1) strong conformational changes take place in a single layer of molecules in order to explain the large deviation from the size the protein has in solution, 2) rodlets are actually made out of not one but two layers with two possible structures: either bilayers are disconnected from the surrounding monolayer, or a monolayer piece is directly adsorbed on the monolayer below. During the compression, a part of the hydrophobin molecules could be expelled from the monolayer and they would form stripes predominantly parallel to the barrier. LB and LS layers homogeneity allows to investigate the wettability by contact angle measurements. Due to the LB method transfer on hydrophilic surface, Vmh2 molecules are attached to the hydrophilic SiO<sub>2</sub> by their hydrophilic parts, while the hydrophobic regions of the protein remain exposed to the air and the contrary is consistently expected for LS films. LB film exhibits a contact angle of 81° which means that it is indeed more hydrophobic than

hydrophobin LS film that displays a contact angle of  $43^\circ$ . The value obtained for LS film is consistent with values reported in Ref. [2] for class I hydrophobins on Teflon (from  $36^\circ$  to  $63^\circ$ ). The dispersion in the contact angle values<sup>2, 6</sup> appears related to the hydrophobin exact nature but also to the dispersion of preparation method. In this context, it is worthwhile to notice that the LB and LS techniques allow to obtain hydrophobin layers with not only well defined thickness, but also well defined molecular orientation.

### Surface Measurements at the Nanoscale.

**Modeling Phase Distance Curves.** AFM in tapping mode works with a tip attached to an oscillating cantilever, at a frequency close to its resonance frequency,  $\omega_0$ . For AFM imaging, the oscillation amplitude is fixed in order to record the surface topography. In AFS, the variations of the oscillation amplitude,  $A$  and phase,  $\phi$ , are recorded in function of the average tip-sample distance  $d_0$ . They reflect the perturbation of the cantilever dynamics by the interaction between the tip and the sample. The AFM cantilever can be modeled as a forced harmonic oscillator with  $k_c$  the stiffness and  $Q$  the quality factor associated with damping in air. In presence of tip-sample interactions  $F_{ts}(d)$ , the equation of motion is given by :

$$\frac{k_c}{\omega_0^2} \frac{d^2 z(t)}{dt^2} + \frac{k_c}{\omega_0 Q} \frac{dz(t)}{dt} + k_c z(t) = F_0 \cos(\omega t) + F_{ts}(d_0 + z(t)) \quad (1)$$

where  $z(t)$  is the oscillation of the tip. Notice that  $d_0$  in simulations and the vertical displacement in experimental curves are equivalent except for an arbitrary offset value. Contact occurs when  $d_0 + A = a_0$  with  $a_0$  the tip-sample distance at which contact interactions start taking place. The tip-sample interaction  $F_{ts}(d)$  may be defined by a combination of van der Waals forces (vdW) and Derjaguin-Muller-Toporov contact mechanics (DMT). The presence of viscoelasticity is taken into account through a damping within the sample:

$$\begin{cases} d_0 + z(t) \geq a_0, F_{ts} = -\frac{HR}{6(d_0 + z(t))^2} \\ d_0 + z(t) \leq a_0, F_{ts} = \frac{4}{3} E(R(d_0 + z(t))^3)^{1/2} - \frac{HR}{6a_0^2} - \frac{k_c}{\omega_0 Q_{dis}} \frac{dz(t)}{dt} \end{cases} \quad (2)$$

In this equation,  $H$  represents the Hamaker constant of the tip-sample system,  $E$  is the reduced Young modulus, and  $R$  is the tip radius which is herein assumed to be spherical.  $Q_{dis}$  is the quality factor associated with damping of the tip within the sample. The numerical integration of the equation of motion was performed by using a fourth order Runge-Kutta algorithm<sup>22</sup>. The phase values calculated are plotted as a function of  $d_0$  in Fig. 2. The transition between regime dominated by attractive long range forces and repulsive ones has a clear signature in phase curves given by a jump from values larger than  $90^\circ$  to values below  $90^\circ$ <sup>23</sup>. When viscoelasticity is taken into account, this shift is modified, as shown on Fig. 2. Phase/distance curves can also be used to calculate the power dissipated by the tip-sample interaction. When the cantilever is excited at its resonance frequency, the power dissipated by the tip when it probes periodically the sample surface (i.e. energy dissipation per period) is obtained using the following equation<sup>24</sup>:

$$P_{tip} = \frac{1}{2} \frac{k_c A^2 \omega_0}{Q} \left[ \frac{A_0}{A} \sin \phi - 1 \right] \quad (3)$$

where  $A_0$  is the free amplitude of the cantilever. For conservative forces like vdW or DMT ones, the power dissipated by the tip is expected to be zero. The calculation of the power dissipation thus allows to highlight non conservative interactions like viscoelastic ones.

### **Hydrophobicity investigation at the nanoscale.**

Wetting properties of Vmh2 monolayers were further investigated at the nanoscale, using AFS. Changes in humidity have a role in adhesion forces between an AFM tip and a sample due to the formation and growth of a water bridge between both surfaces<sup>25, 26</sup>. In Fig. 3A, phase versus distance curves performed on LS monolayer are presented for 4 RH values. At low RH (smaller than 30%) the phase jump from the attractive regime to the repulsive one takes place at ca. 7 nm from the onset of tip-sample interactions (marked with "A" in the plot). At 34 %RH the phase jump suddenly moves at ca. 10 nm from "A". This behavior is ascribed to the absence of meniscus between the tip and the sample at low RH: the water vapor does not condensate between tip and sample, and tip-sample interaction is mainly dominated by attractive vdW and repulsive contact forces. Formation of a water bridge between the tip and the LS film results in a shift of the jump toward the left when the RH attains 34%; this is associated with energy dissipation that is required to break the meniscus<sup>27</sup>. This kind of evolution was systematically observed on LS films for all the tips used with a threshold humidity only varying between 25%RH and 38%RH. In contrast, Fig. 3B, for LB films, evidences no variation in the position of the jump in the phase-distance curves for humidity varying from 3%RH to 79%RH. This confirms that, at the local scale also, the LB film is more hydrophobic than the LS film, with no water nano-condensation between tip and surface. These results confirm the ability of AFM in tapping mode to probe the wettability of surfaces at the nanoscale, which allows now to investigate locally the hydrophobicity of rodlets in comparison to the LB monolayer. Notice that this task would not have been possible to perform using contact angle measurements where wettability is averaged over a large sample area including rodlets and the LB film.

We have thus localized the AFM tip on rodlets (co-existing in the same sample with LB monolayer (see Fig. 1C)). On the top of the rodlets, we observe no changes in the AFS curves (Fig. 3C), similarly to the LB monolayer around the rodlets. This behavior is contrary to results obtained for LS monolayers suggesting that the surface exposed by rodlets is not hydrophilic. Yet, we have demonstrated previously that the thickness of the rodlets is ca. 5 nm<sup>18</sup> which corresponds to the thickness of Vmh2 bilayers. This bilayer being formed at the air/water interface, rodlets could be considered as monolayers fragments facing each other, with hydrophilic parts pointing outwards and hydrophobic parts inwards if we assume that hydrophobic parts of hydrophobins interact with each other. However, such a structure seems unlikely to occur because, in addition to contradict our observations, this arrangement is not expected to be stable at the air/water interface. We can consider that two monolayers interact between their hydrophilic and hydrophobic parts, due to the presence of hydrophobic forces. Hydrophobic forces indeed appeared dominant for hydrophobins of class II<sup>10</sup>. However in such a case we would not expect a strong stability of rodlets on substrates at air, contrary to our observations. Consequently, our results evidence conformational changes within rodlets<sup>15, 16</sup>. We can consider that rodlets are elongated to reach 5nm, which is unlikely to occur due to the tight binding cores of hydrophobins. A conformational change may thus occur in the corresponding bilayer system. It appeared thus interesting to study the local properties of Vmh2 bilayers by AFM for comparison with the rodlets properties. Using the Langmuir trough, we have prepared two kinds of bilayers, LB+LS ones (LB below, LS on top, deposited on a SiO<sub>2</sub> substrate) and LS+LB ones (LS below, LB on top, deposited on a silanized SiO<sub>2</sub> substrate). AFM images evidence the similarity in the topography of the two bilayers (Fig. 4). The roughness has increased with respect to monolayers, up to 0.8 nm. (Fig. 4) shows that, whatever the tip used is, wettability of LS+LB and LB+LS bilayers appears characterized by no formation of water meniscus between tip and surface, even at high RH. As expected, the LS+LB bilayer is hydrophobic, similarly to LB layers and rodlets. Surprisingly, the LB+LS bilayer displays also a hydrophobic wetting behavior, while it is expected to present wetting properties comparable to LS films. In order to account for this observation we conclude that structural changes must have occurred in the LB+LS bilayer.

**Variations of Viscoelasticity at the Nanoscale.** We have compared LS and LB layers, with the same tip under dry atmosphere to avoid any influence from capillarity. Systematically, as shown in Fig. 5A, the



jump position for the LB monolayer is shifted with respect to the one of the LS layer by roughly 4 nm. Two hypotheses may explain such shift: either a particular attractive interaction exists between tip and LB layer; or viscoelasticity is different between both layers. In order to discriminate between the two hypotheses, we have used amplitude and phase-distance curves to obtain the power dissipated between tip and surface (equation 3). The dissipated power becomes different between LS and LB film for average distance between tip and surface smaller than the one associated with the jump between attractive and repulsive regimes (Fig. 5B). A different contact interaction thus occurs between the two films which can be attributed to differences in viscoelasticity, in agreement with numerical simulation results (see Fig. 2). The higher viscoelasticity would correspond to the LB film which presents larger power dissipation. It is known that a class I hydrophobin is constituted by a tight binding core with a large flexible loop, markedly hydrophobic, between the Cys3 and Cys4<sup>13, 17</sup>. The hydrophobic loop which is particularly flexible is also known to be much larger in the class I hydrophobin in comparison to the class II<sup>17</sup>. The higher viscoelasticity for the LB monolayer cannot be attributed to the core and must be related to the presence of the flexible loop. Due to its hydrophobicity the loop is expected to be in contact with air in the LB monolayer in order to minimize contact with the hydrophilic substrate; while in the LS monolayer the loop is expected to interact with the hydrophobic substrate, away from the air interface<sup>28</sup>. The flexibility of the loop at air may thus explain the difference in viscoelasticity observed for the two kinds of hydrophobin layers. This result emphasizes the difference of structure between LB and LS layers, associated with the localization of the loop, which could not be detected with the AFM topography only.

Fig. 6A displays the comparison of phase distance curves, obtained with the same AFM tip, in dry conditions, related to LB monolayer and rodlets coexisting in the same sample. Systematically, the jump for the LB layer appears shifted towards smaller average tip-sample distances with respect to rodlets, with a shift of 3 nm for the tip used for the measurements reported on Fig. 6a. This shows that the dissipative term is less important in the rodlets than in LB layers, although both display similar hydrophobic character. In contrast to the LB films, rodlets do not expose the hydrophobic loop at the air interface. Similarly, Fig. 6B displays comparison between phase curves performed on top of bilayers and of rodlets (still with the same tip). The position of the jump from the attractive regime to the repulsive one appears very similar for the two bilayers and for the rodlets with jump shifts differences not exceeding 1 nm. This suggests that the three surfaces have comparable viscoelasticity. In particular, unlike the LB film, the LS+LB bilayer does not expose the flexible loops to the air. This demonstrates that, similarly to LB+LS bilayers, the hydrophobin molecules reorganize in LS+LB bilayers leading to an hydrophobic bilayer without the flexible loops in contact with air. The properties of these films, as probed by AFM spectroscopy, appear finally very close to the ones of LB+LS as well as to the ones of rodlets. These results, associated with the fact that rodlets present the same thickness than bilayers, led us to conclude that the three systems are equivalent. In other words, a stable configuration for interacting hydrophobins induced a rearrangement within LB+LS and LS+LB bilayers resulting in a structure very similar to that of the rodlets. This observation could explain why homogeneous multilayers of hydrophobins are not possible to obtain<sup>29</sup>. Contrary to rodlets which always display an elongated form, LS+LB and LB+LS bilayers form uniform isotropic films. This difference may be associated with the formation of bilayers in two steps. The first LS or LB layer being isotropic, it may induce isotropy of the hydrophobin aggregates in bilayers. Rodlets, on the contrary, may show their characteristic preferential alignment as a direct result from the uniaxial compression in the Langmuir trough<sup>18, 20</sup>. This implies in particular that rodlet units are already formed at the air/water interface before the film is transferred onto the substrate.

It was already known that structural modifications occurred during spontaneous self-assembly of hydrophobins, at air/water interfaces or on substrates<sup>13, 15, 27, 30</sup>. We now demonstrate that modifications also occur when bilayers are formed with Langmuir techniques and simply deposited onto hydrophilic or reversely onto hydrophobic substrates, independently of the nature of the substrate (hydrophilic SiO<sub>2</sub> or hydrophobic silanized SiO<sub>2</sub> substrates), leading to similar air interfaces. Similar modifications can occur when rodlets are formed. It is interesting to notice that on hydrophobic silanized substrate, these

modifications lead to formation of hydrophobic bilayers, in contrast to hydrophobic Teflon, on which reversed rodlets could be formed<sup>31</sup>.

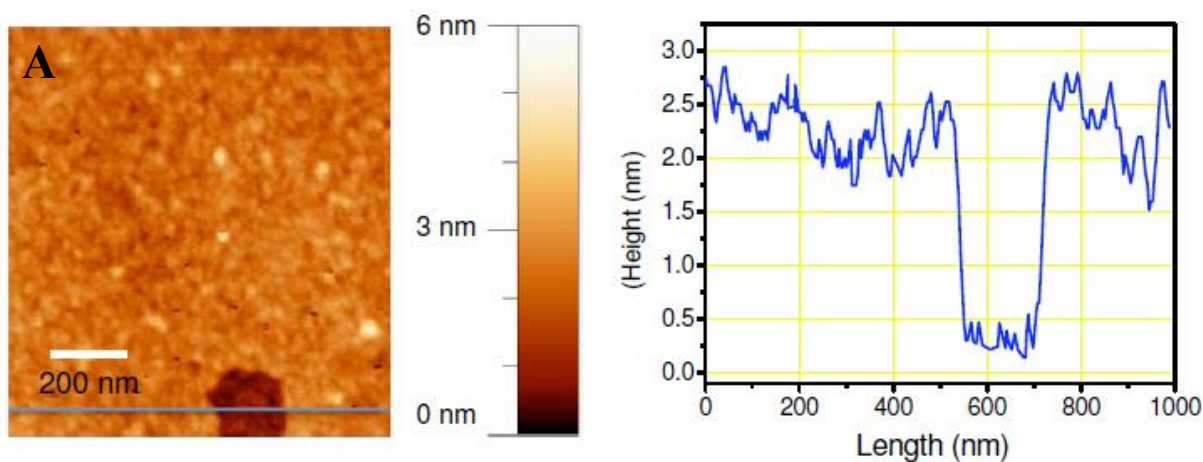
Rodlets are bilayers, hydrophobic, with a smaller visco-elasticity than monolayers. This evidences in particular a modification of the loop localization compared to hydrophobic LB monolayers, the loop being no more freely localized at the air/water interface and possibly involved in interactions between hydrophobins. It had already been pointed in previous publications<sup>15, 30</sup> that structural modification of the hydrophobin occurred in the rodlets. Although the loop is not mandatory for the formation of rodlets, it may be involved in the lateral packing of rodlets<sup>17</sup>, which appears in agreement with the disappearance of free loops from the air interface. Together with modification of hydrophobin structure within rodlets, previously demonstrated<sup>15</sup>, future models should now take into account these new features for new modelizations of rodlets.

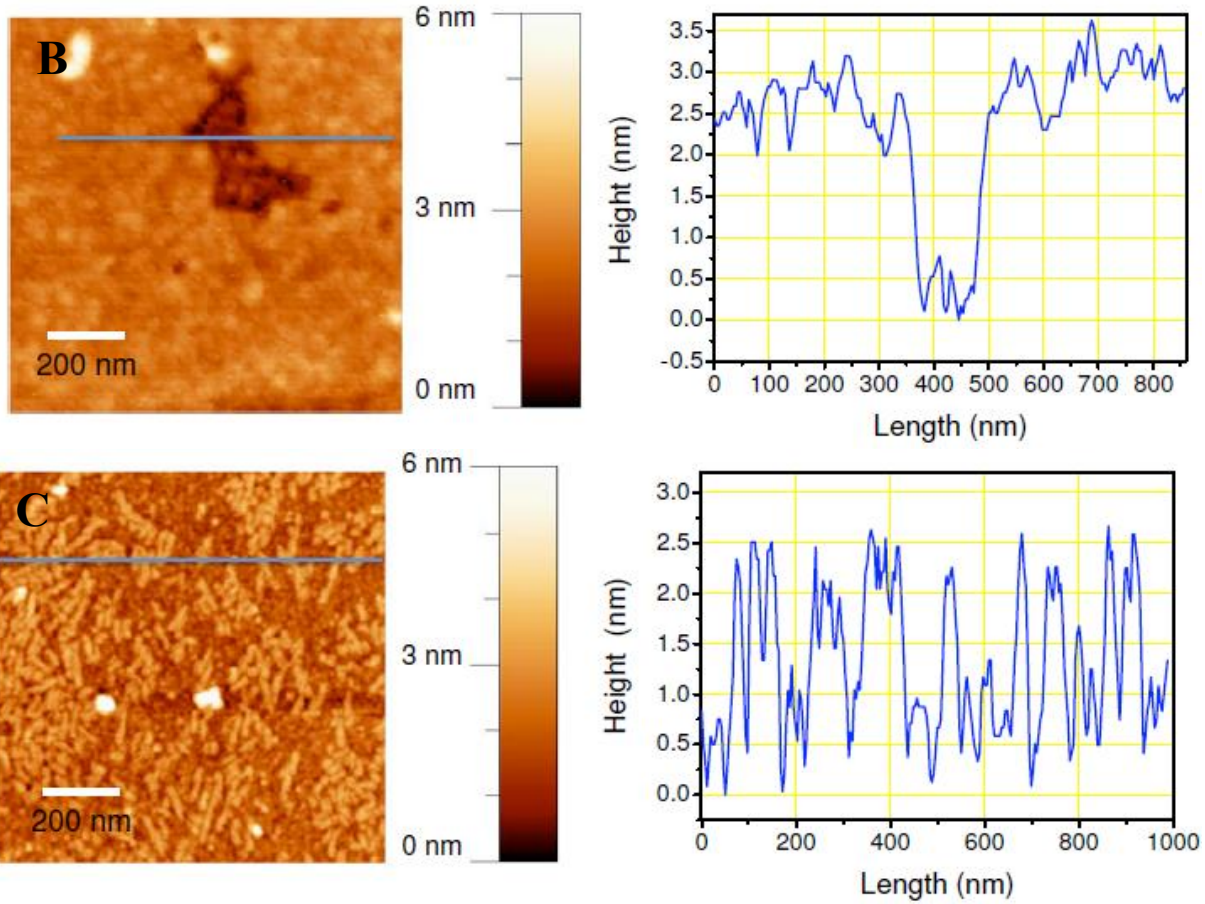
## Conclusion

In summary, using force spectroscopy measurements in dynamic mode we have investigated Vmh2 LS and LB monolayers, rodlets and LS+LB, LB+LS bilayers at the nanoscale level. Concerning monolayers, we have confirmed the hydrophilicity of LS monolayer at the nanoscale by detecting the water meniscus formation between the AFM tip and the monolayer and demonstrated in contrast that no meniscus is formed between tip and LB monolayer. A higher viscoelasticity for LB monolayers has been evidenced with respect to the LS ones. This is related to the presence of the loop, which is exposed to the air in the LB film, due to its hydrophobicity, but interact with the substrate in the LS film.

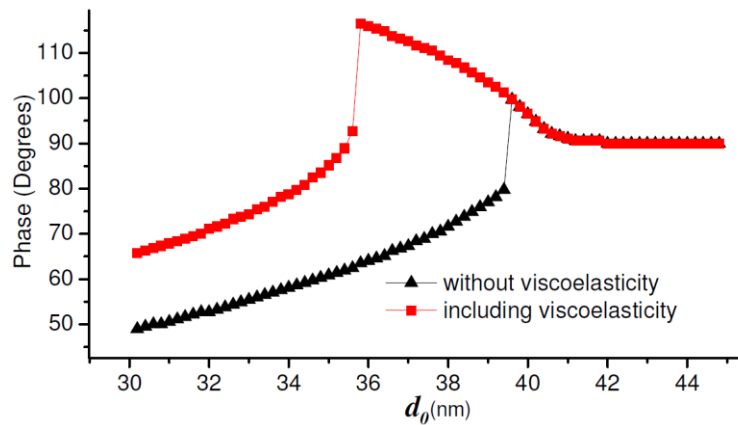
The fact that rodlets and bilayer films display similar hydrophobicity and viscoelasticity strongly suggests that rodlets are actually fragments of bilayers associated with structural modifications that lead to a common stable hydrophobic structure. This hydrophobic bilayer is associated with loops no more freely located at the air interface and possibly involved in interactions between hydrophobins. It would be particularly interesting now to start simulations in order to build a model of interacting molecules in rodlets based on these experimental results.

ACKNOWLEDGMENTS. We thank Dr L. De Stefano for fruitful discussions, Dr I. B. Malham and Dr L. Bureau for substrate silanization and contact angle measurements and D. Limagne for technical support. RR and EL thank Dr. J. Jupille for valuable discussions.

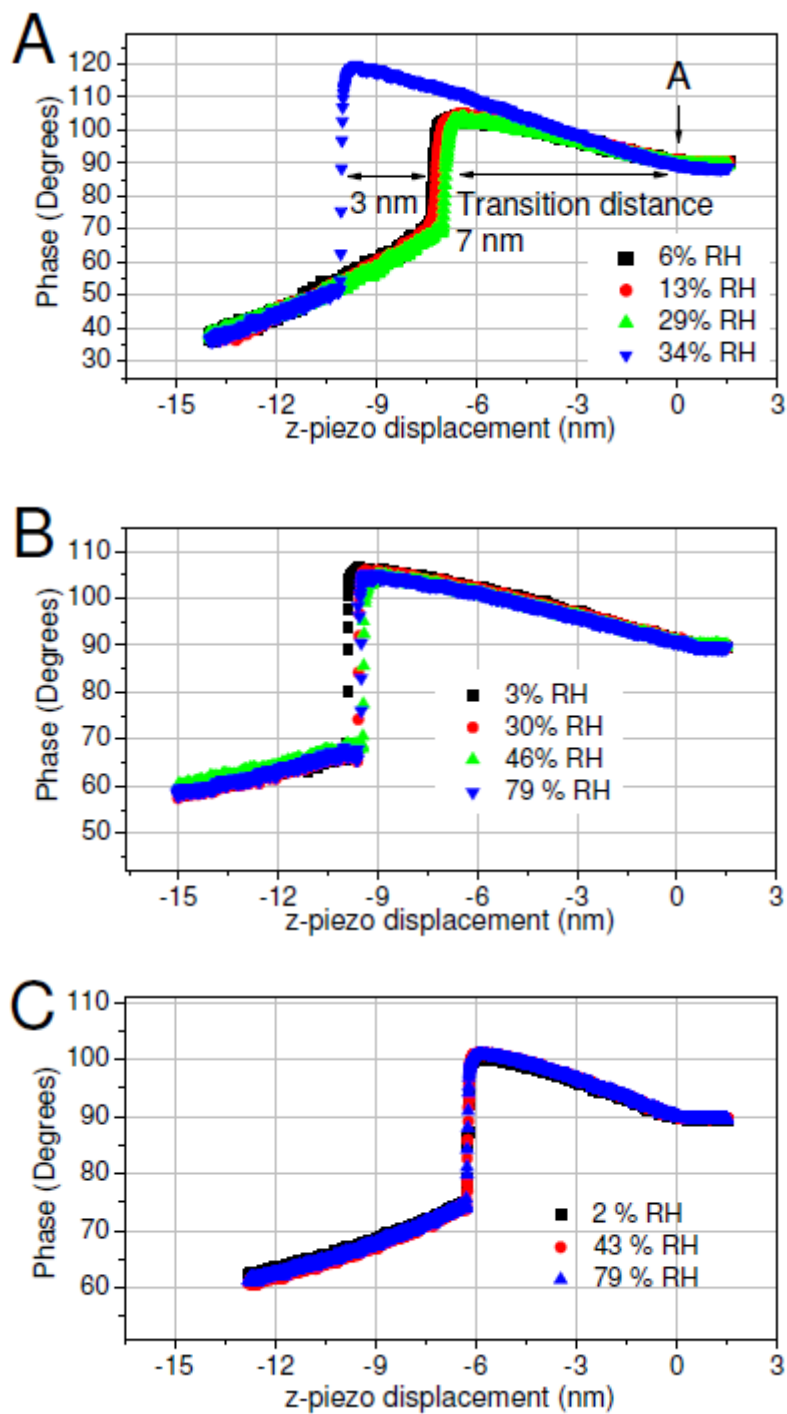




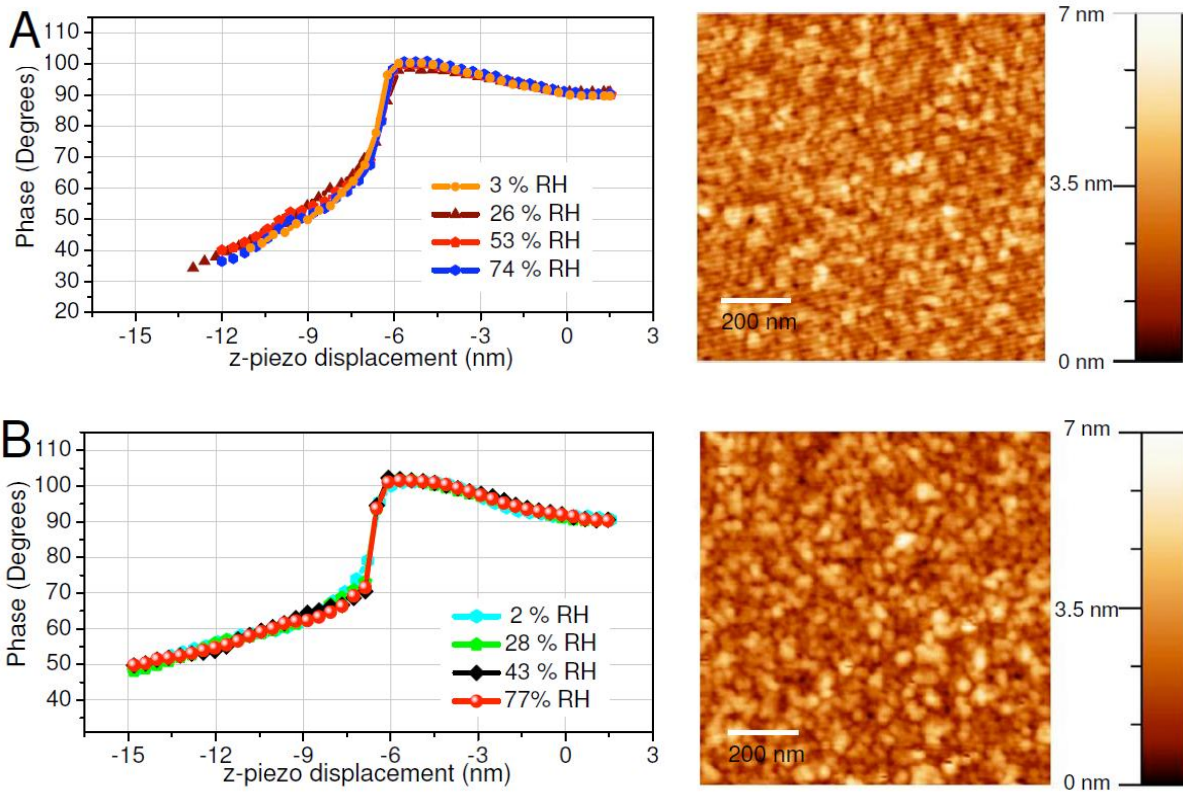
**Figure 1.** AFM topography images and height profiles of : (A), Vmh2 LB monolayer, (B) LS monolayer, (C) coexistence of LB monolayer and rodlets.



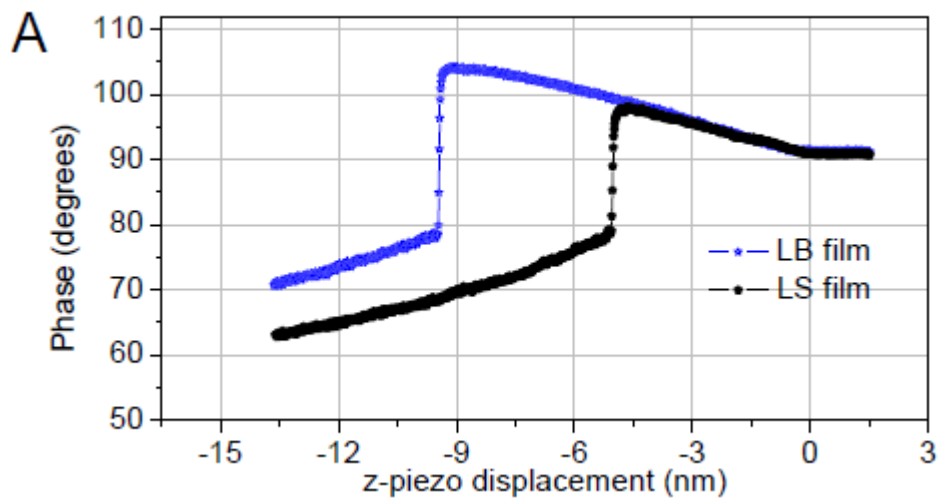
**Figure 2.** Simulated phase-distance curves without taking into account visco-elasticity (black color, triangles) and taking into account visco-elasticity (green color, squares). Parameters for the simulations are :  $\omega_0/2\pi=142\text{kHz}$ ,  $A_0=40\text{nm}$ ,  $k_c=5.1\text{N/m}$ ,  $Q = 550$ ,  $Q_{\text{dis}} = 0.5$ ,  $E=65\text{GPa}$ ,  $a_0=0.1\text{nm}$ ,  $H= 6\times 10^{-20}\text{J}$ ,  $R = 10\text{nm}$ .

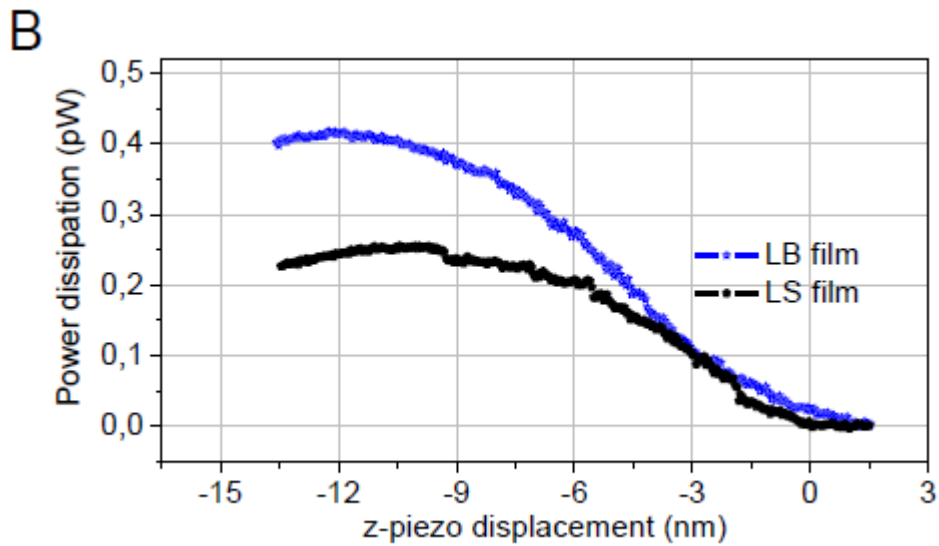


**Figure 3.** (A) Phase distance curves performed for Vmh2 LS film at different humidity RH. “A” indicates the onset of tip/sample interactions. (B) Phase distance curves performed for Vmh2 LB film at different humidities. (C) Phase distance curves for the rodlets at different humidities. For clarity purpose, phase signals measured at 10, 15, 20, 40, 50, 60 and 65 %RH are not shown in the graphs (B) and (C).

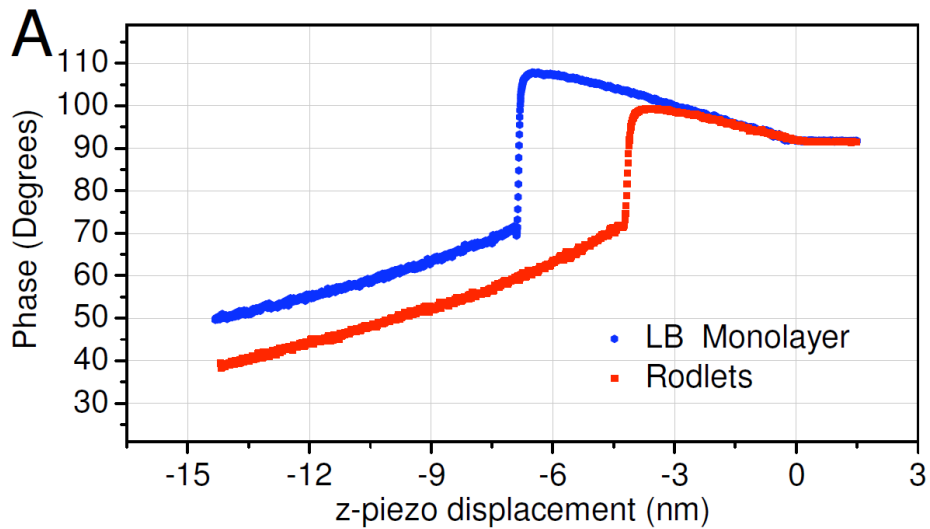


**Figure 4.** AFM topography images of the Vmh2 bilayers with the corresponding phase-distance curves for different humidities : (A) LB+LS bilayer deposited onto SiO<sub>2</sub> surface. (B) LS+LB bilayer deposited onto silanized SiO<sub>2</sub> surface.





**Figure 5.** Experimental phase distance curve performed with the same tip for Vmh2 LB and LS monolayers in dry conditions (A), and the corresponding energy dissipation per period (B). The maximum dissipation observed for LB film ( 0.42 pW) is about 1.7 times larger than the one observed for LS film ( 0.25 pW). The energy dissipation was evaluated using equation 3.





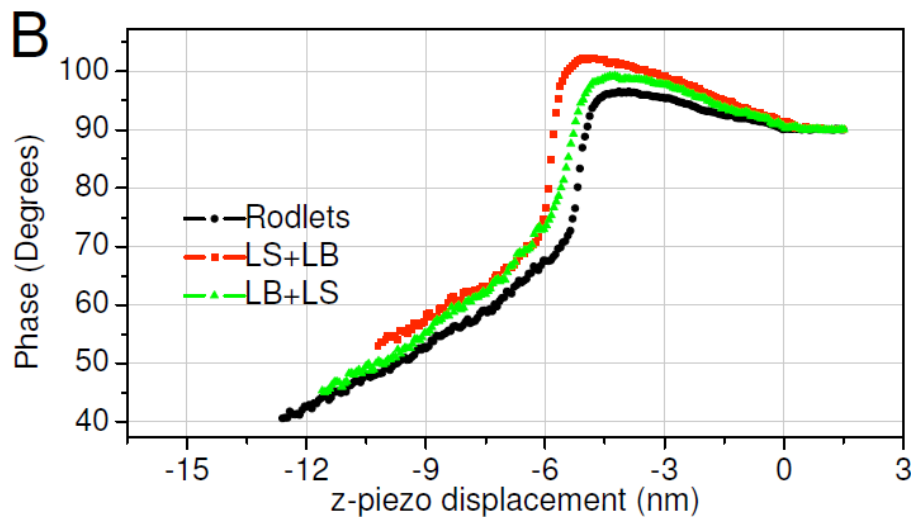


**Figure 6.** (A) Experimental phase distance curves performed in dry conditions with the same tip for LB monolayer and rodlets. (B) Experimental phase distance curves for hydrophobin bilayers and rodlets performed in dry conditions with the same tip.

#### References

- (1) Linder, M. B.; Szilvay, G. R.; Nakari-Setälä, T.; Penttilä, M. E. *FEMS Microbiol. Rev.* **2005**, *29*, 877–896.
- (2) Wosten, H. A. B.; de Vocht M. L. *Biochim. et Biophys. Acta* **2000**, *1469*, 79-86.
- (3) Linder, M. B. *Current Opinion in Coll. Interf. Science* **2009**, *14*, 356-363.
- (4) De Stefano, L.; Rea, I.; Giardina, P.; Armenante, A.; Rendina, I. *Adv. Mat.* **2008**, *20*, 1529-1533.
- (5) Qin, M.; Wang, L. K.; Feng, X. Z. *Langmuir* **2007**, *23*, 4465-4471.
- (6) Scholtmeijer, K.; Janssen, M. I.; Gerssen, B.; de Vocht, M. L.; van Leeuwen, B. M.; van Kooten, T. G.; Wosten, H. A.; Wessels, J. G. *Appl. Environ. Microbiol.* **2002**, *68*, 1367–1373.
- (7) Wang, R.; Yang, Y. L.; Qin, M.; Wang, L. K.; Yu, L.; Shao, B.; Qiao, M. Q.; Wang, C.; Feng, X. Z. *Chem. Mater* **2007**, *19*, 3227-3231.
- (8) Wang, Z.; Huang, Y.; Li, S.; Xu, H.; Linder, M. B. ; Qiao, M. *Biosens. Bioelectr.* **2010**, *26*, 1074-1079.
- (9) Wang, Z.; Lienemann, M.; Qiao, M.; Linder, M. B. *Langmuir* **2010**, *26*, 8491-8496.
- (10) Basheva, E. S.; Kralchevsky, P. A.; Danov, K. D.; Stoyanov, S. D.; Blijdenstein, T. B. J.; Pelan, E. G.; Lips, A. *Langmuir* **2011**, *27*, 4481–4488
- (11) Janssen, M. I.; van Leeuwen, M. B.; Scholtmeijer, K.; van Kooten, T. G.; Dijkhuizen, L.; Wosten, H. A. *Biomaterials* **2002**, *23*, 4847–4854.
- (12) Wessels J. *Annual Review of Phytopathology* **1994**, *32*, 413-437.
- (13) Kwan, A. H. Y.; Winefield, R. D.; Sunde, M.; Matthews, J. M.; Haverkamp, R. G.; Templeton, M. D.; Mackay, J. P. *Proceedings of the National Academy of Sciences of the United States of America* **2006**, *103*, 362-3626.
- (14) Yang, K.; Deng, Y.; Zhang, C.; Elasri, M. *BMC bioinformatics* **2006**, *7*(Suppl 4) S16.
- (15) de Vocht, M. L.; Reviakine, I.; Ulrich, W. P.; Bergsma-Schutter, W.; Wosten, H. A. B.; Vogel, H.; Brisson, A.; Wessels, J. G. H.; Robillard, G. T. *Protein Sci.* **2002**, *11*, 1199–1205
- (16) Askolin, S. Characterization of the *Trichoderma reesei* hydrophobins HFBI and HFBII. *PhD Thesis (Helsinki University of Technology, Espoo)* **2006**, VTT Publications 601, ISSN 1235-0621.
- (17) Kwan AH, et al. Macindoe, I.; Vukašin, P. V.; Morris, V. K.; Kass, I.; Gupte, R.; Mark, A. E.; Templeton, M. D.; Mackay, J. P.; Sunde, M. *Journal of molecular biology* **2008**, *382*, 708-720.
- (18) Houmadi, S.; Ciuchi, F.; De Santo, M. P.; De Stefano, L.; Rea, I.; Giardina, P.; Armenante, A.;

- Lacaze, E.; Giocondo, M. *Langmuir* **2008**, 24, 12953-12957.
- (19) Armenante, A.; Longobardi, S.; Rea, I.; De Stefano, L.; Giocondo, M.; Silipo, A.; Molinaro, A.; Giardina, P. *Glycobiology* **2010**, 20, 594-602.
- (20) Malham, I. B.; Bureau L. *Langmuir* **2009**, 25, 5631-5636.
- (21) Yu, L.; Zhang, B.; Szilvay, G. R.; Sun, R.; Jänis, J.; Wang, Z.; Feng, S.; Xu, H.; Linder, M. B.; Qiao, M. *Microbiology* **2008**, 154, 1677-1685.
- (22) Butcher, J. C. *Wiley and Sons, Ltd., Chichester*, West Sussex PO19 8SQ, England 2003.
- (23) Garcia, R.; San Paulo, A. *Physical Review B* **1999**, 60, 4961-4967.
- (24) Cleveland, J.; Anczykowski, B.; Schmid, A.; Elings, V. *Applied Physics Letters* 72, 2613.
- (25) Paajanen, M.; Katainen, J.; Pakarinen, O. H.; Foster, A. S.; Lahtinen, J. *Journal of colloid and interface science* **2006**, 304, 518-523.
- (26) van Honschoten, J.; Tas, N.; Elwenspoek, M. *American Journal of Physics* **2010**, 78, 277- 286.
- (27) Zitzler, L.; Herminghaus, S.; Mugele, F. *Physical Review B* **2002**, 66, 155436.
- (28) Wang, X.; Permentier, H. P.; Rink, R.; Kruijtzter, J. A.; Liskamp, R. M.; Wösten, H. A.; Poolman, B.; Robillard, G. T. *Biophysical journal* **2004**, 87, 1919-1928.
- (29) Kisko, K.; Torkkeli, M.; Vuorimaa, E.; Lemmetyinen, H.; Seeck, O. H.; Linder, M.; Serimaa, R. *Surf. Sci.* **2005**, 584, 35-40.
- (30) Wang, X.; De Vocht, M. L.; De Jonge, J.; Poolman, B.; Robillard, G. T. *Protein Science* **2002**, 11, 1172-1181.
- (31) Scholtmeijer, K.; de Vocht, M. L.; Rink, R.; Robillard, G. T.; Wosten, H. A. B. *Journal of Biological Chemistry* **2009**, 284, 26309-26314



## Ringraziamenti

I primi doverosi ringraziamenti vanno al Prof. Giovanni Sannia, non solo come Coordinatore del corso di Dottorato, ma soprattutto per il supporto che ha saputo darmi in questi anni, riuscendo sempre a farmi capire che credeva in me (sia con le parole buone ma anche con quelle “meno buone”). Un ringraziamento va anche al Prof. Gennaro Marino, un vulcano di idee e suggerimenti.

Un semplice grazie non basterebbe per esprimere la mia riconoscenza al mio tutor, la professoressa Paola Giardina, con la quale mi sono “tuffata” in questo oceano di idrofobine, tra alti e bassi, soddisfazioni e delusioni. Senza il suo prezioso appoggio, i quotidiani confronti, la sua costante guida, il mio lavoro sarebbe stato molto più arduo. Insieme abbiamo affrontato questo percorso con piena collaborazione e reciproco rispetto, costruendo un rapporto che mai avrei immaginato potesse nascere con un supervisore.

Un Grazie di cuore al Dr Luca De Stefano del CNR di Napoli, e ai suoi preziosissimi collaboratori, Dr Ilaria Rea e Dr Emanuele Orabona, per tutto il meraviglioso lavoro fatto insieme; alla prof. Delia Picone e al Dr Carmine Ercole del dipartimento di Chimica, per la proficua collaborazione; alla Dr Emmanuelle Lacaze e al Dr Said Houmadi per lo straordinario periodo trascorso nella straordinaria Parigi.

Un ringraziamento più che speciale va alla piccola grande famiglia degli “idrofobini”, per tutto il contributo che ha apportato, sia dal lato scientifico che umano. Dalla dottoressa Nunzia Armenante (capostipite) ai Dottori Nunzio Damiano e Vincenzo Riso, passando per la Dr. Katia Iannicelli, il Dr Valerio Caldovino e il Dr Mattia De Stefano, finendo con Rossella Migliaccio, Stefania Passato e Daniele Boccamino: è stato meraviglioso lavorare con voi! Questa dedica va a voi perché, come qualcuno ha detto prima di me, il mio lavoro è anche il vostro lavoro.

Grazie a tutti i membri, passati e presenti, del gruppo BMA (“funghi, freddi e massa”) che in questi anni hanno incrociato la mia strada e che hanno contribuito a rendere l’ambiente di lavoro sereno e amichevole. Un ringraziamento particolare va a tre amici: la Dr Maria Squillace, preziosissimo punto fermo, che mi è sempre vicina anche se è lontana; la Dr Claudia Del Vecchio, che ha condiviso con me lo stesso percorso per 20 lunghi anni; e il Dr Vincenzo Lettera, “vicino di banco” formidabile che ha reso piacevole ogni giorno trascorso insieme.

Non saprei da che parte iniziare per esprimere tutta la gratitudine ai miei genitori, che mi hanno sempre sostenuto, incoraggiato e consolato quando serviva. Sono stati dei perfetti esempi di come si può lavorare non solo con impegno, ma soprattutto con passione!

Per concludere, la valutazione che sempre accompagna la fine di un ciclo non può che essere positiva, se non altro perché il corso di dottorato mi ha permesso di incontrare una persona talmente speciale che in un batter d’occhio è passata da collega a nientemeno che marito. L’ultimo (e più importante) grazie va quindi al Dr Eugenio Galano, per tutto ciò che è, che siamo e che saremo...

